Laboratoire National Henri Becquerel
LNE-LNHB

NOTE TECHNIQUE

Référence de la note	LNHB 06/28

TITRE : **DDEP Training Session**
Summary Report of the first DDEP – TS dedicated to decay data evaluation

RESUME :
Cette note rassemble les exposés qui ont été présentés lors de la session de formation : "DDEP Training Session" centrée sur l'évaluation des données de décroissance radioactive qui s'est tenue à Saclay du 6 au 10 mars 2006

A		
O		
IND.	**DATE**	**OBJET**

	Auteur(s)	Vérificateur(s)	Chef de laboratoire	Chef du Service
Noms	M.-M. Bé C. Dulieu V. Chisté	C. Dulieu	M.-M. Bé	B. Chauvenet

DECAY DATA EVALUATION PROJECT – TRAINING SESSION

Summary Report of the first DDEP – TS dedicated to decay data evaluation

Laboratoire National Henri Becquerel, CEA- Saclay, France
6 – 10 March 2006

Prepared by

Marie-Martine Bé, Christophe Dulieu and Vanessa Chisté

ABBREVIATIONS

ANL	Argonne National Laboratory, USA
BIPM	Bureau International des Poids et Mesures
BNL	Brookhaven National Laboratory, USA
CIEMAT	Centro de Investigationes Energéticas, Medioambiantales y Tecnológicas, Spain
CCRI	Comité Consultatif pour les Rayonnements Ionisants
CEA	Commissariat à l'Énergie Atomique, France
CNEA	Comisión Nacional de Energía Atómica, Argentina
DDEP	Decay Data Evaluation project
IAEA	International Atomic Energy Agency
IEAv-CTA	Centro Técnico Aerospacial, Brazil
IFIN	"Horia Hulubei" Nat. Inst. for Phys. & Nucl. Eng. (IFIN-HH), Romania
KRISS	Korea Research Institute of Standards and Science, South Korea
LNHB	Laboratoire National Henri Becquerel, France
NNDC	National Nuclear Data Center, USA
NPL	National Physical Laboratory, U.K.

Table of contents

Foreword

Basic properties of radionuclides such as half-life, decay mode and branchings, as well as radiation energies and emission probabilities are commonly used in various research fields. To meet the demand for these data the Laboratoire de Métrologie des Rayonnnements Ionisants (LMRI, France*)* produced a table that was published in four volumes that covered the 1982-1987 period. In 1993, a cooperative agreement was established between the Laboratoire National Henri Becquerel (CEA- LNHB, France) and the Physikalisch-Technische Bundesanstalt (PTB*,* Germany) to continue and expand this work. In 1995 the Decay Data Evaluation Project (DDEP), a new international collaboration with the same objectives, was formed. Along with the evaluators from LNHB and PTB, this collaboration has included others from Idaho National Engineering and Environmental Laboratory (INEEL, USA), Brookhaven National Laboratory (BNL, USA), Lawrence Berkeley National Laboratory (LBNL, USA), and Khlopin Radium Institute (KRI, Russia). The goal of the DDEP collaboration has been to produce carefully evaluated radiation properties, which eventually may be accepted as standard data. Thus, the collaboration has adopted a uniform evaluation methodology that emphasizes the following aspects:

- Critical compilation and evaluation of relevant publications;
- Accounting of all published experimental results;
- Uniform approach to the statistical analysis of the data;
- Hardcopy or electronic publications of atomic and nuclear radiation properties;
- Evaluation reviews by two other members of the DDEP collaboration.

Another objective of the *DDEP* collaboration has been to disseminate these critically evaluated data so they may be included in other decay data collections, thus avoiding possible duplication of efforts. The collaboration published its first evaluations in two volumes in 1999: one with the recommended data, the other with a description of the data analysis.

The DDEP collaboration became larger with new members from the International Atomic Energy Agency (IAEA, Austria), Argonne National Laboratory (ANL, USA), University of Sao Paulo (USP, Brazil), National Physical Laboratory (NPL, UK). At present, DDEP evaluations may be found in a Monographie from the Bureau International des Poids et Mesures (BIPM), in NUCLÉIDE, a CD-Rom published by the LNHB, and on Internet at:

http://www.nucleide.org/NucData.htm

Recently, new scientists from the National Institute for Physics and Nuclear Engineering (IFIN, Romania), the Centro de Investigaciones Energeticas, Medioambientales y Tecnologicas (CIEMAT, Spain), the National Physical Laboratory (NPL, UK), the Korea Research Institute of Standards and Science (KRISS, South Korea), and the Comisión Nacional de Energia Atómica (CNEA, Argentina) have expressed their interest in evaluating nuclear decay data. Therefore it seemed useful to organize a training workshop for these new members. This workshop was held at the Commissariat à L' Énergie Atomique (CEA, Saclay, France), from March 6 to March 10, 2006. Experienced evaluators gave lectures on evaluation and statistical analysis of data. Practical sessions were devoted to the use of pertinent computer codes, and some specific evaluations were presented. Finally, students were invited to talk about the evaluations they had prepared.

Thursday, March 9, a visit of the BIPM (Pavillon de Breteuil, Sèvres) was organized in the morning. Professor Giorgio Moscati, President of the *CCRI*, welcomed the participants and underlined the importance of producing carefully evaluated data that may be used as standards. Also, he encouraged evaluators to pursue the publication of another Monographie. The members of the DDEP express theirs thanks for their lectures to Professor Moscati, as well as to Carine Michotte and Guy Ratel, also from BIPM.

DDEP – Training session 6-10 March 2006

List of participants

Marie-Martine Bé CEA/LNHB – Bt. 602 91191 Gif sur Yvette Cedex France	e-mail : mmbe@cea.fr phone : + 33 1 69 08 46 41 fax : + 33 1 69 08 26 19 web : www.nucleide.org
Desmond MacMahon 31, Sarum Bracknell, Berkshire RG12 8XZ United Kingdom	e-mail : desmondmacm@yahoo.co.uk phone : + 44 1344 421712
Edgardo Browne 2546 Tamalpais Ave. El Cerrito, California 94530 U.S.A.	e-mail : ebrowne@lbl.gov
Ruy M. Castro Rod Tamoios, km 5.5 CEP 12228-840 Sao José Dos Campos SP BRAZIL	e-mail : rmcastro@ieav.cta.br
K. B. Lee Korea Research Institute of Standard and Science Po Box 200 Kinveorg, Korea	e-mail : lee@kriss.re.kr
Andy Pearce NPL Hampton Road Teddington Middlesex, TW11 0LW U.K.	e-mail : andy.pearce@npl.co.uk
Arzu Arinc NPL Hampton Road Teddington, Middlesex - TW11 OLW U.K.	e-mail : Arzu.arinc@npl.co.uk phone : + 44 208943 8510
Mark A. Kellett IAEA Nuclear Data Section Wagramerstrasse 5 A – 1200 VIENNA, AUSTRIA	e-mail m.a.kellett@iaea.org phone : 00 431260021708 Fax : 00 4312600721708
Aurelian Luca « Horia Hulubei » Nat. Inst. For Phys. And Nucl. Eng. (IFIN-HH), 407 Atomistilor Street, PO Box MG-6, Magurele, jud. Ilfov, postcode 077125, ROMANIA	e-mail : aluca@ifin.nipne.ro aurelian@digicom.ro phone : 0040 21 404.61.63 fax : 0040 21 457.44.32
Pablo Arenillas CNEA – Argentina Centro Atomico Ezeiza Pro. Borlenghi N°15 1806 – Ezeiza – Argentina	e-mail : arenilla@cae.cnea.gov.ar phone : + 54 11 6779 8408 fax : + 54 11 6779 8554

Juan Carlos Furnari CNEA – Argentina Centro Atomico Ezeiza Pro. Borlenghi N°15 1806 – Ezeiza – Argentina	e-mail : furnari@cae.cnea.gov.ar phone : + 54 11 6779 8596 fax : + 54 11 6779 8126
Monica Galan Laboratorio de Metrologia de Radiaciones Ionizantes CIEMAT Av. Complutense,22 28040-Madrid Espagne	e-mail : monica.galan@ciemat.es phone : + 34 91 346 6222 fax : + 34 91 346 6772 web : www.ciemat.es
Filip G. Kondev Nuclear Engineering Division Argonne National Laboratory 9700 S. Cass Avenue Argonne, IL 60439 USA	e-mail : kondev@anl.gov phone : + 1 630 252 4484 fax : + 1 630 252 4978
Tibor Kibedi Dept. Of Nuclear Physics Australian National University Canberra, ACT 0200	e-mail tibor.kibedi@anu.edu.au phone : + 61 2 61252093 fax : + 61 2 61250748
Jagdish K. Tuli National Nuclear Data Center Brookhaven National Laboratory Building 197D Upton, NY 11973-5000 USA	e-mail : tuli@bnl.gov web : www.nndc.bnl.gov phone : + 1 (631) 344-5080 fax : + 1 (631) 344-2806
Vanessa Chisté CEA/LNHB – Bt. 602 91191 Gif sur Yvette Cedex	e-mail : vanessa.chiste@cea.fr phone : + 33 1 69 08 63 07 fax : + 33 1 69 08 26 19 web : www.nucleide.org
Christophe Dulieu CEA/LNHB – Bt. 602 91191 Gif sur Yvette Cedex	e-mail : christophe.dulieu@cea.fr phone : + 33 1 69 08 57 85 fax : + 33 1 69 08 26 19 web : www.nucleide.org
Bruno Chauvenet CEA/LNHB – Bt. 602 91191 Gif sur Yvette Cedex France	e-mail : bruno.chauvenet@cea.fr phone : + 33 1 69 08 89 81 fax : + 33 1 69 08 26 19
Elvire Leblanc CEA/LNHB – Bt. 602 91191 Gif sur Yvette Cedex France	e-mail : elvire.leblanc@cea.fr phone : + 33 1 69 08 23 32 fax : + 33 1 69 08 26 19
Marie-Christine Lépy CEA/LNHB – Bt. 602 91191 Gif sur Yvette Cedex France	e-mail : marie-christine.lepy@cea.fr phone : + 33 1 69 08 24 48 fax : + 33 1 69 08 26 19
Marie-Noëlle Amiot CEA/LNHB – Bt. 602 91191 Gif sur Yvette Cedex France	e-mail : marie-noelle.amiot@cea.fr phone : + 33 1 69 08 46 52 fax : + 33 1 69 08 26 19

Philippe Cassette CEA/LNHB – Bt. 602 91191 Gif sur Yvette Cedex, France	e-mail : philippe.cassette@cea.fr phone : + 33 1 69 08 48 -_ fax : + 33 1 69 08 26 19
Georges Audi CSNSM – IN2P3 CNRS F- 91405 Orsay Campus France	http://csnwww.in2p3.fr/amdc/web/amdc_fr.html

Absolute Activity Measurement Methods and Decay Data

B. Chauvenet

MEASUREMENT METHODS

- Indirect

$$A = A_0 \times \frac{L}{L_0}$$

A : unknown activity of source S

A_0 : activity of standard source S_0

L : response resulting from source S

L_0 : response resulting from source S_0

- Direct

$$A = \frac{L}{R}$$

R : detection efficiency (source + detector)

R unknown

can be :

- measured
- calculated
- extrapolated to 1

13

DIRECT MEASUREMENT METHODS

Defined solid angle methods :

detection efficiency close to 1 in a measured solid angle

Coincidence methods :

Using simultaneity of emission of radiation of different types

4π measurement methods

Radioactive nuclides surrounded by detecting material in order to approach efficiency of 1 for detecting a disintegration

DEFINED SOLID ANGLE

Applying to radiation emitted by solid sources, with low scattering (alpha particles, low-energy X-rays)

Low solid angle (≈ 1 %) to detect only radiation emitted normally to the source

For a point source and a circular collimator

A = N / G

with N, corrected count rate

G, solid angle of detection = $\frac{1}{4\pi} 2\pi(1 - \cos\theta)$

$$G = \frac{1}{2}\left(1 - \frac{z}{\sqrt{z^2 + r^2}}\right)$$

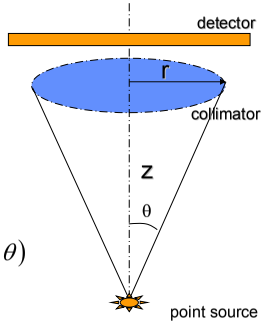

Corrections to be applied

- Dead time
- Source position
- Spread of the source
- Self absorption in the source
- Extrapolation of counts below energy threshold
- Possible scattering of particles in the collimator
- Decay
- Background
- Radioactive impurities

Solid alpha source

Radon 222 frozen point source

4πβ–γ COINCIDENCE METHODS

Applying to radionuclides emitting simultaneously at least two radiation of different types per disintegration : β-γ, α-γ, X or Auger - γ

$N_\beta = A \times \overline{\varepsilon_\beta}$

$N_\gamma = A \times \overline{\varepsilon_\gamma}$

$N_{\beta\gamma} = A \times \overline{\varepsilon_\beta \times \varepsilon_\gamma}$

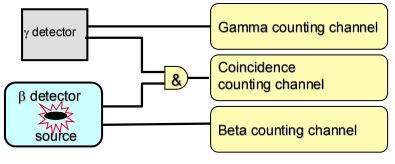

If detection efficiencies are uncorrelated :

$N_{\beta\gamma} = A \times \overline{\varepsilon_\beta} \times \overline{\varepsilon_\gamma}$

$$A = \frac{N_\beta \times N_\gamma}{N_{\beta\gamma}}$$

Condition for validity of the formula $N_{\beta\gamma} = A \times \overline{\varepsilon_\beta} \times \overline{\varepsilon_\gamma}$

No directional correlations ⇒ 4π beta counter

in practice - 4π proportional counter

- liquid scintillation counter

Uniformity of efficiency for at least one detector ⇒ point sources in PC

System using TDCR scintillation detection system in the beta counting channel

Effects to be corrected for

« Beta » efficiency of the gamma channel : wall effect or detection medium effect (gas or scintillator)

« Gamma transition» efficiency of the beta channel :
- probability of detection of gamma photons in the beta detector
- detection of electrons (conversion, Auger) or X rays in case of electron conversion of the gamma transition

Accidental coincidences : two events from two different disintegrations detected and counted in the coincidence resolving time

Dead times : non extending dead times, extending dead times

Complex decay schemes :

-different beta branches of different energies
-different electron capture decay branches with different capture probabilities (P_K,P_L) } different « beta » detection efficiencies

Significant time distribution between true coincident events :
- time jitter (detectors and electronics)
- metastable states (decay scheme)

Extrapolation model : linear, polynomial fitting
Background, half life

Extrapolation procedure to beta detection efficiency 1

$$\varepsilon_\beta \longrightarrow 1,\ N_\beta \longrightarrow A,\ \frac{N_\beta N_\gamma}{N_C} \longrightarrow A$$

$$N_\beta = A(\varepsilon_\beta + (1-\varepsilon_\beta)\left(\frac{\varepsilon_{\beta\gamma}}{1+\alpha} + \alpha\frac{\varepsilon_{ce}}{1+\alpha}\right))$$

$$1-\varepsilon_\beta = \frac{N_\gamma - N_c}{N_\gamma}$$

or

$$\frac{N_\beta \times N_\gamma}{N_C}$$

$$\frac{1-\varepsilon_\beta}{\varepsilon_\beta} = \frac{N_\gamma - N_c}{N_C}$$

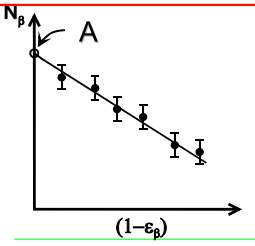

Methods of beta efficiency variation :

For solid point sources :
- Adding absorption foils sandwiching the deposit
- Varying electronic threshold

For liquid scintillation sources
- Defocalisation of PM's

15

Extrapolation models :

Extrapolation curves depend on gamma energy windows

Some curves can be non-linear (curvatures)

- due to variation of gamma efficiency in the beta counter in function of beta efficiency

- due to the decay scheme

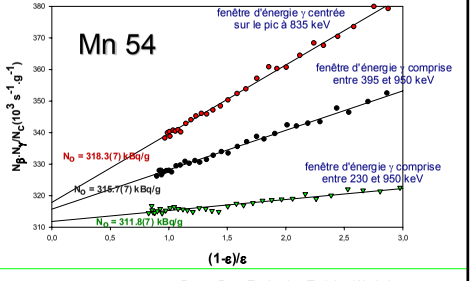

Anti-coincidence method

Applying to beta-gamma, capture-gamma emitters, especially those with metastable states

Beta counting channel

Gamma counting channel :
- dead times common to beta and gamma pulses
- delayed (so that all coincident gamma pulse occurs always after the associated beta pulse)

$$N_\beta = A(\varepsilon_\beta + (1-\varepsilon_\beta)\left(\frac{\varepsilon_{\beta\gamma}}{1+\alpha} + \alpha\frac{\varepsilon_{ce}}{1+\alpha}\right))$$

$$N_\gamma - N_c = A\varepsilon_\gamma(1-\varepsilon_\beta)$$

Extrapolation procedure :

$$\varepsilon_\beta \longrightarrow 1,\ N_c \longrightarrow N_\gamma, N_\beta \longrightarrow A$$

Efficiency tracer method

Applying to pure beta emitters

- Mixed with a **tracer** : a beta-gamma emitter of known activity concentration
  (previously determined by $4\pi\beta\gamma$ coincidence measurement)
- Beta energies of the same order
- Chemical compatibility to get well mixed sources, homogeneous distribution of both nuclides in the source (solid deposit or solution).

- Extrapolation procedure according to beta detection efficiency of the tracer :
- Result = Activity of tracer + Activity of the beta emitter

Coincidences are magical !

Mr Black is one-eyed and Mrs White is short-sighted. In the smoky cabaret,
they are far from the magician but they want to determine the number of rabbits appearing from his hat.
They decide to put their efforts in common…Of course, they count all the rabbits they see.
In addition, they count the number of rabbits seen by them simultaneously…

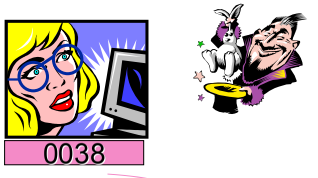

« Common » rabbits
(those seen at the same time by Mr Black and Mrs White)

0022

$$n_{rabbits} = \frac{38 \times 29}{22} = 50{,}01$$

$$\varepsilon_{Mr\ Black} = \frac{29}{50} = 58\%$$

$$\varepsilon_{Mrs\ White} = \frac{38}{50} = 76\%$$

16

4π METHODS

4πγ well-type crystal (NaI(Tl) or CsI)

Applying to nuclides decaying through complex decay schemes

$$R_{global} = 1 - \prod(1 - R_i)$$

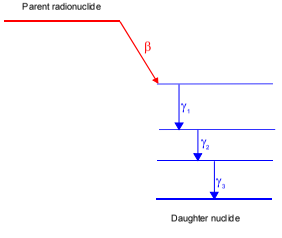

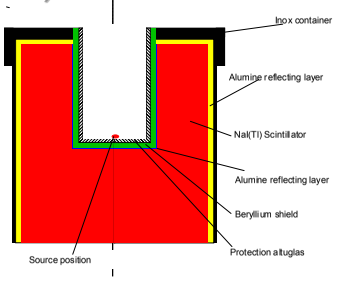

If $R(\gamma_1) = R(\gamma_2) = R(\gamma_3) = 0{,}80 \pm 0{,}02$

then $R_{global} = 0{,}992\ 0 \pm 0{,}002\ 4$

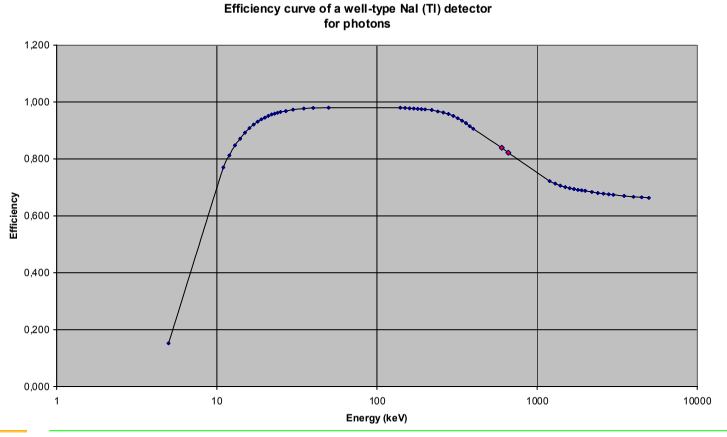

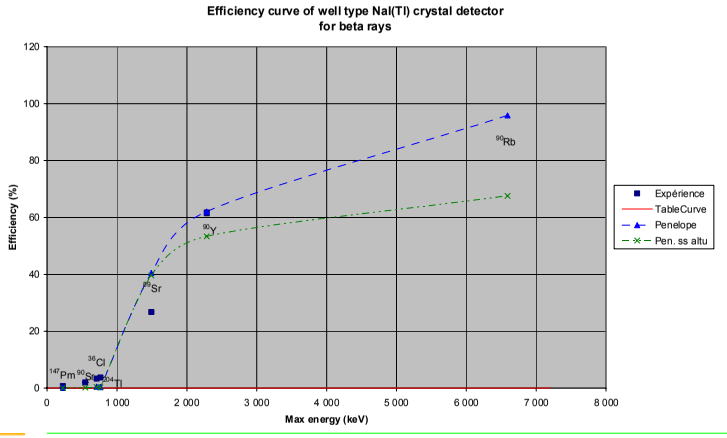

Efficiency curve : experimental, using mono-energetic photon emitters

calculated, using Monte Carlo codes

Efficiency R of detection of disintegration for a given radionuclide

depending of : - efficiency curve

- decay scheme and photon emission intensities

Uncertainty components due to :

- decay scheme data
- efficiency curve

decrease when the efficiency of detection of disintegration goes close to 1

Undirect ⟶ quasi « Direct » method

17

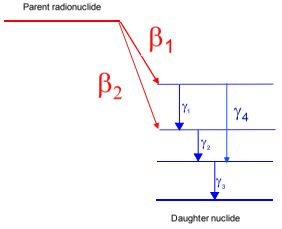

Example of calculation of R for a given decay scheme

Determine the probability per disintegration of each decay path

Determine the probability of no detection of each decay path

Determine the total probability of no detection

Efficiciency = 1 – Total probability of no detection

$$R = 1 - I_{\gamma 1}(1 - R_1)(1 - R_2)(1 - R_3)$$
$$- I_{\gamma 4}(1 - R_4)(1 - R_3)$$
$$- p_{\beta 2}(1 - R_2)(1 - R_3)$$

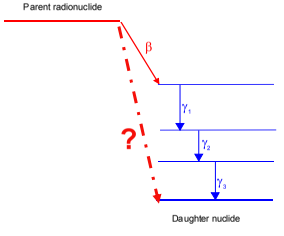

Remark :

Doubt about possible beta branch to the daughter fundamental state…

The problem can be solved by a comparison between results obtained by :

- the coincidence method, whose result does not depend on this possible beta branch

- the 4πγ method, whose result (disintegration detection efficiency value) depend on it

Using several independent activity measurement methods is a way to point out and identify problems in the decay scheme of the measured radionuclide

Effects to be corrected for

•Dead time

•Source position
•Spread of the source
•Self absorption in the source

} If significant difference with conditions for efficiency curve

•Extrapolation of counts below energy threshold
•Half life
•Background
•Radioactive impurities

Differential internal proportional counters

Applying to gaseous radionuclides emitting beta rays and electrons (tritium, krypton 85, xenon 127, xenon 131, xenon 133)

Use of cylindrical internal proportional counters, strictly identical except for their length.
Correct for end effects (inhomogeneity of electrical field in the vicinity of the counters extremities)

→ Use perfect virtual counters obtained by subtraction of counts for the pairs of counters

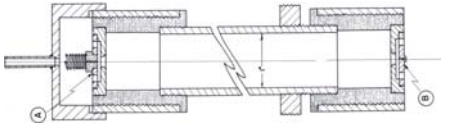

NIST counter

-Known volumes
-Known masses of gas (measured pressure and temperature)
-Radioactive gas mixed with detecting gas (methane, argon-methane, propane)

Effects to be corrected for :

•Dead time

•Lateral wall effect (calculation, extrapolation to 1/P =0)

•Extrapolation of counts below energy threshold

•Decay

•Background

•Radioactive impurities

OTHER METHODS

- **Liquid scintillation : NIST-CIEMAT , TDCR**

- **Calorimetry**

Total energy absorption :

Knowledge of mean energy of particles emitted per disingration

Effects to be corrected for :

•Heat defect
•Particle escape
•Background
•Half life

Conclusions

- Absolute activity measurements are required for the experimental determination of intensities of the particles resulting from the disintegration of a radionuclide and deexcitation of the daughter nuclide
- The precision and accuracy of these measurements contribute directly to those of these intensities
- Each activity measurement method can generate specific biases : it is of major interest to compare results obtained through independent methods.
- For evaluation, one of the minimal requirements is to get the information about the activity measurement methods used, at least to evaluate the claimed uncertainties of the results, but also possible pending problems

Alpha and Beta Spectrometry Techniques for nuclear data determination

Elvire Leblanc – CEA/LNHB
Elvire.leblanc@cea.fr

LNE

Which nuclear data do we want to determine ?

- **Alpha emission : discrete spectrum**
  - ✓ Absolute energies
  - ✓ Absolute alpha-particle emission probabilities
  - ✓ *Half-life*
  - ✓ *Hindrance factor*

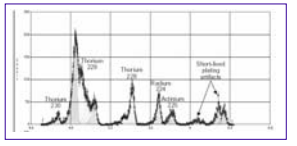

- **Beta emission : continuous spectrum**
  - ✓ Spectrum shape factor
  - ✓ Average energy
  - ✓ Maximum energy
  - ✓ *Log ft (comparative half-life)*

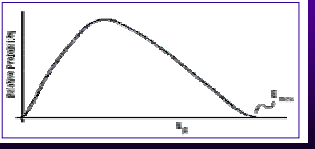

LNE

Source
- Which energy ?
- Which intensity ?

electrons, alpha, …

Loss of energy
Loss of particles

Absorbing material (window, electrode, …)

Loss of energy
Loss of particles

Sensitive part of detector

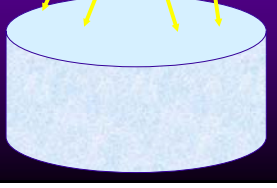

Energy detection threshold

Detection efficiency

Energy resolution

alphas, electrons, …

Sensitive part of detector

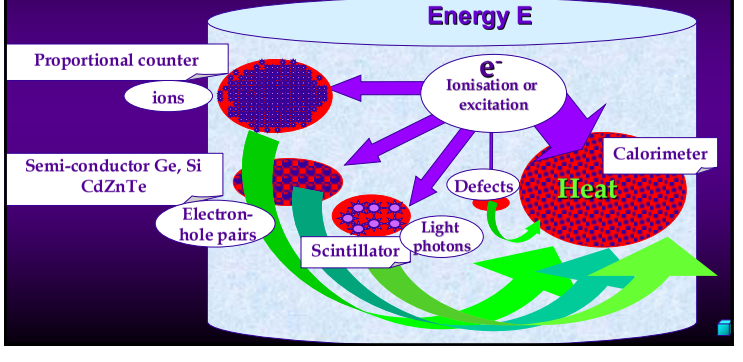

Alpha spectrometry techniques

1

Detector	Advantages	Disadvantages
Silicon semiconductor ❖silicon surface barrier ❖Particle implanted and passivated (PIPS)	low cost easy to use high detection efficiency	Energy loss limited energy resolution 8 ~10 keV overlapping peaks sophisticated fitting procedures
Magnetic spectrometer	energy resolution < 0.1 %	poor detection efficiency (< 1 %) (poor statistics) small energy range heavy equipment
Alpha bolometer	no energy loss energy resolution = 0.1 % large energy range	poor counting rate (poor statistics) recent equipment (has to be validated)

Silicon surface barrier detector

2

- Gold is evaporated on the surface of a N-type crystal (or Al on P-type crystal)
  - ❖Creation of high concentration of traps for e^- (depleted layer)
- Advantage :
  - ❖Relatively thin dead layer
- Disadvantages :
  - ❖Very sensitive to light (ion pair production)
  - ❖Fragile (chemistry, manipulation)

22

Particle implanted and passivated silicon detector (PIPS)

3

Most recent technique

- Silicon chip, photolithographic process, ion implantation (^{11}B)
- Compared to silicon surface barrier detector :
  - ❖very thin dead layer < 50 nm
  - ❖better energy resolution
  - ❖better stability

Energy losses in the case of silicon detectors

4

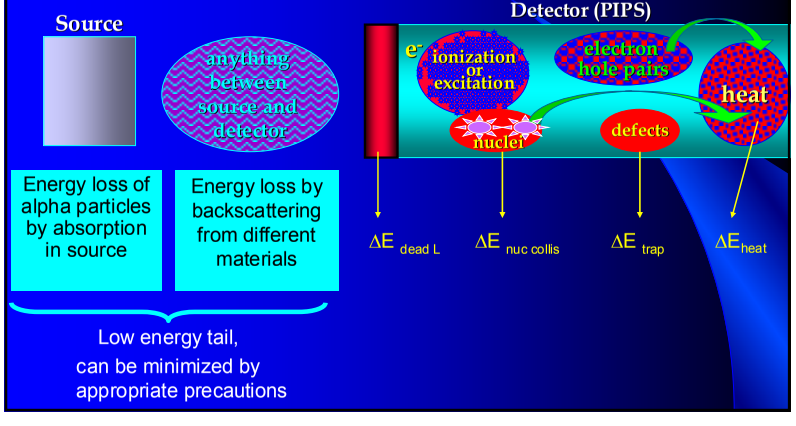

Alpha particle emission probabilities : uncertainty components with a silicon detector

5

Emission probability ➡ peak area

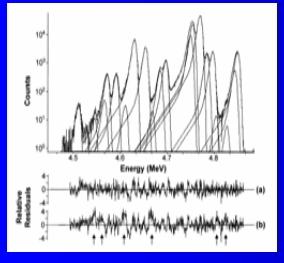

Spectrum with the 20 fitted alpha-particle peaks of ^{237}Np

- **Fitting procedure**
- **Counting statistics**
- **Coincidence summing corrections**
  - conversion electrons
- **Interference peaks**
  - Isotopes
  - Background
  - Source impurities

Alpha particle emission probabilities : uncertainty components Case of ^{238}U, ref. Garcia-Torano, 2000

6

^{238}U Energy (keV)	Alpha emission probability	total uncertainty	fitting and counting	coincidence summing	interference peaks
4038	0.0013	0.0003 *23%*	0.00028 *22%*	0.0004 *31%*	
4151	0.2233	0.005 *2%*	0.0049 *2%*	0.0005 *0.2%*	
4198	0.7754	0.005 *1%*	0.0049 *1%*	0.0005 *0.1%*	0.001 *0.1%*

23

How to reduce uncertainties on emission probabilities ?

7

- Counting statistics :
  - ❖Increase source activity ? You want high quality source
  - ❖Increase solid angle ? You want to reduce coincidence
  - ❖Increase counting time ? You want electronics stability ➡ stabilize temperature
- Coincidence summing corrections (conversion electrons)
  - ❖small solid angle and magnetic deflection
- Interference peaks
  - Isotopes
  - Background
  - Source impurities

  ➡ improve energy resolution
- Fitting procedure requires better energy resolution
  - reduce source activity, change detector

Magnetic spectrometer

8

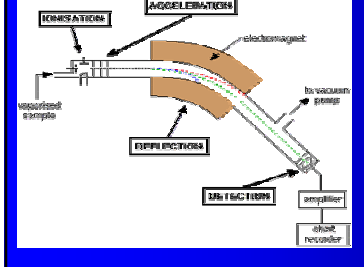

- ***Ionisation***
  - ❖ The atom is ionised by knocking one or more electrons off to give a positive ion.
- ***Acceleration***
  - ❖ The ions are accelerated so that they all have the same kinetic energy.
- ***Deflection***
  - ❖ The ions are then deflected by a magnetic field according to their masses.
  - ❖ The more the ion is charged, the more it gets deflected.
- ***Detection***
  - ❖ For one given magnetic field, only a corresponding ***mass/charge ratio is detected.***

Magnetic spectrometer

- Precise determination of alpha-particle energy
  - ❖Uncertainties ?
- Alpha-particle emission probabilities
  - ❖Uncertainty components :
    - Statistics
    - Backgroung due to contamination
    - Magnetic field stability

Physics principle of bolometer

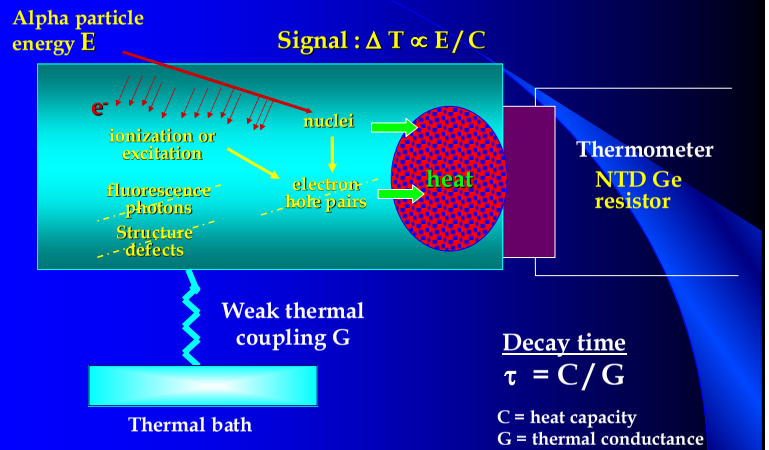

24

Detector design

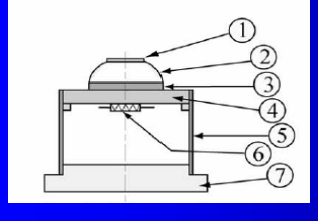

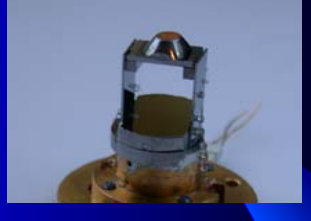

- 1 metallic absorber : copper
- 2,3 thermalisation volume
- 4 NTD Ge resistance thermometer (phonons)
- 5 thermal coupling : Ge
- 6 heating resistor for calibration
- 7 mechanical support

Experimental set-up

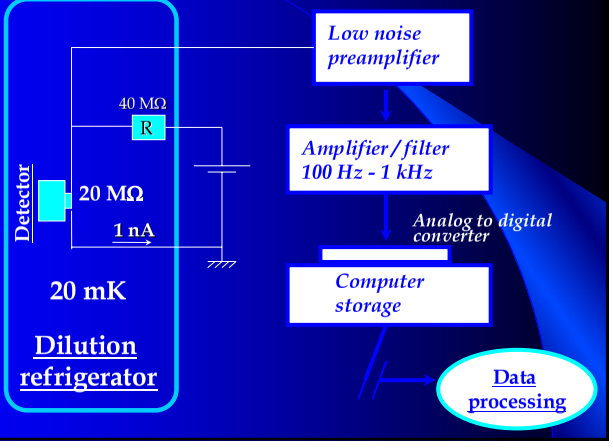

External sputtered ^{241}Am source measured with bolometer B306

13

(time of measurement : 12 hours)

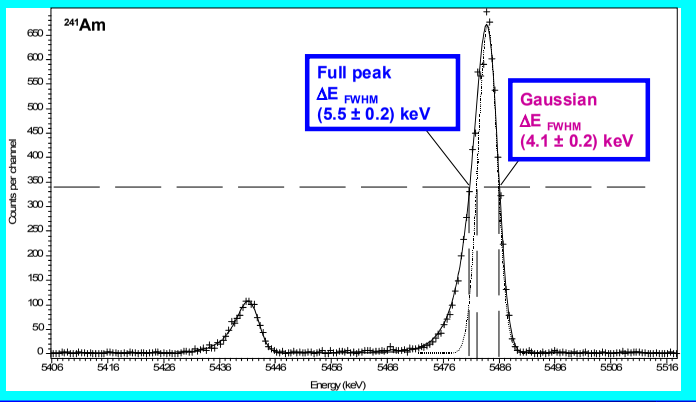

External electrodeposited ^{238}Pu source measured with conventional silicon detector and with bolometer B306

14

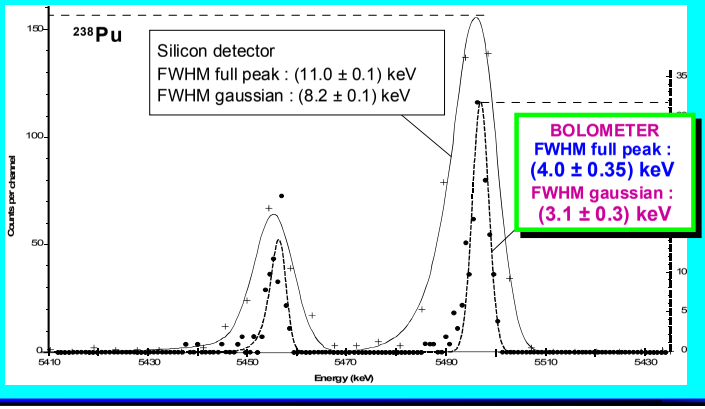

Alpha particle emission probabilities : uncertainty components with a bolometer

15

- Main contribution : counting statistics
  - Increase counting time ?
    - ➡ stabilize detector temperature
- Coincidence summing corrections (conversion electrons)
  - Can be made negligible with small solid angle and magnetic deflection
- Minor contributions :
  - Interference peaks: isotopes, background sources impurities (contribution minimized by energy resolution)
  - Fitting procedure (contribution minimized by energy resolution)

beta spectrometry techniques

1

Detector	Advantages	Disadvantages
Silicon semiconductor Si-PIN Si(Li)	low cost easy to use good detection efficiency	limited energy resolution non-linearity no detection at low energies Detection efficiency is energy dependant
Magnetic spectrometer	excellent energy resolution < 0.1 %	poor detection efficiency (< 1 %) (poor statistics) small energy range heavy equipment
Beta bolometer	energy resolution = 0.1 % **no energy loss** **linearity over a large energy range**	counting rate (limited statistics) recent equipment (has to be validated)

Beta decay nuclear data and associated uncertainties

2

- End point energy
  - Large uncertainty with solid state detector
    - ^{36}Cl (Spejewski, 1967) E = (708.7 ± **0.6**) keV
  - Use mass spectrometry
    - ^{36}Cl (Audi, 2003) E = (709.68 ± **0.08**) keV
- Average energy
  - Calculated : discrepancies in literature > 10 %
  - Experimental : You need to measure beta spectrum
- Beta spectrum shape factor
  - How can one measure it ?

^{36}Cl beta decay

3

- tables of Behrens and Szybisz (1976) gather most of experimental beta shape factors published since 1950 (not exhaustive)
- Spectra can be calculated from statistical Fermi distribution corrected by experimental shape factor expressed as : $q^2 + \lambda_2.p^2$

Calculated ^{36}Cl beta spectrum with λ_2 experimentally determined :

Magnetic spectrometer	(FELDMAN, 1952)	$\lambda_2 = 1.67 \pm ?$
4 pi Scintillator	(JOHNSON, 1956)	$\lambda_2 = 1.75 \pm 0.09$
Semiconductor	(WILLETT, 1967)	$\lambda_2 = 2.11 \pm ?$
Semiconductor	(SASTRY, 1972)	$\lambda_2 = 1.58 \pm ?$
Semiconductor	(REICH, 1974)	$\lambda_2 = 1.68 \pm 0.10$

^{36}Cl measured with magnetic bolometer

4

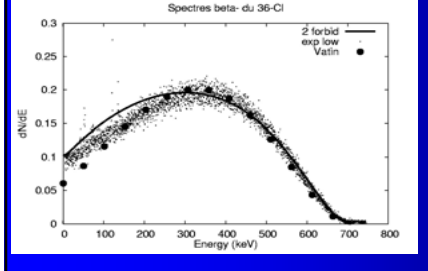

Comparison of experimental data (magnetic calorimeter, acquisition 2005), with the calculation performed by Olivier Bersillon with program SDF2NDF (second forbidden unique transition)
and spectrum calculated by R. Vatin (internal technical note, to be published).

- Detection efficiency
  > 99 %
  for 7 to 710 keV electrons
- Linearity
  better than 1 %
  over 2 decades of energy

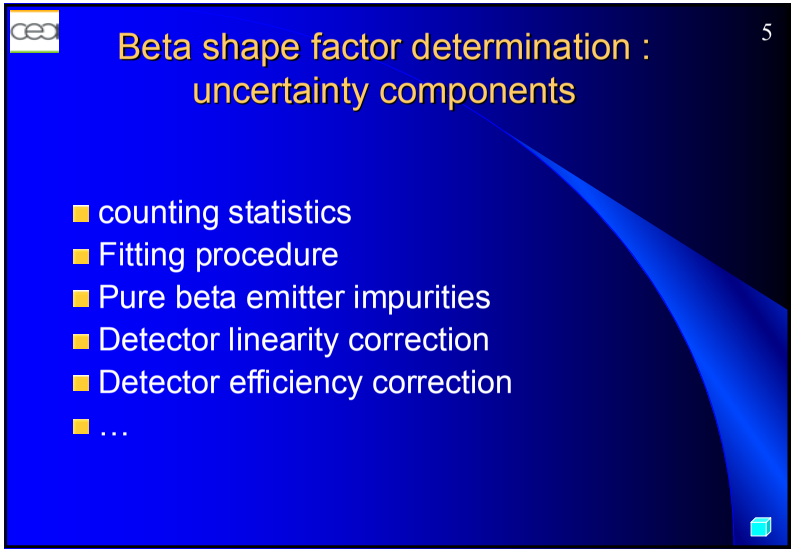
Beta shape factor determination :
uncertainty components
5
counting statistics
Fitting procedure
Pure beta emitter impurities
Detector linearity correction
Detector efficiency correction
…

Direct measurement of electron capture probability

1

Source enclosed in a gold absorber thermally coupled to a magnetic thermometer

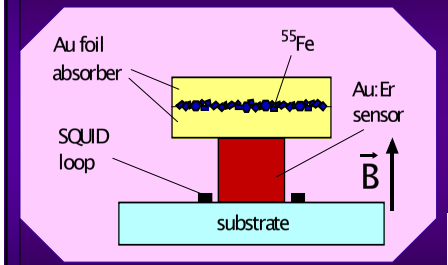

- All emitted Auger electrons and X-ray photons following a capture are detected and their energies are summed up

Detector counts one event for one capture of total energy equal to the binding energy of the electron that has been captured

Does it work ?

Absolute activity measurement with magnetic microcalorimeters (CEA/LNHB, University of Heidelberg)

2

Theoretical absorption spectrum of an enclosed ^{55}Fe source

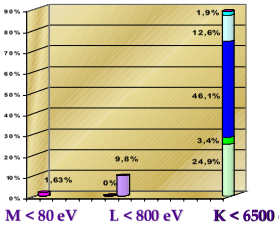

Total absorption spectrum of an enclosed ^{55}Fe source

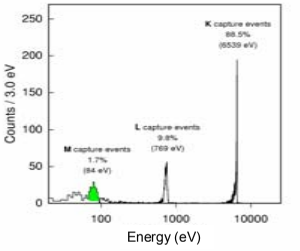

- Efficient thermalization of electron energy :
  - ✓ K, L and M captures perfectly separated
- Good energy resolution
- Energy detection threshold : **< 80 eV**
- Detection efficiency for photons of 100 eV - 6,5 keV : **99 %**

Spectrométrie X haute résolution en énergie

1

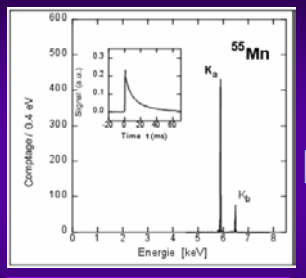

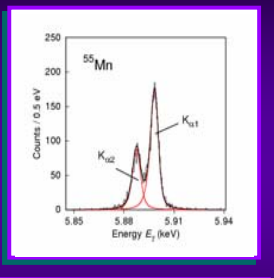

Rendement de détection pour des photons (100 eV à 6,5 keV) > 99 %

Bolomètre magnétique Electronique à 2 SQUIDs

FWHM = 3,4 eV à 6 keV

Université de Heidelberg

spectrométrie gamma

2

Enjeux : **abaisser les limites de détection des actinides**

Thèse : M. Rodrigues

Limite de détection d'un radionucléide $\propto \sqrt{RC}$

- **R = résolution en énergie du pic**
  - ✓ dépend de la physique du détecteur
- **C = amplitude moyenne du fond sous le pic considéré** *(diffusion Compton, rayonnement de freinage)*
  - ✓ dépend en partie du matériau du détecteur
    - effet photoélectrique varie avec $Z^{4,5}$

Importance du numéro atomique Z du matériau

3

Comparaison du fond (Compton) dans 2,5 cm de germanium et 300 µm d'or du à l'interaction de photons de 200 keV

Même rendement d'absorption photoélectrique à 200 keV = 40 %

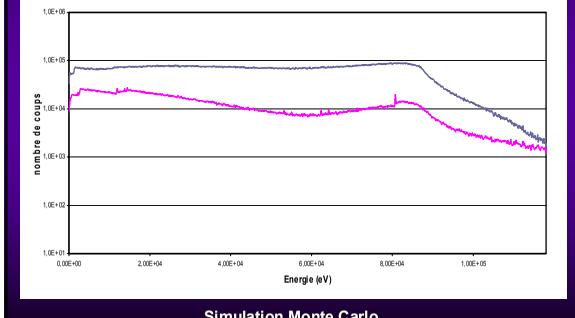

Germanium Z = 32

Au Z = 79

Simulation Monte Carlo

Importance de la résolution en énergie

4

Si un détecteur en germanium avait une résolution en énergie de 110 eV au lieu de 450 eV à 122 keV …

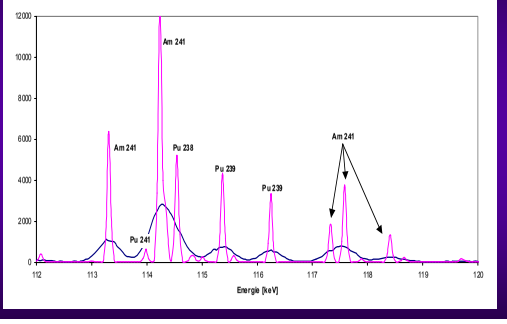

Résolution en énergie (FWHM) à 122 keV

110 eV

450 eV

Simulation Monte Carlo de l'interaction d'un mélange isotopique de plutonium dans du germanium convolué par une gaussienne représentant différentes résolutions en énergie

BrIcc - New Theoretical Conversion Coefficients
Comparison with experimental values

T. Kibédi
Dept. of Nuclear Physics, Australian National University, Canberra, Australia
T.W. Burrows
National Nuclear Data Center, Brookhaven National Laboratory, Upton, U.S.A.
M.B. Trzhaskovskaya
Petersburg Nuclear Physics Institute, Gatchina, Russia
C.W. Nestor, Jr.
Oak Ridge National Laboratory, Oak Ridge , U.S.A
P. M. Davidson
Dept. of Nuclear Physics, Australian National University, Canberra, Australia

Outline

- Internal conversion process
- Theoretical conversion coefficients
- Can we ignore the vacancy created during conversion? Other effects.
- Raman et al. *(2002)*: **"*How good are the internal conversion coefficients now?*"**
- An improved review of high precision conversion coefficient
- Conversion coefficient and Ω(E0) data tables
- BrIcc: calculating conversion coefficients

Conversion electrons (CE)

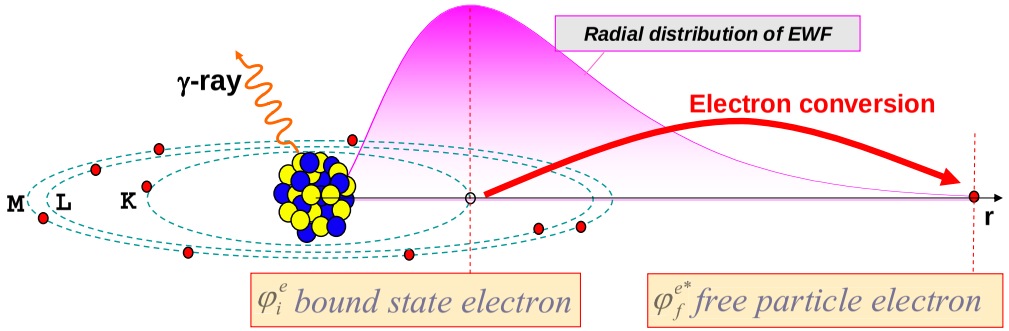

Energetics of CE-decay (i=K, L, M,....)

$E_i = E_f + E_{ce,i} + E_{BE,i} + \cancel{T_r}$

γ-, CE-decays and electron positron creation (π) are independent processes

Transition probability

$\lambda_T = \lambda_\gamma + \lambda_{CE} = \lambda_\gamma + \lambda_K + \lambda_L + \lambda_M \ldots\ldots + \lambda_\pi$

Conversion coefficient

$\alpha_i = \lambda_{CE,i} / \lambda_\gamma$

The physics of conversion coefficients

$$\alpha_K \equiv \frac{\lambda_{e,K}}{\lambda_\gamma}$$

$$\lambda_e = \frac{2\pi}{\hbar}\left|m_{fi}\right|^2 \frac{d\rho}{dE}$$ *Fermi's golden rule*

Density of final electron state (continuum)

$$m_{fi} = \psi_f^{N*}\ \varphi_f^{e*}\ F_{\ell,m}\ \psi_i^N\ \varphi_i^e$$

Nuclear *Electron* *Multipolar source*

Same for γ and CE

φ_i^e *bound state electron*

φ_f^{e*} *free particle electron*

ICC calculations considered

- **HSICC: Hager-Seltzer**, Nucl. Data. Sect. **A4**, 1 (1968)

  Used for ENSDF, RadWare, etc.

- **RSICC: Rösel-Fries-Alder-Pauli**, ADNDT **21**, 91 (1978)

  Used for DDEP

- **BRICC: Band-Trzhaskovskaya-Nestor-Tikkanen-Raman**, ADNDT **81**, 1 (2002)

  BTNTR – No Hole approximation

  RNIT(2) – "Frozen orbital", effect of the hole taken into account

  Adopted for ENSDF (2005)

  Recommended for DDEP (2006)

Underlying assumptions in ICC calculations

Common in all models

Physical model

- **Calculations up to the first nonvanishing order of the perturbation theory**

Atomic field model

- **One-electron approximation**
- **Free neutral atom**
- **Screening of the nuclear field by the atomic electrons**
- **Spherically symmetric atomic potential**
- **Relativistic electron wave functions**
- **Experimental electron binding energies**

Nuclear model

- **Finite nuclear size**
- **Spherically symmetric nucleus**

Underlying assumptions in ICC calculations

HSICC	RSICC	BRICC
	Atomic field model	
Self-consistent field calculated Hatree-Fock-Slater	Self-consistent potential Hatree-Fock-Slater	Self-consistent field calculated Dirac-Fock
	Exchange interaction between electrons	
APPROXIMATED (C=2/3)	APPROXIMATED (C=1)	EXACT TREATMENT
	Consideration of the hole	
YES	NO	BTNTR: NO RNIT(2): YES
	Nuclear model	
Fermi nuclear charge distribution	Homogeneously charged sphere	Homogeneously charged sphere
	Finite nuclear size - penetration	
NOT	NOT	YES, Surface Current model Manual correction for hindered M1 transitions
	Higher-order effect	
Vacuum polarization, electron corr.	NO	NO
	Range	
Z=30-103; Shells:K,L,M; $E_\gamma \leq 1650$ keV	Z=30-104; Shells:All; $E_\gamma \leq 5000$ keV	Z=10-95; Shells:All; $E_\gamma \leq 6000$ keV

Higher order and atomic effects

- **Atomic many body correlations: factor ~2 for E_{kin}(ce) < 1 keV**
- **Partially filled valence shell: non-spherical atomic field**
- **Shake effect: increases ICC**
- **Resonance/sub threshold internal conversion in hydrogen-like ion**
  E_{tran} ≈ BE, M1 multipolarity
  ^{125}Te 35.492 keV
  ^{171}Yb 70.6 keV, $T_{1/2}$(ion) reduced by ~10^{+5}
- **Hindered nuclear decay in fully ionized atoms**
  Isomers in $^{144m}Tb^{65+}$, $^{149m}Dy^{66+}$, $^{151m}Er^{68+}$: up to factor 30
- **Binding energy uncertainty: <0.5% for E_{kin}(ce) > 10 keV**
- **Chemical effects: <<1%**
- **Penetration effect decreases ICC**
  ***n s1/2* shells (K, L1, M1,..); M1, M2, M3,... multipolarities**
  For M1 transition:
  0.01% (Z=10)
  ~15% (Z=112)

Can we ignore the atomic vacancies?

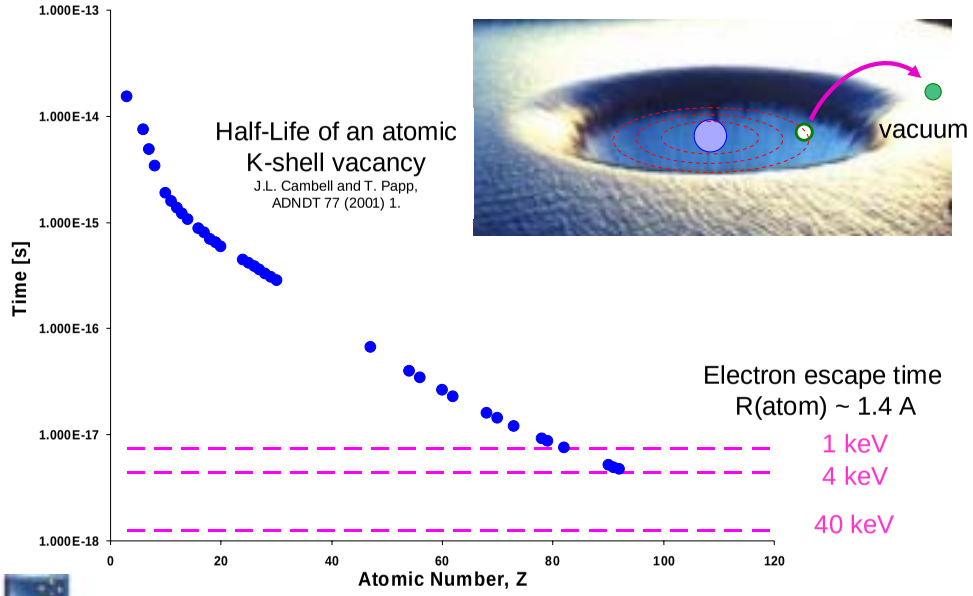

Inclusion of the Hole in BRICC

Band-Trzhaskovskaya-Nestor-Tikkanen-Raman (2002)

- **BTNTR**
  - Bound and Continuum wave functions are calculated in the SCF of a neutral atom
- **RNIT(1)**
  - Bound wave function is calculated in the SCF of a neutral atom
  - Continuum wave function is calculated in the SCF of an ion.
- **RNIT(2) – "Frozen Orbital" approximation:**
  - Bound wave function is calculated in the SCF of a neutral atom
  - Continuum wave function is calculated in an ion field, which is not SCF. Constructed using bound wave functions of the neutral atom.
  - *"There is insufficient time for the rearrangement of the atomic orbitals"*

Initial and Final wave functions are NOT ORTHOGONAL!

Hole / No Hole – how sizable is it?

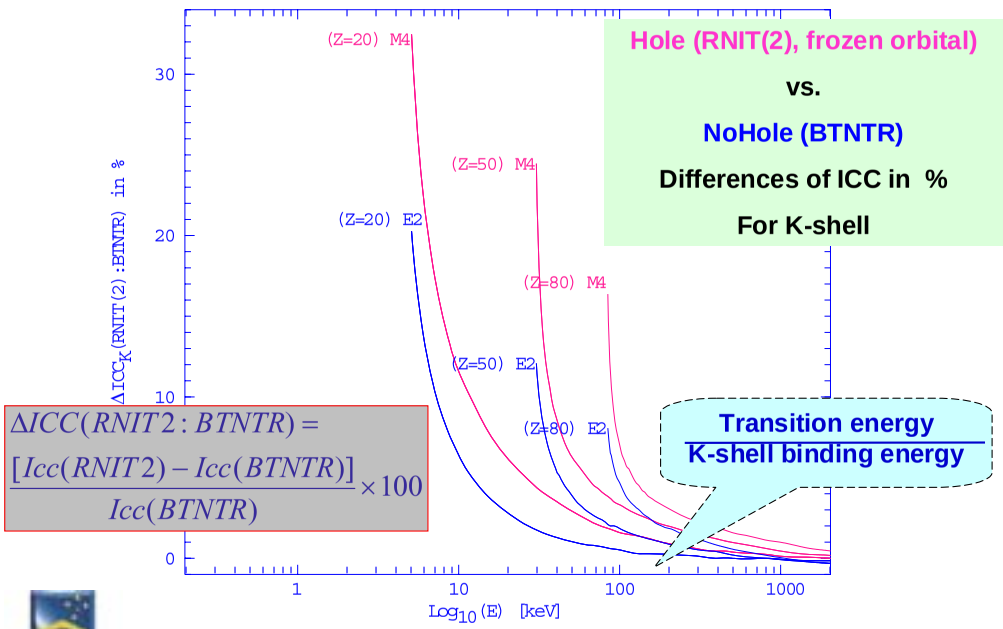

Hole (RNIT(2), frozen orbital)

vs.

NoHole (BTNTR)

Differences of ICC in %

For K-shell

$$\Delta ICC(RNIT2:BTNTR) = \frac{[Icc(RNIT2) - Icc(BTNTR)]}{Icc(BTNTR)} \times 100$$

Transition energy / K-shell binding energy

Hole (RNIT(2), frozen orbit) vs. NoHole (BTNTR)

Differences of ICC in %

For TOTAL ICC

Frequency distribution of known multipolarities

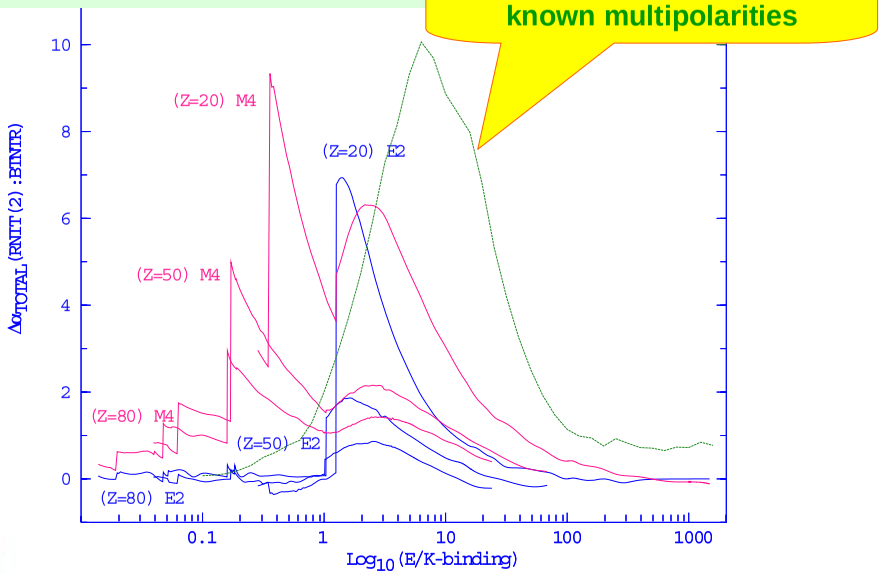

Raman et al. *(2002)*

"How good are the internal conversion coefficients now?"

- **100 experimental ICC**
- **Deviation of ICC**

$$\Delta ICC(Exp:Theory) = \frac{[Icc(Exp) - Icc(Theory)]}{Icc(Theory)} \times 100$$

HSICC	**-3.01(24)%**
RSICC	-2.71(24)%
BTNTR NO Hole	+0.19(26)%
RNIT(1) With Hole	-0.94(24)%
RNIT(2) With Hole	-1.18(24)%

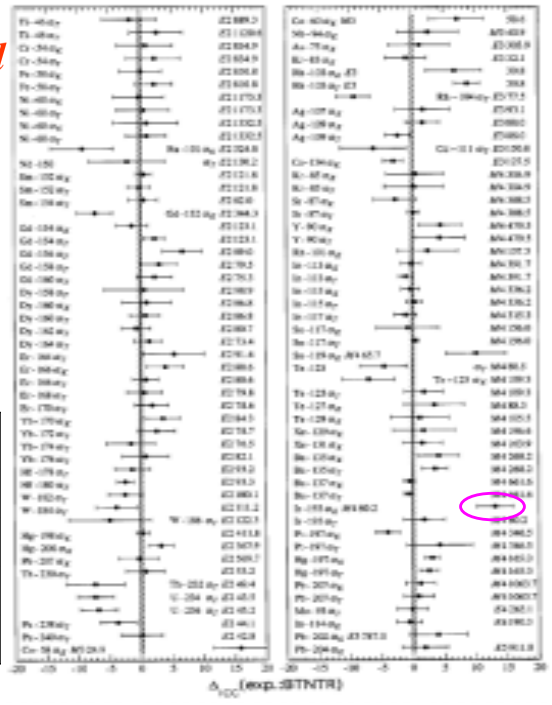

Hole / No Hole - the saga continues

Nica-Hardy-Iacob-Raman-Nestor-Trzhaskovskaya, PRC 70 (2004) 054305.

- **^{193}Ir, 10.5 days isomer, 80.236(7) keV M4, (no other transition)**
- **From singles X and gamma measurement**

$$\alpha_K \times \varpi_K = \frac{N_K}{N_\gamma} \times \frac{\varepsilon_\gamma}{\varepsilon_K}$$

α_{Total}(Exp) = 21300(400)

	α_K	Difference
Exp.	103.0(8)	
BTNTR NO Hole	92.0(3)	+10.7(8)%
RNIT(1) With Hole	99.6(3)	+3.3(8)%
RNIT(2) With Hole	103.3(3)	-0.3(8)

BrIcc - Increased Numerical Accuracy

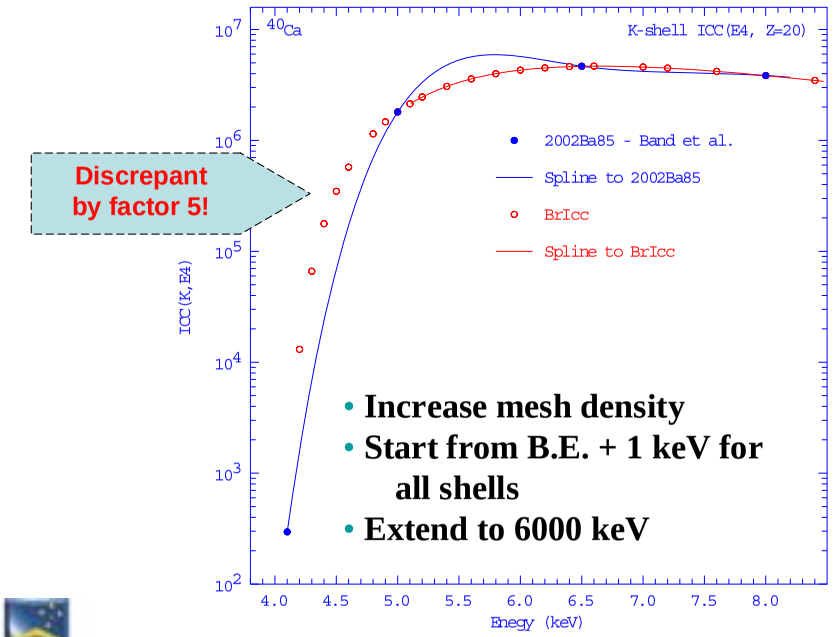

Discrepant by factor 5!

- **Increase mesh density**
- **Start from B.E. + 1 keV for all shells**
- **Extend to 6000 keV**

BrIcc - Cubic spline interpolation

Th – calculated directly with RAINE

Int – Interpolated over 186 Points

Diff - difference

$$\Delta ICC(Int:Th) = \frac{[Icc(Int) - Icc(Th)]}{Icc(Th)} \times 100$$

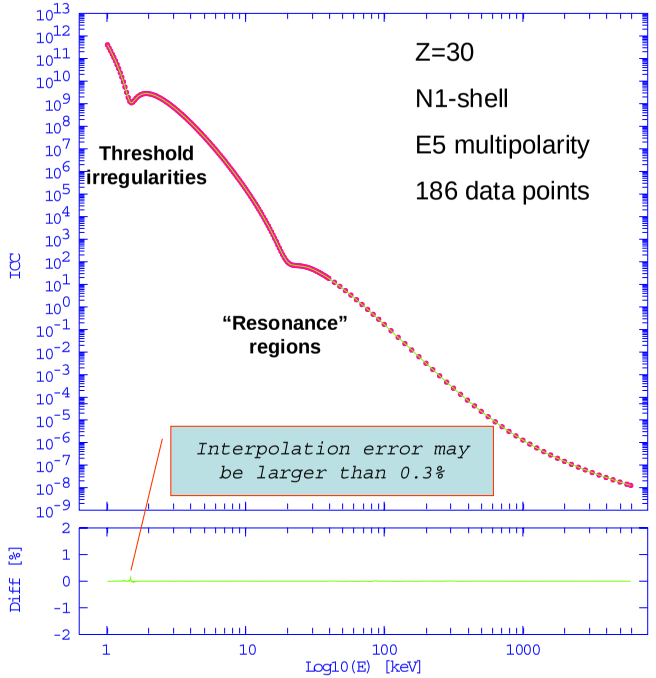

Irregular behavior

Resonance regions
ICC → 0 (in non-relativistic approximation)

Threshold non-irregularities
Rapid rise of ICC, cause not clear

BrIcc – extra care to increase density of tabulations

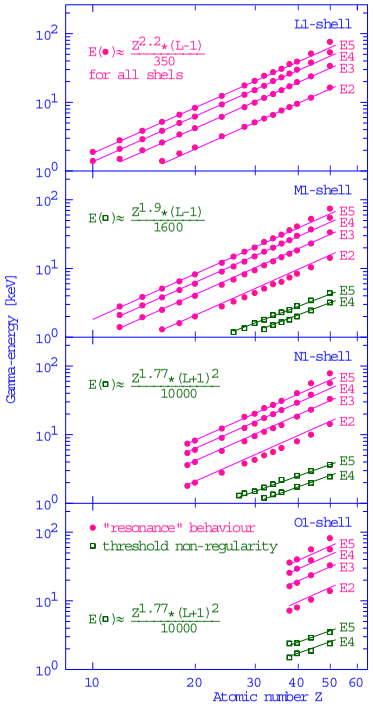

Review of High Precision Experimental ICC`s

General policies

- **Δα/α ≤ 5%, Searched entire ENSDF file**
- **Only E2, M3, E3, E4, M4, E5.**
- **Excluded E1(hindered) and M1 (mixed with E2)**

Results

- **Adopted 140+ ICC values of Total, K-, L-shells and K/L ratio**
- **More than 80% of the ICC values (~1 %) and/or uncertainties have been changed.**

	ENSDF	Raman	Present work
645.9859(20) keV E2(+M3) in 124Te, α_K (NPG changed α_K(557))	0.00340(14)	---	0.00345(14)
24.889(21) keV M3 in 58Co, α_K (XPG changed ω_K)	1860(100)	2030(90)	1860(70)
1063.656(3) keV M4+E5 in 207Pb α_K, (Re-evaluated by Murray Martin 2005; 6 measurements)	0.0972(23)	0.0945(22)	0.0949(19)

How good are the internal conversion coefficients now? (March 2006)

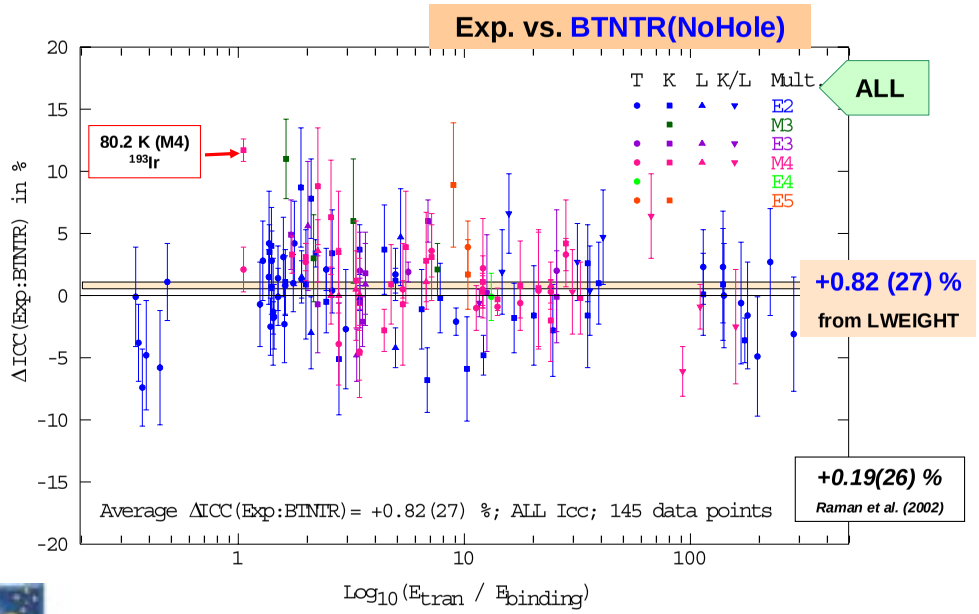

How good are the internal conversion coefficients now? (March 2006)

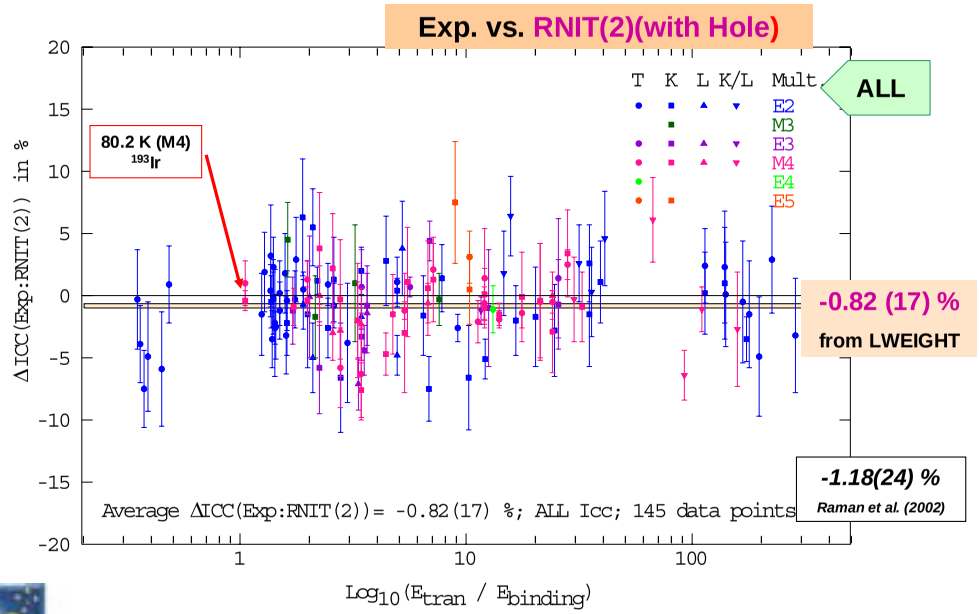

How good are the internal conversion coefficients now? (March 2006)

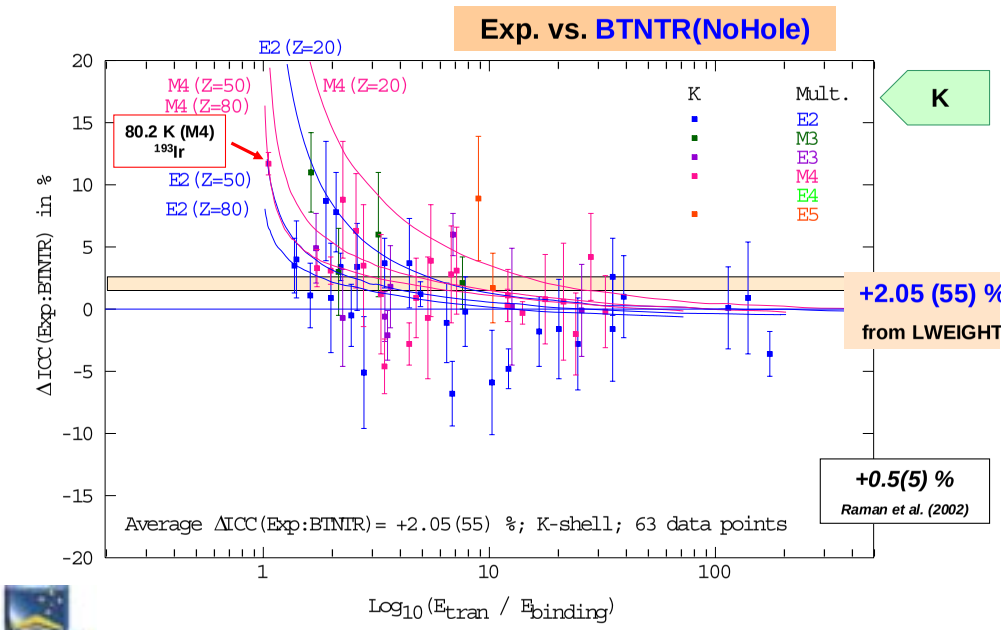

How good are the internal conversion coefficients now? (March 2006)

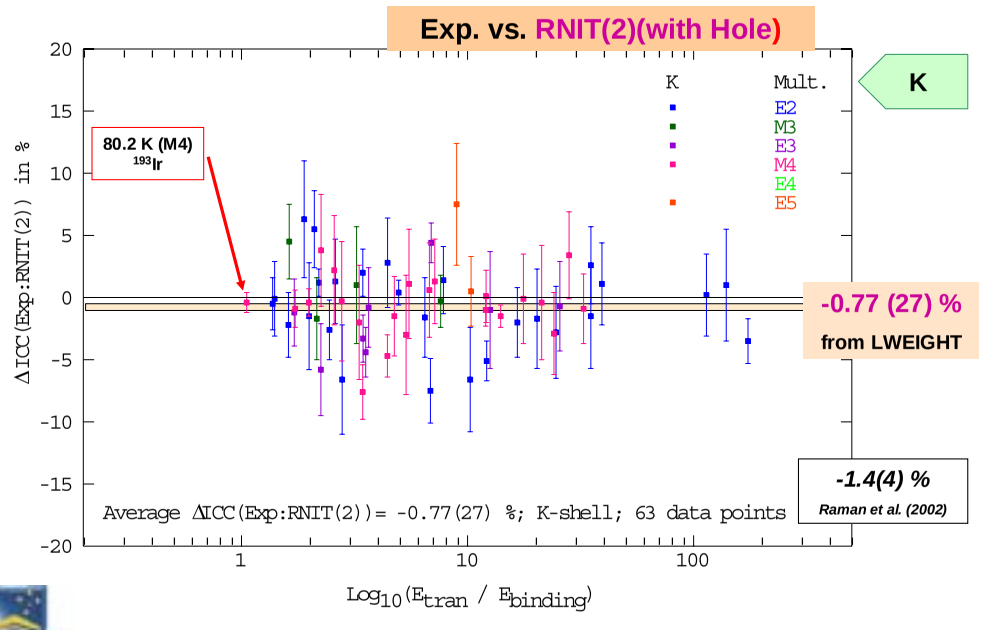

Review of High Precision Experimental ICC`s

What next

- New compilation of ratios of sub-shell ICCs identified ~100 new values – need to be evaluated! (*Raman et. al., Atomic Data and Nuclear Data Tables 92 (2006) 207)*
- Extend statistical analysis to treat discrepant data
  - Normalized residual method
  - Rajeval technique
- BrIcc: extend for Z (1-9 and 96-126)

Data points should be re-measured

				Exp	BTNTR	Difference (Exp:BTNTR)	RNIT(2)	Difference (Exp:RNIT(2))
^{73}Ge	13.2845(15)	E2	K	296(26) UNC > 5%	264.8	+11.8(98)%	298.7	-0.9(87)%
^{104}Rh	115.960(1)	E2	K	0.6893(10) UNC too small	0.6273	+9.9(2)%	0.6356	+8.4(2)%
^{188}W	155.032(12)	E2	K	0.345(1) UNC too small	0.317	+8.8(4)%	0.324	+6.4(4)%

Data Table	Reference	Z	Shells or IPF	L	Transition energy [keV][a]
Internal Conversion Coefficient (ICC) using the 'Frozen Orbitals' approximation					
BrIccFO	Based on the model of 2002Ba85 and 2002Ra45	10–95	All shells	1–5	ε_{ic}+1–6000
Pair Conversion Coefficient (PCC)					
ScPcc	1979Sc31	0–100[b]	IPF	1–3	1100–8000
HoPcc	1996Ho21	50–100	IPF	1–3	1100–8000
Electronic factor Ω(E0)[c]					
HsOmg	1969Ha61	30–42	K[d],L_1[e],L_2[f]	0	ε_{ic}+6–1500
BeOmg	1970Be87	40–102	K	0	51[f]–2555
		40–102	L_1,L_2	0	51–2555
PaOmg	1986PaZM	8–40	K[e]	0	511–12775
		8–40	IPF	0	1431–12775

[a] ε_{ic} is the binding energy for the ic-shell
[b] Used for Z < 50
[c] Electronic factors are only calculated for even Z values at present
[d] Not used
[e] Used for Z < 40
[f] For Z=40–58: 51.1 keV; for Z=60–82: 102.2 keV; for Z=84–96: 153.3 keV and for Z=98–102: 204.4 keV

CalcBrIcc (FORTRAN90)

Input: Z & E_γ

Output:

- **ICC for K, L1, L2, L3, M1,…R2 and for E1-E5, M1-M5**
- **ICC for L, K/L, M, L/M, N, L/N,…R, L/R**
- **ICC for IPF**
- **Total ICC; sum of electron conversion and pair production**
- **Ω(E0) electronic factor for K, L1, L2, IPF, Total, K/Total**

Warning messages for cases of

BE/Threshold(IPF) ≤ $E_\gamma \pm \Delta E_\gamma$ ≤ first tabulation energy

or

last tabulation energy ≤ $E\gamma \pm \Delta E\gamma$

Mixed multipolarities & uncertainties

$$\delta^2 = \frac{I_\gamma(E2)}{I_\gamma(M1)} \qquad \alpha(M1/E2) = \frac{\alpha_{M1} + \delta^2 \alpha_{E2}}{1+\delta^2}$$

Uncertainty is a sum off :

- **Theory + interpolation, set to 1.36% of the ICC value**
- **Uncertainty on E:**

$$\Delta\alpha_{DE\_H} = \alpha(E_\gamma + \Delta E_H) - \alpha(E_\gamma),$$
$$\Delta\alpha_{DE\_L} = \alpha(E_\gamma - \Delta E_L) - \alpha(E_\gamma).$$

- **Uncertainty on MR:**

$$\Delta\alpha_{DMR\_H} = \frac{[\alpha(\pi L) + \delta_H^2 \alpha(\pi' L')]}{1+\delta_H^2} - \frac{[\alpha(\pi L) + \delta^2 \alpha(\pi' L')]}{1+\delta^2},$$
$$\Delta\alpha_{DMR\_L} = \frac{[\alpha(\pi L) + \delta_L^2 \alpha(\pi' L')]}{1+\delta_L^2} - \frac{[\alpha(\pi L) + \delta^2 \alpha(\pi' L')]}{1+\delta^2},$$

Total:

$$\Delta\alpha = \sqrt{(\Delta\alpha_{theo})^2 + (\Delta\alpha_{DE})^2 + (\Delta\alpha_{DMR})^2}$$

Treats limits on E_γ and δ according to ENSDF (see manual)

Stand alone program for Windows/Linux/Unix form NNDC:

http://www.nndc.bnl.gov/nndcscr/ensdf_pgm/analysis/BrIcc/

Manual:

http://www.nndc.bnl.gov/nndcscr/ensdf_pgm/analysis/BrIcc/BrIccManual.pdf

Web Interface:

http://www.rsphysse.anu.edu.au/nuclear/bricc/

Workshop on
DECAY DATA EVALUATION

- **Saclay, March 6 – 10, 2006**
- **Edgardo Browne**

1

γ-ray Properties

2

- Photon energy and intensity
- Transition energy and intensity
- Relative and absolute intensities
- Equilibrium intensity

3

- Photon energy and intensity

Guidelines

- When possible use evaluated values:

Recommended standards for γ-ray energy calibration (1999), R.G. Helmer, C. van der Leun, Nucl. Instrum. and Methods in Phys. Res. **A450**, 35 (2000)

X-ray and gamma-ray standards for detector calibration, IAEA-TECDOC-**619**, September 1991.

4

Guidelines

- Weighted averages of values from the same type of measurements (e.g. with Ge detectors).
- The uncertainty on the average (recommended) value should not be smaller than the smallest input uncertainty.
- For discrepant data use the "Limitation of Relative Statistical Weight" method (Program *LWEIGHT*).

5

- Transition Energy

$$E_T = E_\gamma + E_R,$$

where

$E_R = E_\gamma^2/2\, M_R c^2$ is the nuclear recoil energy

E_γ is the photon energy (in MeV)

$M_R \sim A$ is the mass of the daughter nucleus

$M_R\, c^2 \sim 931.5 \times A$

6

- Transition Intensity

$$I_T = I_\gamma\, (1 + \alpha),$$

where

I_γ is the photon intensity,

α is the total conversion coefficient (theoretical interpolated value)

7

- Relative and Absolute Intensities

- Relative intensities (relative to the intensity of the strongest γ ray, usually taken as 100). Also called *relative emission probabilities*.

- Absolute intensities (per 100 disintegrations of the emitting radionuclide, usually given in %). Also called *absolute emission probabilities*, usually given "per decay.")

8

^{66}Ga γ-ray energies

1993Al15, 1994En02 E_γ (keV) Unevaluated	2000He14 E_γ (keV) Evaluated	Fitted E_γ (keV)
2173.334 (18)	**2173.319 (15)**	**2173.319 (15)**
2189.631 (9)	**2189.616 (6)**	**2189.616 (6)**
2213.19 (11)	**2213.181 (9)**	**2213.181 (9)**
2265.86 (24)		2265.84 (24)
2292.188 (13)		2292.171 (13)
2341.691 (11)		2341.673 (11)
2393.153 (10)	**2393.129 (7)**	**2393.129 (7)**
2422.544 (9)	**2422.525 (7)**	**2422.525 (7)**
2433.826 (18)		2433.807 (18)
2467.99 (7)		2467.97 (7)
2492.44 (3)		2492.42 (3)
2537.11 (5)		2537.09 (5)
2588.573 (13)		2588.553 (13)
2631.46 (9)		2631.44 (9)
2698.94 (5)		2698.92 (5)
2713.75 (5)		2713.73 (5)
2751.852 (6)	**2751.835 (5)**	**2751.835 (5)**
2780.12 (18)	**2780.095 (16)**	**2780.095 (16)**
2785.7 (3)		2785.7 (3)
2802.8 (5)		2802.8 (5)
2843.153 (16)		2843.130 (16)

Combining evaluated and unevaluated energies

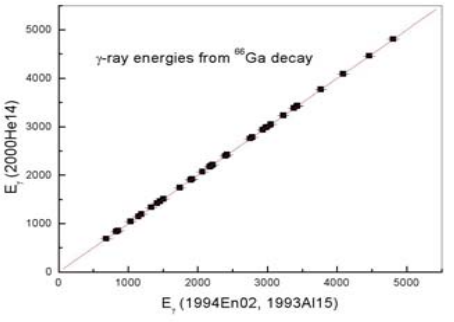

^{66}Ga relative γ-ray intensities

Table 1
Comparison of measured relative γ-ray emission probabilities for ^{66}Ga

E_γ (keV) Helmer [16]	I_γ (rel.) Camp et al. [2]	I_γ (rel.) Raman et al. [8]	I_γ (rel.) Berkeley	I_γ (rel.) Budapest	I_γ (rel.) Recommended
833.5324 (21)	15.92 (17)	16.02 (24)	15.94 (14)	15.92 (6)	15.93 (5)
1039.220 (3)	100.0	100.0 (16)	100.0 (9)	100.0 (3)	100.0 (3)
1333.112 (5)	3.25 (4)	3.17 (5)	3.20 (3)[a]	3.171 (13)	3.175 (12)
1418.754 (5)	1.70 (3)		1.640 (23)	1.659 (8)	1.657 (8)
1508.158 (7)	1.520 (24)		1.503 (23)	1.496 (7)	1.497 (7)
1898.823 (8)	1.09 (4)		1.062 (23)	1.050 (8)	1.051 (8)
1918.329 (5)	5.63 (8)	5.33 (8)	5.44 (6)	5.360 (23)[b]	5.368 (21)
2189.616 (6)	15.06 (18)	14.54 (21)	14.50 (13)	14.39 (6)	14.42 (5)
2422.525 (7)	5.16 (5)	5.12 (8)	5.15 (6)	5.072 (24)	5.085 (22)
2751.835 (5)	61.2 (6)	61.2 (8)	61.5 (6)	61.34 (26)	61.35 (23)
3228.800 (6)	3.96 (4)	4.06 (8)	4.07 (4)	4.087 (22)	4.082 (19)
3380.850 (6)	3.78 (4)	3.96 (8)	3.99 (4)	3.950 (23)	3.960 (19)
3422.040 (8)	2.18 (4)		2.29 (3)	2.321 (16)	2.314 (14)
3791.036 (8)[c]	2.68 (3)	2.96 (5)	2.96 (4)	2.929 (24)	2.941 (19)
4085.853 (9)	3.07 (4)	3.38 (8)	3.42 (4)	3.455 (20)	3.445 (18)
4295.224 (10)[c]	9.17 (11)	10.24 (26)[d]	10.54 (15)[e]	10.25 (7)[f]	10.30 (8)[g]
4461.202 (9)	1.875 (22)		2.20 (4)	2.275 (23)	2.26 (3)
4806.007 (9)	3.82 (4)	4.93 (11)	5.00 (7)	5.04 (3)	5.03 (3)

^{66}Ga Measured Relative γ-Ray Emission Probabilities

```
Limitation of relative statistical weight (LWM)
 Program LWEIGHT, version 1.3, March 2000
 Current date: 06/17/2003

 833 keV

 INP. VALUE  INP. UNC.     R. WGHT  chi**2/N-1 REFERENCE
 .160200E+02 .240E+00       .502E-01  .735E-01  00Ra00
 .159400E+02 .140E+00       .147E+00  .370E-02  02Ba00
 .159200E+02 .600E-01 MIN *.802E+00* .881E-02  02Mo00

 No. of Input Values N= 3  CHI**2/N-1=   .09  CHI**2/N-1(critical)=  4.60

 UWM    :.159600E+02  .305505E-01
 WM     :.159280E+02  .537480E-01(INT.)  .157651E-01(EXT.)
```

Limitation of relative statistical weight (LWM)

```
Program LWEIGHT, version 1.3, March 2000
 Current date: 06/16/2003

 3256 keV

 INP. VALUE  INP. UNC.      R. WGHT  chi**2/N-1 REFERENCE
 .320000E+00 .300E-01       .270E-01  .530E+01  70Ph01
 .249000E+00 .500E-02 MIN *.973E+00* .147E+00  71Ca14

 No. of Input Values N= 2  CHI**2/N-1=  5.45  CHI**2/N-1(critical)=  6.60

 UWM    :.284500E+00  .355000E-01
 WM     :.250919E+00  .493197E-02(INT.)  .115135E-01(EXT.)
```


Something to think about …

2. Photon Intensities

Problem #1: How to obtain the best γ-ray relative intensities from several independent measurements.

A Simple Example

Author A measures: $I_1 = 10$ $I_2 = 50$ $I_3 = 125$
Author B measures: $Y_1 = 28$ $Y_2 = 100$ $Y_3 = 300$

1. Normalize to $I_1 = 10$

$Y_1 = 10$ $Y_2 = 35.7$ $Y_3 = 107.1$

Now we average:

$\bar{I}_1 = 10$ $\bar{I}_2 = 42.9$ $\bar{I}_3 = 116.0$ ---(1)

2. Normalize to $I_2 = 50$

$Y_1 = 14$ $Y_2 = 50$ $Y_3 = 150$

Now we average:

$\bar{I}_1 = 12$ $\bar{I}_2 = 50$ $\bar{I}_3 = 137.5$

We normalize to $\bar{I}_1 = 10$ and compare with (1)

$\bar{I}_1 = 10$ $\bar{I}_2 = 41.7$ $\bar{I}_3 = 114.6$ ---(2)

SOMETHING IS WRONG !!

A Solution

Both photon intensities are on a different internal scale

Let's assume that these scales are linearly related through a factor α, such that:

$$\sum_{K=1}^{L}\sum_{i=1}^{N}\left(\alpha_K B_i - I_{Ki}\right)^2 / \delta_{iK}^2$$

is a minimum.

Where:

$B_i \equiv$ i-th γ-ray branching (unknown).

$\alpha_K \equiv$ is the scale factor for the K-th author (unknown)

$I_{Ki} \equiv$ experimental γ-ray intensity.

THIS IS A NON-LINEAR MINIMIZATION PROBLEM

2. γ-ray Intensities

2.1. Formulation of the Problem

The following statistical procedures provide a method for analyzing γ-ray intensities so that one consistent set of branching ratios is adopted for the deexcitation of each nuclear level. γ-ray intensities depopulating a level are typically measured on unrelated scales, which are independent of the various parent isotopes or nuclear reactions populating the level. Following the procedures of Tepel[22] and Lederer,[23] the scales are assumed to be linearly related by factors α_j, such that the expression

$$Q = \sum_i \sum_j \frac{(I_{ij}\alpha_j - \bar{I}_i)^2}{(\alpha_j \Delta I_{ij})^2} \qquad (1)$$

is minimized. Here I_{ij} is the intensity of the i-th γ-ray in the j-th measurement, ΔI_{ij} is the uncertainty in I_{ij}, $\bar{I}_i$ is the adopted branching ratio for the i-th γ ray, and the summations are over all γ rays. Equation (1) can be rewritten as

$$Q = \sum_i \sum_j \omega_{ij}(I_{ij} - \beta_j \bar{I}_i)^2 , \qquad (2)$$

where $\omega_{ij} = \Delta I_{ij}^{-2}$, $\beta_j = \alpha_j^{-1}$, and $\beta_1 = 1$. Equation (2) can be minimized, following the method of Tepel,[22] by iteratively solving the following system of equations:

$$\bar{I}_i = \frac{\sum_j \omega_{ij} I_{ij} \beta_j}{\sum_j \omega_{ij} \beta_j^2} \qquad (3)$$

$$\beta_j = \frac{1}{\alpha_j} = \frac{\sum_i \omega_{ij} I_{ij} \bar{I}_i}{\sum_i \omega_{ij} \bar{I}_i^2} \qquad (4)$$

Initially, $\beta_j = 1$ is assumed for all values of j. $\bar{I}_i$'s are then calculated from equation (3) and substituted into equation (4) to recalculate β_j. This process is iterated until β_j converges. The intensities are then converted to the original relative scale

$$\bar{I}_{ij} = \bar{I}_i \beta_j , \qquad (5)$$

where $\bar{I}_{ij}$ is the adopted intensity for the i-th γ-ray in the j-th measurement. The uncertainty in $\bar{I}_i$ is calculated from the final parameters and the covariance matrix C, as shown in the equation

$$\Delta\bar{I}_i = (\beta_j^2 C_{ii} + \bar{I}_i^2 C_{jj} + 2\beta_j \bar{I}_i C_{ij})^{1/2} . \qquad (6)$$

This procedure is equally valid for the analysis of γ-ray intensities, whether for different measurements with the same parent isotope or nuclear reaction, or for the decay of a single level, which has been populated by various parent isotopes or nuclear reactions.

Workshop on
DECAY DATA EVALUATION
Decay Scheme Normalization

Paris, France, March 3, 2006
Jagdish K. Tuli

1.Relative intensity is what is generally measured

2. Multipolarity and mixing ratio (δ).

3. Internal Conversion Coefficients

- Theoretical Values:
- From BRICC

- Experimental values:

For very precise values ($\leq$ 3% uncertainty).

E_γ = 661 keV ; ^{137}Cs (α_K=0.0902 $\pm$ 0.0008, M4)

Nuclear penetration effects.

^{233}Pa β^- decay to ^{233}U.

E_γ = 312 keV almost pure M1 from electron sub-shell ratios.

However α_K(exp) = 0.64 $\pm$ 0.02.

($\alpha_K{}^{th}$(M1)=0.78, $\alpha_K{}^{th}$(E2)=0.07)

For mixed E0 transitions (e.g., M1+E0).

^{227}Fr β^- ^{227}Ra

E_γ = 379.1 keV (M1+E0); α(exp) = 2.4 $\pm$ 0.8

α^{th}(M1) = 0.40; α^{th}(E2) = 0.08

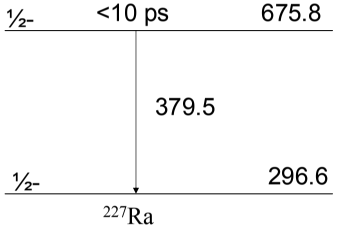

Notation

Relative γ-ray intensity: I_γ

Absolute γ-ray intensity: $\%I_\gamma$ (photons per 100 parent decays)

Relative transition intensity: TI

$TI = I(\gamma+ce) = I_\gamma(1+\alpha)$

Absolute transition intensity: %TI

$\%TI = \%I(\gamma+ce)$

Total internal conversion coefficient: α

Normalization factor: N

$\%I_\gamma = N \times I_\gamma$, $\%TI = N \times TI$

Note: In terms of quantities, NR and BR, defined in ENSDF,

$N = NR \times BR$

Where,

$I_\gamma \times NR$ is the photon intensity per 100 decays through this decay mode, and

BR is the ratio of parent decays through this mode to parent decays through all modes.

44

Decay Scheme Normalization

Rel. Int.	Norm. Factor	Abs. Int.
I_γ	NR × BR	$\%I_\gamma$
I_t	NT × Br	$\%I_t$
I_β	NB × BR	$\%I_\beta$
I_ε	NB × BR	$\%I_\varepsilon$
I_α	NB × BR	$\%I_\alpha$

BR: Factor for Converting Intensity Per 100 *Decays Through This Decay Branch*, to Intensity Per 100 *Decays of the Parent Nucleus*

NR: Factor for Converting Relative I_γ to I_γ Per 100 Decays Through This Decay Branch.

NT: Factor for Converting Relative TI to TI Per 100 Decays Through This Decay Branch.

NB: Factor for Converting Relative B^- and E Intensities to Intensities Per *100 Decays of This Decay Branch.*

1. Absolute intensity is measured

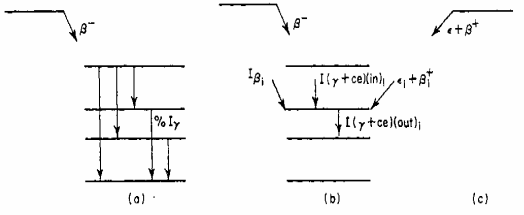

Absolute intensities

"Intensities per 100 disintegrations of the parent nucleus"

- Measured (Photons from β^-, $\varepsilon+\beta^+$, and α decay)
  Simultaneous singles measurements
  Coincidence measurements

a. When the absolute intensity of one of the gamma radiations in the daughter nucleus has been measured, the normalization factor for the relative gamma intensities is calculated as follows:

$$\text{Normalization factor } N = \frac{\%I_\gamma}{I_\gamma}$$

If instead of the photon intensity the transition intensity, which is γ+ce, is known in absolute units, then the normalization factor is calculated as follows:

$$\%I_\gamma = \frac{\%I(\gamma+ce)}{(1+\alpha)}$$

$$\text{Normalization factor } N = \frac{\%I_\gamma}{I_\gamma}$$

If absolute intensities for more than one transition are known, an average of normalization factors, calculated for each transition, should be taken.

45

Normalization Procedures

1. Absolute intensity of one gamma ray is known ($\%I_\gamma$)

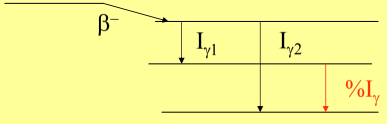

Relative intensity $I_\gamma \pm \Delta I_\gamma$

Absolute intensity $\%I_\gamma \pm \Delta\%I_\gamma$

Normalization factor $N = \%I_\gamma / I_\gamma$

Uncertainty $\Delta N = [(\Delta\%I_\gamma/\%I_\gamma)^2+(\Delta I_\gamma/ I_\gamma)^2]^{1/2} \times N$

Then $\%I_{\gamma l} = N \times I_{\gamma l}$

$\Delta\%I_{\gamma l} = [(\Delta N/N)^2 + (\Delta I_{\gamma 1}/ I_{\gamma 1})^2]^{1/2} \times I_{\gamma l}$

2. From Decay Scheme

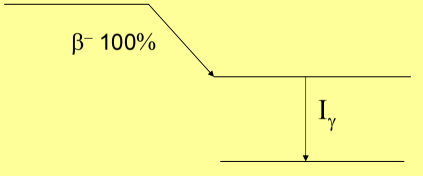

Iγ: Relative γ-ray intensity; α: total conversion coefficient

$$N \times I_\gamma \times (1 + \alpha) = 100\%$$

Normalization factor $N = 100/ I_\gamma \times (1 + \alpha)$

Absolute γ-ray intensity $\%\ I_\gamma = N \times I_\gamma = 100/ (1 + \alpha)$

Uncertainty $\Delta\%\ I_\gamma = 100 \times \Delta\alpha/(1 + \alpha)^2$

Total intensity from transition-intensity balance

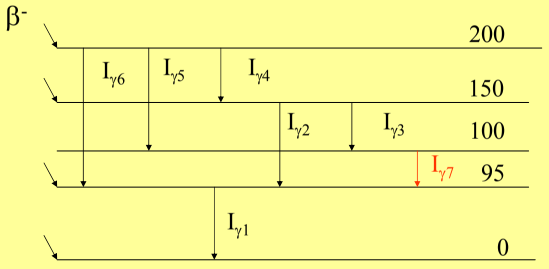

$TI(\gamma_7) = TI(\gamma_5) + TI(\gamma_3)$

If $\alpha(\gamma_7)$ is known, then

$I\gamma_7 = TI(\gamma_7) / [1 + \alpha(\gamma_7)]$

b. If the β^- intensity for a transition to a level other than the ground state has been measured in absolute units, and in addition one knows all the transition intensity feeding and leaving that level, one can calculate the normalization factor as follows:

Transition intensity (γ+ce) leaving level i (in rel units) = $\dfrac{TI(out)_i}{I(\gamma+ce)(out)_i}$

Transition intensity (γ+ce) feeding level i (in rel units) = $\dfrac{TI(in)_i}{I(\gamma+ce)(in)_i}$

β^- intensity to level i per 100 parent decays = $\%I\beta_i$

$$\text{Normalization factor } N = \frac{\%I\beta_i}{I(\gamma+ce)(out)_i - I(\gamma+ce)(in)_i}$$

c. If the β^+ intensity for a transition to a level other than the ground state has been measured in absolute units, and Q(ε) is known, then if one knows all the transition intensity feeding and leaving that level, one can calculate the normalization factor as follows:

Transition intensity (γ+ce) leaving level i (rel units) = $\dfrac{TI(out)_i}{I(\gamma+ce)(out)_i}$

Transition intensity (γ+ce) feeding level i (rel units) = $\dfrac{TI(in)_i}{I(\gamma+ce)(in)_i}$

β^+ intensity to level i per 100 parent decays = $\%I\beta^+_i$

Electron capture intensity to level i per 100 parent decays

$$\%I\varepsilon_i = (\varepsilon/\beta^+)_i(\text{theory}) \times \%I\beta^+_i$$

$$\text{Normalization factor } N = \frac{(\%I\varepsilon_i + \%I\beta^+_i)}{TI(out)_i - TI(in)_i}$$

Equilibrium Decay Chain

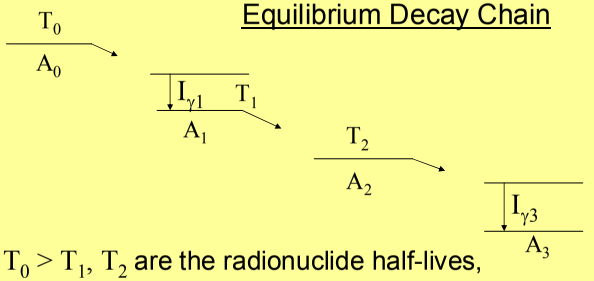

$T_0 > T_1$, T_2 are the radionuclide half-lives,

For t = 0 only radionuclide A_0 exists,

% $I_{\gamma 3}$, $I_{\gamma 3}$, and $I_{\gamma 1}$ are known.

Then, at equilibrium

$$\% I_{\gamma 1} = (\% I_{\gamma 3}/I_{\gamma 3}) \times I_{\gamma 1} \times (T_0/(T_0 - T_1)) \times (T_0/(T_0 - T_2))$$

Normalization factor $N = \%I_{\gamma 1}/ I_{\gamma 1}$

$$\%I(\gamma_1) = \frac{\%I(\gamma_3)\times I(\gamma_1)}{I(\gamma_3)} \times \frac{T_0}{T_0-T_1} \times \frac{T_0}{T_0-T_2}$$

Normalization factor $N = \frac{\%I_{\gamma_1}}{I_{\gamma_1}}$

2. Direct feeding to the ground state is known

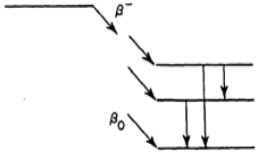

In this case, one sums up the transition intensity, I(γ+ce), for all γ's decaying directly to the g.s. and the normalization factor is calculated as follows:

$$\text{Normalization factor} = \frac{(100\text{-direct feeding of g.s.})}{\Sigma I(\gamma+ce) \text{ to g.s.}}$$

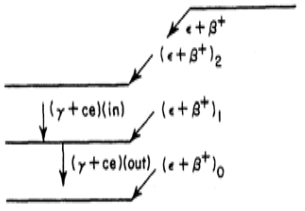

47

If in ε+β+ decay, the intensity for $\gamma^{\pm}$ radiation is known, then one can proceed to calculate the γ-ray normalization as follows:

i. Let measured annihilation intensity = $\%I(\gamma^{\pm})$

ii. Assume $\varepsilon+\beta^+$ branch to g.s. is $b_0 = \%I(\varepsilon+\beta^+)_0$

iii. Intensity imbalance, X_i, for level i, in relative units,
$X_i = [(\gamma+ce)(out)_i - (\gamma+ce)(in)_i]$

iv. Then normalization factor $N = \frac{(100-b_0)}{\Sigma X_i}$

v. The $\varepsilon+\beta^+$ branch to level i is $b_i = X_i \times N$

vi. For level i let r_i denote the theoretical electron capture to positron ratio, $r_i = \varepsilon/\beta+$ (theory)

vii. Total annihilation radiation =

$$2\left[\frac{b_0}{1+r_0} + \frac{b_1}{1+r_1} + \frac{b_2}{1+r_2} + \ldots\right] = \%I(\gamma^{\pm})$$

viii. Substituting for b_i from (v) one calculates the only unknown, b_0, and the normalization factor is calculated from (iv).

Note: If there are gamma transitions in the decay scheme that undergo significant pair conversion, then their contribution to annihilation radiation should be subtracted out of $I(\gamma^{\pm})$

4. X-ray intensity is known

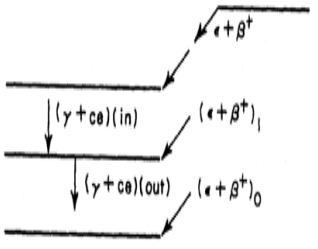

If, in $\varepsilon+\beta^+$ decay, the x-ray intensity, say for the K x-ray, is known, then one can proceed to calculate the normalization as follows:

i. Let the measured K x-ray intensity = $\%I(K\ x\text{-ray})$

ii. Assume $\varepsilon+\beta^+$ branch to g.s. is $b_0 = \%I(\varepsilon+\beta^+)_0$

iii. Intensity imbalance for level i (in relative units),
$X_i = [(\gamma+ce)(out)_i - (\gamma+ce)(in)_i]$

iv. Normalization factor, $N = \dfrac{(100 - b_0)}{\Sigma X_i}$

v. For level i let r_i denote the theoretical electron capture to position ratio, $r_i = \varepsilon/\beta+$ (theory)

vi. The ε intensity for level i is then given as $I(\varepsilon_i) = \dfrac{b_i x r_i}{(1+r_i)}$

vii. The K x-ray intensity, KX_i, resulting from electron capture to the level i is then given by

$$KX_i = I(\varepsilon_i) \times P_{ki} \times \omega_k$$

where P_{ki} is the fraction of the decay proceeding by K capture (from, say, the program LOGFT) and ω_k is the K-shell fluorescence yield (given by Bambynek et al., Rev. Mod. Phys. 44, 716 (1972))

viii. Sum of intensities calculated in (vii) is equal to I(K x-ray)

$$\Sigma KX_i = \%I(K\ x\text{-ray})$$

Only unknown b_0 can then be calculated, which in turn gives the normalization factor.

Note: If there are gamma transitions in the decay scheme that undergo significant internal conversion, then their contribution to I(x-ray) should be subtracted from (i) above.

- 6 -

5. X-ray-γ coincidence is measured

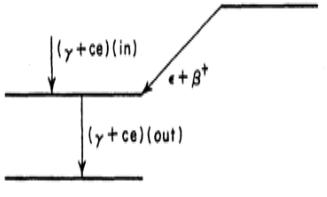

In some simple decay schemes the normalization factor can be calculated from x-ray-γ ray coincidences. It is important to single out the x-ray intensity (KX_i) as being due to the ε branch to level i which emits the γ ray.

The normalization is calculated in a manner similar to that described in (4) above. From (4)(vii),

$$I\varepsilon_i = \frac{KX_i}{P_{ki} \times \omega_k}$$

Since,

$$b_i = \frac{I\varepsilon_i(1+r_i)}{r_i = X_i \times N}$$

one can calculate N (normalization factor). X_i is the intensity imbalance for level i.

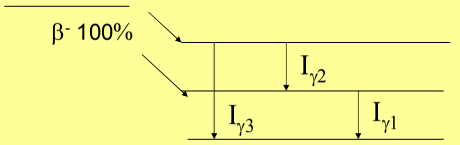

Normalization factor $N = 100 / I_{\gamma 1}(1 + \alpha_1) + I_{\gamma 3}(1 + \alpha_3)$

$\% I_{\gamma 1} = N \times I_{\gamma 1} = 100 \times I_{\gamma 1} / I_{\gamma 1}(1 + \alpha_1) + I_{\gamma 3}(1 + \alpha_3)$

$\% I_{\gamma 3} = N \times I_{\gamma 3} = 100 \times I_{\gamma 3} / I_{\gamma 1}(1 + \alpha_1) + I_{\gamma 3}(1 + \alpha_3)$

$\% I_{\gamma 2} = N \times I_{\gamma 2} = 100 \times I_{\gamma 2} / I_{\gamma 1}(1 + \alpha_1) + I_{\gamma 3}(1 + \alpha_3)$

Calculate uncertainties in $\% I_{\gamma 1}$, $\% I_{\gamma 2}$, and $\% I_{\gamma 3}$. Use 3% fractional uncertainty in α_1 and α_3.

See Nucl. Instr. and Meth. **A249**, 461 (1986).

To save time use computer program GABS

4. Annihilation radiation intensity is known

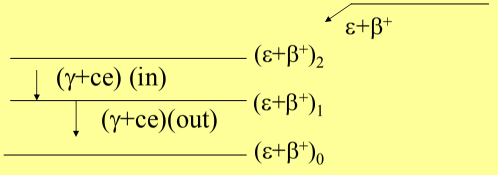

$I(\gamma\pm)$ = Relative annihilation radiation intensity

X_i = Intensity imbalance at the ith level = (γ+ce) (out) – (γ+ce) (in)

$r_i = \varepsilon_i / \beta^+_i$ theoretical ratio to ith level

$X_i = \varepsilon_i + \beta^+_i = \beta^+_i (1 + r_i)$, therefore $\beta^+_i = X_i / 1 + r_i$

$$2 [X_0 / (1 + r_0) + \Sigma X_i / (1 + r_i)] = I(\gamma\pm) \ldots\ldots\ldots (1)$$

$$[X_0 + \Sigma I_{\gamma i} (\gamma + ce) \text{ to gs }] N = 100 \ldots\ldots\ldots (2)$$

Solve equation (1) for X_0 (rel. gs feeding).

Solve equation (2) for N (normalization factor).

5. X-ray intensity is known

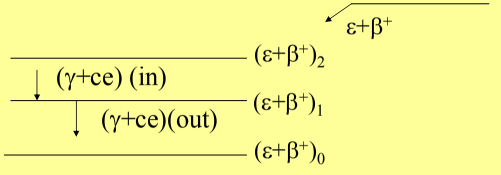

I_K = Relative Kx-ray intensity

X_i = Intensity imbalance at the ith level = (γ+ce) (out) – (γ+ce) (in)

$r_i = \varepsilon_i / \beta^+_i$ theoretical ratio to ith level

$X_i = \varepsilon_i + \beta^+_i$, so $\varepsilon_i = X_i r_i / 1 + r_i$ (atomic vacancies); ω_K=K-fluorsc.yield

P_{Ki} = Fraction of the electron-capture decay from the K shell

$I_K = \omega_K [\varepsilon_0 \times P_{K0} + \Sigma \varepsilon_i \times P_{Ki}]$

$$I_K = \omega_K [P_{K0} \times X_0 r_0 / (1 + r_0) + \Sigma P_{Ki} \times X_i r_i / 1 + r_i] \ldots (1)$$

$$[X_0 + \Sigma I_i(\gamma + ce) \text{ to gs}] N = 100 \ldots. (2)$$

Solve equation (1) for X_0, equation (2) for N.

Gamma-ray spectrometry and decay data

Marie-Christine Lépy, CEA/LNHB
Marie-christine.lepy@cea.fr

- Introduction
- Calibration principles
  - Energy calibration
  - Efficiency calibration
  - Associated uncertainties
- Some difficulties
  - Peak shape characteristics
  - Peak area determination
  - Case of X-rays
  - Corrective terms

Processing of the gamma-ray spectra

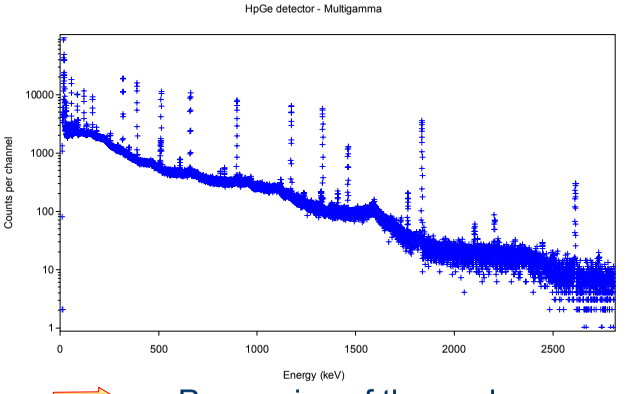

Processing of the peaks

Information contained in a peak

position = energy (E)

nuclide identification (E, $I\gamma(E)$)

area = number of emitted photons (N(E), $\varepsilon(E)$)

nuclide activity $A = \frac{N(E)}{\varepsilon(E) \cdot I_\gamma(E)}$

Calibration principle

- Energy calibration
- Efficiency calibration
- Combined standard uncertainty

Calibration

- Gamma-ray spectrometry : 2 kinds of information
  - Qualitative : Nuclide identification -> requires energy calibration
  - Quantitative : Activity determination -> requires efficiency calibration

$$A = \frac{N(E)}{\varepsilon(E) \cdot I_\gamma(E)}$$

Energy calibration (1)

- Relation between the channel (peak position) and the energy

E = f (channel) ~ α + β channel

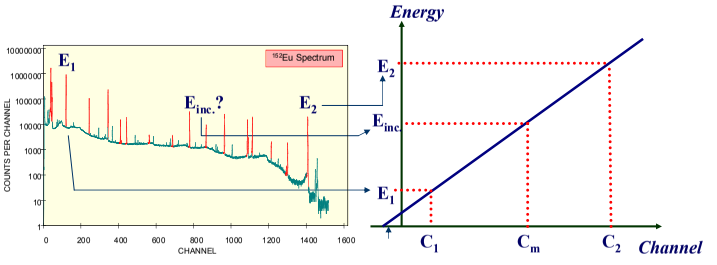

Energy calibration (2)

This is performed using reference radionuclides with photon emission energies well known :

The γ-ray energies are based on the « gold standard » : the 411.802 05 (17) keV transition from ^{198}Au decay

Some other values :

^{109}Cd :	88.033 60 (103)
^{57}Co :	122.060 65 (12)
^{137}Cs :	661.662 1 (54)
^{60}Co :	1 173.233 1 (62)
	1 332.495 9 (70)
^{152}Eu :	121.781 68 (29)

Reference : « Recommended standards for γ-ray energy calibration (1999) »
R.G. Helmer, C. Van der Leun, NIM in PR A 450 (2000) 35-70

Energy calibration (3)

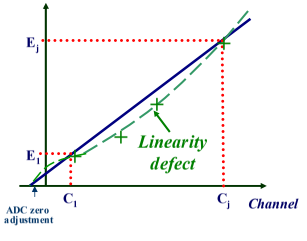

Using two energy references in the low and high energy range :

^{57}Co : 122 keV

^{60}Co : 1332 keV

-> linear function :

$$E\ (keV) = a_0 + a_1 C$$

C : channel number

a_0 and a_1 : calibration coefficients

A third energy can be used to get adjust quadratic function to take account of linearity defect.

Efficiency calibration (1)

$$A = \frac{N(E)}{\varepsilon(E) \cdot I_\gamma(E)} \quad \Longleftrightarrow \quad \varepsilon(E) = \frac{N(E)}{A \cdot I_\gamma(E)}$$

This is performed using standard with standardized activity A (Bq) with photon emission intensities, I_γ well known

N (E) : peak area

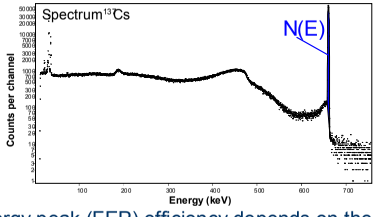

ε(E) Full-energy peak (FEP) efficiency depends on the energy and on the source-detector geometrical arrrangement

Efficiency calibration (2)

To get an efficiency values at any energy : energy calibration over the whole energy range

1. Use different radionuclides to get energies regularly spaced over the range of interest
   - Single gamma-ray emitters : ^{51}Cr (320 keV), ^{137}Cs (662 keV)
   - ^{54}Mn (834 keV) : one efficiency value per one measurement

⚠ Multigamma emitters : ^{60}Co, ^{133}Ba, ^{152}Eu, ^{56}Co : several efficiencies values per one measurement , but coincidence summing effects !

For each energy, discrete values of the FEP efficiency $\varepsilon(E_1)$, $\varepsilon(E_2)$, … $\varepsilon(E_n)$

2. Computation of the efficiency for
   1. Local interpolation
   2. Fitting a mathematical function to the experimental values

Efficiency calibration (3)

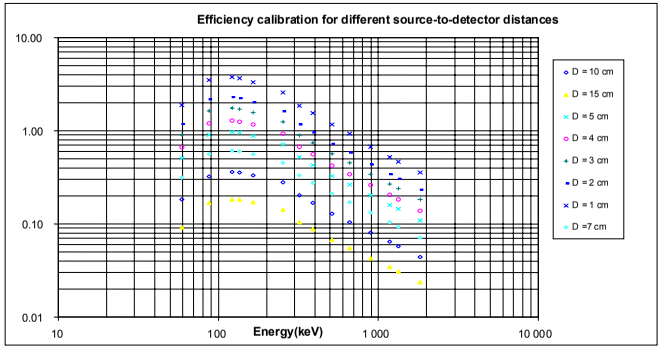

Efficiency calibration (4)

Local interpolation

E_1 -> ε_1

E_2 -> ε_2

To get ε(E) for $E_1 < E < E_2$

Solution 1 : linear interpolation ⟶ $\varepsilon(E) = \varepsilon_1 + \frac{(E - E_1)}{(E_2 - E_1)} \cdot (\varepsilon_2 - \varepsilon_1)$

⚠ : valid only for close energies

Solution 2 : logarithmic interpolation

$$\ln(\varepsilon(E)) = \ln(\varepsilon_1) + \frac{(\ln E - \ln E_1)}{(\ln E_2 - \ln E_1)} \cdot (\ln \varepsilon_2 - \ln \varepsilon_1)$$

Efficiency calibration (5)

Local interpolation : example

Determine efficiency for E = 662 keV (^{137}Cs) knowing :

1. E_1 = 569 keV (^{134}Cs) $\varepsilon_1 = 2{,}21\ 10^{-3}$
   E_2 = 766 keV (^{95}Nb) $\varepsilon_2 = 1{,}67\ 10^{-3}$

   Linear interpolation : $\varepsilon(E) = 1{,}96\ 10^{-3}$
   Logarithmic interpolation : $\varepsilon(E) = 1{,}92\ 10^{-3}$

2. E_1 = 122 keV (^{57}Co) $\varepsilon_1 = 8{,}22\ 10^{-3}$
   E_2 = 1 173 keV (^{60}Co) $\varepsilon_2 = 1{,}13\ 10^{-3}$

   LInear interpolation : $\varepsilon(E) = 4{,}57\ 10^{-3}$
   Logarithmic interpolation : $\varepsilon(E) = 1{,}87\ 10^{-3}$

Actual value (at 662 keV) : $\varepsilon(E) = 1{,}90\ 10^{-3}$

Conclusion : approximation to be used only if high uncertainties (> 10 %) are acceptable

Efficiency calibration : mathematical fitting(1)

Determination of the best fitted function to a given set of experimental data (energy, efficiency)

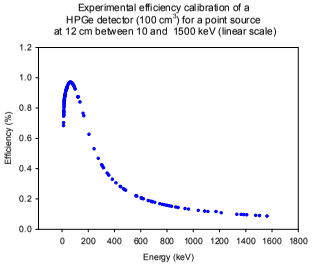

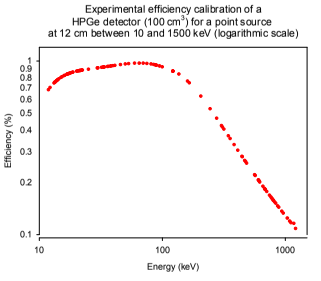

In the logarithmic scale , the shape is smoother than in the linear scale.

54

Efficiency calibration : mathematical fitting(2)

Functions most frequently used :

Polynomial fitting in the log-log scale : $$\ln \varepsilon(E) = \sum_{i=0}^{n} a_i \cdot (\ln E)^i$$

$$\ln \varepsilon(E) = \sum_{i=0}^{n} a_i \cdot E^{-i}$$

Remarks :

- a_i coefficients are determined using a least-squares fitting method
- experimental data must be weighted
- the polynomial degree (n) must be adjusted depending on the number of experimental data (p) : n << p
- in some case two different functions can be used with a cross point
- check the resulting fitted curves !

Efficiency calibration : mathematical fitting(3)

Example : 57 experimental data
In the 122-to-1836 keV range

Fitting function :

$$\ln \varepsilon(E) = \sum_{i=0}^{n} a_i \cdot (\ln E)^i$$

Fitted coefficients :

fitting	122 to 1836 keV
deg0	-4.616E+01
deg1	6.683E+01
deg2	-3.701E+01
deg3	8.907E+00
deg4	-7.976E-01

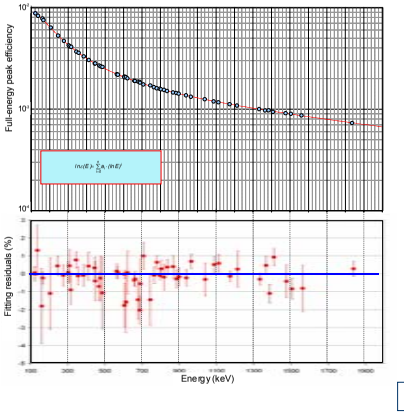

Efficiency calibration : mathematical fitting(4)

Efficiency fitting must be visually checked

In the case of cross points be carefull :

- Avoid zones with important inflexion
- Avoid high degree polynomials

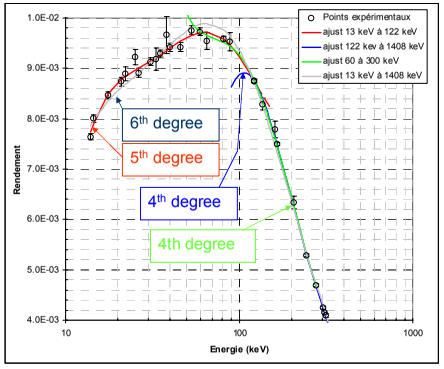

Example of efficiency calibration for a planar HPGe detector (low-energy)

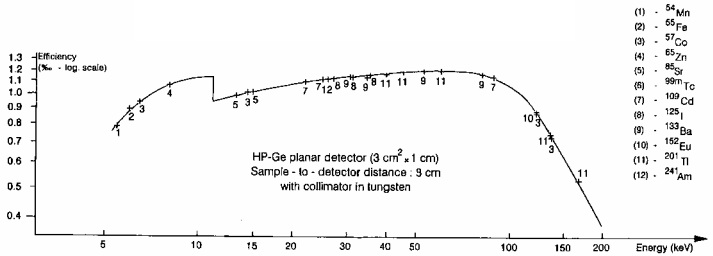

Efficiency calibration : remarks

- Efficiency calibration for reference geometry
- Correlation between input data
- Corrective factors needed if different measurement geometry
- Monte Carlo simulation

Combined standard uncertainty (1)

Efficiency calibration $\varepsilon(E) = \frac{N(E)}{A \cdot I(E) \cdot t}$

$$\left(\frac{u\varepsilon(E)}{\varepsilon}\right)^2 = \left(\frac{uN(E)}{N}\right)^2 + \left(\frac{uA}{A}\right)^2 + \left(\frac{uI(E)}{I(E)}\right)^2$$

Uncertainty on t negligible

$$\frac{uA}{A} = 5 \cdot 10^{-3} \qquad \frac{uN(E)}{N(E)} = \frac{\sqrt{N(E)}}{N(E)} = \frac{1}{\sqrt{N(E)}}$$

If $N(E) = 10^4 \Rightarrow \frac{uN(E)}{N(E)} = 10^{-2}$

Influence of the peak area : If $N(E) = 10^5 \Rightarrow \frac{uN(E)}{N(E)} = 3.1\ 10^{-3}$

Combined standard uncertainty (2)

$$\frac{uA}{A} = 5 \cdot 10^{-3} \qquad \text{If } N(E) = 10^5 \Rightarrow \frac{uN(E)}{N(E)} = 3.1\ 10^{-3}$$

For gamma-rays

$$\frac{uI_\gamma(E)}{I_\gamma(E)} = 1.10^{-3} \Rightarrow \frac{u\varepsilon(E)}{\varepsilon(E)} = 6 \cdot 10^{-3}$$

For X-rays

$$\frac{uI_X(E)}{I_X(E)} = 2.10^{-2} \Rightarrow \frac{u\varepsilon(E)}{\varepsilon(E)} = 2.1\ 10^{-2}$$

$$\varepsilon(E) = \frac{N(E)}{A \cdot I(E) \cdot t} \Longleftrightarrow I(E) = \frac{N(E)}{A \cdot \varepsilon(E) \cdot t}$$

… and no standard radionuclide for E < 5 keV

Activity determination

- Activity determination $A = \dfrac{N(E)}{I_\gamma(E) \cdot \varepsilon(E)}$
- Relative standard uncertainty :

$$\left(\frac{uA}{A}\right)^2 = \left(\frac{uN(E)}{N}\right)^2 + \left(\frac{u\varepsilon(E)}{\varepsilon(E)}\right)^2 + \left(\frac{uI_\gamma(E)}{I_\gamma(E)}\right)^2$$

$$\frac{uN(E)}{N(E)} = \frac{\sqrt{N(E)}}{N(E)} = \frac{1}{\sqrt{N(E)}} \qquad \frac{u\varepsilon(E)}{\varepsilon(E)} = 1 \cdot 10^{-2} \qquad \frac{uI_\gamma(E)}{I_\gamma(E)} = 1 \cdot 10^{-3}$$

Influence of the peak area :

if $N = 10^4$ $uN/N = 10^{-2}$ -> $uA/A = 1{,}4\ 10^{-2}$

if $N = 10^5$ $uN/N = 3{,}110^{-3}$ -> $uA/A = 1{,}05\ 10^{-2}$

At the best, $u\varepsilon/\varepsilon = 5\ 10^{-3}$ and $uN/N = 110^{-3}$ -> $uA/A = 5{,}2\ 10^{-3}$

Gamma emission intensity determination

$$I_\gamma(E) = \frac{N(E)}{A \cdot \varepsilon(E)}$$

$$\left(\frac{uI_\gamma(E)}{I_\gamma(E)}\right)^2 = \left(\frac{uN(E)}{N}\right)^2 + \left(\frac{u\varepsilon(E)}{\varepsilon(E)}\right)^2 + \left(\frac{uA}{A}\right)^2$$

$$\frac{uN(E)}{N(E)} = \frac{\sqrt{N(E)}}{N(E)} = \frac{1}{\sqrt{N(E)}} \qquad \frac{uN(E)}{N(E)} = 5 \cdot 10^{-3} \qquad \frac{uA}{A} = 2 \cdot 10^{-3}$$

For gamma-rays

$$\frac{u\varepsilon(E)}{\varepsilon(E)} = 1.10^{-3} \Rightarrow \frac{uI_\gamma(E)}{I_\gamma(E)} = 6 \cdot 10^{-3}$$

For X-rays

$$\frac{u\varepsilon(E)}{\varepsilon(E)} = 2.10^{-2} \Rightarrow \frac{uI_X(E)}{I_X(E)} = 2.1 \cdot 10^{-2}$$

Monte Carlo simulation

Generation of spectra for any source-to-detector geometry.

Principle : follows each photon "story" along its whole path (from the source to the detector volume), simulation of secondary particles (electrons, X-ray rearrangement …).

- Advantages :
  - Accurate 3D description of complex geometries
  - Physicals processes are taken into account
- Drawbacks :
  - Computation time
  - Unaccurate knowledge of some geometrical parameters (inside of the detector)
  - Uncertainties on cross sections
- Hazardous for absolute efficiency calibration
- but can be used with good results for efficiency transfer.

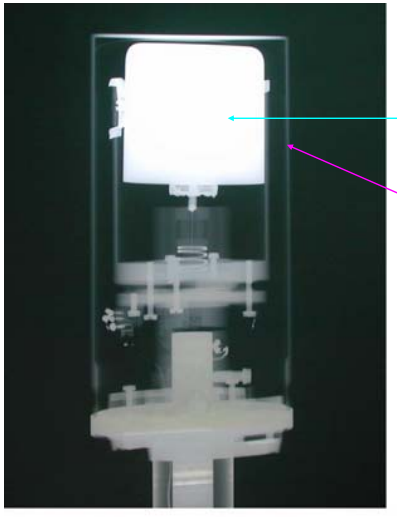

Detector radiography

Ge Crystal

Al cap

HPGe detector GeHP :

- rounded crystal
- shifted / vertical axis
- tilted …

25

Gamma-ray spectrometry (2)

Marie-Christine Lépy, CEA/LNHB
Marie-christine.lepy@cea.fr

- Introduction
- Calibration principles
  - Energy calibration
  - Efficiency calibration
  - Associated uncertainties
- Some difficulties
  - Peak shape characteristics
  - Peak area determination
  - Case of X-rays
  - Corrective terms

Processing of the gamma-ray spectra

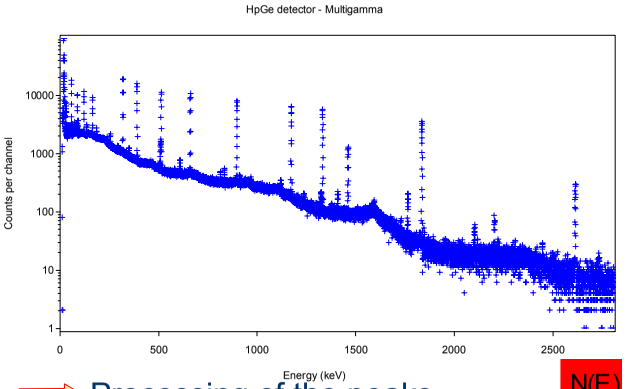

Processing of the peaks $\varepsilon(E) = \frac{N(E)}{A \cdot I_\gamma(E)}$

Information contained in a peak

position = energy (E)

→ nuclide identification (E, $I_\gamma(E)$)

area = number of emitted photons (N(E), $\varepsilon(E)$)

→ nuclide activity
detector efficiency $\varepsilon(E) = \frac{N(E)}{A \cdot I_\gamma(E)}$
photon emission intensity

Region of interest

- For quantitative analysis : determination of N(E) = peak area

  (number of photons with energy E that deposited all their energy in the detector)
- Spectrum - > "Regions Of Interest" (ROI's) containing one or several peaks

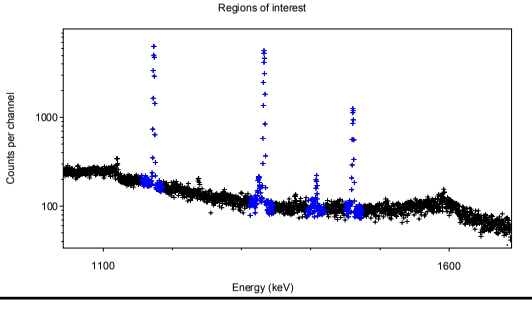

Energy resolution

- Initial photon emission : Monoenergetic line (source)
- Widening and distortion of the resulting peak (spectrum)
  - Widening : gaussian effects
    - fluctuation of the number of charge carriers : ΔE_S
    - electronic noise : ΔE_E
  - Non gaussian effects
    - Charges collection : ΔE_C
    - Drift of the operating system (detector + electronics)
    - Pile-up
- Result : in the resulting spectrum : 'peak' with finite width (keV) and more or less symmetrical shape
- First approximation : Gaussian shape

Gaussian distribution

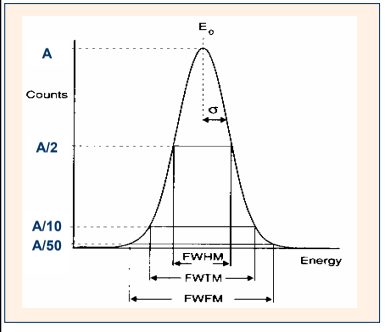

$$G(E) = A \cdot \exp\left(-\frac{(E-E_0)^2}{2\sigma^2}\right)$$

- Distribution centered on the E_0 energy with σ standard deviation
- Full width at half maximum of the Gaussian :

$$FWHM = 2{,}355\ \sigma$$

- Gaussian area :

$$S = (2\pi)^{1/2}\ \sigma\ A$$

Peak full width at half maximum

$$\Delta E = \left(\Delta E_S^2(E) + \Delta E_C^2 + \Delta E_E^2\right)^{1/2}$$

- ΔE_S = statistical noise (dependent on the energy)
- ΔE_C = charge collection
- ΔE_E = electronical noise

- First approximation : $\Delta E = \left(K + \Delta E_S^2(E)\right)^{1/2}$

$$\Delta E^2 = K + \Delta E_S^2(E) = K + (2{,}355)^2 \cdot F \cdot w \cdot E$$

FWHM versus energy

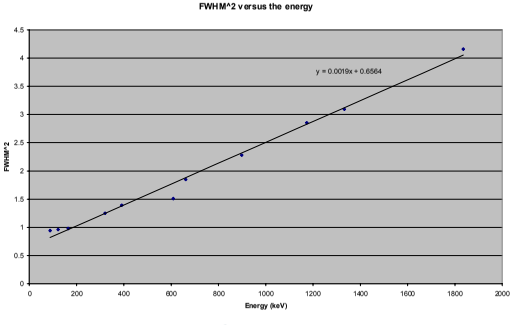

- Linear fitting : $FWHM^2 = 0{,}0019E + 0{,}6564$
- K = 0,656 keV (electronics + charge collection)
- $(2{,}355)^2\ F\ w = 0{,}0019$ -> F = 0,116

- Energy resolution : ΔE (keV) : FWHM : Full Width at Half Maximum of a peak
  - Evolves as the square root of the energy
  - From 0,16 keV to 2,5 keV, depending on the detector and on the photon energy
- Resolving power : $\Delta E / E$ (%) : Some 10^{-3}
  (5 – 10 % for NaI)
- Caracteristic of the quality of the spectrometer :
  - separation of closely spaced peaks
  - detection limit

Some values

Type	Size		Resolution (keV)		
			5,9 keV	122 keV	1332 keV
Si(Li)	Area (cm^2)				
	0,12		0,14 - 0,17		
	0,28		0,17 – 0,18		
	0,80		0,18 – 0,19		
	2,0		0,22 – 0,25		
Ge planar	Depth (cm)	Diameter (cm)			
	0,5	0,6	0,145	0,55 – 0,48	
	0,5 – 1,0	1,0	0,24 – 0,18	0,57 – 0,49	
	0,5 – 1,0	1,6	0,29 – 0,20	0,59 – 0,50	
	0,5 – 1,3	2,5	0,46 – 0,30	0, 72 – 0,54	
	1,0 – 1,3	5,1	0,62 – 0,54	0, 77 – 0,72	
	Efficiency (%)				
Ge coaxial n-type	10		0,66 – 0,74	0,8 – 1,0	1,8 – 2,0
	20		0,69 – 0,79	0,85 – 1,0	1,8 – 2,0
	30		0,72 – 0,84	0,9 – 1,0	1,9 – 2,2
Ge coaxial p-type	10			0,82 – 1,0	1,7 – 2,0
	20			0,85 – 1,1	1,8 – 2,0
	40			0,88 – 1,2	1,9 – 2,2
	50			0,95 – 1,2	2,1 – 2,5

Other peak shape characteristics

- FWTM (Full Width at Tenth Maximum)
- FWFM (Full Width at Fiftieth Maximum)
- These values can be compared to those characteristic of a Gaussian (ideal ?) peak :
  FWTM / FWHM = 1,82
  FWFM / FWHM = 2,38
- Information about the peak shape, particularly on its base (collection defects)

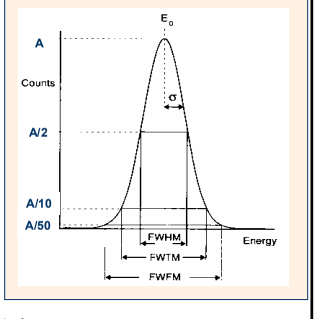

Processing of a ROI

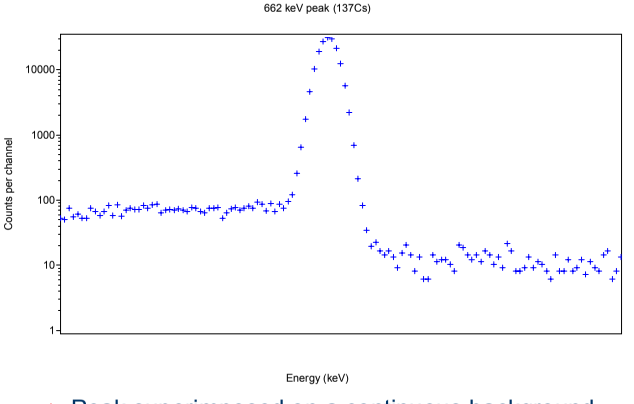

- Peak superimposed on a continuous background

Background

Peak with energy E_0 in region [f,l] first channel = f ; last channel = l

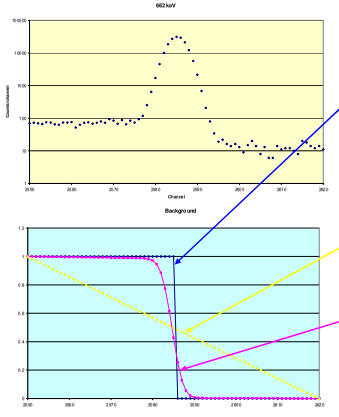

Step :

F(i) = 1 for E < E0

F(i) = 0 for E > E0

Linear : $F(i) = 1 - \frac{(i - f)}{(l - f)}$

Galton curve : $F(i) = 1 - \frac{\sum_{f}^{i} Y_i}{\sum_{f}^{l} Y_i}$

Peak area determination (1)

- Approximation : peak = Gaussian

$$G(E) = A \cdot \exp\left(-\frac{(E-E_0)^2}{2\sigma^2}\right)$$

- E_0 = energy, A = amplitude, σ = standard deviation
- Gaussian area : $S[-\infty, +\infty] = (2\pi)^{1/2}\ \sigma\ A$
- Approximation (without peak fitting) : sum of channels in the region [-3σ, +3 σ] around the peak centroïd = 99,7 % of the Gaussian total area (S)

Peak area determination (2)

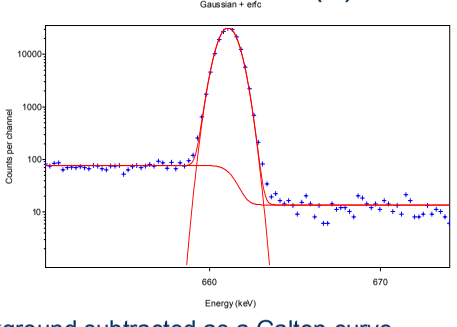

- Background subtracted as a Galton curve
- Peak fitted with a Gaussian : fitted parameters :
  A = 31360 σ = 0,53 -> N = 164 200
- Using a linear background and summing of channel contents :
  N = 164 600

Peak area determination (3)

- Peak with low-energy tailing : G(E) + T(E)
- Tail = exponential background ↳ Gaussian shape (detector response)

$$T(E) = \int_{-\infty}^{E_0} A \cdot T \cdot \exp(\tau \cdot E) \cdot \exp\left[\frac{-(E-E_0)^2}{2\sigma^2}\right] \cdot dE$$

$$T(E) = A \cdot \frac{T}{2} \cdot \exp\left[(E-E_0)\tau + \frac{\sigma^2\tau^2}{2}\right] \cdot \operatorname{erfc}\left[\frac{1}{\sqrt{2}}\left(\frac{(E-E_0)}{\sigma} + \sigma\tau\right)\right]$$

$$\operatorname{erfc}(x) = \frac{2}{\sqrt{\pi}} \int_x^{\infty} e^{-t^2}\, dt$$

Overlapping peaks (1)

If peaks with about the same width : individuals areas area can be obtained from the total net area weighted by the relative amplitude of each peak

Case of 511 keV region :

Example : ^{85}Sr

(Gamma at 514 keV)

Net area = 48 500

Amplitude 511 = 1000

Amplitude 514 = 10 000

Area of 511 = 4 400

Area of 514 = 44 100

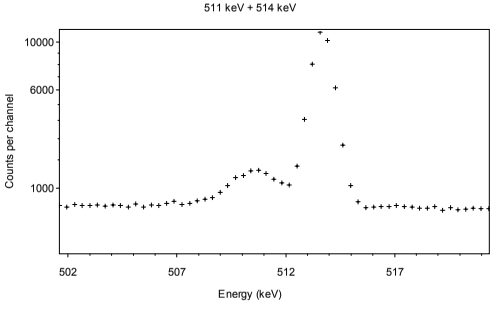

Overlapping peaks (2)

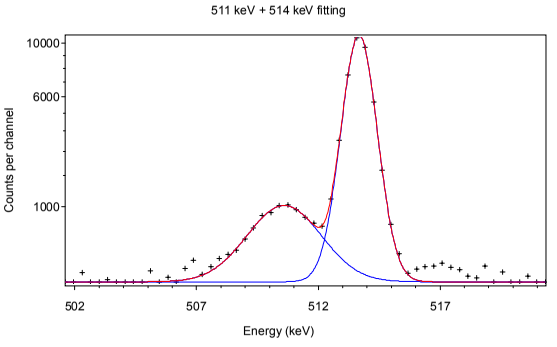

Fitting : 511 = 7730 514 = 40 400

σ = 1,07 σ = 0,53

Bias on the 514 keV area = 9 % !!!

Case of X-rays (1)

Scattered photons -> energy close to the one of the main peak
-> depending on the source –detector geometrical arrangement

^{152}Eu spectrum – KX-ray region (40-45 keV)

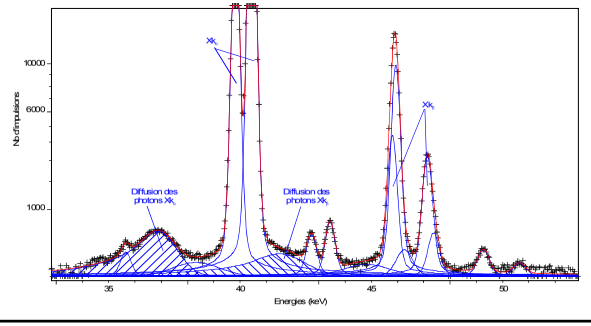

Case of X-rays (2)

Photons = transitions between excited levels

Gamma = nuclear levels

X = atomic levels

For monoenergetic emission, there is a finite line shape

that is Lorentzian (Γ) $$L(E) = \frac{\Gamma/2\pi}{(E - E_0)^2 + (\Gamma/2)^2}$$

Transition width (Γ) = initial state energy width + final state energy width $\Gamma = \Delta E_i + \Delta E_f$

Natural linewidth (2)

Energy levels = uncertainty (ΔE)

Heisenberg uncertainty principle : $\Delta E \cdot \Delta t \geq h / 2\pi$

h (Planck constant) = 6,582 122 . 10^{-16} eV.s

Δt uncertainty of the level half-life = $1/\lambda = 1{,}4427\ t_{1/2}$

($\lambda = \ln 2 / t_{1/2}$)

- Examples : gamma lines
  - $^{137}Cs \rightarrow {}^{137}Ba^{m}$: excited level = 661,7 keV
  - level half-life = 2,552 min → $\Delta E \approx 3\ 10^{-18}$ eV
  - ^{60}Co at 1 332,5 keV
  - level half-life = 7 10^{-13} s → $\Delta E \approx 6{,}5\ 10^{-4}$ eV

Natural linewidth (1)

Gamma-ray line width = some 10^{-3} eV (maximum)

X-ray lines : some eV

Detector widening (Gaussian) : some hundreds of eV

Element	Z	Energy (keV)	Level width (eV) K	L 3	Kα1 linewidth Γ(eV)	σ (eV)	Γ / σ
Nickel	28	7,45	1,44	0,48	1,94	155	0,030
Cadmium	48	22,98	7,28	2,50	9,8	200	0,115
Lead	82	72,80	60,4	5,8	66,2	350	0,445
Uranium	92	94,65	96,1	7,4	103,5	415	0,587

Peak = *Lorentzian ⊗ Gaussian (Voigt profile)*

For high Z X-ray lines, the natural linewidth is not negligible versus the detector resolution

Natural linewidth (2)

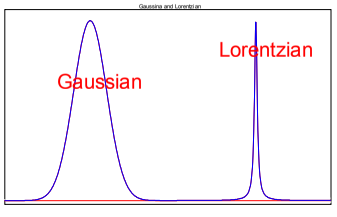

σ = 50 eV – Γ = 10 eV

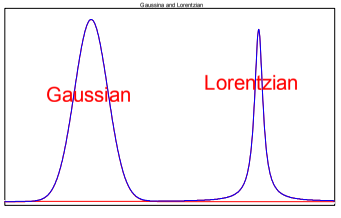

σ = 50 eV – Γ = 30 eV

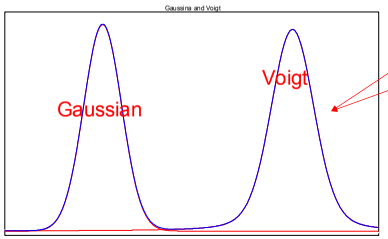

Peak = *Lorentzian ⊗ Gaussian (Voigt profile)*

$$V(E) = \int_{-\infty}^{+\infty} L(E') \cdot G(E - E') \cdot dE'$$

Processing of X-ray regions (1)

- Example : ^{241}Am spectrum (10 – 30 keV region)
  - Gamma at 26 keV
  - Np L X-rays in the 12-20 keV

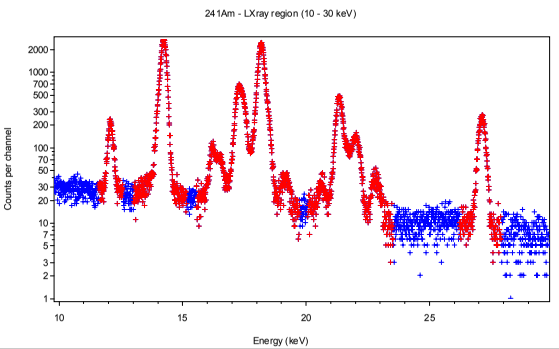

Processing of X-ray regions (2)

- Processing of the Np L beta region

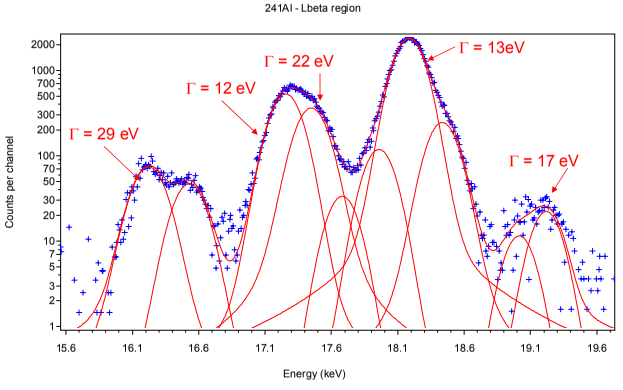

Main corrective terms

$$A = \frac{N(E)}{\varepsilon(E)\cdot I_\gamma(E)} \cdot C_T \cdot C_D \cdot C_G \cdot C_P \cdot C_C$$

- Half-life : C_T
- Decay during measurement C_D
- Geometry : C_G
- Contribution of background or escape peaks : C_P
- Coincidence summing : C_C

Half-life

- T : radionuclide half-life
- t_0 : reference date
- t_m : measurement date

$$C_T = \exp^{(\ln(2)\cdot\frac{(t_m - t_0)}{T})}$$

- τ : acquisition time (real time !)
- the radionuclide decays during the measurement

If τ not negligible vesus T :

$$C_D = \frac{\lambda\cdot\tau}{1-\exp^{(-\lambda\cdot\tau)}} \quad \text{where} \quad \lambda = \frac{\ln(2)}{T}$$

Source-to-detector geometry

- Source-to-detector distance can be adapted according to the counting rate
  - Small distance : Higher count rate
    - -> Smaller counting time
    - -> Less influence of the environmental background
    - -> Possiblitlity to use smaller samples (less self-absorption)
  - Large distance : Lower count rate
    - -> Less pile-up
    - -> Reduction of the coincidence summing effect
    - -> Accuracy of the position

Compromise between counting time and corrective factors

High counting rates (1)

Detector + electronics response slow versus pulses frequency

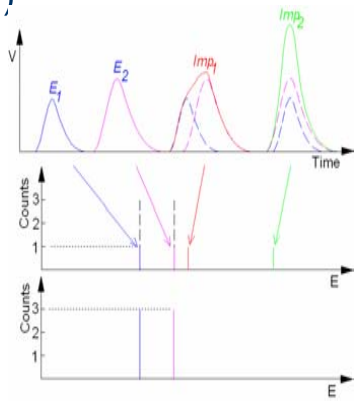

- Consequences
  - spectrum degradation
  - Counting losses

High counting rates (2)

2 kinds of solutions

- Use an absorber -> requires absorption correction

$$C_{abs}(E) = e^{\mu(E)\cdot x}$$

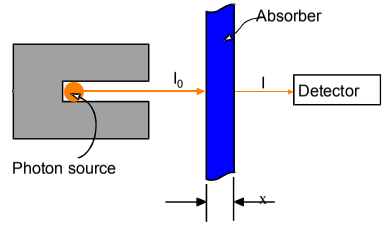

$$I(E) = I_0(E)\cdot e^{-\mu(E)\cdot x}$$

  - X = absorber thickness
  - μ(E) = absorber linear attenuation coefficient for energy E

- Use adapted electronic modules
  - Short shaping time
  - Pile-up rejector

Pile-up rejector : effect the spectrum shape

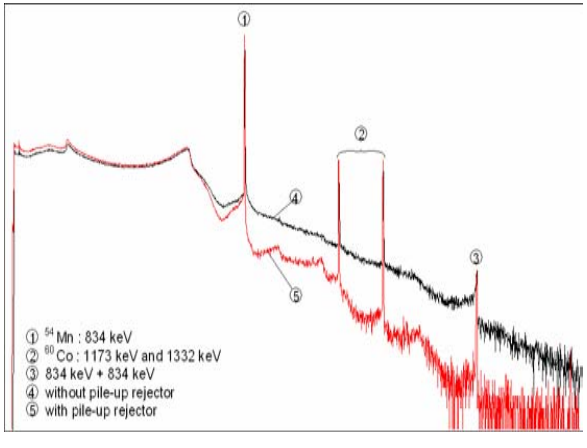

Pile-up rejector : effect the peak area

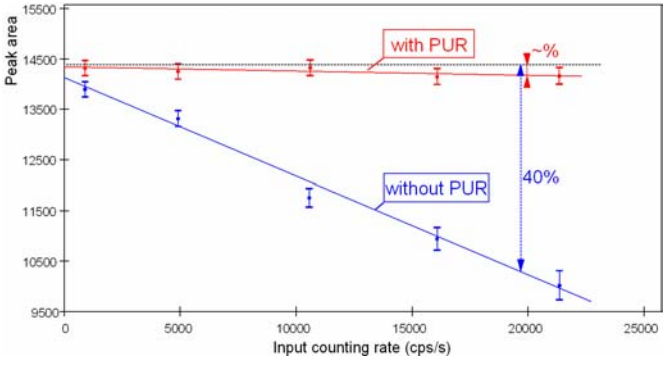

Better conservation of the peak area

Geometry correction

- Efficiency calibration
  - Characteristic of the detector.
  - Defined for an incident energy and source-detector geometry

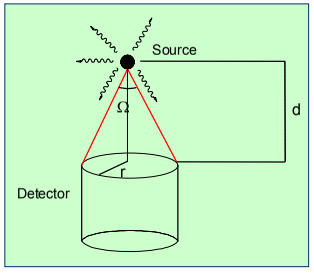

- Sample with different geometry to be measured
  - - self-absorption
  - - geometry variation (solid angle)

Types of geometries and matrixes

- Large number of geometries and matrixes :
  - - point source
  - - disk-shape samples (filters)
  - - cylindrical geometries
    - - liquid
    - - solid
    - - gas
  - - Marinelli geometries (Environment)
    - - liquid
    - - solid
    - - gas

General principle (1)

- Efficiency :
  - The photon impinges on the detector :
    (source-to-detector solid angle)
  - The energy is totally absorbed

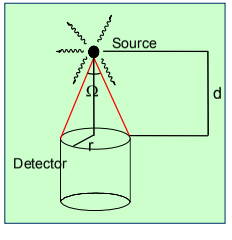

$$\varepsilon^P(E) = \varepsilon^G \cdot \varepsilon^I(E)$$

$$\varepsilon^G = \frac{\Omega}{4\pi}$$

ε^G = geometrical efficiency ($\nless$ E)

$\varepsilon^I(E)$ = intrinsic efficiency (depends on E)

General principle (2)

- For the calibration geometry : $\varepsilon_0(E)$

$$\varepsilon_0(E) = \varepsilon_0^G \cdot \varepsilon^I(E) \qquad \text{with :} \qquad \varepsilon_0^G = \frac{\Omega_0}{4\pi}$$

- For the measurement geometry : $\varepsilon_m(E)$

$$\varepsilon_m(E) = \varepsilon_m^G \cdot \varepsilon^I(E) \qquad \text{with :} \qquad \varepsilon_m^G = \frac{\Omega_m}{4\pi}$$

$$\varepsilon_m(E) = \varepsilon_0(E) \cdot \frac{\Omega_m}{\Omega_0}$$

Example : Displacement of a point source

- Calibration conditions :

Detector : radius : r = 2 cm

$$\Omega_0 = 2\pi\left(1 - \frac{d}{\sqrt{d^2 + r^2}}\right) = 0{,}122$$

Source-to-detector distance : d =10 cm

Efficiency calibration at 100 keV = 0,0171

- Measurement conditions
  - Source-to-detector distance : d1 = 20 cm $\Omega_{m1} = 0{,}031$
  - Source-to-detector distance : d2 = 5 cm $\Omega_{m2} = 0{,}449$

$$\varepsilon_{m1}(100\,\text{keV}) = \varepsilon_0(100)\cdot\frac{\Omega_{m1}}{\Omega_0} = 0{,}0171\cdot\frac{0{,}031}{0{,}122} = 0{,}0043$$

$$\varepsilon_{m2}(100\,\text{keV}) = \varepsilon_0(100)\cdot\frac{\Omega_{m2}}{\Omega_0} = 0{,}0171\cdot\frac{0{,}449}{0{,}122} = 0{,}0629$$

Volume samples

Adaptation of the « Moens method » including :

- Geometrical factors
- Absorption and self-absorption factors

Self-absorption

Self-absorption in the sample volume : depends on the energy E

For a small slab with thickness dx : $I = I_0 \exp(-\mu(E)\,dx)$

μ = linear attenuation coefficient of the sample material

For the whole sample with total thickness x :

$$I = \int_0^x I_0 \exp(-\mu(E)\cdot x')\cdot\frac{dx'}{x} = I_0\cdot\frac{1-\exp(-\mu(E)\cdot x)}{\mu(E)\cdot x}$$

Self-absorption factor : $F_{aut}(E) = \dfrac{1-\exp(-\mu(E)\cdot x)}{\mu(E)\cdot x}$

Matrix effect (1)

Matrix change with the same source-to-detector geometrical characteristics)

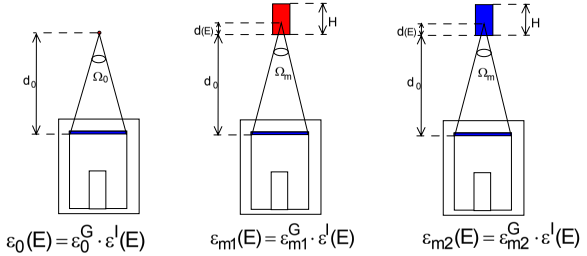

$$\varepsilon_0(E) = \varepsilon_0^G\cdot\varepsilon^I(E) \qquad \varepsilon_{m1}(E) = \varepsilon_{m1}^G\cdot\varepsilon^I(E) \qquad \varepsilon_{m2}(E) = \varepsilon_{m2}^G\cdot\varepsilon^I(E)$$

$$\varepsilon_{m1}^G = \Omega_1\cdot F_{aut1} \qquad \varepsilon_{m2}^G = \Omega_2\cdot F_{aut2}$$

Same geometries (1 and 2): $\Omega_1 = \Omega_2$

Thus : $\varepsilon_{m2}^G = \varepsilon_{m1}^G\cdot\dfrac{F_{aut2}}{F_{aut1}}$

Matrix effect (2)

$$\varepsilon_2(E) = \varepsilon_1(E)_0 \cdot \frac{F_{aut\ 2}(E)}{F_{aut\ 1}(E)} = \varepsilon_1(E)_0 \cdot \frac{\mu_1(E)}{\mu_2(E)} \cdot \frac{1 - \exp(-\mu_2(E) \cdot x)}{1 - \exp(-\mu_1(E) \cdot x)}$$

Example : Volume sample (x = 5 cm)

Calibration using liquid (H_20/HCl) sample

Measurement of solid matrixes (silica and sand)

Density :

H_20/HCl = 1,016

silica = 0,25

sand = 1,54

Energy (*keV*)	100	200	300	500
μ_{eau} (cm^{-1})	0,174	0,139	0,121	0,0985
Faut (water)	0,668	0,721	0,750	0,790
μ_{silice} (cm^{-1})	0,042	0,031	0,027	0,022
Faut (silica)	0,902	0,926	0,935	0,947
Correction	1,35	1,29	1,25	1,20
μ_{sable} (cm^{-1})	0,262	0,202	0,174	0,142
Faut(sand)	0,557	0,629	0,668	0,716
Correction	0,83	0,87	0,89	0,91

Background spectrum (1)

- Spectrum without any sample
  - Picture of the detector-environment response
  - To take into account in the spectrum processing
    - Natural radioactivity
    - Influence of the shielding (Fluorescence X rays)
    - Presence of any radioactive impurity

Background spectrum (2)

Whole spectrum – t = 250 000"

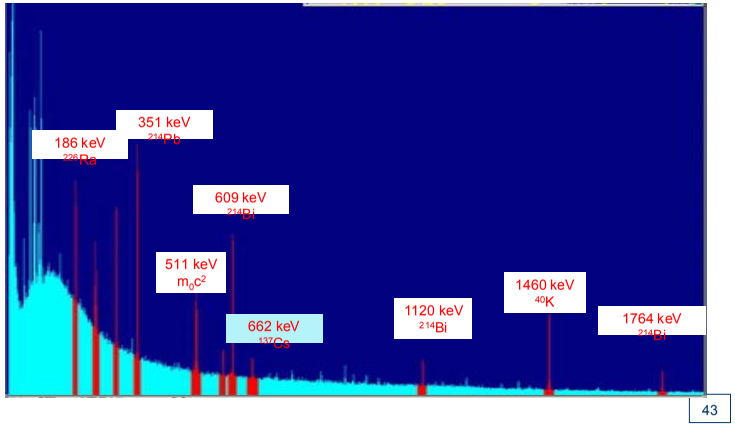

Background spectrum (3)

t = 250 000" - low-energy part

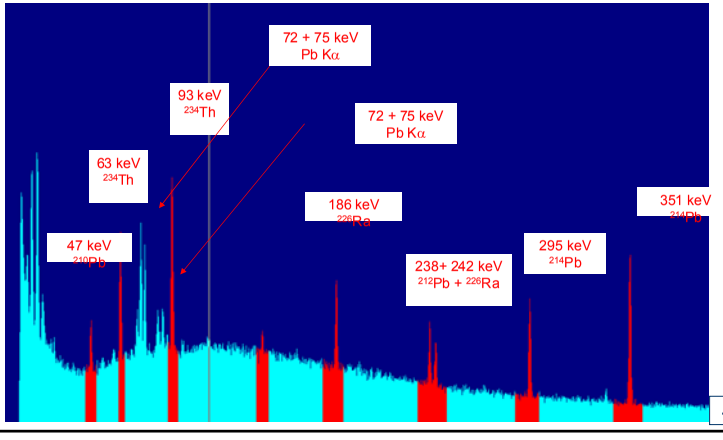

Main background lines

- Natural radioactivity
  - Ra (^{210}Pb, ^{214}Bi, ^{214}Pb) and Th (^{208}Tl, ^{224}Ra, ^{228}Ac, ^{212}Bi, ^{212}Pb) decay chains
  - ^{40}K (1 460 keV)

  Reduced by ventilation + shielding
- Fluorescence lines
  - Pb (shielding) : XKα : 72 and 75 keV
    XKβ : 85 and 87 keV
  - Cd (shielding) : XK : 23 and 26 keV
  - Cu (shielding) : XK : 8 and 9 keV
  - Ba (concrete) : XK : 32 and 36 keV
- 511 keV (annihilation)

Other "peak corrections"

Presence of any escape peak

- E – Ge X_K (10 keV)
- E – m_0c2 (511 keV)
- E – 2 m_0c2 (1 022 keV)

^{88}Y – Ge(Li) detector – 55 cm^3 – point source at 20 cm

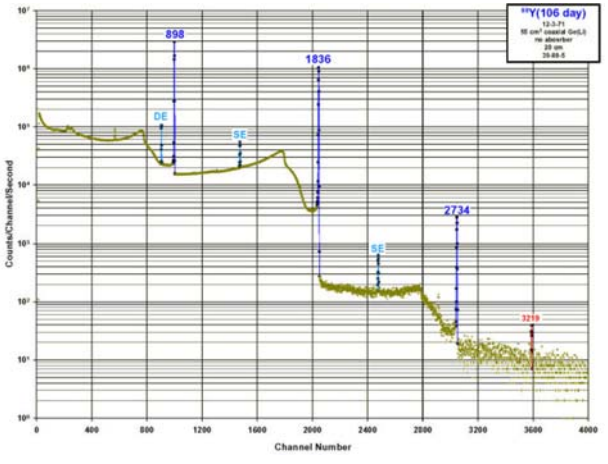

Coincidence summing

- Due to decay scheme
- Consequence :
  - spectrum degradation
  - Counting losses

- Even with low counting rate

- Decay scheme :

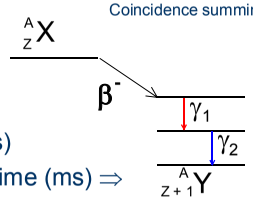

- Life-time of the intermediate level (ps)

<< Detector (+ electronics) response time (ms) ⇒

- In the detector :

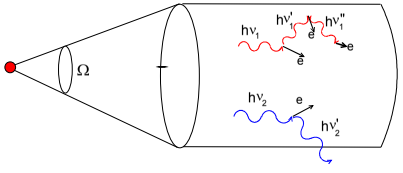

Output signal

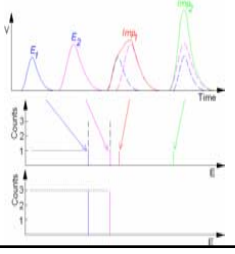

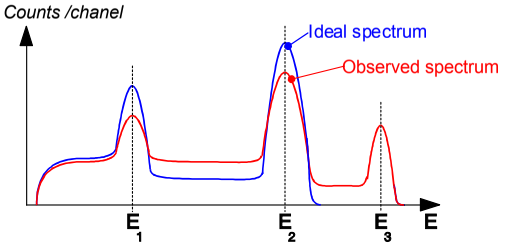

- Simultaneous detection of two cascade photons :
- 2 kinds of consequences :
- Loss of a pulse in peak E1
- Loss of a pulse in peak E2
- Gain of a pulse with total or partial sum energy E1+E2

- Phenomenon due to the decay scheme

Efficiency (reminder)

- Monoenergetic gamma emission
- Emission intensity : Iγ(E)
- Full-energy peak (FEP) efficiency :

$$\varepsilon^P(E) = \frac{N^P(E)}{A \cdot I\gamma(E)}$$

Total absorption of the energy

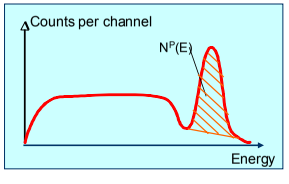

- Total efficiency :

$$\varepsilon^T(E) = \frac{N^T(E)}{A \cdot I\gamma(E)}$$

Partial absorption of the energy

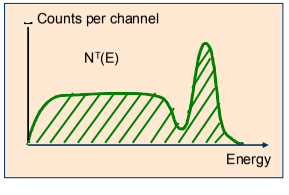

Total efficiency $\varepsilon^T(E)$

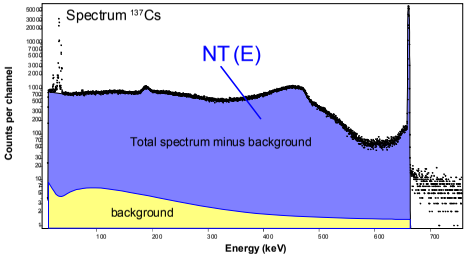

$$\varepsilon^T(E) = \frac{NT(E)}{A.I_\gamma(E)}$$

Correction formulation

Simple case: decay scheme with 2 excited levels

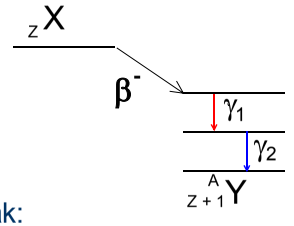

1. Correction concerning γ_1 peak:

Ideal counting in the peak corresponding to energy E_1 :

$$N_1 = A \cdot I(E_1) \cdot \varepsilon^P(E_1) = A \cdot I_{\gamma 1} \cdot \varepsilon^P{}_1$$

Counting losses in peak corresponding to energy E_1 :

If :
- photon E_1 emitted and totally absorbed : $A \cdot I(E_1) \cdot \varepsilon^P(E_1)$
- photon E2 emitted just after photon E1 (cascade) : P_{12}
- photon E2 absorbed in the detector (totally or partially)$\varepsilon^T(E_2)$

Then :

$$n_1 = A \cdot I(E_1) \cdot \varepsilon^P(E_1) \cdot P_{12} \cdot \varepsilon^T(E_2) = N_1 \cdot P_{12} \cdot \varepsilon^T(E_2)$$

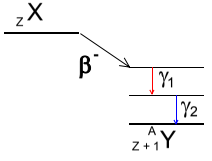

Observed counting : $N'_1 = N_1 - n_1$

$$N'_1 = N_1(1 - P_{12} \cdot \varepsilon^T(E_2))$$

Correction for the peak

$$C_1 = \frac{N_1}{N'_1} = \frac{1}{1 - P_{12} \cdot \varepsilon^T(E_2)}$$

P_{12} = Probability that E_2 photon is emitted just after the emission of E_1 photon

Starting point : level 1

What is possible : transition $\gamma 2$
What will give E_2 photon :
emission $\gamma 2$

$$P_{12} = \frac{I_{\gamma 2}}{T_{\gamma 2}}$$

$$C_1 = \frac{1}{1 - \frac{I_{\gamma 2}}{T_{\gamma 2}} \cdot \varepsilon^T(E_2)}$$

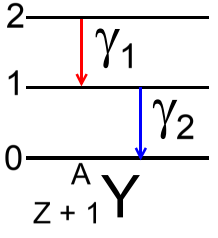

T_γ = gamma transition probability

I_γ = gamma emission intensity

Decay with 3 transitions :

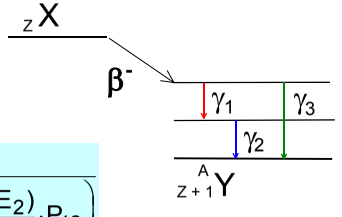

$$C_3 = \frac{N_3}{N'_3} = \frac{1}{\left(1 + \frac{I_{\gamma 1}}{I_{\gamma 3}} \cdot \frac{\varepsilon^P(E_1) \cdot \varepsilon^P(E_2)}{\varepsilon^P(E_3)} \cdot P_{12}\right)}$$

Example of a scheme with 2 levels :

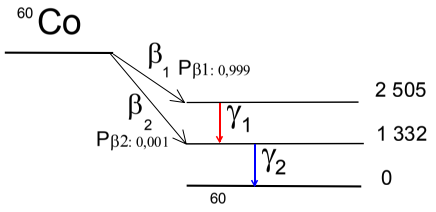

HPGe detector 60 cm³

Source-to-detector distance : 7 cm

	E (keV)	P_γ (%)	α^T	ε^P	ε^T
γ1	1 173	99,9	1,7 10^{-4}	1,35 10^{-2}	9 10^{-2}
γ2	1 332	100	1,3 10^{-4}	1,22 10^{-2}	9 10^{-2}

- Correction C_1:

$$C_1 = \frac{1}{1 - P_{12} \cdot \varepsilon^T(E_2)} = \frac{1}{1 - \frac{I_{\gamma 2}}{T_{\gamma 2}} \cdot \varepsilon^T(E_2)} = \frac{1}{1 - \frac{\varepsilon^T(E_2)}{1+\alpha_2}}$$

C_1 = 1/0,91 = 1,10

- Correction C_2 :

$$C_2 = \frac{1}{1 - P_{21} \cdot \varepsilon^T(E_1)} = \frac{1}{1 - \frac{I_{\gamma 1}}{T_{\gamma 1} + T_{\beta 2}} \cdot \varepsilon^T(E_1)} \approx \frac{1}{1 - \varepsilon^T(E_1)}$$

C_2 = 1/0,91 = 1,10

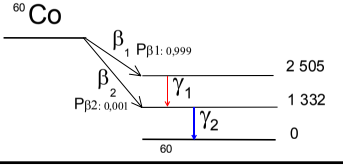

Correction examples for HPGe 100 cm³

Radionucléide	Energy (keV)	Point source at 1 cm	Point source at 10 cm	50 cm² vial at contact	500 cm² vial at contact
^{56}Co	846.8	1.241	1.018	1.122	1.060
	1238.3	1.317	1.023	1.167	1.080
	2598.5	1.169	1.011	1.065	1.031
^{57}Co	122.1	1.136	1.007	1.004	1.001
	136.5	0.941	0.995	0.978	0.992
^{60}Co	1173.2	1.092	1.008	1.061	1.030
	1332.5	1.095	1.008	1.062	1.031
^{88}Y	898.0	1.193	1.013	1.069	1.032
	1836.1	1.211	1.014	1.079	1.036
^{133}Ba	81.0	1.306	1.019	1.173	1.082
	356.0	1.246	1.014	1.114	1.046
^{139}Ce	165.9	1.110	1.006	1.054	1.023
^{152}Eu	121.8	1.263	1.018	1.157	1.076
	778.9	1.154	1.011	1.092	1.043
	1408.0	1.277	1.016	1.133	1.054

- Correction summing computation requires :
  - Knowledge of the decay scheme
  - Efficiency calibration (total and FEP)
- Consider all possible cascades
- Corrections gamma-X (N-type detector)
  - X resulting from internal conversion (competition with photon emission)
  - X resulting from electron capture
- B+ decay : coincidence with two 511 keV photons (annihiliation)

→ this can be taken into account using a modified decay scheme

- Remark : we neglected angular correlations between two photons …

Statistical noise : $\Delta E_S(1)$

- Cause : Statistical fluctuations of the number of charge carriers

  E : incident energy

  w : mean pair creation energy

$$n = \frac{E}{w}$$

- Hypothesis : Poisson statistics :

Standard deviation on the number of charge carriers $\sigma_n = \sqrt{n}$

-> Standard deviation on the deposited energy (n w)

$$\sigma_{E_S} = \sigma_n \cdot w = \sqrt{n} \cdot w = \sqrt{\frac{E}{w}} \cdot w = \sqrt{E \cdot w}$$

Statistical noise : $\Delta E_S(2)$

Example : (at 77K : w = 2,96 eV in Ge
w = 3,76 eV in Si)

E = 1 MeV -> in Ge : n = 3,3 10^5

$$\sigma_{E_S} = \sqrt{w \cdot E} = \sqrt{2{,}96 \cdot 10^6} = 1{,}72 \text{ keV}$$

$$FWHM = 2{,}355 \cdot \sigma_{E_S} = 4{,}05 \text{ keV}$$

The observed width is lower (< 2 keV)

-> F = Fano factor : $F = \frac{\text{Observed variance}}{\text{Poisson predicted variance}}$

Statistical noise : $\Delta E_S(3)$

$$\Delta E_S(E) = 2{,}355 \cdot \sqrt{F \cdot w \cdot E}$$

- Fano factor < 1 (charge creation are not independent : correlations)
- Measured for Ge and Si : value depending on the quality of the crystal ?

  Experimental values : (increasing versus time …)
  Ge : 0,07 to 0,12
  Si : 0,08 to 0,12

Electronical noise : ΔE_E

- Preamplifier – amplifier
  - Independent on the energy
  - Can be determined using a pulser : input at the preamplifier

Charge collection : ΔE_C

Resolution

- Cause : loss of charge carriers (ballistic effect)
  - Trapping (impurities or crystal imperfections) :
    loss of charge or slowing of the rate of charge collection
  - Depends on the quality of the crystal and on the electric field (position of the interaction in the detector)

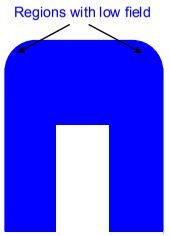

- Consequence of the loss of charge :
  Low-energy tailing
- Improvement :
  - Increasing the voltage
  - Rejecting pulses with slow rise-time
  - Using collimator to avoid interaction in low electric field regions (front corners)

Thank you very much for your attention

Log *ft* values in Beta Decay

Filip G. Kondev

kondev@anl.gov

Nuclear Engineering Division

Argonne National Laboratory

A U.S. Department of Energy
Office of Science Laboratory
Operated by The University of Chicago

Some useful references

Books

- ✓**"Week interaction and nuclear beta decay", H.F. Schopper, 1966**
- ✓**"Handbook of nuclear spectroscopy", J. Kantele, 1995**
- ✓**"Radiation detection and measurements", G.F. Knoll, 1989**
- ✓**"Alpha-, Beta- and Gamma-ray Spectroscopy", Ed. K. Siegbahn, 1965**

Journal Articles

- ✓**W. Bambynek et al., Rev. Mod. Phys. 49 (1977) 77**
- ✓**N.B. Gove and M.J. Martin, Nuclear Data Tables 10 (1971) 205**
- ✓**S. Raman and N.B. Gove, Phys. Rev. C7 (1973) 1995**
- ✓**B. Singh et al., Nuclear Data Sheets 84 (1998 487**

Plenty of information available on the Web

Introduction

Beta Decay: universal term for all weak-interaction transitions between two neighboring isobars

Take place is 3 different forms
β–, β+ & EC (capture of an atomic electron)

β+: p → n + e+ + ν

EC: p + e- → n + ν

β–: n → p + e- + $\tilde{\nu}$

a nucleon inside the nucleus is transformed into another

Classification of β decay transition

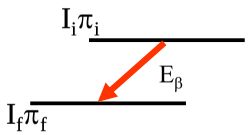

$$I_i = I_f + L_\beta + S_\beta \qquad \pi_i\pi_f = (-1)^{L_\beta}$$

$$L_\beta = l_{\beta-(\beta+)} + l_{\tilde{\nu}(\nu)} \qquad S_\beta = s_{\beta-(\beta+)} + s_{\tilde{\nu}(\nu)} = \begin{cases} 0 \\ 1 \end{cases} \begin{matrix} \uparrow\downarrow \\ \downarrow\downarrow or \uparrow\uparrow \end{matrix}$$

$L_\beta = n$ defines the degree of forbiddenness (n)

allowed

when $L_\beta = n = 0$ and $\pi_i\pi_f = +1$

$$\Delta I = |I_i - I_f| \equiv 0,1$$

forbidden

when the angular momentum conservation requires that $L_\beta = n > 0$ and/or $\pi_i\pi_f = -1$

Classification of allowed decay

$(\pi_i \pi_f = +1)$

Fermi

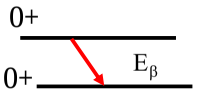

$\Delta I = |I_i - I_f| \equiv 0$

$L_\beta = 0 \quad S_\beta = 0 \downarrow\uparrow$

Gamow-Teller

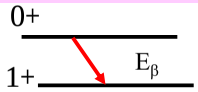

$\Delta I = |I_i - I_f| \equiv 1$

$L_\beta = 0 \quad S_\beta = 1 \uparrow\uparrow or \downarrow\downarrow$

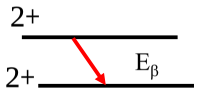

mixed Fermi & Gamow-Teller

$\Delta I = |I_i - I_f| \equiv 0 \qquad I_i \neq 0$

Classification of β decay transitions

Type of transition	Order of forbiddenness	ΔI	$\pi_i\pi_f$
Allowed		0,+1	+1
Forbidden unique	1	∓2	-1
	2	∓3	+1
	3	∓4	-1
	4	∓5	+1
	.	.	.
Forbidden	1	0, ∓1	-1
	2	∓2	+1
	3	∓3	-1
	4	∓4	+1
	.	.	.

Some useful empirical rules

The fifth power beta decay rule:

the speed of a β transition increases approximately in proportion to the fifth power of the total transition energy (if other things are being equal, of course)

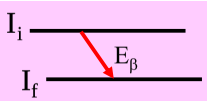

$$\frac{1}{\tau} \propto [(M(Z) - M(Z \pm 1))c^2]^5$$

- **depends on spin and parity changes between the initial and final state**
- **additional hindrance due to nuclear structure effects – isospin, "l-forbidden", "K-forbidden", etc.**

β decay lifetime

$t \equiv T_{1/2}^{\beta_i} = \frac{T_{1/2}^{\exp}}{P_{\beta_i}}$ partial half-life of a given $\beta^-(\beta^+,EC)$ decay branch (i)

$$\frac{\ln 2}{T_{1/2}^n} = \frac{g^2}{2\pi^3} \int^W p_e W_e (W_0 - W_e)^2 F(Z, W_e) C_n dW_e$$

g – week interaction coupling constant

p_e – momentum of the β particle

W_e – total energy of the β particle

W_0 – maximum energy of the β particle

$F(Z,W_e)$ – Fermi function – distortion of the β particle wave function by the nuclear charge

C_n – shape factor

Z – atomic number

β decay Hindrance Factor

$$HF_{\beta}^{n} = \frac{T_{1/2}^{\beta_i}}{T_{1/2}^{n}} = \left(\frac{g^2\eta^2}{2\pi^3 \ln 2}\right) f_n t$$

$$f_n = \int^{W} p_e W_e (W_0 - W_e)^2 F(Z, W_e)(C_n/\eta^2) dW_e$$

statistical rate function (phase-space factor): the energy & nuclear structure dependences of the decay transition

η^2 contains the nuclear matrix elements

Log *f*

- ENSDF analysis program LOGFT – both Windows & Linux distribution
  http://www.nndc.bnl.gov/nndcscr/ensdf_pgm/analysis/logft/
- LOGFT Web interface at NNDC http://www.nndc.bnl.gov/logft/

Log *ft* values

$$\log ft = \log f + \log t$$

coming from calculations — coming from experiment

Decay Mode	Type	ΔI ($\pi_i\pi_f$)	log *f*
β– EC + β+	allowed	0, +1 (+)	$\log f_0^-$ $\log(f_0^{EC} + f_0^+)$
β– EC + β+	1st-forb unique	∓2 (-)	$\log f_0^- + \log(f_1^-/f_0^-)$ $\log[(f_1^{EC} + f_1^+)/(f_0^{EC} + f_0^+)]$

N.B. Gove and M. Martin, Nuclear Data Tables **10** (1971) 205

Log *t*

$$t \equiv T_{1/2}^{\beta_i} = \frac{T_{1/2}^{\exp}}{P_{\beta_i}}$$

$$P_{\beta_i} = \eta[I^{tot}(out) - I^{tot}(in)]$$

$$I^{tot}(out/in) = \sum_i I_{\gamma_i}(1+\alpha_{T_i})$$

$$\alpha_T(M1+E2) = \frac{\alpha_T(M1) + \delta^2 \alpha_T(E2)}{1+\delta^2}$$

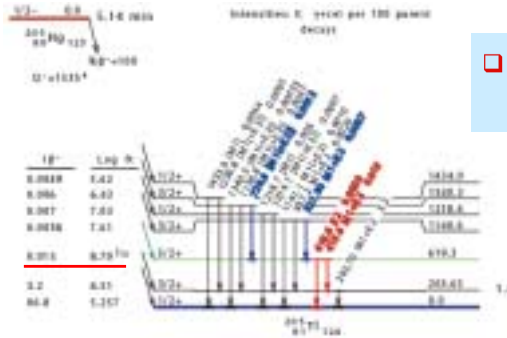

- What we want to know accurately
  ✓$T_{1/2}$, I_γ, α_T & δ

In

$$\frac{I^{tot}(521+721) = 0.086(16)}{I^{tot}(416+619) = 0.78(10)} = 0.69(10) \text{ (net)}$$

Out

$\eta = 0.0022 \rightarrow t = 2.056\times10^6[s] \rightarrow \log t = 6.31 \rightarrow \log f = 2.386 \rightarrow \log ft = 8.7$

Rules for Spin/Parity Assignments

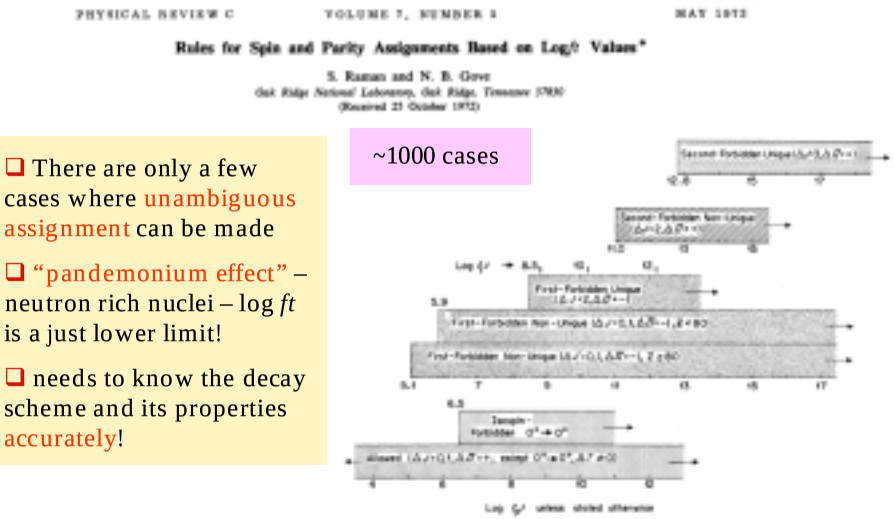
PHYSICAL REVIEW C VOLUME 7, NUMBER 5 MAY 1973

Rules for Spin and Parity Assignments Based on Log f Values*

S. Raman and N. B. Gove

- There are only a few cases where unambiguous assignment can be made
- "pandemonium effect" – neutron rich nuclei – log *ft* is a just lower limit!
- needs to know the decay scheme and its properties accurately!

~1000 cases

Log *ft* values review

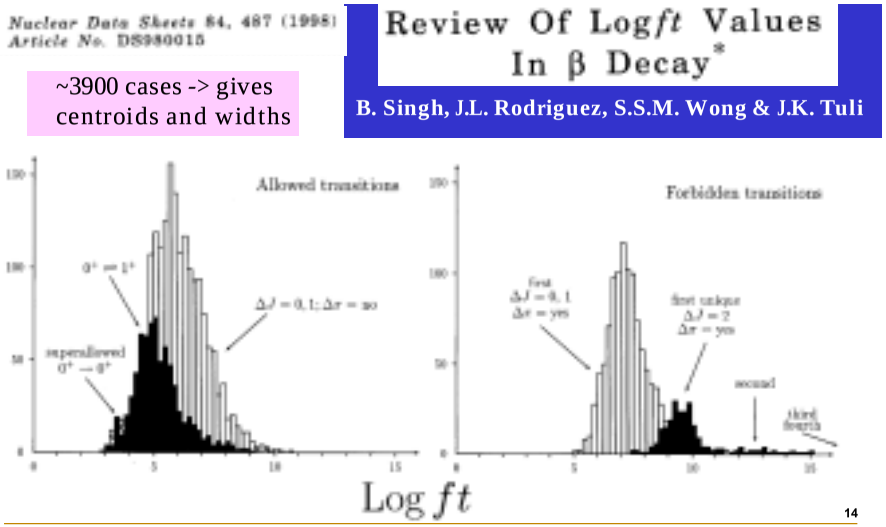
Nuclear Data Sheets 84, 487 (1998)
Article No. DS980015

Review Of Log*ft* Values In β Decay*

B. Singh, J.L. Rodriguez, S.S.M. Wong & J.K. Tuli

~3900 cases -> gives centroids and widths

Allowed transitions

Forbidden transitions

superallowed $0^+ \rightarrow 0^+$

$\Delta J = 0, 1; \Delta\pi = no$

first $\Delta J = 0, 1$ $\Delta\pi = yes$

first unique $\Delta J = 2$ $\Delta\pi = yes$

second

third fourth

Log *ft*

Implications to DDEP evaluations

$$\log ft = a \qquad t \equiv T_{1/2}^{\beta_i} = \frac{T_{1/2}^{\exp}}{P_{\beta_i}}$$

$$\log f + \log T_{1/2}^{\exp} - \log P_{\beta_i} = a$$

$$\log f + \log T_{1/2}^{\exp} - a = \log P_{\beta_i}$$

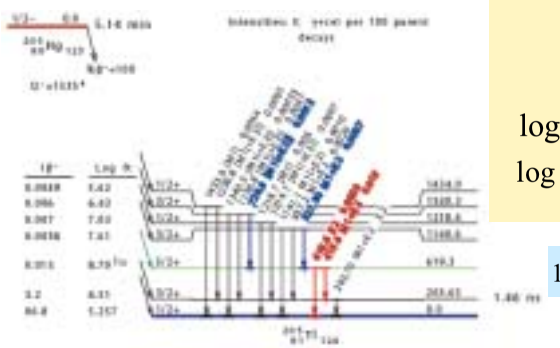

$$a = \log ft = 9.5(8)$$

from systematics

$\log f = 2.39$ **from calculations**

$\log T_{1/2}^{\exp} = 2.49$ **from experiment**

$$1.5\times10^{-2} > P_{\beta_i} > 3.8\times10^{-4}$$

$$P_{\beta_i}(\exp t) = 0.012(8)$$

...but be careful, nuclear structure is important

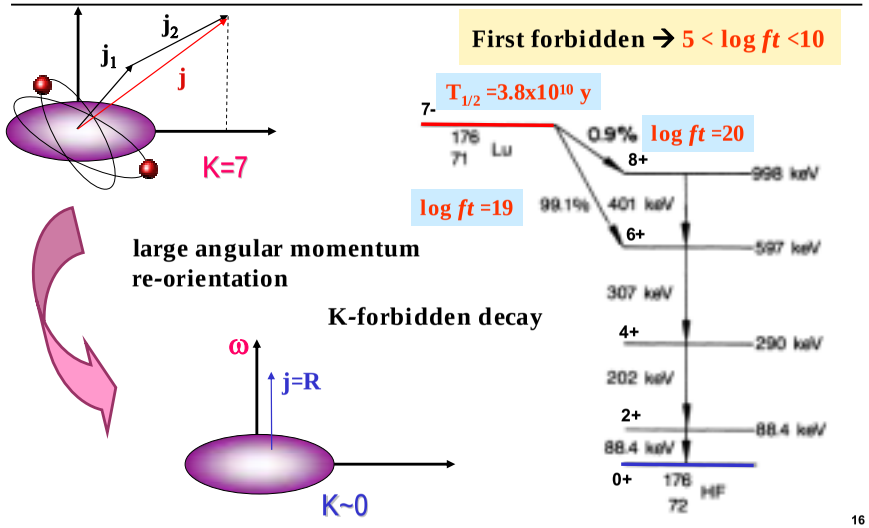

Workshop on
DECAY DATA EVALUATION

Saclay, March 6 – 10, 2006

Edgardo Browne

α Hindrance factors

The probability of α decay depends on the:

- Energy of the α particle
- Parent and daughter nuclear structure configurations

A useful definition of *hindrance factor* is:

$$HF = T_{1/2}(\alpha)\ exp./T_{1/2}(\alpha)\ theor.$$

Notice that $T_{1/2}(\alpha) = T_{1/2}/\ \alpha$ branching.

HF depends only on the nuclear structure configurations. The energy dependence has been removed.

$T_{1/2}(\alpha)$ theor. is from "The Theory of Alpha Radioactivity," M.A. Preston, *Phys. Rev.* ***71****, 865 (1947!!)*

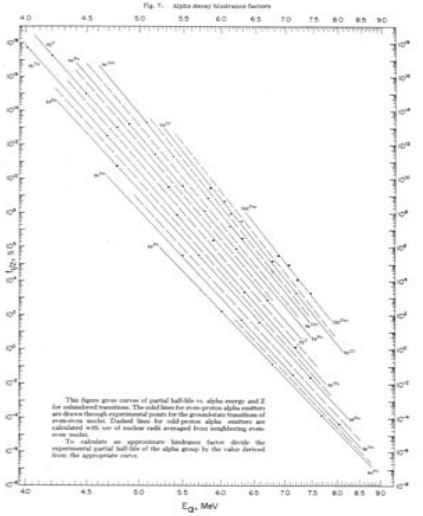

HF(0+ to 0+, even-even nucleus) = 1
by definition. All other hindrance factors are relative to this value.

Hindrance factors for odd-A and odd-odd nuclei are relative to HF values for the 0+ to 0+ α transitions in the neighboring even-even nuclei

The Radius Parameter r_0

This parameter is roughly equivalent to the nuclear radius, and it may be determine for each nucleus from the 0+ to 0+ α transition in even-even nuclei, and assuming HF=1.

See "Review of Alpha-Decay Data from Doubly-Even Nuclei," Y.A. Akovali, *Nucl. Data Sheets* ***84****, 1 (1998).*

Favored alpha-particle transition in odd-A nuclei

If HF < 4 then initial and final levels have the same spin (J) and parity (π).

For even-A nuclei

If one of the levels has J=0, the parity change is given by

$$\Delta\pi = (-1)^{\Delta J}$$

The radius parameter r_0 (Y. Akovali, Oak Ridge)

- Odd-N nucleus (Z, A)
  $r_0(Z, N) = [r_0(Z, N-1) + r_0(Z, N+1)]/2$
- Odd-Z nucleus (Z, A)
  $r_0(Z, N) = [r_0(Z-1, N) + r_0(Z+1, N)]/2$
- Odd-Odd nucleus (Z, A)
  $r_0(Z, N) = [r_0(Z, N-1) + r_0(Z, N+1)]/2 =$
  $[r_0(Z-1, N+1)+r_0(Z-1, N-1)+r_0(Z+1, N+1) +r_0(Z+1, N-1)]/4$

Example

$^{219}Rn \Rightarrow ^{215}Po$ (Odd-N)

r_0 (Z=84, N=131) = [r_0(84, 130) + r_0(84, 132)] /2

From 1998Ak04:

r_0(84,214) = 1.559 *8*

r_0(84,216) = 1.5555 *2*, therefore

r_0 (Z=84, N=131) = 1.557

Use Table 1 – "Calculated r_0 for even-even nuclei" (1998Ak04). Insert R0= … in *comment* record:

CA HF R0=…

Run program ALPHAD to calculate hindrance factors.

HF(401 keV) = 3.4 (Favored α decay).

Estimating an α-decay branching

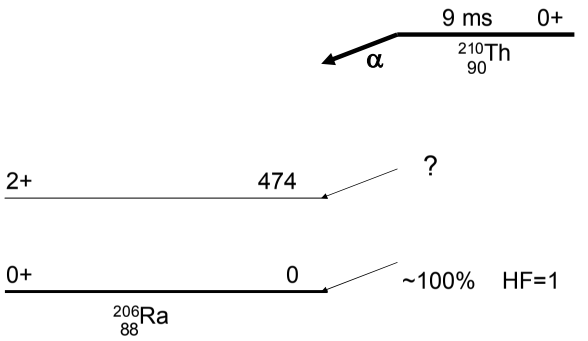

HF Systematic for Even-even Thorium Nuclei

Parent nucleus	Jπ	Daughter nucleus	Jπ	HF
^{210}Th	0+	^{206}Ra	2+	**?**
^{228}Th	0+	^{224}Ra	2+	0.92
^{230}Th	0+	^{226}Ra	2+	1.1
^{232}Th	0+	^{228}Ra	2+	1.0

We expect HF(^{210}Th) ~ 1

Computer Program ALPHAD

		Z	A			
		90.	210.			
Q ALPHA	E TOTAL	ALPHA HALF LIFE	RADIUS	RZERO	TOTAL HALF LIFE	ALPHA BRANCH
8.0530	8.0881	1.042E-07 D	9.0867E-13	1.5386	9.000E-03 S	1.000E+00

ENERGY LEVEL	ABUNDANCE	CALC. HALF LIFE	HINDRANCE FACTOR
0.00	1.00E+00	1.04E-07	1.00E+00
474.00	1.00E-01	3.35E-06	3.11E-01
474.00	5.00E-02	3.35E-06	6.22E-01
474.00	3.00E-02	3.35E-06	1.04E+00
474.00	1.00E-02	3.35E-06	3.11E+00
474.00	5.00E-03	3.35E-06	6.22E+00
474.00	3.00E-03	3.35E-06	1.04E+01
474.00	1.00E-03	3.35E-06	3.11E+01
474.00	1.00E-04	3.35E-06	3.11E+02

So α(474)~ 3%

Decay Data Evaluation Project

"Training workshop"

Saclay, Laboratoire National Henri Becquerel

The evaluation of atomic masses present and future

Georges Audi Csnsm March 7, 2006

- nuclear data: dynamic and static large lines
- evaluation of static nuclear data: Ensdf - Ame - Nubase
- the Atomic Mass Evaluation (AME)
  - the experimental data
  - data evaluation • data treatment + some special treatments
  - adjusted masses
  - regularity - estimated unknown masses
- the future of Ame & Nubase
- conclusion: best possible experimental masses
  & best possible evaluation of data

Ame2003 and Nubase2003

Aaldert H. Wapstra Amsterdam
Olivier Bersillon Bruyères-le-Châtel
Catherine Thibault Orsay
Jean Blachot Grenoble

Ame2008 and Nubase2008

Aaldert H. Wapstra Amsterdam
....

"THE 2003 ATOMIC MASS EVALUATION"

Nuclear Physics A729 (2003) 129

"THE NUBASE EVALUATION OF NUCLEAR AND DECAY PROPERTIES"

Nuclear Physics A729 (2003) 3

- -

1993	1995	1997	2003	2008	2013
Ame'93	Ame'95	Nubase'97	Ame2003	Ame2008	Ame2013
full	update		Nubase2003	Nubase2008	Nubase2013

texts, tables, figs and bonus on the Web of Amdc

http://amdc.in2p3.fr/

http://www.nndc.bnl.gov/amdc/

ISOMERS AND NUBASE

- gs – isomer identification
  - if γ-emission $\Rightarrow$NSDD
  - if no γ $\Rightarrow$decay energy to other nuclide
    $\Longrightarrow$ AME
- NUBASE 'horizontal' evaluation
  - half-lives
  - spin and parities
  - decay modes
    - $\Longrightarrow$which state is the ground-state
    - $\Longrightarrow$which states are involved in a mass relation
- Other needs for NUBASE
  - radioactive parameters for calculations
    - reactors
    - waste management
    - nuclear astrophysics
    - prepare nuclear physics experiment

csnsm *G. Audi*

NUCLEAR DATA

- Static Nuclear Data
  - masses
  - $T_{1/2}$ & J^{π}
  - excitation energies
  - decay modes at rest and intensities
  - decay from excited states
  - neutron capture cross-sections
  - magnetic moments & radii
  - ...
- Dynamic Nuclear Data
  - reaction cross-sections
  - reaction rates
  - reaction mechanisms
  - spectroscopic factors
  - ...

csnsm *G. Audi*

"HORIZONTAL EVALUATIONS"

- Atomic Mass Evaluation AME
  - Wapstra since 1959 + G.A. since 1981
- NUBASE
  - Blachot, Bersillon, Wapstra, GA (1993)
- Radii, spins and moments from
  - isotope shifts - hyperfine structure - Otten 1989
  - ... isotope shifts: Aufmuth (1987)
  - ... moments: Raghavan (1989) + Stone(1999)
  - ... radii: Angeli 1991 – Nadjakov 1994
- Isotopic abundances
  - Holden
- E_{2^+} and $B(E2)$ of e-e nuclides
  - Raman et al.
- ...
  - ...

csnsm *G. Audi*

"Static" Nuclear Data

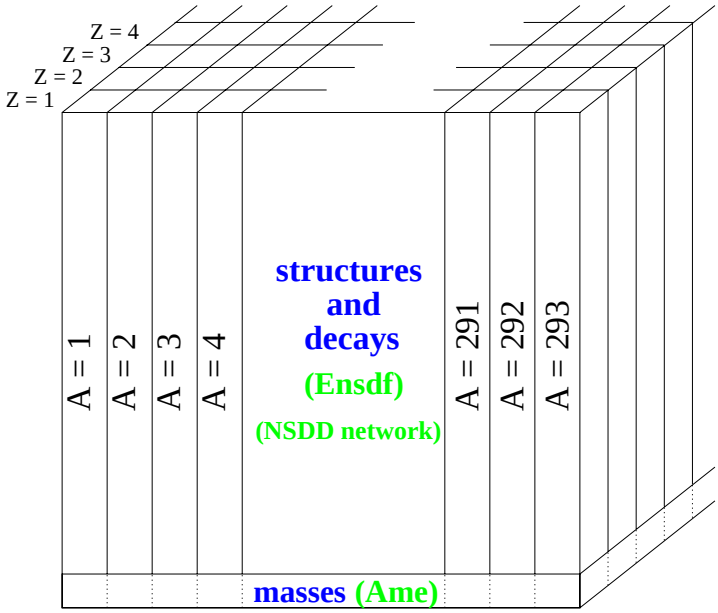

Ame: created by A.H. Wapstra (Amsterdam) in 1959
since 1981 together with G. Audi (Csnsm − Orsay)

interaction Ame ⟷ Ensdf

=> NUBASE : masses
isomers E^m
$T_{1/2}$
J^{π}
decay modes & intensities

The Ame ("Atomic Mass Evaluation")

- Experimental Data
  - Energy relation: reactions - decays $\longrightarrow$ relative meas.
  - Inertial mass in EM field $\longrightarrow$ relative measurement
- Data Evaluation
- Treatment of Data
  - Least Squares Method
  - Flow of Information
  - Consistency of Data
- Estimates for Unknown Masses
  - From S_{2n} - S_{2p} - Q_α - ...
  - From difference with a smooth function

Experimental Data

- Energy Relation
  expressed in eV or keV

  keV*: *standard* volt
  adopt a value for $2e/h$ in Josephson

  keV: *international* volt
  from evaluation of fundamental constants
- Inertial mass in EM field
  expressed in u or μu, the
  "unified mass unit"
  $1\text{u} = \mathcal{M}(^{12}\text{C})/12$ since 1960

Conversion factor:

$1\text{u} = 931\,494.009\,0 \pm 0.007\,1$ keV*
$1\text{u} = 931\,494.013 \pm 0.037$ keV

Precision for ^{28}Si

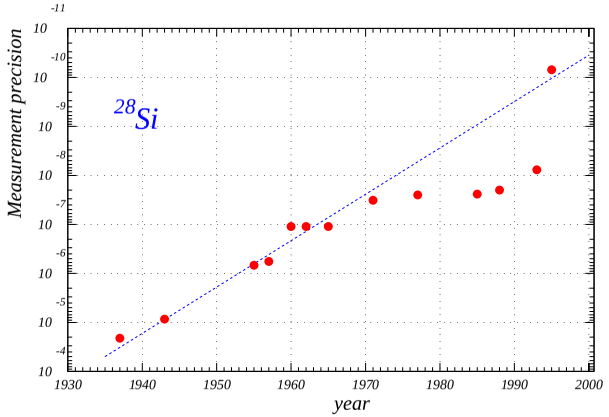

One order of magnitude every 10 years

- 1937: 600 keV
- 1970-1990's "plateau" at 0.7 keV
- 1993: Stockholm-trap + (p,γ) + Manitoba-Spectr + (p,α)
- 1995: pure MIT-trap 2 eV
- 2005: expected 0.2 eV who & where

DATA EVALUATION

1 - Data Collection
* hidden data
* all available experimental data
even poor ones (flagged accordingly)

2 - Careful Reading
* evaluate or re-evaluate
calibration procedures & calibrants
accuracies of the measurements
* examine spectra
* select PRIMARY information

3 - Comparison
* to previous results
$\longrightarrow$ direct results
$\longrightarrow$ combination of other results
* to estimates from extrapolations
(regularity of the Mass-Surface)
* to estimates from models

4 - Dialogue
* asking complementary information
* suggesting different analyses
* suggesting new measurements

evaluator = referee $\oplus$ anonymous collaborator $\oplus$ .....

csnsm G. Audi

G. Audi slide 984-16

DATA-file

```
205 890806000a1 W    40Kr08     1620    200    205Hg(B-)205Tl
205 890806000a2 W    51Ly10     1750    200    205Hg(B-)205Tl
205 890816000c1 B    78Pe08     41.4    1.1    205Pb(e)205Tl          .525    .008 LM
205 890826000b1 P    62Bo25,W   2701.4  10.    205Bi(B+)205Pb         976     10   E+
205 890826000b2 P    62Pe08,W   2715.4  10.    205Bi(B+)205Pb         990     10   E+
205 890826000b3 W    AHW  *W E+ to 703.44 level
205 890836000b1 W    69Ho37,W   3390    150    205Po(B+)205Bi         3E-3    1    p+
205 890836000b2 W    AHW  *W Positrons to 849.83 and 1001.22 levels
```

REFERENCE-file

```
78Pa11 PRVCA  18,1249  Pardo,R.C., E.Kashy, W.Benenson, L.W.Robinson
78Pa12 .PRVCA 18,1277  Paschopoulos,I., E.Muller, H.J.Korner, I.C.Oelrich, K.E.Rehm, H.J.Scheerer
78Pe08 NUPAB 302,   1  Pengra,J.G., H.Genz, R.W.Fink
78Pf01 PRLTA  41,   63 Pfeiffer,L.P., A.P.Mills,Jr., R.S.Raghavan, F.Achandros
78Ra15 PRVCA  18,1085  Rao,G.R., G.Azuelos, J.C.Kim, J.P.Martin, P.Taras
```

MASS-file

```
204 0880   5990#   270#   204Ra
205 0800  -22311      6   205Hg   5.2  m   1/2-
205 0810  -23845      4   205Tl   stbl     1/2+
205 0820  -23791      4   205Pb   15.2 My  5/2-
205 0830  -21083      8   205Bi   15.3 d   9/2-
```

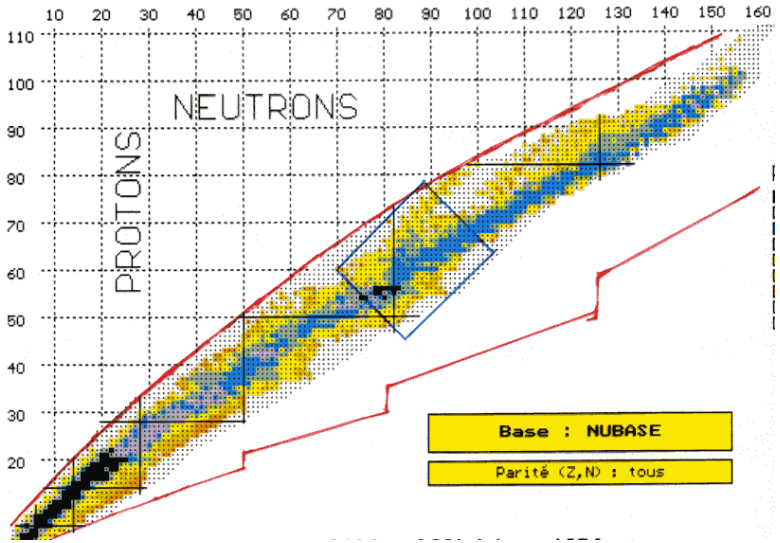

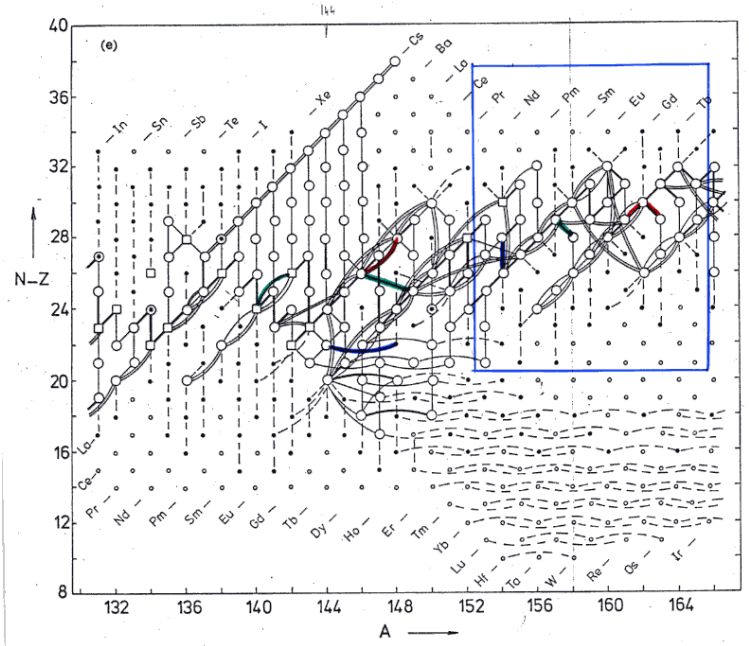

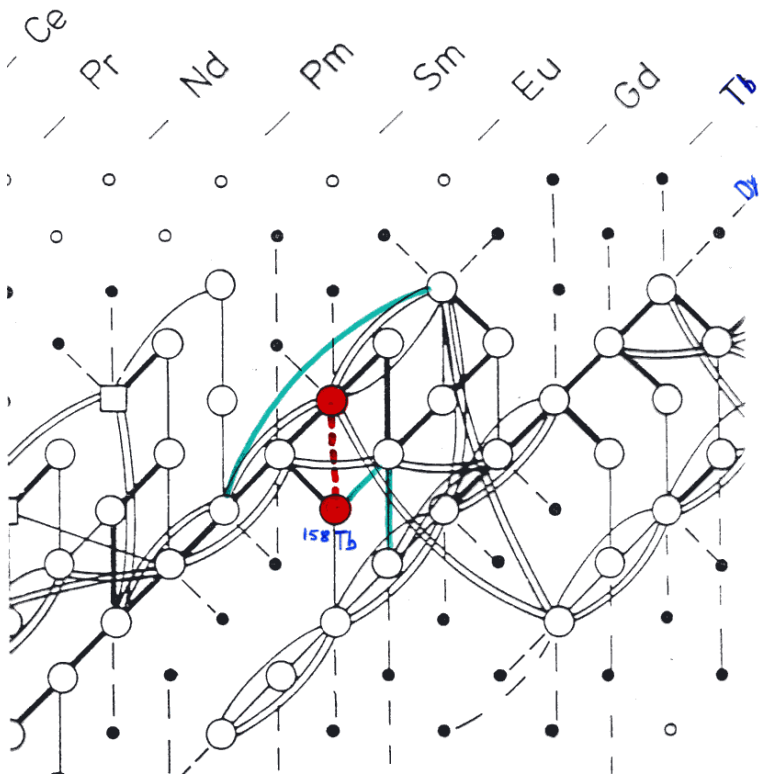

The Ame ("Atomic Mass Evaluation")

- Treatment of Data
  - Least Squares Method
    - answer vector
    - adjusted values for the data
  - Flow of Information
    - influence of each datum on each mass
  - Consistency of Data
    - with other combination(s)
    - with expectation from extrapolations
    - with expectation from models

Treatment of Data - LSM - 1

Q data $q_i \pm dq_i$

M unknown quantities m_μ with $Q > M$

Q equations to M parameters overdetermined

$\sum_{\mu=1}^{M} k_i^\mu m_\mu = q_i \pm dq_i \Rightarrow \boxed{\mathbf{K}|m\rangle = |q\rangle}$

and the diagonal weight matrix $\mathbf{W}$: $w_i^i = 1/(dq_i dq_i)$

Very simple construction

$${}^{t}\mathbf{KWK}|m\rangle = {}^{t}\mathbf{KW}|q\rangle$$

$$\mathbf{A}|m\rangle = {}^{t}\mathbf{KW}|q\rangle$$

$\mathbf{A}$ normal matrix square, positive, symmetric and regular

$\Rightarrow$ invertible : $\mathbf{A}^{-1}$

$|\overline{m}\rangle = \mathbf{A}^{-1}\ {}^{t}\mathbf{KW}|q\rangle \Rightarrow \boxed{|\overline{m}\rangle = \mathbf{R}|q\rangle}$

"Flow-of-information" matrix : $\Rightarrow \boxed{\mathbf{F} = {}^{t}\mathbf{R} \otimes \mathbf{K}}$

NIM 249 (1986) 443

Treatment of Data - LSM - 1a

adj. value of exp. data $\Rightarrow \boxed{|\overline{q}\rangle = \mathbf{KR}|q\rangle}$

Consistency of data

$v_i = (\overline{q}_i - q_i)/dq_i \Rightarrow \chi^2 = \sum_{i=1}^{Q} v_i^2$

expected $\chi_{expect} = Q - M \pm \sqrt{2(Q-M)}$

normalized χ_n = consistency factor = Birge ratio

$\chi_n = \sqrt{\chi^2/(Q-M)}$ $\chi_{n-expected} = 1 \pm 1/\sqrt{2(Q-M)}$

Partial consistency factor, χ_n^p, for a group of p data:

$$\chi_n^p = \sqrt{\frac{Q}{Q-M}\ \frac{1}{p}\ \sum_{i=1}^{p} v_i^2}.$$

Treatment of Data - Least Squares Method - 2

Typical Sizes (Ame'2003 numbers)

6848 experimental data

(but U=1230 B=207 C=58 D=37 F=72)

5244 valid input exp. data + 887 estim. $\Rightarrow Q = 6131$

3504 masses (including 1073 estimates for unknowns) $\Rightarrow M = 3504$

Reducing the System

Pre-averaging $\Rightarrow Q = 4038$ $M = 3504$

Separating "Secondaries" (2657) $\Rightarrow Q = 1381$ $M = 847$

Least Squares Adjustment

Total χ^2= 814 (expected 534 ± 33)

$\Rightarrow$ on the average σ's underestimated by 27% for energy data and 16% for mass spectrometry

Distribution of the deviations (v/s)

$\sigma > 1$	$\sigma > 2$	$\sigma > 3$
15%	3.2%	0.007%

TREATMENT OF DATA - Least Squares Method - 3

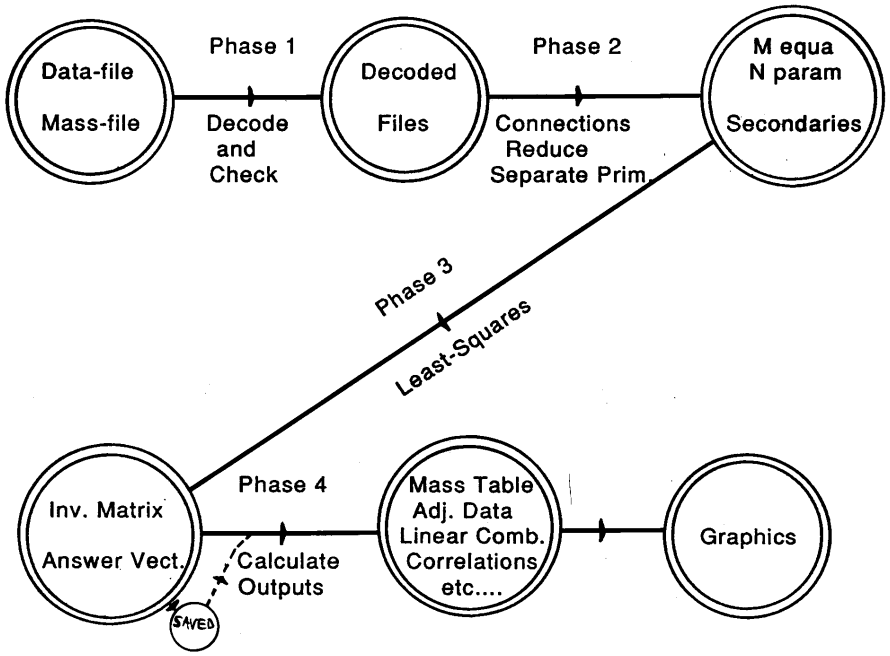

Special Treatments I

- Asymmetric Errors X^{+a}_{-b}

  Symmetrize the probab. distribution:

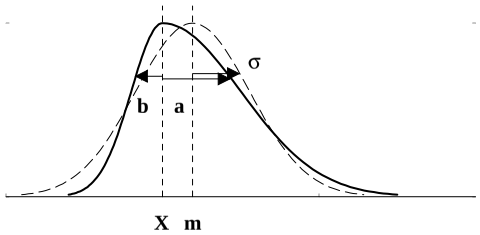

  - Rough symmetrization

    $X+\frac{1}{2}(a-b) \quad \pm \quad \frac{1}{2}(a+b)$
  - Rigourous symmetrization (cf. Nubase2003)

    $X+0.64(a-b) \quad \pm \quad \sqrt{(1-\frac{2}{\pi})\,(a-b)^2+ab}$

Special Treatments II

- Range of Values X_{min}-X_{Max}

  Moments of the probab. distribution:

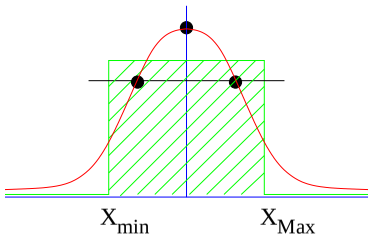

$\frac{1}{2}(X_{min}+X_{Max}) \quad \pm \quad 0.29(X_{Max}-X_{min})$

Special Treatments III-a

- Mixture of two lines

  Two lines are known to exist at: M_{gs} M_m

  but relative population NOT known

  Assume equal probablitiy for all population ratio

  The mixture will appear at any value between M_{gs} and M_m

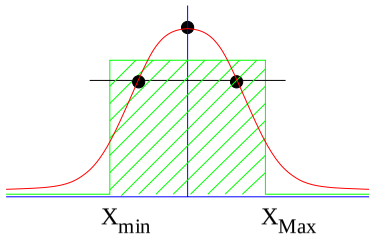

same as preceding view: $M_{exp}=\frac{1}{2}(M_{gs}+M_m) \quad \pm \quad 0.29(M_m-M_{gs})$

the ground-state mass ($E_1=M_m-M_{gs}$) :

$M_{gs}=M_{exp}-0.5E_1 \quad \pm \quad \sqrt{(\sigma^2_{exp}+(\frac{1}{2}\sigma_1)^2+(0.29E_1)^2}$

Special Treatments III-b

- Mixture of three lines

  Three lines are known to exist at: M_{gs} M_{m1} M_{m2}

  (see demonstration in Ame2003, p. 176):

  the ground-state mass:

  $$M_{gs} = M_{exp} - \tfrac{1}{3}(E_1 + E_2)$$

  and its error:

  $$\sigma_{gs}^2 = \sigma_{exp}^2 + (\tfrac{1}{3}\sigma_1)^2 + (\tfrac{1}{3}\sigma_2)^2 + \tfrac{1}{18}(E_1^2 + E_2^2 - E_1 E_2)$$

The Ame ("Atomic Mass Evaluation")

- Regularity of the mass-surface

  Smoothness and structures

  Surface in 3D space

  Structures on the Surface: Shells - Deformations - Wigner

  Regularity is a basic property of the surface of masses

  Consequences :

  New Physics

  Outliers

  Conflict among Data

  Estimate unknown masses

Regularity of the Mass Surface I

- Surface in 3D space
- Pairing Energy ⇒ 4-sheets
  - nearly parallel in all directions
  - smooth variations in N and Z

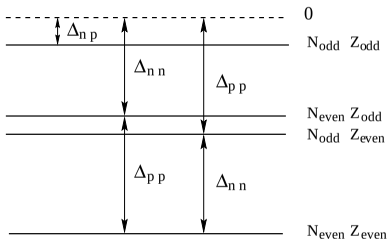

Caveat: smooth = continuous non-staggering

smooth ≠ slow

- Structures on the Surface:

  Shells - Deformations - Wigner

- Conclusion: Regularity is a Basic Property

Regularity of the Mass Surface II

- New Physics
  - Coherent deviations in (N, Z)

    ⇒ new physical property (e.g. $^{23}N_{15}$ $N = 108 - 115$ Cs_{63-112})
- Outliers
  - One single 'Irregularity'

    ⇒ question correctness of datum

    re-measure same and/or measure neighbors

    strongly deviating 1-experiment (chaotic surf.):

    ⇒ replace by estimated 'recommended' value
- Conflict among Data

  ⇒ which one agrees with estimate?
- Unknown Masses

  ⇒ Estimates : Interpolate - Extrapolate

Regularity of the Mass Surface III

- Extrapolations (short extrapolations)
  - from regularity of the surface of masses
    - for medium and heavy nuclides
  - knowledge of n-stable or n-unstable
    - for light n-rich nuclides
    - similar for p-rich ← but Coulomb !!
  - mirror and IMME
    - for light p-rich nuclides

Csnsm Georges Audi

Scrutinizing the surface of masses

Derivatives of the Mass Surface

Separation energies : S_n S_{2n} S_p S_{2p}
Decay energies: Q_α Q_β $Q_{\beta\beta}$
Pairing energies : Δ_{nn} Δ_{np} Δ_{pp}

function of Z N A $N-Z$ $2Z-N$
1-2 isolines Z N A $N-Z$ $2Z-N$
(pb: same sheet - extrap. - double movement - ....)

Subtracting a simple function

subtracting results from a model
- spherical Groote-Hilf-Takahashi
- spherical Duflo-Zuker
  - (pb: shell migrations ...)

subtracting a Bethe and Weizsäcker formula
$\mathcal{M}(N,Z) = N\mathcal{M}_n + Z\mathcal{M}_H - \alpha A + \beta\frac{(N-Z)^2}{A} + \gamma A^{\frac{2}{3}} + \frac{3}{5}\frac{e^2Z^2}{r_0 A^{\frac{1}{3}}}$
- plus a pairing term to lessen oscillations

Csnsm Georges Audi

06

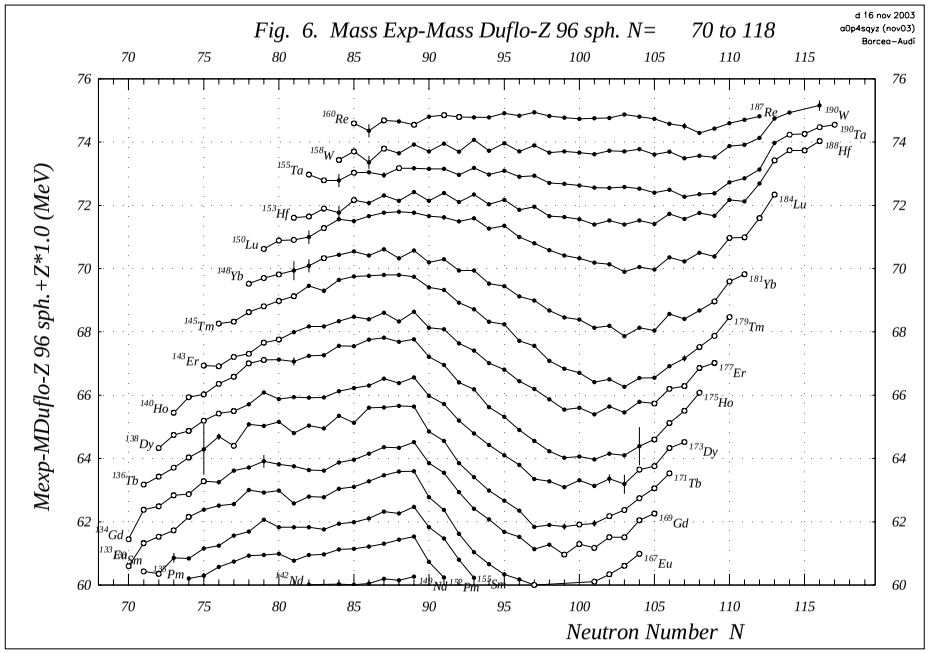

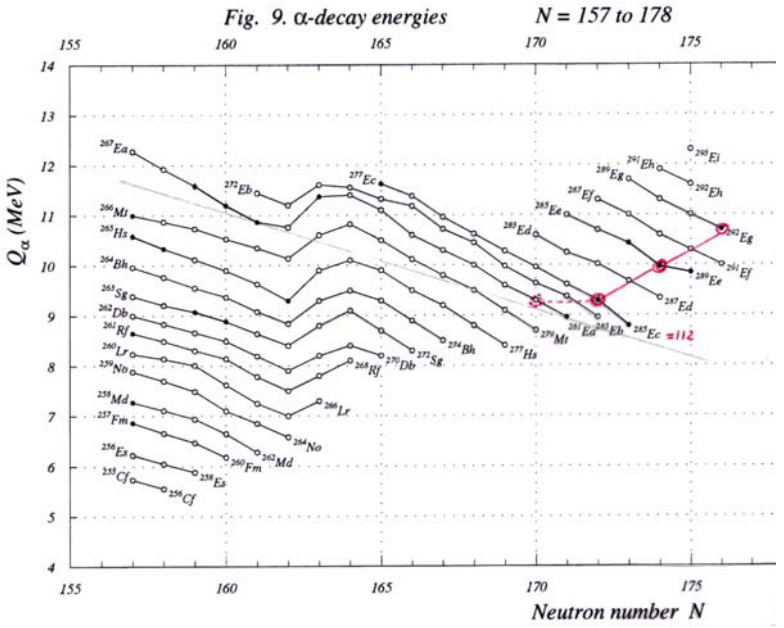

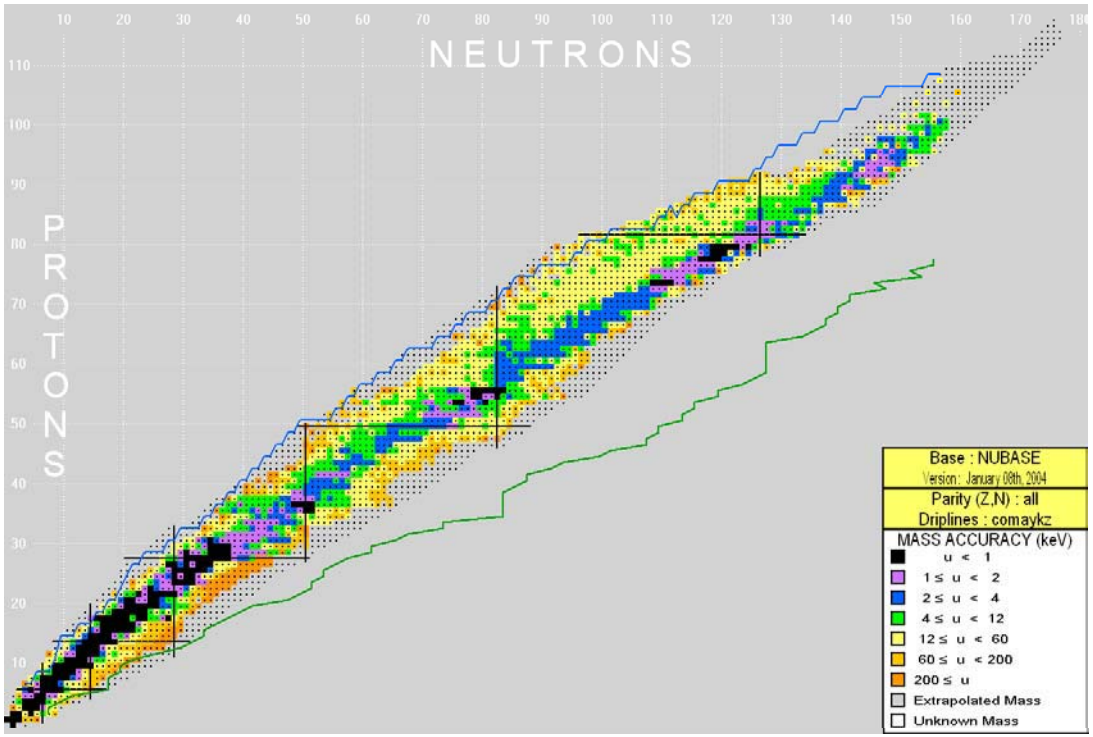

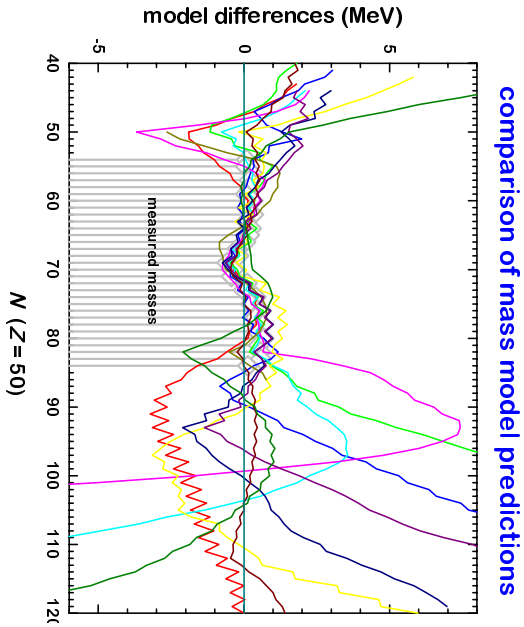

TO CONCLUDE

- Deriving a mass value from one or several experiments

  sometimes not easy

- Mathematical tools (LSM)

  + computer tools
  + evaluator's judgment

  are essential ingredients to reach the best possible mass-values

---

- unknown masses
  - close to last ones : predicted from extension of mass surface
  - further out : derived from models.

    but models diverge!!! (10's of MeV in region of r-process)

- therefore (besides best possible experimental data):
  - best possible evaluation of masses ⟶ best set of mass values

    on which models may 1) adjust their parameters
    2) improve predictions further away

A Lecture on the Evaluation of Atomic Masses

Georges Audi

First edition: September 2000, updated December 2, 2004

Centre de Spectrométrie Nucléaire et de Spectrométrie de Masse, CSNSM, IN2P3-CNRS, et UPS, Bâtiment 108, F-91405 Orsay Campus, France

Abstract

The ensemble of experimental data on the 2830 nuclides which have been observed since the beginning of Nuclear Physics are being evaluated, according to their nature, by different methods and by different groups. The two "horizontal" evaluations in which I am involved: the Atomic Mass Evaluation AME and the NUBASE evaluation belong to the class of "static" nuclear data. In this lecture I will explain and discuss in detail the philosophy, the strategies and the procedures used in the evaluation of atomic masses.

Résumé *L'évaluation des masses atomiques* - Les données expérimentales sur les 2830 nucléides observés depuis les débuts de la Physique Nucléaire sont évaluées, suivant leur nature, par différentes méthodes et par différents groupes. Les deux évaluations "horizontales" dans les- quelles je suis impliqué : l'Évaluation des Masses Atomiques AME et l'évaluation NUBASE appartiennent à la classe des données nucléaires "statiques". Dans ce cours je vais expliquer et discuter de manière approfondie la philosophie, les stratégies et les procédures utilisées dans l'évaluation des masses atomiques.

PACS. 21.10.Dr ; 21.10.Hw ; 21.10.Tg ; 23.40.-s ; 23.50.+z ; 23.60.+e
Keywords: Binding energies - atomic masses - horizontal evaluation - nuclear data - least-squares - predictions of unknown masses

1 Introduction

Nuclear Physics started a little bit more than 100 years ago with the discoveries of natural radioactivity by Henri Becquerel and Pierre and Marie Curie; and of the atomic nucleus in 1911 by Ernest Rutherford with his assistants Ernest Marsden and Hans Geiger. First, it was a science of curiosity exhibiting phenomena unusual for that time. It is not until the late thirties, well after the discovery of artificial radioactivity by Frédéric and Irène Joliot-Curie, that the research in that domain tended to accelerate drastically and that Nuclear Physics became more and more a quantitative science.

Since then, scientists have accumulated a huge amount of data on a large number of nuclides. Today there are some 2830 variations on the combination of protons and neutrons that have been observed. Although this number seems large, specially compared to the 6 000 to 7 000 that are predicted to exist, one should be aware that the numbers of protons and neutrons constituting a nuclide are not really independent. Their special correlation form a relatively narrow band around a line called the bottom of the valley of stability. In Fig. 1 this is illustrated for the known masses (colored ones) across the chart of nuclides. In other words, nuclear data put almost no constraint in isospin on nuclear

models. From there follows the tendency of nuclear physicists to study nuclides at some distance from that line, which are called *exotic* nuclides.

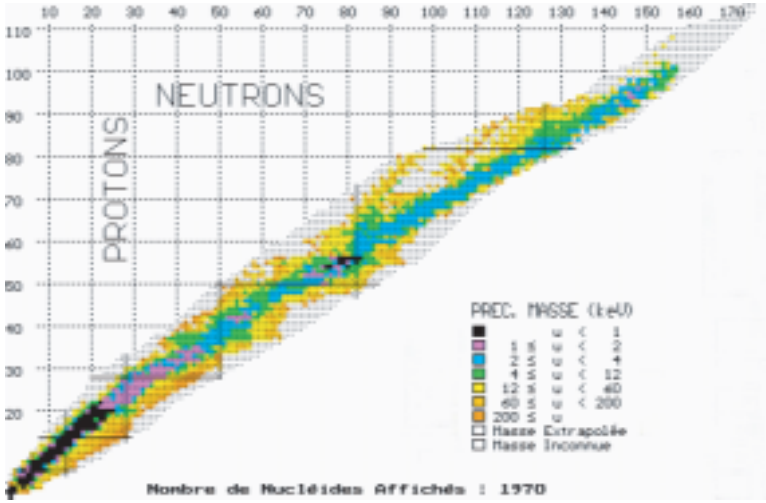

Figure 1: Chart of nuclides for the precision on masses. Only the known masses are colored, exhibiting crudely the narrowness of the valley of our knowledge in this immense landscape. Would these 1970 known masses been scattered around in the (N, Z) plane, our understanding of the nucleus would have been completely changed.

Sometimes remeasurement of the same physical quantity improved a previous result; sometimes it entered in conflict with it. The interest of the physicist has also evolved with time: the quantities considered varied importantly, scanning all sort of data from cross sections to masses, from half-lives to magnetic moments, from radii to superdeformed bands.

Thus, we are left nowadays with an enormous quantity of information on the atomic nucleus that need to be sorted, treated in a homogeneous way, while keeping traceability of the conditions under which they were obtained. When necessary, different data yielding values for the same physical quantity need to be compared, combined or averaged to derive an adopted value. Such values will be used in domains of physics that can be very far from nuclear physics, like half-lives in geo-chronology, cross-sections in proton-therapy, or masses in the determination of the α fine structure constant.

There are two classes of nuclear data: one class is for data related to nuclides at rest (or almost at rest); and the other class is for those related to nuclidic dynamics. In the first class, one finds ground-state and level properties, whereas the second encompasses reaction properties and mechanisms.

Nuclear ground-state masses and radii; magnetic moments; thermal neutron capture cross-sections; half-lives, spins and parities of excited and ground-state levels; the relative position (excitation energies) of these levels; their decay modes and the relative intensities of these decays; the transition probabilities from one level to another and the level width;

the deformations; all fall in the category of what could be called the "static" nuclear properties.

Total and differential (in energy and in angle) reaction cross-sections; reaction mechanisms; and spectroscopic factors could be grouped in the class of "dynamic" nuclear properties.

Certainly, one single experiment, for example a nuclear reaction study, can yield data for both 'static' and 'dynamic' properties.

It is out of the scope of the present lecture to cover all aspects of nuclear properties and nuclear data. The fine structure of "static" nuclear data will be shortly described and the authors of the various evaluations presented. Then I will center this lecture on the two "horizontal" evaluations in which I am involved: the atomic mass evaluation AME and the NUBASE evaluation, both being strongly related, particularly when considering isomers.

2 "Static" nuclear data

2.1 The NSDD: data for nuclear structure

The amount of data to be considered for nuclear structure is huge. They are represented schematically in Fig. 2 for each nuclide as one column containing all levels from the ground-state at the bottom of that column to the highest known excited state. All the known properties for each of the levels are included. Very early, it was found convenient to

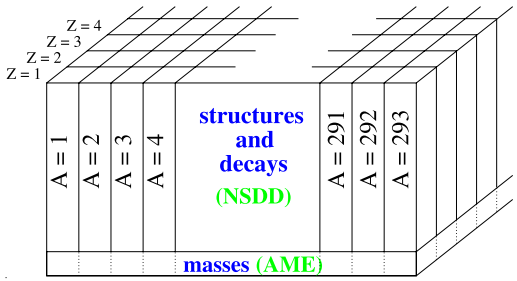

Figure 2: Schematic representation of all the available "static" nuclear data (structure, decay, mass, radius, moments,...). Each nuclide is represented as a building with its ground-state at the ground floor. The mass evaluation is represented on the ground floor, across all buildings. It includes also data for upper levels if they represent an energy relation to another nuclide, like a foot-bridge between two buildings that will allow to derive the level difference between their ground floors.

organize their evaluation in a network, splitting these data according to the mass of the nuclides, the A-chains. Such a division makes sense, since most of the decay relations among nuclides are β-decays where A is conserved. This is, of course, less true for heavier nuclides where α-decay is the dominant decay-mode connecting an A-nuclide to an $A-4$ daughter. This structure is the one adopted by the Nuclear Structure and Decay Data network (the NSDD) organized internationally under the auspices of the IAEA in Vienna. An A-chain or a group of successive A-chains is put under the responsibility of one member

of the network. His or her evaluation is refereed by another member of the network before publication in the journal 'Nuclear Data Sheets' (or in the 'Nuclear Physics' journal for $A \leq 44$). At the same time the computer files of the evaluation (the ENSDF: 'Evaluated Nuclear Structure Data Files') are made available at the NNDC-Brookhaven [1]. In this evaluation network, most of the "static" nuclear data are being considered.

The NSDD evaluation for each nuclide is not dependent, at first order, on the properties of a neighboring nuclide, except when there is a decay relation with that neighbor. Such evaluation, conducted nuclide by nuclide, is called a 'vertical' evaluation.

2.2 The atomic mass evaluation AME

However, the evaluation of data for energy relations between nuclides is more complex due to numerous links that overdetermine the system and exhibit sometimes inconsistencies among data. This ensemble of energy relations is taken into account in the 'horizontal' structure of the Atomic Mass Evaluation AME [3, 4]. By 'horizontal' one means that a unique nuclear property is being considered across the whole chart of nuclides, here the ground-state masses. Only such a structure allows to encompass all types of connections among nuclides, whether derived from β-decays, α-decays, thermal neutron-capture, reaction energies, or mass-spectrometry where any nuclide, e.g. ^{200}Hg can be connected to a molecule like $^{12}C^{13}C^{35}Cl_5$ or, in a Penning trap mass spectrometer, to ^{208}Pb.

The AME, the main subject of this lecture, will be developed below, in Section 3.

2.3 The isomers in the AME and the emergence of NUBASE

At the interface between the NSDD and the AME, one is faced with the problem of identifying - in some difficult cases - which state is the ground-state. The isomer matter is a continuous subject of worry in the AME, since a mistreatment can have important consequences on the ground-state masses. Where isomers occur, one has to be careful to check which one is involved in reported experimental data, such as α- and β-decay energies. Cases have occurred where authors were not (yet) aware of isomeric complications. The matter of isomerism became even more important, when mass spectrometric methods were developed to measure masses of exotic atoms far from β-stability and therefore having small half-lives. The resolution in the spectrometers is limited, and often insufficient to separate isomers. Then, one so obtains an average mass for the isomeric pair. A mass of the ground-state, our primary purpose, can then only be derived if one has information on the excitation energy and on the production rates of the isomers. And in cases where e.g. the excitation energy was not known, it may be estimated, see below.

When an isomer decays by an internal transition, there is no ambiguity and the assignment as well as the excitation energy is given by the NSDD evaluators. However, when a connection to the ground-state cannot be obtained, most often a decay energy to (and sometimes from) a different nuclide can be measured (generally with less precision). In the latter case one enters the domain of the AME, where combination of the energy relations of the two long-lived levels to their daughters (or to their parents) with the masses of the latter, allows to derive the masses of both states, thus an excitation energy (and, in general, an ordering).

Up to the 1993 mass table, the AME was not concerned with all known cases of isomerism, but only in those that were relevant to the determination of the ground-

state masses. In 1992 it was decided, after discussion with the NSDD evaluators, to include all isomers for which the excitation energy "is not derived from γ-transition energy measurements (γ-rays and conversion electron transitions), and also those for which the precision in γ-transitions is not decidedly better than that of particle decay or reaction energies leading to them" [2].

However, differences in isomer assignment between the NSDD and the AME evaluations cannot be all removed at once, since the renewal of all A-chains in NSDD can take several years. In the meantime also, new experiments can yield information that could change some assignments. Here a 'horizontal' evaluation should help.

The isomer matter was one of the main reasons for setting up in 1993 the NUBASE collaboration leading to a thorough examination and evaluation of those ground-state and isomeric properties that can help in identifying which state is the ground-state and which states are involved in a mass measurement [5]. NUBASE appears thus as a 'horizontal' database for several nuclear properties: masses, excitation energies of isomers, half-lives, spins and parities, decay modes and their intensities. Applications extend from the AME to nuclear reactors, waste management, astrophysical nucleo-synthesis, and to preparation of nuclear physics experiments.

Setting up NUBASE allowed in several cases to predict the existence of an unknown ground-state from trends of isomers in neighboring nuclides, whereas only one long-lived state was reported. A typical example is ^{161}Re, for which NUBASE'97 [6] predicted a $(1/2^+\#)$ proton emitting state below an observed 14 ms α-decaying high-spin state. (Everywhere in AME and NUBASE the symbol # is used to flag values estimated from trends in systematics.) Since then, the 370 μs, $1/2^+$, proton emitting state was reported with a mass 124 keV below the 14 ms state. For the latter a spin $11/2^-$ was also assigned [7]. Similarly, the $11/2^-$ bandhead level discovered in ^{127}Pr [8] is almost certainly an excited isomer. We estimate for this isomer, from systematical trends, an excitation energy of 600(200)# keV and a half-life of approximatively 50# ms.

In some cases the value determined by the AME for the isomeric excitation energy allows no decision as to which of the two isomers is the ground-state. This is particularly the case when the uncertainty on the excitation energy is large compared to that energy, e.g.: $E^m(^{82}\mathrm{As}) = 250 \pm 200$ keV; $E^m(^{134}\mathrm{Sb}) = 80 \pm 110$ keV; $E^m(^{154}\mathrm{Pm}) = 120 \pm 120$ keV.

Three main cases may occur. In the first case, there is no indication from the trends in J^π systematics of neighboring nuclides with same parities in N and Z, and no preference for ground-state or excited state can be derived from nuclear structure data. Then the adopted ordering, as a general rule, is such that the obtained value for E^m is positive. In the three examples above, ^{82}As will then have its (5^-) state located at 250±200 keV above the (1^+); in ^{134}Sb the (7^-) will be 80±110 keV above (0^-); and ^{154}Pm's spin (3,4) isomer 120±120 keV above the (0,1) ground-state. In the second case, one level could be preferred as ground-state from consideration of the trends of systematics in J^π. Then, the NUBASE evaluators accept the ordering given by these trends, even if it may yield a (slightly) negative value for the excitation energy, like in ^{108}Rh (high spin state at −60±110 keV). Such trends in systematics are still more useful for odd-A nuclides, for which isomeric excitation energies of isotopes (if N is even) or, similarly, isotones follow usually a systematic course. This allows to derive estimates both for the relative position and for the excitation energies where they are not known. Finally, there are cases where data exist on the order of the isomers, e.g. if one of them is known to decay into the other one, or if the Gallagher-Moszkowski rule [9] for relative positions of combinations

points strongly to one of the two as being the ground-state. Then the negative part, if any, of the distribution of probability has to be rejected (Fig. 3). Value and error are then calculated from the moments of the positive part of the distribution.

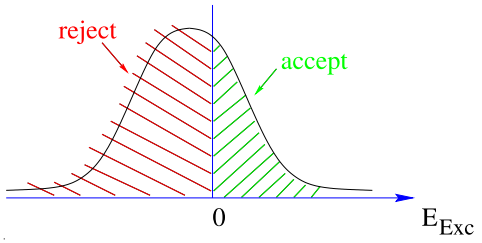

Figure 3: Truncated distribution of probability when there is a strong indication about ordering of ground-state and isomer.

2.4 Other 'horizontal' evaluations

There might be other reasons for 'horizontal' evaluations. The splitting of data among a large number of evaluators - like in the NSDD network described above - does not always allow having a completely consistent treatment of a given nuclear property through the chart of nuclides. In addition, some quantities may fall at the border of the main interest of such a network. This is the reason why a few 'horizontal' compilations or evaluations have been conducted for the benefit of the whole community. For example, one can quote the work of Otten [10] for isotope shift and hyperfine structure of spectral lines and the deduced radii, spins and moments of nuclides in their ground-state and long-lived isomeric states. An evaluation of isotope shifts has been published also by Aufmuth and coworkers [11], and Raghavan [12] gave a table of nuclear moments, updated recently by Stone [13]. More recent tables for nuclidic radii were published by Angeli [14] in 1991 and by Nadjakov *et al* [15] in 1994. Two other 'horizontal' evaluations are worth mentioning. One is the evaluation of isotopic abundances, by Holden [16]. The second one is the evaluation of Raman and coworkers [17] for the energy E_{2^+} and the reduced electric quadrupole transition probability $B(E2)$ of the first excited 2^+ state in even-even nuclides.

3 The evaluation of atomic masses (AME)

The atomic mass evaluation is particular when compared to the other evaluations of data reviewed above, in that there are almost no absolute determinations of masses. All mass determinations are relative measurements. Each experimental datum sets a relation in energy or mass among two (in a few cases, more) nuclides. It can be therefore represented by one link among these two nuclides. The ensemble of these links generates a highly entangled network. This is the reason why, as I mentioned earlier (cf. Section 2.2), a 'horizontal' evaluation is essential.

I will not enter in details in the different types of mass experiments, since there are other lectures devoted to this subject [18]. Nevertheless, I need to sketch the various

classes of mass measurements to outline how they enter the evaluation of masses and how they interfere with each other.

Generally a mass measurement can be obtained by establishing an energy relation between the mass we want to determine and a well known nuclidic mass. This energy relation is then expressed in electron-volts (eV). Mass measurements can also be obtained as an inertial mass from its movement characteristics in an electro-magnetic field. The mass, thus derived from a ratio of masses, is then expressed in 'unified atomic mass' (u) (cf. Section 3.1.3), or its sub-unit, μu. Two units are thus used in the present work.

The mass unit is defined, since 1960, by $1\,\mathrm{u} = \mathcal{M}(^{12}\mathrm{C})/12$, one twelfth of the mass of one free atom of Carbon-12 in its atomic and nuclear ground-states. Before 1960, as Wapstra once told me, two mass units were defined: the physical one $^{16}\mathrm{O}/16$, and the chemical one which considered one sixteenth of the average mass of a standard mixture of the three stable isotopes of oxygen. Physicists could not convince the chemists to drop their unit; "The change would mean millions of dollars in the sale of all chemical substances", said the chemists, which is indeed true! Joseph H.E. Mattauch, the American chemist Truman P. Kohman and Aaldert H. Wapstra [19] then calculated that, if $^{12}\mathrm{C}/12$ was chosen, the change would be ten times smaller for chemists, and in the opposite direction ... That lead to unification; 'u' stands therefore, officially, for 'unified mass unit'! Let us mention to be complete that the chemical mass spectrometry community (e.g. bio-chemistry, polymer chemistry) widely use the dalton (symbol Da, named after John Dalton [20]), which allows to express the number of nucleons in a molecule. It is thus not strictly the same as 'u'.

The energy unit is the electronvolt. Until recently, the relative precision of $M - A$ expressed in keV was, for several nuclides, less good than the same quantity expressed in mass units. The choice of the volt for the energy unit (the electronvolt) is not evident. One might expect use of the *international* volt V, but one can also choose the *standard* volt V_{90} as maintained in national laboratories for standards and defined by adopting an exact value for the constant $(2e/h)$ in the relation between frequency and voltage in the Josephson effect. In the 1999 table of standards [21]: $2e/h = 483597.9\,(\mathrm{exact})\,\mathrm{GHz}/\mathrm{V}_{90}$. An analysis by Cohen and Wapstra [22] showed that all precision measurements of reaction and decay energies were calibrated in such a way that they can be more accurately expressed in V_{90}. Also, the precision of the conversion factor between mass units and *standard* volts V_{90} is more accurate than that between it and *international* volts V:

$$\begin{aligned} 1\,\mathrm{u} &= 931\,494.009\,0 \pm 0.007\,1\ \mathrm{keV}_{90} \\ 1\,\mathrm{u} &= 931\,494.013\ \ \pm 0.037\ \ \ \mathrm{keV} \end{aligned}$$

The reader will find more information on the energy unit, and also some historical facts about the electronvolt, in the AME2003 [3], page 134.

3.1 The experimental data

In this section we shall examine the various types of experimental information on masses and see how they enter the AME.

3.1.1 Reaction energies

The energy absorbed in a nuclear reaction is directly derived from the Einstein's relation $E = mc^2$. In a reaction A(a,b)B requiring an energy Q_r to occur, the energy balance writes:

$$Q_r = \mathcal{M}_\mathrm{A} + \mathcal{M}_\mathrm{a} - \mathcal{M}_\mathrm{b} - \mathcal{M}_\mathrm{B} \tag{1}$$

This reaction is often endothermic, that is Q_r is negative, requiring input of energy to occur. Other nuclear reactions may release energy. This is the case, for example, for thermal neutron-capture reactions (n,γ) where the (quasi)-null energetic neutron is absorbed and populates levels in the continuum of nuclide 'B' at an excitation energy exactly equal to Q_r. With the exception of some reactions between very light nuclides, the the masses of the projectile 'a' and of the ejectile 'b' are known with a much higher accuracy than those of the target 'A', and of course the residual nuclide 'B'. Therefore Eq. 1 reduces to a linear combination of the masses of two nuclides:

$$\mathcal{M}_\mathrm{A} - \mathcal{M}_\mathrm{B} = q \pm dq \tag{2}$$

where $q = Q_r - \mathcal{M}_\mathrm{a} + \mathcal{M}_\mathrm{b}$.

A nuclear reaction usually deals with stable or very-long-lived target 'A' and projectile 'a', allowing only to determine the mass of a residual nuclide 'B' close to stability. Nowadays with the availability of radioactive beams, interest in reaction energy experiments is being revived.

It is worth mentioning in this category the very high accuracies attainable with (n,γ) and (p,γ) reactions. They play a key-rôle in providing many of the most accurate mass differences, and help thus building and strengthening the "backbone"[1] of masses along the valley of β-stability, and determine neutron separation energies with high precision[2].

Also very accurate are the self-calibrated reaction energy measurements using spectrometers. When measuring the difference in energy between the spectral lines corresponding to reactions A(a,b)B and C(a,b)D with the same spectrometer settings [24] one can reach accuracies better than 100 eV. Here the measurement can be represented by a linear combination of the masses of four nuclides:

$$\delta Q_r = \mathcal{M}_\mathrm{A} - \mathcal{M}_\mathrm{B} - \mathcal{M}_\mathrm{C} + \mathcal{M}_\mathrm{D} \tag{3}$$

The most precise reaction energy is the one that determined the mass of the neutron from the neutron-capture energy of ^{1}H at the ILL [25]. The $^1\mathrm{H}(\mathrm{n},\gamma)^2\mathrm{H}$ established a relation between the masses of the neutron, of ^{1}H and of the deuteron with the incredible precision of 0.4 eV.

3.1.2 Disintegration energies

Disintegration can be considered as a particular case of reaction, where there is no incident particle. Of course, here the energies Q_β, Q_α or Q_p are almost always positive, i.e. these particular reactions are exothermic. For the A(β^-)B, A(α)B or A(p)B disintegrations[3],

[1] the 'backbone' is the ensemble of nuclides along the line of stability in a diagram of atomic number Z versus neutron number Z [23]. The energy relations among nuclides in the backbone are multiple.

[2] The number of couples of nuclides connected by (n,γ) reactions with an accuracy of 0.5 keV or better was 243 in AME2003, against 199 in AME93, 128 in AME83 and 60 in the 1977 one. The number of cases known to better than 0.1 keV was 100 in AME2003, 66 in AME93 and 33 in AME83. Several reaction energies of (p,γ) reactions are presently (AME93)known about as precisely (25 and 8 cases with accuracies better than 0.5 keV and 0.1 keV respectively).

[3] The drawing for α-decay is taken from the educational Web site of the Lawrence Berkeley Laboratory: http://www.lbl.gov/abc/.

one can write respectively:

$$Q_{\beta^-} = \mathcal{M}_{\rm A} - \mathcal{M}_{\rm B} \quad (4)$$
$$Q_{\alpha} = \mathcal{M}_{\rm A} - \mathcal{M}_{\rm B} - \mathcal{M}_{\alpha} \quad (5)$$
$$Q_{p} = \mathcal{M}_{\rm A} - \mathcal{M}_{\rm B} - \mathcal{M}_{\rm p} \quad (6)$$

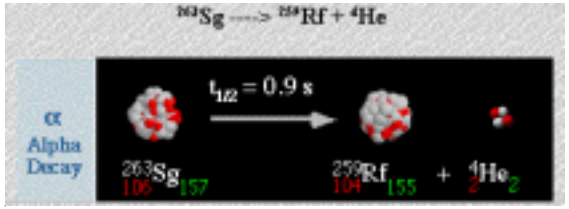

These measurements are very important because they allow deriving masses of unstable or very unstable nuclides.

This is more specially the case for the proton decay of nuclides at the drip-line, in the medium-A region [26]. They allow a very useful extension of the systematics of proton binding energies. But in addition they give in several cases information on excitation energies of isomers. This development is one more reason why we have to give more attention to relative positions of isomers than was necessary in earlier evaluations.

α-decays have permitted to determine the masses of the heavy nuclides. Moreover, the time coincidence of α lines in a decaying chain allows very clear identification of the heaviest ones. Quite often, and more particularly for even-even nuclides, the measured α-decay energies yield quite precise mass differences between parent and daughter nuclide.

3.1.3 Mass Spectrometry

Mass-spectrometric determination of atomic masses are often called 'direct' mass measurements because they are supposed to determine not an energy relation between two nuclides, but directly the mass of the desired one. In principle this is true, but only to the level of accuracy of the parameter of the spectrometer that is the least well known, which is usually the magnetic field in which the ions move. It follows that the accuracy in such absolute direct mass determination is very poor.

This is why, in all precise mass measurements, the mass of an unknown nuclide is always compared, in the same magnetic field, to that of a reference nuclide. Thus, one determines a ratio of masses, where the value of the magnetic field cancels, leading to a much more precise mass determination. As far as the AME is concerned, here again we have a mass relation between two nuclides.

One can distinguish three sub-classes in the class of mass measurement by mass-spectrometry (see also [18]):

1. Classical mass-spectrometry, where the electromagnetic deflection plays the key-rôle. More exactly, the two beams corresponding to the ion of the investigated nuclide and to that of the reference are forced to follow the same path in the magnetic field.

The ratio of the voltages of some electrostatic devices that make this condition true determines the ratio of masses. These voltages are determined either from the values of resistors in a bridge [27] or directly from a precision voltmeter [28].

2. Time-of-Flight spectrometry, where one measures simultaneously the momentum of an ion (from its magnetic rigidity $B\rho$) and its velocity (from the time of flight along a path of well-determined length) [29]. Calibration in this type of experiment requires a large set of reference masses, so that the AME cannot establish a simple relation between two nuclides. Nevertheless, the calibration function thus determined, together with its contribution to the error is generally well accounted for. The chance is small that recalibration might be necessary. In case it appears to be so in some future, one could consider a global re-centering of the published values. It is interesting to note that Time-of-Flight spectrometers can be also set-up in cyclotrons [30] or in storage rings [31].

3. Cyclotron Frequency, when measured in a homogeneous magnetic field, yields mass value of very high precision due to the fact that frequency is the physical quantity that can be measured with the highest accuracy with the present technology. Three types of spectrometers follow this principle:

   - the *Radio-Frequency Mass Spectrometer* (Fig. 4) invented by L.G. Smith [32] where the measurement is obtained in-flight, as a transmission signal, in only one turn;

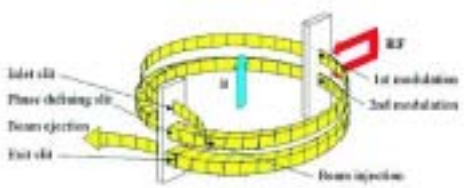

Figure 4: Principle of the *Radio-Frequency Mass Spectrometer*. Ions make two turns following a helicoidal path in a homogeneous field $\vec{B}$. Two RF excitations are applied at one turn interval. Only ions for which the two excitations are in opposite phase (and then cancel) will exit the spectrometer and be detected. Typical diameter of the helix is 0.5-1 meter. This scheme is from the MISTRAL Web site: http://csnwww.in2p3.fr/groupes/massatom/.

   - the *Penning Trap Spectrometer* (Fig. 5) where the ions are stored for 0.1–2 seconds to interact with a radio-frequency excitation signal [33]; and
   - the *Storage Ring Spectrometer* where the ions are stored and the ion beam cooled, while a metallic probe near the beam picks up the generated Schottky noise (a signal induced by a moving charge) [34].

Penning traps, as well as storage rings and the MISTRAL on-line Smith-type spectrometer, are now also used for making mass measurements of many nuclides further away from

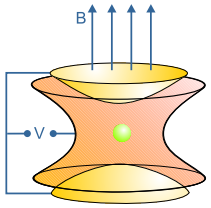

Figure 5: Principle of the *Penning Trap Spectrometer*. Ions follow a cyclotron motion in the horizontal plane due to $\vec{B}$ and cannot escape axially due to repulsion by the end-cup electrodes. The ring electrode is split to allow RF excitation. Typical inner size is 1-2 cm. This scheme is from the ISOLTRAP Web site: http://cern.ch/isoltrap/.

the line of stability. As a result, the number of nuclides for which experimental mass values are now known is substantially larger than in the previous atomic mass tables. These mass-spectrometric measurements of exotic nuclides are often made with resolutions that do not allow separation of isomers. Special care is needed to derive the mass value for the ground-state (cf. Section 2.3).

Nowadays, several mass measurements are made on fully (bare nuclei) or almost fully ionized atoms. Then, a correction must be made for the total binding energy of all removed electrons $B_e(Z)$. They can be found in the table for calculated total atomic binding energy of all electrons of Huang et al. [35]. Unfortunately, the precision of the calculated values $B_e(Z)$ is not clear; this quantity (up to 760 keV for $_{92}$U) cannot be measured easily. Very probably, its precision for $_{92}$U is rather better than the 2 keV accuracy with which the mass of, e.g., ^{238}U is known. A simple formula, approximating the results of [35], is given in the review of Lunney, Pearson and Thibault [36]:

$$B_{el}(Z) = 14.4381\, Z^{2.39} + 1.55468 \times 10^{-6}\, Z^{5.35}\ \text{eV} \qquad (7)$$

Penning traps have allowed to reach incredible accuracies in the measurement of masses. If one observes the increase of accuracies over the last seven or eight decades, for example on ^{28}Si, see Fig. 6, one would see that after a regular increase of one order of magnitude every ten years until 1970, the mass accuracy of ^{28}Si seemed to have reached a limit at the level of 5×10^{-7}. Until the arrival of high precision Penning traps, that allowed to catch up with the previous tendency and yielded an accuracy slightly better than 10^{-10} in 1995 [37]. Such precision measurements with Penning traps have considerably improved the precision in our knowledge of atomic mass values along the backbone.

3.2 Data evaluation in the AME

The evaluation of masses share with most other evaluations many procedures. However, the very special character in the treatment of data in the mass evaluation is, as said above (header of the present Section), that all measurements are relative measurements. Each

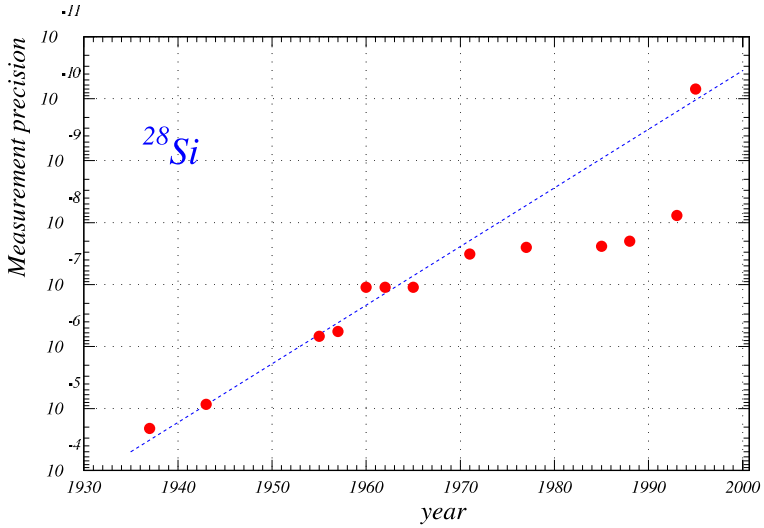

Figure 6: Our knowledge of the mass of ^{28}Si has increased by one order of magnitude per decade since 1935. Extrapolating this tendency, one could expect that we will reach a 10^{-12} accuracy in 2015.

experimental datum will be thus represented by a link connecting two or three nuclei (cf. Section 3.3.1). The set of connections results in a complex canvas where data of different type and origin are entangled. Here lies the very challenge to extract values of masses from the experiments. The counterpart is that the overdetermined data system will allow cross-checks and studies of the consistencies within this system. The other help to the evaluator will be the property of regularity of the surface of masses that will be described in the last section of this lecture.

The first step in the evaluation of data is to make a compilation, i.e. a collection of all the available data. This collection must include the 'hidden' data: a paper does not always say clearly that some of the information it contains is of interest for mass measurement. The collection includes also even poorly documented datum, which is labelled accordingly in the AME files.

The second step is the critical reading, which might include:

1. the evaluation or re-evaluation of the calibration procedures, the calibrators, and of the precisions of the measurements;

2. spectra examination: peaks position and relative intensities, peaks symmetry, quality of the fit;

3. search for the PRIMARY information, in the data, which do not necessarily appear always as clearly as they should. (i.e. in cases the authors combined the original result with other data, to derive a mass value, the AME should retain only the

former). It also happened that the authors gave only the derived mass value. Then the evaluator has to reconstruct the original result and ask for authors' confirmation.

The third step in the data evaluation will be to compare the results of the examined work to earlier results if they exist (either directly, or through a combination of other data). If there are no previous results, comparison could be done with estimates from extrapolations, exploiting the above mentioned regularity of the mass surface (cf. Section 4), or to estimates from mass models or mass formulae.

Finally, the evaluator often and on has to establish a dialog with the authors of the work, asking for complementary information when necessary, or suggesting different analysis, or suggesting new measurements.

The new data can now enter the data-file as one line. For example, for the electron capture of ^{205}Pb, the evaluator enters:

```
205 890816000c1 B  78Pe08   41.4   1.1   205Pb(e)205Tl    0.525  0.008 LM
```

where besides a 14 digits ID-number, there is a flag (as described in Ref. [3], p. 184), here 'B', then the NSR reference-code [38] for the paper '78Pe08' where the data appeared, the value for the Q of the reaction with its error bar (41.4 ± 1.1 keV), and the reaction equation, where 'e' stands for electron-capture. The information in the last columns says that this datum has been derived from the intensity ratio (0.525 ± 0.008) of the L and M lines in electron capture. The evaluator can add as many comment lines as necessary, following this data line, for other information he judges useful for exchange with his fellow evaluator. Some of these comments, useful for the user of the mass tables, will appear in the AME publication.

3.3 Data treatment

In this section, we shall first see how the network of data is built, then how the system of data can be reduced. In the third and fourth subsections, I shall describe shortly the least-squares method used in the AME and the computer program that will decode data and calculate the adjusted masses. A fifth part will develop the very important concept of 'Flow-of-Information' matrix. Finally, I shall explain how checking the consistency of data (or of sub-group of data) can help the evaluator in his judgment.

3.3.1 Data entanglement - Mass Correlations

We have seen in Section 3.1 that all mass measurements are RELATIVE measurements. Each experimental piece of data can be represented by a link between two, sometimes three, and more rarely four nuclides. As mentioned earlier, assembling these links produces an extremely entangled network. A part of this network can be seen in Fig. 7. One notices immediately that there are two types of symbols, the small and the large ones. The small ones represent the so-called SECONDARY nuclides; while the nuclides with large symbols are called PRIMARY. Secondary nuclides are represented by full small circles if their mass is determined experimentally, and by empty ones if estimated from trends in systematics. Secondary nuclides are connected by SECONDARY data, represented by dashed lines. A chain of dashed lines is at one end free, and at the other end connected to one unique[4]

[4]Sometimes a chain of secondary nuclides can be free at both ends. These nuclides have no connection to the backbone of known masses, but are connected to each other by α-chains of sometime high or very

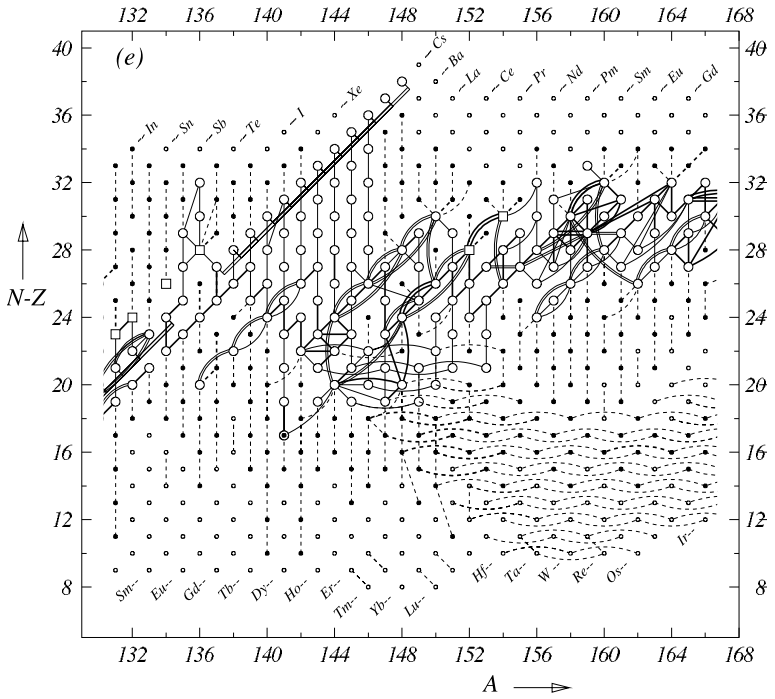

Figure 7: Diagram of connections for the experimental data. Each symbol represents one nuclide and each line represents one piece of data connecting two nuclides. When a nuclide is connected to Carbon-12 (often the case for mass spectrometry), it is represented by a square symbol.

primary nuclide (large symbol). This representation means that all secondary nuclides are determined uniquely by the chain of secondary connections going down to a primary nuclide. The latter are multiply determined and enter thus the entangled canvas. They are inter-connected by PRIMARY data, represented by full lines.

We see immediately from Fig. 7 that the mass of a primary nuclide cannot be determined straightforwardly. One may think of making an average of the values obtained from all links, but such a recipe is erroneous because the other nuclides on which these links are built are themselves inter-connected, thus not independent. In other words these PRIMARY data, connecting the primary nuclides, are correlated, and the correlation coefficients are to be taken into account.

Caveat: the word *primary* used for these nuclides and for the data connecting them does not mean that they are more important than the others, but only that they are

high precision. The chain is floating and no experimental mass can be derived. The evaluator makes an estimate for one of the masses in the chain in order to have it fixed. These non-experimental masses are all quoted as ('systematics') in the Tables.

subject to the special treatment below. The labels *primary* and *secondary* are not intrinsic properties of data or masses. They may change from primary to secondary or reversely when other information becomes available.

3.3.2 Compacting the set of data

We have seen that *primary* data are correlated. We take into account these correlations very easily with the help of the least-squares method that will be described below. The *primary* data will be improved in the adjustment, since each will benefit from all the available information.

Secondary data will remain unchanged; they do not contribute to χ^2. The masses of the secondary nuclides will be derived directly by combining the relevant adjusted primary mass with the secondary datum or data. This also means that secondary data can easily be replaced by new information becoming available (but one has to watch since the replacement can change other secondary masses down the chain as seen from the diagram Fig. 7).

We define DEGREES for *secondary* masses and *secondary* data. They reflect their distances along the chains connecting them to the network of primaries; they range from 2 to 16. Thus, the first secondary mass connected to a primary one will be a mass of degree 2, and the connecting datum will be a datum of degree 2 too. Degree 1 is for primary masses and data.

Before treating the primary data by the least-squares method, we try as much as possible to reduce the system, but without allowing any loss of information. One way to do so is to PRE-AVERAGE identical data: two or more measurements of the same physical quantities can be replaced by their average value and error. Also the so-called PARALLEL data can be pre-averaged: they are data that give essentially values for the mass difference between the same two nuclides, e.g. ^{9}Be(γ,n)^{8}Be, ^{9}Be(p,d)^{8}Be, ^{9}Be(d,t)^{8}Be and ^{9}Be(^{3}He,α)^{8}Be. Such data are represented together, in the main least-squares calculation, by one of them carrying their average value. If the Q data to be pre-averaged are strongly conflicting, i.e. if the consistency factor (or Birge ratio, or normalized χ)

$$\chi_n = \sqrt{\frac{\chi^2}{Q-1}} \tag{8}$$

resulting in the calculation of the pre-average is greater than 2.5, the (internal) error σ_i in the average is multiplied by the Birge ratio ($\sigma_e = \sigma_i \times \chi_n$). The quantity σ_e is often called the 'external' error. However, this treatment is not used in the very rare cases where the errors in the values to be averaged differ too much from one another, since the assigned errors loose any significance (three cases in AME'93). We there adopt an arithmetic average and the dispersion of values as error, which is equivalent to assigning to each of these conflicting data the same error.

In AME'93, 28% of the 929 cases in the pre-average had values of χ_n beyond unity, 4.5% beyond two, 0.7% beyond 3 and only one case beyond 4, giving a very satisfactory distribution overall. With the choice above of a threshold of χ_n^0=2.5 for the Birge ratio, only 1.5% of the cases are concerned by the multiplication by χ_n. As a matter of fact, in a complex system like the one here, many values of χ_n beyond 1 or 2 are expected to exist, and if errors were multiplied by χ_n in all these cases, the χ^2-test on the total adjustment would have been invalidated. This explains the choice made in the AME of a rather high

threshold ($\chi_n^0 = 2.5$), compared e.g. to χ_n^0=2 recommended by Woods and Munster [39] or, even, χ_n^0=1 used in a different context by the Particle Data Group [40], for departing from the rule of internal error of the weighted average (see also [41]).

Another method to increase the meaning of the final χ^2 is to exclude data with weights at least a factor 10 less than other data, or combinations of other data giving the same result. They are still kept in the list of input data but labelled accordingly; comparison with the output values allows to check that this procedure did not have unwanted consequences.

The system of data is also greatly reduced by replacing data with isomers by an equivalent datum for the ground-state, if a γ-ray energy measurement is available from the NNDC (cf. Section 2.3). Excitation energies from such γ-ray measurements are normally far more precise than reaction energy measurements.

Typically, we start from a set of 6000 to 7000 experimental data connecting some 3000 nuclides. After pre-averaging, taking out the data with very poor accuracy and separating the secondary data, we are left with a system of 1500 primary data for 800 nuclides.

3.3.3 Least-squares method

Each piece of data has a value $q_i \pm dq_i$ with the accuracy dq_i (one standard deviation) and makes a relation between 2, 3 or 4 masses with unknown values m_μ. An overdetermined system of Q data to M masses ($Q > M$) can be represented by a system of Q linear equations with M parameters:

$$\sum_{\mu=1}^{M} k_i^\mu m_\mu = q_i \pm dq_i \tag{9}$$

(a generalization of Eq. 2 and Eq. 3), e.g. for a nuclear reaction $A(a,b)B$ requiring an energy q_i to occur, the energy balance writes:

$$m_{\rm A} + m_{\rm a} - m_{\rm b} - m_{\rm B} = q_i \pm dq_i \tag{10}$$

thus, $k_i^{\rm A} = +1$, $k_i^{\rm a} = +1$, $k_i^{\rm B} = -1$ and $k_i^{\rm b} = -1$.

In matrix notation, $\mathbf{K}$ being the (Q, M) matrix of coefficients, Eq. 9 writes: $\mathbf{K}|m\rangle = |q\rangle$. Elements of matrix $\mathbf{K}$ are almost all null: e.g. for reaction $A(a,b)B$, Eq. 2 yields a line of $\mathbf{K}$ with only two non-zero elements.

We define the diagonal weight matrix $\mathbf{W}$ by its elements $w_i^i = 1/(dq_i dq_i)$. The solution of the least-squares method leads to a very simple construction:

$$^{\mathbf{t}}\mathbf{KWK}|m\rangle = {}^{\mathbf{t}}\mathbf{KW}|q\rangle \tag{11}$$

the NORMAL matrix $\mathbf{A} = {}^{\mathbf{t}}\mathbf{KWK}$ is a square matrix of order M, positive-definite, symmetric and regular and hence invertible [42]. Thus the vector $|\overline{m}\rangle$ for the adjusted masses is:

$$|\overline{m}\rangle = \mathbf{A^{-1}}\ {}^{\mathbf{t}}\mathbf{KW}|q\rangle \qquad \text{or} \qquad |\overline{m}\rangle = \mathbf{R}|q\rangle \tag{12}$$

The rectangular (M, Q) matrix $\mathbf{R}$ is called the RESPONSE matrix.

The diagonal elements of $\mathbf{A^{-1}}$ are the squared errors on the adjusted masses, and the non-diagonal ones $(a^{-1})_\mu^\nu$ are the coefficients for the correlations between masses m_μ and m_ν.

3.3.4 The AME computer program

The four phases of the AME computer program perform the following tasks:

1. decode and check the data file;
2. build up a representation of the connections between masses, allowing thus to separate primary masses and data from secondary ones and then to reduce drastically the size of the system of equations to be solved, without any loss of information;
3. perform the least-squares matrix calculations (see above); and
4. deduce the atomic masses, the nuclear reaction and separation energies, the adjusted values for the input data, the *influences* of data on the primary masses described in next section, and display information on the inversion errors, the correlations coefficients, the values of the χ^2 (cf. Section 3.3.6), and the distribution of the normalized deviations v_i.

3.3.5 Flow-of-Information

One of the most powerful tools in the least-squares calculation described above is the flow-of-information matrix. This matrix allows to trace back, in the least-squares method, the contribution of each individual piece of data to each of the parameters (here the atomic masses). The AME uses this method since 1993.

The flow-of-information matrix $\mathbf{F}$ is defined as follows: $\mathbf{K}$, the matrix of coefficients, is a rectangular (Q, M) matrix, the transpose of the response matrix ${}^{\mathbf{t}}\mathbf{R}$ is also a (Q, M) rectangular one. The (i, μ) element of $\mathbf{F}$ is defined as the product of the corresponding elements of ${}^{\mathbf{t}}\mathbf{R}$ and of $\mathbf{K}$. In reference [43] it is demonstrated that such an element represents the *"influence"* of datum i on parameter (mass) m_μ. A column of $\mathbf{F}$ thus represents all the contributions brought by all data to a given mass m_μ, and a line of $\mathbf{F}$ represents all the influences given by a single piece of data. The sum of influences along a line is the *"significance"* of that datum. It has also been proven [43] that the influences and significances have all the expected properties, namely that the sum of all the influences on a given mass (along a column) is unity, that the significance of a datum is always less than unity and that it always decreases when new data are added. The significance defined in this way is exactly the quantity obtained by squaring the ratio of the uncertainty on the adjusted value over that on the input one, which is the recipe that was used before the discovery of the $\mathbf{F}$ matrix to calculate the relative importance of data.

A simple interpretation of influences and significances can be obtained in calculating, from the adjusted masses and Eq. 9, the adjusted data:

$$|\overline{q}\rangle = \mathbf{KR}|q\rangle. \tag{13}$$

The i^{th} diagonal element of $\mathbf{KR}$ represents then the contribution of datum i to the determination of $\overline{q_i}$ (same datum): this quantity is exactly what is called above the *significance* of datum i. This i^{th} diagonal element of $\mathbf{KR}$ is the sum of the products of line i of $\mathbf{K}$ and column i of $\mathbf{R}$. The individual terms in this sum are precisely the *influences* defined above.

The flow-of-information matrix $\mathbf{F}$, provides thus insight on how the information from datum i flows into each of the masses m_μ.

3.3.6 Consistency of data

The system of equations being largely over-determined ($Q >> M$) offers the evaluator several interesting possibilities to examine and judge the data. One might for example examine all data for which the adjusted values deviate importantly from the input ones. This helps to locate erroneous pieces of information. One could also examine a group of data in one experiment and check if the errors assigned to them in the experimental paper were not underestimated.

If the precisions dq_i assigned to the data q_i were indeed all accurate, the normalized deviations v_i between adjusted $\overline{q}_i$ and input q_i data (cf. Eq. 13), $v_i = (\overline{q}_i - q_i)/dq_i$, would be distributed as a gaussian function of standard deviation $\sigma = 1$, and would make χ^2:

$$\chi^2 = \sum_{i=1}^{Q} \left(\frac{\overline{q}_i - q_i}{dq_i} \right)^2 \qquad \text{or} \qquad \chi^2 = \sum_{i=1}^{Q} v_i^2 \tag{14}$$

equal to $Q - M$, the number of degrees of freedom, with a precision of $\sqrt{2(Q-M)}$.

One can define as above the NORMALIZED CHI, χ_n (or 'consistency factor' or 'Birge ratio'): $\chi_n = \sqrt{\chi^2/(Q-M)}$ for which the expected value is $1 \pm 1/\sqrt{2(Q-M)}$.

For our current AME2003 example of 1381 equations with 847 parameters, i.e. 534 degrees of freedom, the theoretical expectation value for χ^2 should be 534±33 (and the theoretical $\chi_n = 1 \pm 0.031$). The total χ^2 of the adjustment is actually 814; this means that, in the average, the errors in the input values have been underestimated by 23%, a still acceptable result. In other words, the experimentalists measuring masses were, on average, too optimistic by 23%. The distribution of the v_i's (the individual contributions to χ^2, as defined in Eq. 14 is also acceptable, with, in AME2003, 15% of the cases beyond unity, 3.2% beyond two, and 8 items (0.007%) beyond 3.

The χ_n value was 1.062 in AME'83 for $Q - M$=760 degrees of freedom, 1.176 in AME'93 for $Q - M = 635$, and 1.169 in the AME'95 update for $Q - M$=622.

Another quantity of interest for the evaluator is the PARTIAL CONSISTENCY FACTOR, χ_n^p, defined for a (homogeneous) group of p data as:

$$\chi_n^p = \sqrt{\frac{Q}{Q-M} \; \frac{1}{p} \; \sum_{i=1}^{p} v_i^2}. \tag{15}$$

Of course the definition is such that χ_n^p reduces to χ_n if the sum is taken over all the input data.

One can consider for example the two main classes of data: the reaction and decay energy measurements and the mass spectrometric data (see Section 3.1). The partial consistency factors χ_n^p are respectively 1.269 and 1.160 for energy measurements and for mass spectrometry data, showing that both types of input data are responsible for the underestimated error of 23% mentioned above, with a better result for mass spectrometry data.

One can also try to estimate the average accuracy for 181 groups of data related to a given laboratory and with a given method of measurement, by calculating their partial consistency factors χ_n^p. A high value of χ_n^p might be a warning on the validity of the considered group of data within the reported errors. In general, in the AME such a situation is extremely rare, because deviating data are cured before entering the 'machinery' of the adjustment, at the stage of the evaluation itself (see Section 3.2). On

the average the experimental errors appear to be slightly underestimated, with as much as 57% (instead of expected 33%) of the groups of data having χ_n^p larger than unity. Agreeing better with statistics, 5.5% of these groups are beyond $\chi_n^p = 2$.

3.4 Data requiring special treatment

It often happens that data require some special treatment before entering the data-file (cf. Section 3.2). Such is the case of data given with asymmetric uncertainties, or when information is obtained only as one lower and one upper limit, defining thus a range of values. We shall examine these two cases.

All errors entering the data-file must be one standard deviation (1 σ) errors. When it is not the case, they must be converted to 1 σ errors to allow combination with other data.

3.4.1 Asymmetric errors

Sometimes the precision on a measurement is not given as a single number, like σ (or dq in Section 3.3.3 above), but asymmetrically X^{+a}_{-b}, as shown in Fig. 8.

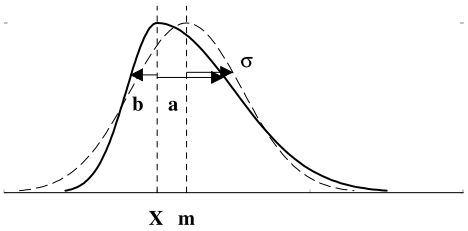

Figure 8: An experimental result is represented by an asymmetric probability density function (heavy solid line) with central value X and errors $+a$ and $-b$. This function is symmetrized as shown by the dashed line with its center m displaced by $0.64 \cdot (a - b)$

Such errors are symmetrized, before entering the treatment procedure. A rough estimate can be used: take the central value to be the mid-value between the upper and lower 1σ-equivalent limits $X + (a - b)/2$, and define the uncertainty to be the average of the two uncertainties $(a + b)/2$. A better approximation is obtained with the recipe described in Ref. [5]. The central value X is shifted to:

$$X + 0.64 \cdot (a - b) \tag{16}$$

and the precision σ is:

$$\sigma^2 = (1 - \frac{2}{\pi})\,(a - b)^2 + ab. \tag{17}$$

In the appendix of Ref. [5] one can find the demonstration and discussion of Eq. 16 and Eq. 17.

3.4.2 Range of values

Some measurements are reported as a range of values with most probable lower and upper limits (Fig. 9). They are treated as a uniform distribution of probabilities [44]. The moments of this distribution yield a central value at the middle of the range and a 1σ uncertainty of 29% of that range.

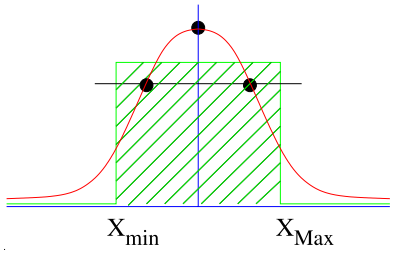

Figure 9: Experimental datum given as a range of values is represented by a rectangular distribution of probabilities.

3.4.3 Mixture of spectral lines

**** to be completed ****

4 Regularity of the mass-surface

When nuclear masses are displayed as a function of N and Z, one obtains a *surface* in a 3-dimensional space. However, due to the pairing energy, this surface splits into four *sheets*. The even-even sheet lies lowest, the odd-odd highest, the other two nearly halfway between as represented in Fig. 10. The vertical distances from the even-even sheet to the

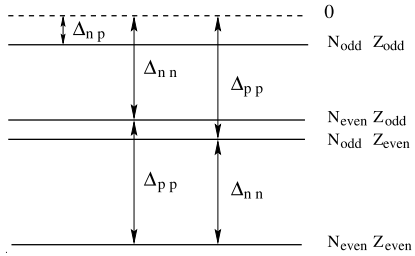

Figure 10: The surface of masses is split into four sheets. This scheme represents the pairing energies responsible for this splitting. The zero energy surface is a purely hypothetical one for no pairing at all among the last nucleons.

odd-even and even-odd ones are the proton and neutron pairing energies Δ_{pp} and Δ_{nn}.

They are nearly equal. The distances of the last two sheets to the odd-odd sheet are equal to $\Delta_{nn} - \Delta_{np}$ and $\Delta_{pp} - \Delta_{np}$, where Δ_{np} is the proton-neutron pairing energy due to the interaction between the two odd nucleons, which are generally not in the same shell. These energies are represented in Fig. 10, where a hypothetical energy zero represents a nuclide with no pairing among the last nucleons.

Experimentally, it has been observed that:

- the four sheets run nearly parallel in all directions, which means that the quantities Δ_{nn}, Δ_{pp} and Δ_{np} vary smoothly and slowly with N and Z; and
- each of the mass sheets varies very smoothly also, but very rapidly[5]. with N and Z. The smoothness is also observed for first order derivatives (slopes, cf. Section 4.2.1) and all second order derivatives (curvatures of the mass surface). They are only interrupted in places by sharp cusps or large depressions associated with important changes in nuclear structure: shell or sub-shell closures (sharp cusps), shape transitions (spherical-deformed, prolate-oblate: depressions on the mass surface), and the so-called 'Wigner' cusp along the $N = Z$ line.

This observed regularity of the mass sheets in all places where no change in the physics of the nucleus are known to exist, can be considered as one of the BASIC PROPERTIES of the mass surface. Thus, dependable estimates of unknown, poorly known or questionable masses can be obtained by extrapolation from well-known mass values on the same sheet. Examination of previous such estimates, where the masses are now known, shows that the method used, though basically simple, has a good predictive power [36].

In the evaluation of masses the property of regularity and the possibility to make estimates are used for several purposes:

1. *New Physics* - Any coherent deviation from regularity, in a region (N, Z) of some extent, could be considered as an indication that some new physical property is being discovered.

2. *Outliers* - However, if one single mass violates the systematic trends, then one may seriously question the correctness of the related datum. There might be, for example, some undetected systematic [45] contribution to the reported result of the experiment measuring this mass. We then reread the experimental paper with extra care for possible uncertainties, and often ask the authors for further information. This often leads to corrections.
   In the case where a mass determined from ONLY ONE experiment (or from same experiments) deviate severely from the smooth surface, replacement by an estimated value would give a more usefull information to the user of the tables and would prevent obscuring the plots for the observation of the mass surface. Fig. 11 for one of the derivatives of the mass surface (cf. Section 4.2.1) is taken from AME'93 and shows how replacements of a few such data by estimated values, can repair the surface of masses in a region, not so well known, characterized by important irregularities. Presently, only the most striking cases, not all irregularities, have been replaced by estimates: typically those that obscure plots like in Fig. 11.

3. *Conflicts among data* - There are cases where some experimental data on the mass of a particular nuclide disagree among each other and no particular reason for rejecting one or some of them could be found from studying the involved papers. In such cases, the measure of agreement with the just mentioned regularity can be used by the evaluators for selecting which of the conflicting data will be accepted and used in the evaluation.

4. *Estimates* - Finally, drawing the mass surface allows to derive estimates for the still unknown masses, either from interpolations or from short extrapolations, as can be seen in Fig. 12.

[5] smooth means continuous, non-staggering; smooth does not mean slow.

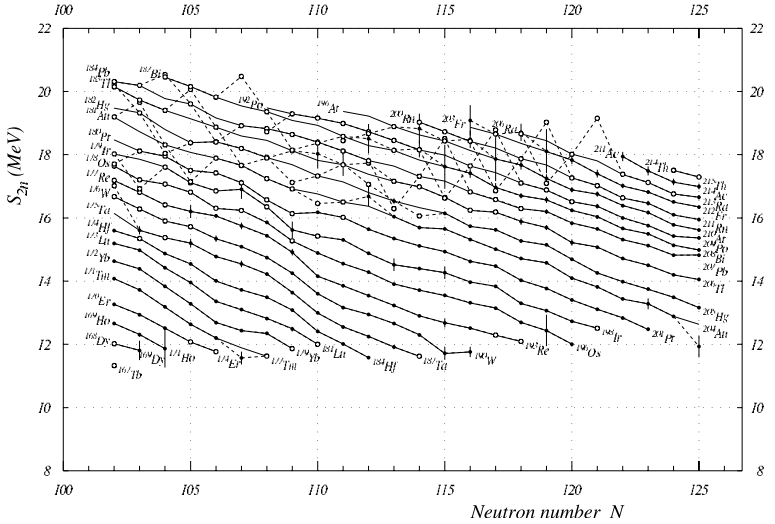

Figure 11: Two-neutron separation energies as a function of N (from AME'93, p. 166). Solid points and error bars represent experimental values, open circles represent masses estimated from "trends in systematics". Replacing some of the experimental data by values estimated from these trends, changes the mass surface from the dotted to the full lines. The use of a 'derivative' function adds to the confusion of the dotted lines, since two points are changed if one mass is displaced. Moreover, in this region there are many α links resulting in large propagation of errors.

4.1 Extrapolations

In the case of extrapolation however, the error in the estimated mass will increase with the distance of extrapolation. These errors are obtained by considering several graphs of systematics with a guess on how much the estimated mass may change without the extrapolated surface looking too much distorted. This recipe is unavoidably subjective, but has proven to be efficient through the agreement of these estimates with newly measured masses in the great majority of cases.

It would be desirable to give estimates for all unknown nuclides that are within reach of the present accelerator and mass separator technologies. But, in fact, the AME only estimates values for all nuclides for which at least one piece of experimental information

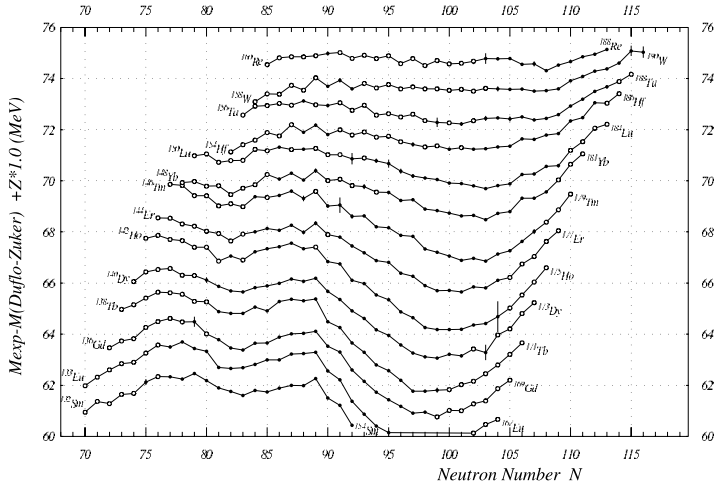

Figure 12: Differences, in the rare-earth region, between the masses and the values predicted by the model of Duflo and Zuker [46]. Open circles represent values estimated from systematic trends; points are for experimental values.

is available (e.g. identification or half-life measurement or proof of instability towards proton or neutron emission). In addition, the evaluators want to achieve continuity in N, in Z, in A and in $N - Z$ of the set of nuclides for which mass values are estimated. This set is therefore the same as the one defined for NUBASE [5].

To be complete, it should be said that REGULARITY is not the only property used to make estimates: all available experimental information is taken into account. The limits for the methods based on REGULARITY appear rapidly when going down to low mass numbers where nuclear structures appear and disappear on very short ranges, not to mention vanishing magic numbers.

Neutron-rich masses could be constrained by our knowledge of nuclides being stable or unstable relative to neutron emission: e.g. stability against neutron emission implies a positive neutron separation energie. This property, however, is usefull only for light species, where the neutron drip-line can be reached. Similarly for proton-rich nuclides, but here one has to be carefull and take into account the Coulomb barrier which may hinder proton emission of a slightly p-unbound nucleus. Light proton-rich masses could be derived from the masses of their mirror companions, or from the IMME (Isobaric Multiplet Mass Equation) which showed, up to now, to be fairly well verified. New developments in these directions are in progress.

4.2 Scrutinizing the surface of masses

Direct representation of the mass surface is not convenient since the binding energy varies very rapidly with N and Z. Splitting in four sheets, as mentioned above, complicates even more such a representation. There are two ways to still be able to observe with some precision the surface of masses: one of them uses the *derivatives* of this surface, the other is obtained by *subtracting a simple function* of N and Z from the masses.

They are both described below and I will end this section with a description of the interactive computer program that visualizes all these functions to allow easier derivation of the estimated values.

4.2.1 The derivatives of the mass surface

By *derivative* of the mass surface we mean a specified difference between the masses of two nearby nuclei. These functions are also smooth and have the advantage of displaying much smaller variations. For a derivative specified in such a way that differences are between nuclides in the same mass sheet, the near parallelism of these leads to an (almost) unique surface for the derivative, allowing thus a single display. Therefore, in order to illustrate the systematic trends of the masses, four derivatives of this last type were traditionally chosen:

1. the two-neutron separation energies versus N, with lines connecting the isotopes of a given element, as in Fig. 11;

2. the two-proton separation energies versus Z, with lines connecting the isotones (the same number of neutrons);

3. the α-decay energies versus N, with lines connecting the isotopes of a given element; and

4. the double β-decay energies versus A, with lines connecting the isotopes and the isotones.

These four derivatives are given in the printed version of the AME2003, Part II, Figs. 1–36 [4].

However, from the way these four derivatives are built, they give only information within one of the four sheets of the mass surface (e-e, e-o, o-e or e-e; e-o standing for even N and odd Z). When observing the mass surface, an increased or decreased spacing of the sheets cannot be observed. Also, when estimating unknown masses, divergences of the four sheets could be unduly created, which is unacceptable.

Fortunately, other various representations are possible (e.g. separately for odd and even nuclei: one-neutron separation energies versus N, one-proton separation energy versus Z, β-decay energy versus A, ...). Such graphs have been prepared and can be obtained from the AMDC web distribution [47].

The method of 'derivatives' suffers from involving two masses for each point to be drawn, which means that if one mass is moved then two points are changed in opposite direction, causing confusion in our drawings Fig. 11.

4.2.2 Subtracting a simple function

Since the mass surface is smooth, one can try to define a function of N and Z as simple as possible and not too far from the real surface of masses. The difference between the mass surface and this function, while displaying reliably the structure of the former, will vary much less rapidly, improving thus its observation.

Subtracting results from a model Practically, we use the results of the calculation of one of the modern models. However, we can use here only those models that provide masses specifically for the spherical part, forcing the nucleus to be un-deformed. The reason is that the models generally describe quite well the shell and sub-shell closures, and to some extent the pairing energies, but not the locations of deformation. If the theoretical deformations were included and not located at exactly the same position as given by the experimental masses, the mass difference surface would show two dislocations for each shape transition. Interpretation of the resulting surface would then be very difficult.

My two choices are the "New Semi-Empirical Shell Correction to the Droplet Model (Gross Theory of Nuclear Magics)" by Groote, Hilf and Takahashi [48]; and the "Microscopic Mass Formulas" of Duflo and Zuker [46], which has been illustrated above (Fig. 12). In AME2003, we made extensive use of such differences with models. The plots we have prepared were not published, they can be retrieved from the AMDC [47].

The difference of mass surfaces shown in Fig. 12 is instructive:

1. the lines for the isotopic series cross the N=82 shell closure with almost no disruption, showing thus how well shell closures are described by the model;
2. the well-known onset of deformation in the rare-earth at N=90 appears very clearly here as a deep large bowl, since deformation is not used in this calculation. The contour of this deformation region is neat. The depth, i.e. the amount of energy gained due to deformation, compared to ideal spherical nuclides, can be estimated; and
3. Fig. 12 shows also how the amplitude of deformation decreases with increasing Z and seems to vanish when approaching Rhenium (Z=75).

Subtracting a Bethe and Weizsäcker formula Since 1975 [49], and now with more and more evidence, it appears that the *'magic'* numbers that were though to occur at fixed numbers of protons or neutrons, are not really so. They might disappear when going away from the valley of stability, or appear at new locations. Where such migrations occur, most models are much in trouble, and the reasoning we made above for not including deformation in the models, now applies also to 'magic' numbers. Excluding shell and sub-shell closures, we are then driven directly back to the pioneering work of Weizsäcker [50]. Recent works [51, 52] on the modern fits of the original Bethe and Weizsäcker's formula seems promising in this respect.

The concept of the liquid drop mass formula was defined by Weizsäcker in 1935 [50] and fine-tuned by Bethe and Bacher [53] in 1936. The binding energy of the nucleus comprises only a volume energy term, a surface one, an asymmetry term, and the Coulomb energy contribution for the repulsion amongst protons. The *total* mass is thus:

$$\mathcal{M}(N,Z) = N\mathcal{M}_{\rm n} + Z\mathcal{M}_{\rm H} - \alpha A + \beta\frac{(N-Z)^2}{A} + \gamma A^{\frac{2}{3}} + \frac{3}{5}\frac{e^2Z^2}{r_0A^{\frac{1}{3}}} \qquad (18)$$

where $A = N+Z$, is the atomic weight, $r_0A^{1/3}$ the nuclear radius, $\mathcal{M}_{\rm n}$ and $\mathcal{M}_{\rm H}$ the masses of the neutron and of the hydrogen atom. The constants α, β, γ and r_0 were determined empirically by Bethe and Bacher: α = 13.86 MeV, β = 19.5 MeV, γ = 13.2 MeV and $r_0 = 1.48 \cdot 10^{-15}$ m (then $\frac{3}{5}e^2/r_0$ = 0.58 MeV). The formula of Eq. (18) is unchanged if $\mathcal{M}(N,Z)$, $\mathcal{M}_{\rm n}$ and $\mathcal{M}_{\rm H}$ are replaced by their respective mass excesses (at that time they were called *mass defects*). When using the *constants* given above one should be aware that when Bethe fixed them, he used for the mass excesses of the neutron and hydrogen atom respectively 7.8 MeV and 7.44 MeV in the ^{16}O standard, with a value of 930 MeV for the atomic mass unit.

If we subtract Eq. (18) from all masses we are left with values that vary much less rapidly than the masses themselves, while still showing all the structures. However, the splitting in four sheets will still make the image fuzzy. One can then add to the right hand side of the formula of Bethe (18) a commonly used pairing term $\Delta_{pp} = \Delta_{nn} = -12/\sqrt{A}$ MeV and no Δ_{np} (Fig. 10), which is sufficient for our purpose. (For those interested, there is a more refined study of the variations of the pairing energies that has been made by Jensen, Hansen and Jonson [54]).

4.3 Far extrapolations

When exploiting these observations one can make extrapolations for masses very far from stability. This has been done already [55], but with a further refinement of this method obtained by constructing an *idealized* surface of masses (or *mass-geoid*) [56], which is the best possible function to be subtracted from the mass surface. In Ref. [55], a local *mass-geoid* was built as a cubic function of N and Z in a region limited by magic numbers for both N and Z, fitted to only the purely spherical nuclides and keeping only the very reliable experimental masses. Then the shape of the bowl (for deformation) was reconstructed 'by hand', starting from the known non-spherical experimental masses. It was found that the maximum amplitude of deformation amounts to 5 MeV, is located at ^{168}Dy, and that the region of deformation extends from N=90 to N=114 and from Z=55 to Z=77, which is roughly in agreement with what is indicated by Fig. 12.

4.4 Manipulating the mass surface

In order to make estimates of unknown masses or to test changes on measured ones, one needs to visualize different graphs, either from the 'derivatives' type or from the 'difference' type. On these graphs, one needs to add (or move) the relevant mass and determine how much freedom is left in setting a value for this mass.

Things are still more complicated, particularly for changes on measured masses, since other masses could depend on the modified one, usually through secondary data. Then one mass change may give on one graph several connected changes.

Another difficulty is that a mass modification (or a mass creation) may look acceptable on one graph, but may appear unacceptable on another graph. One should therefore be able to watch several graphs at the same time.

A supplementary difficulty may appear in some types of graphs where two tendencies may alternate, following the parity of the proton or of the neutron numbers. One may then wish, at least for better comfort, to visualize only one of these two parities.

All this has become possible with the 'interactive graphical tool', called DESINT (from

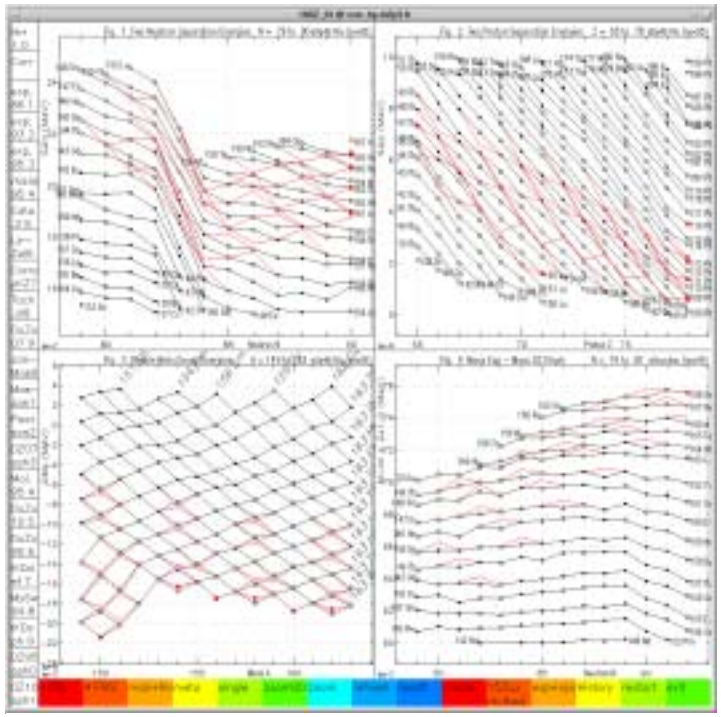

Figure 13: A screen image of DESINT, the interactive graphical display of four cuts in the surface of masses around ^{146}Gd. The four quadrants display respectively $S_{2n}(N)$, $S_{2p}(Z)$, $Q_{2\beta}(A)$ and $(M_{\rm exp} - M_{\rm Duflo-Zuker})(N)$ [46]. The lines in black connect nuclides with same Z, N, (Z and N) and Z respectively. The boxes at left and bottom serve for various interactive commands. The N=82 shell closure is clearly seen in quadrant 1 and in the lower left corner of quadrant 3. The lines in red illustrate the many consequences of an increase of the mass of ^{146}Gd by 500 keV.

the French: 'dessin interactif') written by C. Borcea [57] and illustrated in Fig. 13. Any of the 'derivatives' or of the 'differences' can be displayed in any of the four quadrants of Fig. 13, or alone and enlarged. Any of these functions can be plotted against any of the parameters N, Z, A, $N-Z$, and $2Z-N$; and connect iso-lines in any single or double parameters of the same list (e.g., in the third view of Fig. 13, iso-lines are drawn for Z AND for N). Zooming in and out to any level and moving along the two coordinates are possible independently for each quadrant. Finally, and more importantly, any change appears, in a different color, with all its consequences and in all four graphs at the same time. As an example and only for the purpose of illustration, a change of +500 keV has been applied, in Fig. 13, to ^{146}Gd in quadrant number four; all modifications in all graphs appear in red.

5 The Tables

In December 2003, we succeeded in having published TOGETHER the "Atomic Mass Evaluation" AME [3, 4] and the NUBASE evaluation [5], which have the same "horizontal" structure and basic interconnections at the level of isomers.

After the 1993 tables (AME'93) it was projected to have updated evaluations performed regularly (every two years) and published in paper only partly, while all files should still be distributed on the Web. Effectively, an update AME'95 [2] appeared two years later. Lack of time to evaluate the stream of new quite important data, and also the necessity to create the NUBASE evaluation (see below), prevented the intended further updates of the AME. The NUBASE evaluation was thus published for the first time in September 1997 [6], but in order to have consistency between the two tables, it was decided then that the masses in NUBASE'97 should be exactly those from AME'95. A certain stabilization, that seems to be reached now, encouraged us to publish in 2003 a new full evaluation of masses, together with the new version of NUBASE. This time, the AME2003 and NUBASE2003 are completely 'synchronized'.

Full content of the two evaluations is accessible on-line at the web site of the Atomic Mass Data Center (AMDC) [58] through the *World Wide Web*. One will find at the AMDC, not only the published material, but also extra figures, tables, documentation, and more specially the ASCII files for the AME2003 and the NUBASE2003 tables, for use with computer programs.

The contents of NUBASE can be displayed with a PC-program called "NUCLEUS" [59], and also by a Java program JVNUBASE [60] through the *World Wide Web*, both distributed by the AMDC.

6 Conclusion

Deriving a mass value for a nuclide from one or several experiments is in most cases not easy. Some mathematical tools (the least-squares method) and computer tools (interactive graphical display), and especially the evaluator's judgment are essential ingredients to reach the best possible recommended values for the masses.

Unknown masses close to the last known ones can be predicted from the extension of the mass surface. However, for the ones further out, more particularly those which are essential in many astrophysical problems, like the nucleosynthesis r-process, values for

the masses can only be derived from some of the available models. Unfortunately, the latter exhibit very large divergences among them when departing from the narrow region of known masses, reaching up to tens of MeV's in the regions of the r-process paths. Therefore, one of the many motivations for the best possible evaluation of masses is to get the best set of mass values on which models may adjust their parameters and better predict masses further away.

Acknowledgements

I would like to thank Aaldert H. Wapstra with whom I have been working since 1981. The material used in this lecture is also his material. He was the one who established in the early fifties the AME in its modern shape as we know now. Aaldert H. Wapstra has always been very accurate, very careful and hard working in his analysis in both the AME and the NUBASE evaluations. During these 23 years I have learned and still learn a lot from his methods. I wish also to thank my close collaborators: Jean Blachot who triggered in 1993 the NUBASE collaboration, Olivier Bersillon, Catherine Thibault, and Catalin Borcea who built the computer programs for mass extrapolation, and worked hard at the understanding, the definition and the construction of a *mass-geoid*.

References

[1] T.W. Burrows, *Nucl. Instrum. Meth. A* **286** (1990) 595;
http://www.nndc.bnl.gov/nndc/ensdf/.

[2] G. Audi and A.H. Wapstra, *Nucl. Phys. A* **595** (1995) 409.

[3] A.H. Wapstra, G. Audi and C. Thibault, *Nucl. Phys. A* **729** (2003) 129.

[4] G. Audi, A.H. Wapstra and C. Thibault, *Nucl. Phys. A* **729** (2003) 337.

[5] G. Audi, O. Bersillon, J. Blachot and A.H. Wapstra, *Nucl. Phys. A* **729** (2003) 3.

[6] G. Audi, O. Bersillon, J. Blachot and A.H. Wapstra, *Nucl. Phys. A* **624** (1997) 1.

[7] R.J. Irvine, C.N. Davids, P.J. Woods, D.J. Blumenthal, L.T. Brown, L.F. Conticchio, T. Davinson, D.J. Henderson, J.A. Mackenzie, H.T. Penttilä, D. Seweryniak and W.B. Walters, *Phys. Rev. C* **55** (1997) 1621.

[8] T. Morek, K. Starosta, Ch. Droste, D. Fossan, G. Lane, J. Sears, J. Smith and P. Vaska, *Eur. Phys. Journal A* **3** (1998) 99.

[9] C.J. Gallagher, Jr. and S.A. Moszkowski, *Phys. Rev.***111** (1958) 1282.

[10] E.W. Otten, *Treatise on Heavy-Ion Science*, ed. D.A. Bromley **8**, 517 (1989).

[11] P. Aufmuth, K. Heilig and A. Steudel, *At. Nucl. Data Tables* **37** (1987) 455.

[12] P. Raghavan, *At. Nucl. Data Tables* **42** (1989) 189.

[13] N. Stone, *At. Nucl. Data Tables* to be published (1999).

[14] I. Angeli, *Acta Phys. Hungarica* **69** (1991) 233.

[15] E.G. Nadjakov, K.P. Marinova and Yu.P. Gangrsky, *At. Nucl. Data Tables* **56** (1994) 133.

[16] N.E. Holden, *Report BNL-61460* (1995).

[17] S. Raman, C.W. Nestor, Jr., S. Kahane and K.H. Bhatt, *At. Nucl. Data Tables* **42** (1989) 1.

[18] A. Lépine-Szily, *Experimental Overview of Mass Measurements*, tutorial lecture at the Second Euroconference on Atomic Physics at Accelerators - Mass Spectrometry (APAC-2000), Cargèse (France), 18-23 Septembre 2000, Hyperfine Interactions **132** (2001) 35-57.

[19] T.P. Kohman, J.H.E. Mattauch and A.H. Wapstra, J. de Chimie Physique **55** (1958) 393.

[20] John Dalton, 1766-1844, who first speculated that elements combine in proportions following simple laws, and was the first to create a table of (very approximate) atomic weights.

[21] P.J. Mohr and B.N. Taylor, J. Phys. Chem. Ref. Data **28** (1999) 1713.

[22] E.R. Cohen and A.H. Wapstra, *Nucl. Instrum. Meth.* **211** (1983) 153.

[23] A.H. Wapstra and K. Bos, *At. Nucl. Data Tables* **20** (1977) 1.

[24] V.T. Koslowsky, J.C. Hardy, E. Hagberg, R.E. Azuma, G.C. Ball, E.T.H. Clifford, W.G. Davies, H. Schmeing, U.J. Schrewe and K.S. Sharma, *Nucl. Phys. A* **472** (1987) 419.

[25] E.G. Kessler, Jr., M.S. Dewey, R.D. Deslattes, A. Henins, H.G. Börner, M. Jentschel, C. Doll and H. Lehmann, *Phys. Lett. A* **255** (1999) 221.

[26] C.N. Davids, P.J. Woods, H.T. Penttilä, J.C. Batchelder, C.R. Bingham, D.J. Blumenthal, L.T. Brown, B.C. Busse, L.F. Conticchio, T. Davinson, D.J. Henderson, R.J. Irvine, D. Seweryniak, K.S. Toth, W.B. Walters and B.E. Zimmerman, *Phys. Rev. Lett.* **76** (1996) 592.

[27] R.R. Ries, R.A. Damerow, W.H. Johnson, *Proc. 2nd Int. Conf. Atomic Masses and Fund. Constants (*AMCO-2), Vienna, July 1963, p. 357.

[28] R.C. Barber, R.L. Bishop, L.A. Cambey, H.E. Duckworth, J.D. Macdougall, W. McLatchie, J.H. Ormrod and P. Van Rookhuyzen, *Proc. 2nd Int. Conf. Atomic Masses and Fund. Constants (*AMCO-2), Vienna, July 1963, p. 393.

[29] A. Gillibert, W. Mittig, L. Bianchi, A. Cunsolo, B. Fernandez, A. Foti, J. Gastebois, C. Grégoire, Y. Schutz and C. Stephan, *Phys. Lett. B* **192** (1987) 39;
D.J. Vieira, J.M. Wouters, K. Vaziri, R.H. Krauss, Jr., H. Wollnik, G.W. Butler, F.K. Wohn and A.H. Wapstra, *Phys. Rev. Lett.* **57** (1986) 3253.

[30] M. Chartier, G. Auger, W. Mittig, A. Lépine-Szilly, L.K. Fifield, J.M. Casandjian, M. Chabert, J. Ferme, A. Gillibert, M. Lewitowicz, M. Mac Cormick, M.H. Moscatello, O.H. Odland, N.A. Orr, G. Politi, C. Spitaels and A.C.C. Villari, *Phys. Rev. Lett.* **77** (1996) 2400.

[31] J. Trötscher, K. Balog, H. Eickhoff, B. Franczak, B. Franzke, Y. Fujita, H. Geissel, Ch. Klein, J. Knollmann, A. Kraft, K.E.G. Löbner, A. Magel, G. Münzenberg, A. Przewloka, D. Rosenauer, H. Schäfer, M. Sendor, D.J. Vieira, B. Vogel, Th. Winkelmann and H. Wollnik, *Nucl. Instrum. Meth. B* **70** (1992) 455.

[32] L.G. Smith and C.C. Damm, *Rev. Sci. Instr.* **27** (1956) 638;
L.G. Smith, *Phys. Rev.***111** (1958) 1606.

[33] P.B. Schwinberg, R.S. Van Dyck, Jr. and R.S. Dehmelt, *Phys. Lett. A* **81** (1981) 119;
for a recent review: D. Lunney, *Mesures des propriétés statiques des noyaux : utilisation des pièges ioniques*, notes de l'École Joliot-Curie de Physique Nucléaire (1999) 85.

[34] B. Franzke, K. Beckert, H. Eickhoff, F. Nolden, H. Reich, U. Schaaf, B. Schlitt, A. Schwinn, M. Steck and Th. Winkler, *Phys. Scr.* **T59** (1994) 176.

[35] K.-N. Huang, M. Aoyagi, M.H. Chen, B. Crasemann and H. Mark, *At. Nucl. Data Tables* **18** (1976) 243.

[36] D. Lunney, J.M. Pearson and C. Thibault, *Rev. Mod. Phys.* **75** (2003) 1021.

[37] F. DiFilippo, V. Natarajan, M. Bradley, F. Palmer and D.E. Pritchard, *Phys. Scr.* **T59** (1995) 144.

[38] Nuclear Structure Reference (NSR): a computer file of indexed references maintained by NNDC, Brookhaven National Laboratory; http://ndcnt1.dne.bnl.gov/nsrq/ or http://www.nndc.bnl.gov/.

[39] M.J. Woods and A.S. Munster, *NPL Report RS(EXT)* **95** (1988).

[40] Particle Data Group, 'Review of Particle Properties', *Eur. Phys. Journal C* **3** (1998), 1.

[41] A.H. Wapstra, *Inst. Phys. Conf. Series* **132** (1993) 129.

[42] Y.V. Linnik, *Method of Least Squares* (Pergamon, New York, 1961); *Méthode des Moindres Carrés* (Dunod, Paris, 1963)

[43] G. Audi, W.G. Davies and G.E. Lee-Whiting, *Nucl. Instrum. Meth. A* **249** (1986) 443.

[44] G. Audi, M. Epherre, C. Thibault, A.H. Wapstra and K. Bos, *Nucl. Phys. A* **378** (1982) 443.

[45] Systematic errors are those due to instrumental drifts or instrumental fluctuations, that are beyond control and are not accounted for in the error budget. They might show up in the calibration process, or when the measurement is repeated under different experimental conditions. The experimentalist adds then quadratically a systematic error to the statistical and the calibration ones, in such a way as to have consistency of his data. If not completely accounted for or not seen in that experiment, they can still be observed by the mass evaluators when considering the mass adjustment as a whole.

[46] J. Duflo and A.P. Zuker, *Phys. Rev. C* **52** (1995) 23; and private communication February 1996 to the AMDC, http://www.nndc.bnl.gov/amdc/theory/du_zu_10.feb96.

[47] http://www.nndc.bnl.gov/amdc/masstables/Ame2003/graphs2003/

[48] H.v. Groote, E.R. Hilf and K. Takahashi, *At. Nucl. Data Tables* **17** (1976) 418.

[49] C. Thibault, R. Klapisch, C. Rigaud, A.M. Poskanzer, R. Prieels, L. Lessard and W. Reisdorf, *Phys. Rev. C* **12** (1975) 644.

[50] C.F. von Weizsäcker, *Z. Phys.* **96** (1935) 431.

[51] Julian Michael Fletcher, M.Sc. dissertation, University of Surrey, September 2003.

[52] Piet J. van Isacker, private communication, June 2004.

[53] H.A. Bethe and R.F. Bacher, *Rev. Mod. Phys.* **8** (1936) 82.

[54] A.S. Jensen, P.G. Hansen and B. Jonson, *Nucl. Phys. A* **431** (1984) 393.

[55] C. Borcea and G. Audi, *AIP Conf. Proc.* **455** (1998) 98.

[56] C. Borcea and G. Audi, *Proc. Int. Conf. on Exotic Nuclei and Atomic Masses* (ENAM'95), Arles, June 1995, p. 127.

[57] C. Borcea and G. Audi, *Rev. Roum. Phys.* **38** (1993) 455; *Report CSNSM* **92-38**, October 1992, http://www.nndc.bnl.gov/amdc/extrapolations/bernex.pdf.

[58] The NUBASE and the AME files in the electronic distribution can be retrieved from the Atomic Mass Data Center through the *Web* at http://www.nndc.bnl.gov/amdc/.

[59] B. Potet, J. Duflo and G. Audi, *Proc. Int. Conf. on Exotic Nuclei and Atomic Masses* (ENAM'95), Arles, June 1995, p. 151; http://www.nndc.bnl.gov/amdc/nucleus/arlnucleus.ps

[60] E. Durand, *Report CSNSM* **97-09**, July 1997; http://www.nndc.bnl.gov/amdc/nucleus/stg-durand.doc

Workshop on
DECAY DATA EVALUATION

Saclay, March 6 – 10, 2006

Edgardo Browne

Statistical Analysis of Decay Data

- Relative γ-ray intensities
- α-particle intensities
- Electron capture and β intensities
- Recommended standards for energies and intensities
- Statistical procedures for data analysis
- Discrepant data
- Level energies

1. Relative γ-ray Intensities

$I_\gamma = A \times \varepsilon(E_\gamma)$

$A \pm \Delta A$ … Spectral peak area

$\varepsilon \pm \Delta\varepsilon$ … Detector efficiency

Several measurements with Ge detectors:

$I_{\gamma 1} = A_1 \times \varepsilon_1$, $I_{\gamma 2} = A_2 \times \varepsilon_2$, …

ε_1, ε_2, … are determined with standard calibration sources, thus they are *not independent quantities*.

Best value of I_γ is a weighted average of $I_{\gamma i}$. A realistic uncertainty Δi_γ should not be lower than the *lowest uncertainty in the input values*.

Same criterion applies to γ-ray energies.

An Eckert & Ziegler Company Fax 661•257•8303

CERTIFICATE OF CALIBRATION
GAMMA STANDARD SOURCE

Radionuclide:	Be-133	**Customer:**	U.C. LAWRENCE BERKELEY LAB
Half-life:	3862 ± 15 days	**P.O. No.:**	6513215
Catalog No.:	GF-290	**Reference Date:**	1-Nov-01 12:00 PST
Source No.:	838-18-6	**Contained Radioactivity:**	1.025 µCi 37.93 kBq

Physical description:

A. Capsule type:	M
B. Nature of active deposit:	Evaporated metallic salt
C. Active Diameter:	3 mm
D. Backing:	9.23 mg/cm² kapton
E. Cover:	0.254 mm aluminized mylar

Radioimpurities:

Cs-134 = 0.316% on 1 Nov 01

Method of Calibration:

This source was assayed using gamma ray spectrometry.

Peak energy used for integration:	302.9, 356.0 keV
Branching ratio used:	0.183, 0.619 gammas per decay

Uncertainty of Measurement:

A. Type A (random) uncertainty:	± 0.8 %
B. Type B (systematic) uncertainty:	± 3.0 %
C. Uncertainty in aliquot weighing:	± 0.0 %
D. Total uncertainty at the 99% confidence level:	± 3.1 %

Notes:
- See reverse side for leak test(s) performed on this source.
- IPL participates in a NIST measurement assurance program to establish and maintain implicit traceability

5

Precise half-life values are important for γ-ray calibration standards

The IAEA Coordinated Research Programme (CRP) gives:

$dT_{1/2}/T_{1/2} < 0.00144\ T_{1/2}/T_1$, where

T_1 is the maximum source-in-use period for a given radionuclide (15 years or 5 half-lives), whichever is shorter. Then the contribution to the uncertainty in the radiation intensity calibration using this radionuclide will not exceed 0.1%.

Example: ^{133}Ba - $T_{1/2}$ =10.57± 0.04 y - T_1 = 15 y, then

$dT_{1/2}/T_{1/2}$ = 0.00144 x 10.57/15 = 0.0010,

Experimental value is 0.04/10.57 = 0.0039.

The contribution to the uncertainty is >0.1%.

110

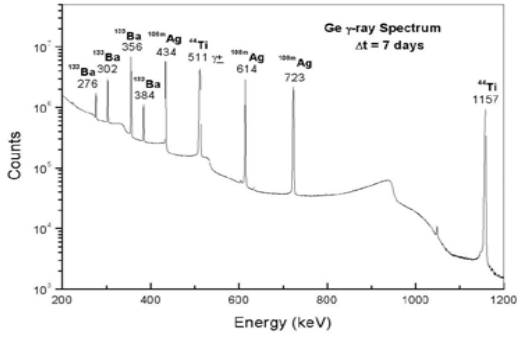

7

$A = A_1(434) + A_2(614) + A_3(723)$

The areas of the individual peaks are not independent of each other.

DO NOT use $A_1(434)$, $A_2(614)$, and $A_3(723)$ to determine $T_{1/2}(434)$, $T_{1/2}(614)$, and $T_{1/2}(723)$, respectively, and then average these values to obtain $T_{1/2}$.

Use "A" to determine $T_{1/2}$.

8

2. α-particle Intensities

$$I_\alpha = A \times \varepsilon$$

$A \pm \Delta A$ … Spectral peak area

ε ……..Geometry (semiconductor detectors)

ε is the same for all α-particle energies.

Best value of I_α is a weighted average of $I_{\alpha i}$.

Uncertainty is the external (multiplied by χ) uncertainty of the average value.

Same criterion applies to α-particle energies, but because of the use of standards for energy calibrations, a realistic uncertainty should not be lower than the *lowest uncertainty in the input values*.

3. Electron Capture and β Intensities

Most electron capture and β intensities are from γ-ray transition intensity balances.

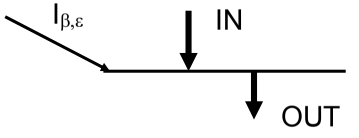

I_β or I_ε = OUT - IN

4. Recommended Standards for Energies and Intensities

Recommended standards for γ-ray energy calibration (1999), R.G. Helmer, C. van der Leun, Nucl. Instrum. and Methods in Phys. Res. **A450**, 35 (2000).

X-ray and gamma-ray standards for detector calibration, IAEA-TECDOC-**619**, September 1991.

Recommended Energy and Intensity Values of Alpha Particles from Radioactive Decay, A. Rytz, Atomic Data and Nuclear Data Tables **47**, 205 (1991)

I strongly suggest reading the following paper

Decay Data: review of measurements, evaluations and compilations, A.L. Nichols, Applied Radiations and Isotopes **55**, 23 (2001).

5. Statistical Procedures for Data Analysis

13

Averages

Unweighted

$x(avg) = 1 / n \sum x_i$

$\sigma_{x(avg)} = [\, 1 / n\,(n-1)\, \sum (x(avg) - x_i)^2]^{1/2}$ Std. dev.

Weighted

$x(avg) = W \sum x_i / \sigma_{xi}^2$; $W = 1 / \sum \sigma_{xi}^{-2}$

$\chi^2 = \sum (x(avg) - x_i)^2 / \sigma_{xi}^2$ Chi sqr.

$\chi_\nu^2 = 1 / (n-1) \sum (x(avg) - x_i)^2 / \sigma_{xi}^2$ Red. Chi sqr

$\sigma_{x(avg)}$ = larger of $W^{1/2}$ and $W^{1/2} \chi_\nu$. Std. dev.

14

Discrepant Data

- **Simple definition**: A set of data for which $\chi_\nu^2 > 1$.
- But, χ_ν^2 has a Gaussian distribution, i.e. it varies with the number of degrees of freedom ($n - 1$).
- **Better definition**: A set of data is discrepant if χ_ν^2 is greater than χ_ν^2 (critical). Where χ_ν^2 (critical) is such that there is a 99% probability that the set of data is discrepant.

15

χ^2_ν (critical)

[$\nu = N-1$]

ν	χ^2_ν (critical)	ν	χ^2_ν (critical)
1	6.6	11	2.2
2	4.6	12	2.2
3	3.8	13	2.1
4	3.3	14	2.1
5	3.0	15	2.0
6	2.8	16	2.0
7	2.6	17	2.0
8	2.5	18 – 21	1.9
9	2.4	22 – 26	1.8
10	2.3	27 – 30	1.7
		> 30	$1 + 2.33 \times 2/\nu$

16

Limitation of Relative Statistical Weight Method (Program *LWEIGHT*)

For discrepant data ($\chi^2_\nu >$ χ^2_ν(critical)) with at least three sets of input values, we apply the *Limitation of Relative Statistical Weight* method. The program identifies any measurement that has a relative weight >50% and increases its uncertainty to reduce the weight to 50%. Then it recalculates χ^2_ν and produces a new average and a best value as follows:

- If $\chi^2_\nu \leq \chi^2_\nu$(critical), the program chooses the weighted average and its uncertainty (the larger of the internal and external values).
- If $\chi^2_\nu > \chi^2_\nu$(critical), the program chooses either the weighted or the unweighted average, depending on whether the uncertainties in the average values make them overlap with each other. If that is so, it chooses the weighted average and its (internal or external) uncertainty. Otherwise, the program chooses the unweighted average. In either case, it may expand the uncertainty to cover the most precise input value.

Simple Example

X= 500±1 1000±100

ν=N - 1

X(avg)= 500 ± 5

χ^2_ν =25, χ^2_ν (critical) =6.6 Data are discrepant

We change to 500±100 (Same statistical weights). Then

X(avg)= 750 ± 250

^{44}Ti Half-life (LWEIGHT)

```
                44Ti Half-life Measurements
 INP. VALUE  INP. UNC.      R. WGHT  chi**2/N-1 REFERENCE
 .607000E+02 .120E+01       .141E+00  .826E-01   99Wi01
 .590000E+02 .600E+00 MIN  *.563E+00* .479E+00   98Ah03
 .603000E+02 .130E+01       .120E+00  .163E-01   98Go05
 .620000E+02 .200E+01       .507E-01  .214E+00   98No06
 .666000E+02 .160E+01       .792E-01  .348E+01   90Al11
 .542000E+02 .210E+01       .460E-01  .149E+01   83Fr27
 No. of Input Values N= 6  CHI**2/N-1=  5.76  CHI**2/N-1(critical)=  3.00
 UWM    :.604667E+02  .164796E+01                              unweighted average
 WM     :.599288E+02  .450317E+00(INT.)  .108057E+01(EXT.)     weighted average
 INP. VALUE  INP. UNC.      R. WGHT  chi**2/N-1 REFERENCE
 .607000E+02 .120E+01       .161E+00  .563E-01   99Wi01
 .590000E+02 .681E+00      *.500E+00* .487E+00   98Ah03
 * Input uncertainty increased .114E+01 times *
 .603000E+02 .130E+01       .137E+00  .663E-02   98Go05
 .620000E+02 .200E+01       .580E-01  .188E+00   98No06
 .666000E+02 .160E+01       .907E-01  .334E+01   90Al11
 .542000E+02 .210E+01       .526E-01  .156E+01   83Fr27
 No. of Input Values N= 6  CHI**2/N-1=  5.63  CHI**2/N-1(critical)=  3.00
 UWM    :.604667E+02  .164796E+01                              unweighted average
 WM     :.600634E+02  .481846E+00(INT.)  .114378E+01(EXT.)     weighted average
 LWM    :.600634E+02  .114378E+01   Min. Inp. Unc.=.600000E+00  LWEIGHT value
 LWM has used weighted average   and external uncertainty
                 Recommended value:  60.0 (11) y
```

I strongly suggest reading the following paper

M.U.Rajput, T.D.Mac Mahon, *Techniques for Evaluating Discrepant Data*, Nucl.Instrum.Methods Phys.Res. **A312**, 289 (1992).

6. Level Energies (*GTOL*)

Simple example

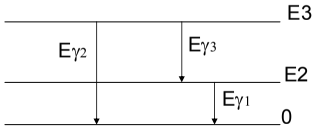

We want to deduce level energies Ei such that

$E\gamma 1 = E2$

$E\gamma 2 = E3$

$E\gamma 3 = E3 - E2$

In matrix form:

$$\begin{vmatrix} E\gamma 1 \\ E\gamma 2 \\ E\gamma 3 \end{vmatrix} = \begin{vmatrix} 1 & 0 \\ 0 & 1 \\ -1 & 1 \end{vmatrix} \begin{vmatrix} E2 \\ E3 \end{vmatrix}$$

For a general case

$$\vec{E\gamma} = \lambda \vec{E}$$

This is a linear regression problem. The solution is

$$\hat{E} = (\lambda \tilde{\lambda})^{-1} \tilde{\lambda} \vec{E\gamma}$$

Program *GTOL* does this calculation. It also does a γ-ray transition intensity balance.

7. ^{44}Sc Electron Capture Decay

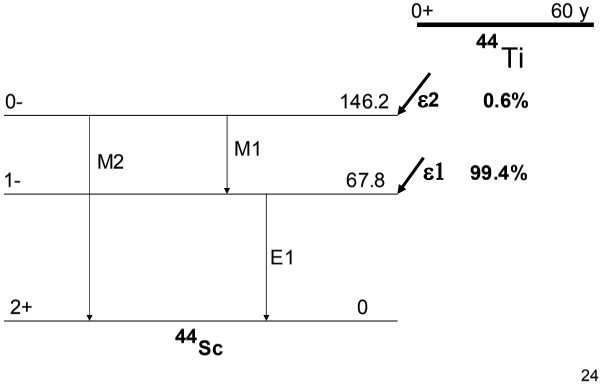

^{44}Sc ENSDF Data Set (GTOL)

LEVEL	TI (OUT)	TI (IN)	TI (NET)	NET FEEDING (CALC)	(USE)
0.0	0.000	104.8 18	-104.8 18	-1.0 17	0.0
67.8679 14	104.7 18	103.0 12	1.6 21	1.6 21	0.6 11
146.224 22	103.1 12	0.000	103.1 12	99.4 11	99.4 11

```
44SC    44TI EC DECAY
44TI  P 0             0+               60.0 Y    11             267.5     19
44SC  N 0.964      13          1.0
44SC  L 0             2+               3.97 H    4
44SC  L 67.8679   141-                154.2 NS  8
44SC  E                           0.6      11
44SC  G 67.8679   14    96.5 16     E1                   0.0845
44SCS G KC=    0.0766  $LC=    0.00664
44SC  L 146.224   220-                50.4 US   7
44SC  E                           99.4     11
44SC  G 78.36      3    100.0 11     M1                   0.0302
44SCS G KC=    0.0273  $LC=    0.00243
44SC  G 146.22     3    0.095 3     [M2]                 0.0460
44SCS G KC=    0.0414  $LC=    0.00385
```


^{44}Sc ENSDF Data Set (LOGFT)

```
• 44SC    44TI EC DECAY
• 44TI  P 0             0+               60.0 Y    11             267.5     19
• 44SC  N 0.964      13          1.0
• 44SC  L 0             2+               3.97 H    4
• 44SC  L 67.8679   141-                154.2 NS  8
• 44SC  E                           0.6   11   9.2    8
• 44SCS E  CK=0.8910 $CL=0.09309 $CM+=0.01592
• 44SC  G 67.8679   14    96.5 16     E1                   0.0845
• 44SCS G KC=    0.0766  $LC=    0.00664
• 44SC  L 146.224   220-                50.4 US   7
• 44SC  E                          99.4   11   6.509 17
• 44SCS E  CK=0.8883 $CL=0.09533 $CM+=0.016352 18
• 44SC  G 78.36      3    100.0 11     M1                   0.0302
• 44SCS G KC=    0.0273  $LC=    0.00243
• 44SC  G 146.22     3    0.095 3     [M2]                 0.0460
• 44SCS G KC=    0.0414  $LC=    0.00385
```

LWeight & LWeight for Excel

- **Lweight :**
  - What is it used to ?
  - A brief presentation.
- **Lweight for Excel :**
  - Why ?
  - How to use it ?

Christophe Dulieu – CEA/LNHB

LWeight

- Fortran program (D. MacMahon & E. Browne)
- Calculation of averages for data sets
- Rejection of outliers input values
- Limitation of Relative Statistical Weight
- One iteration calculation

Lweight for Excel

- Excel data sheet formulas
- Calculation of averages for data sets
- Rejection of outliers input values
- Limitation of Relative Statistical Weight
- One iteration calculation : Lweight41, or …
- Complete calculation : Lweight4

Lweight4 : all iterations

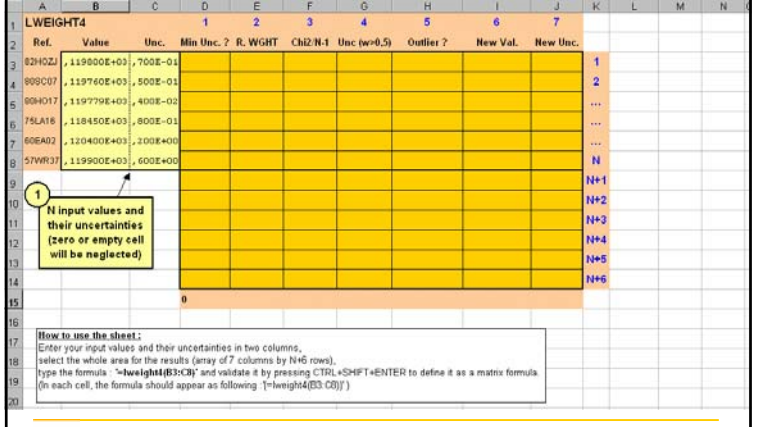

Lweight4 : all iterations (2)

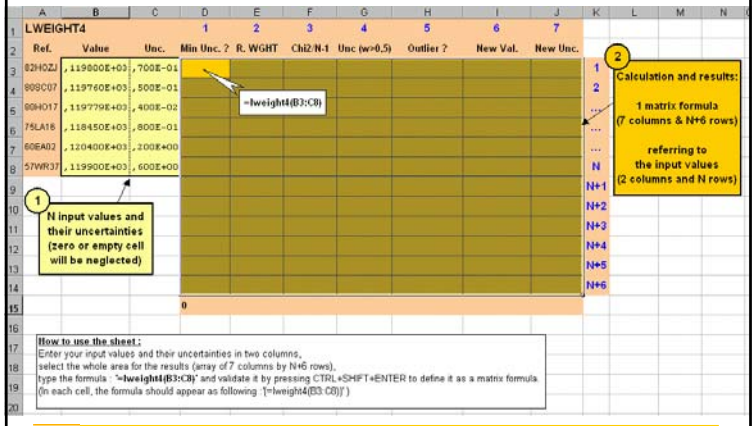

Lweight4 : all iterations (3)

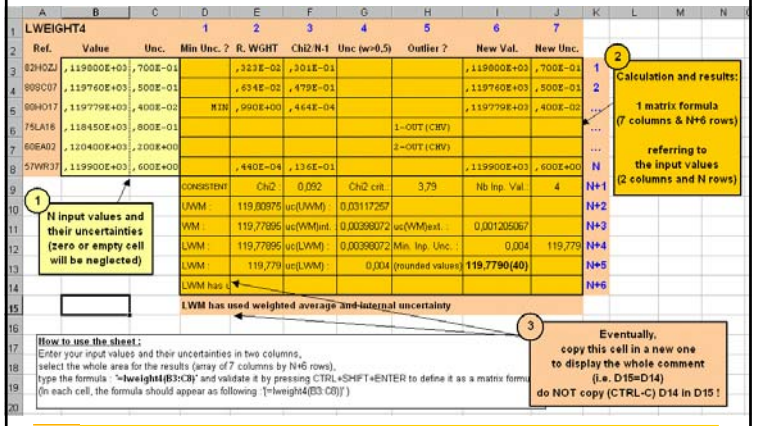

Lweight41 : one iteration

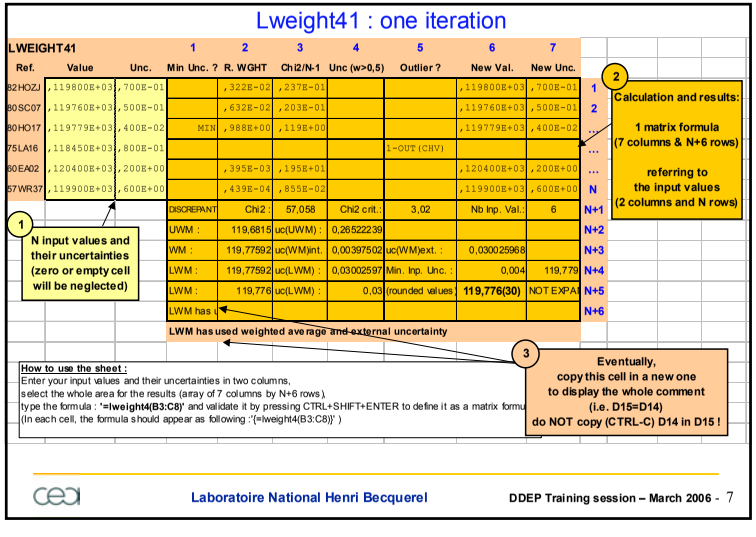

LWEIGHT4 (complete calculation)

1 Min Unc. ?	2 R. WGHT	3 Chi2/N-1	4 Jnc (if w>0,5	5 Outlier ?	6 New Val.	7 New Unc.
	0,040919	0,0400476			0,0185	0,0003
	0,0102298	0,0427083			0,0182	0,0006
	0,0057542	0,0991591			0,0176	0,0008
	0,0102298	0,0651653			0,0195	0,0006
	0,0102298	0,121657			0,0178	0,0006
	0,0012743	0,0233488			0,02	0,0017
	0,0920678	0,0374725			0,0186	0,0002
	0,023017	0,1902815			0,0196	0,0004
	0,0920678	0,1152083			0,0191	0,0002
	0,040919	0,1931454			0,0194	0,0003
	0,0920678	0,000385			0,0188	0,0002
	0,0920678	0,5864879			0,0195	0,0002
	0,0016368	0,2448785			0,0153	0,0015
	0,0102298	0,7775633			0,0163	0,0006
	0,0147309	1,0312696			0,0164	0,0005
	0,0002302	0,0649535			0,014	0,004
	0,023017	0,7106349			0,0172	0,0004
	0,0016368	0,2888978			0,015	0,0015
				1-OUT(3*S		
	0,0009207	0,1987013			0,0146	0,002
	0,0045466	0,0018505			0,0186	0,0009
	0,023017	0,0763484			0,0193	0,0004
MIN	0,3682713	0,0302606			0,0187	0,0001
	0,040919	0,3382782			0,0196	0,0003
DISCREPA	Chi2 :	5,2787036	Chi2 crit.:	1,828652	Nb Inp. Val.:	23
UWM:	0,0178957	uc(UWM) :	0,0003733			
WM :	0,0187816	uc(WM)int :	6,069E-05	uc(WM)ext.	0,0001394	
LWM :	0,0178957	uc(LWM) :	0,0008043	Min. Inp. Ui	0,0001	0,0187
LWM :	0,0179	uc(LWM) :	0,0008	(rounded v	0,0179(8)	EXPANDED
LWM has u						

LWM has used unweighted average and expanded the uncertainty so range includes the most precise value of 0,0187

LWEIGHT41 (1 calculation only)

1 Min Unc. ?	2 R. WGHT	3 Chi2/N-1	4 Jnc (if w>0,5	5 Outlier ?	6 New Val.	7 New Unc.
	0,0405047	0,0173719			0,0185	0,0003
	0,0101262	0,0289539			0,0182	0,0006
	0,005696	0,0806586			0,0176	0,0008
	0,0101262	0,0793114			0,0195	0,0006
	0,0101262	0,0955849			0,0178	0,0006
	0,0012614	0,0258322			0,02	0,0017
	0,0911355	0,0087322			0,0186	0,0002
	0,0227839	0,2252098			0,0196	0,0004
	0,0911355	0,1830467			0,0191	0,0002
	0,0405047	0,2437799			0,0194	0,0003
	0,0911355	0,0132406			0,0188	0,0002
	0,0911355	0,7138026			0,0195	0,0002
	0,0016202	0,2220212			0,0153	0,0015
	0,0101262	0,689654			0,0163	0,0006
	0,0145817	0,9117233			0,0164	0,0005
	0,0002278	0,0597626			0,014	0,004
	0,0227839	0,6029891			0,0172	0,0004
	0,0016202	0,2630604			0,015	0,0015
				1-OUT(3*S)		
	0,0009114	0,1817943			0,0146	0,002
	0,0045005	0,0004312			0,0186	0,0009
	0,0227839	0,1012366			0,0193	0,0004
MIN	0,3645422	0,0004675			0,0187	0,0001
	0,0405047	0,400373			0,0196	0,0003
DISCREPA	Chi2 :	14,909118	Chi2 crit.:	1,8078651	Nb Inp. Val.:	24
UWM:	0,0175542	uc(UWM) :	0,0004943			
WM :	0,0186896	uc(WM)int :	6,038E-05	uc(WM)ext. :	0,0002331	
LWM :	0,0175542	uc(LWM) :	0,0011458	Min. Inp. Un	0,0001	0,0187
LWM :	0,0176	uc(LWM) :	0,0011	(rounded va	0,0176(11)	EXPANDED
LWM has u						

LWM has used unweighted average and expanded the uncertainty so range includes the most precise value of 0,0187

NNDC Data Services

Jagdish K. Tuli
National Nuclear Data Center
Brookhaven National Laboratory
Upton, NY 11973

Overview of US Nuclear Data Program's nuclear structure and decay data activities

Content:

- How do our evaluation and dissemination activities fit into the global picture?
- Who is involved?
- What are the major products?
- How can our products be accessed?
- Other activities

The International Connection

The US structure and decay data evaluation effort is part of an international effort coordinated by the IAEA
via two-yearly Advisory Group meetings

Long-Term Non-US Contributors:	Emerging Non-US Contributors:
BELGIUM	ARGENTINA
CANADA	AUSTRALIA
CHINA	BRAZIL
FRANCE	BULGARIA
JAPAN	INDIA
KUWAIT	
RUSSIA	

Structure Evaluation Responsibilities

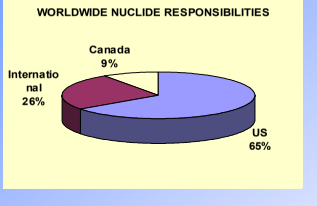

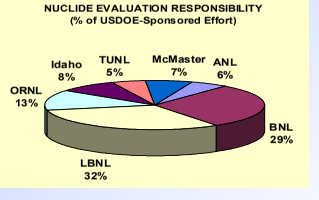

The US contribution is a very significant one

Responsible for two thirds of the known ~2900 nuclides.

However, there is an extremely important international component to the overall structure evaluation effort!

USNDP Evaluators – Who Are We?

US Network (~6 FTE)

(US-DOE Office of Science funded)

ANL

BNL
INEEL

LBNL

ORNL

McMASTER

TUNL

TUNL Nuclear Data Evaluation Project

NNDC Web Portal

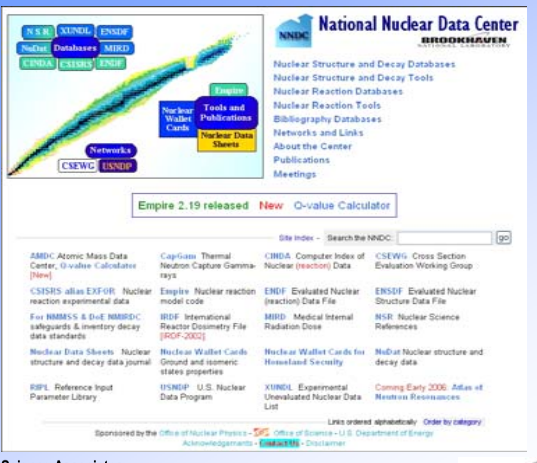

120

Geographical Distribution of NNDC Users in 2004

- USA - 41.87%
- EU - 25.72%
- Japan - 6.06%
- China - 3.75%
- Former USSR - 3.28%
- India - 3.13%
- Canada - 2.47%
- Korea - 1.09%
- Australia - 0.78%
- Brazil - 0.77%
- The rest- 4.14%
- Unresolved - 6.94%

Our Major Products

Evaluated (or compiled) structure & decay data, A=1-294, and the means to access them

PRINCIPAL DATABASES ....
Web accessible from NNDC or mirror sites;
http://www.nndc.bnl.gov.

- **NSR** - Nuclear Science References (bibliographic).
- **ENSDF** - Evaluated Nuclear Structure Data File; comprehensive, peer reviewed, publicly available; the primary data source for other special purpose databases and the starting point for several major publications.
- **XUNDL** – Experimental Unevaluated Data List compiled from recently published literature; primarily high-J papers.

ENSDF Database: Major Contributors and Derivatives

Contributing Databases: Atomic Masses (Audi, Wapstra); Nuclear Science References (NSR); XUNDL Compilation

ENSDF

Derivative Databases: NuDat; MIRD; RADWARE Hi-J

Derivative Publications: (value added): Nuclear Data Sheets (Elsevier); Nuclear Wallet Cards; Table of Isotopes (1996-9); Table of Super - deformed Bands; Table of Radioactive Isotopes (1986)

ENSDF Database Structure

ENSDF

A=1 .... A .... A=294

Abs Z_{min} .... Z .... Z_{max} Ref

Adopted
(best values)
Q values
Levels:
(E, Jπ, T1/2, μ, Q, config, excitn.)
Gammas:
(E, Br, Mult, δ)
1 dataset

Decays
β^-
$\varepsilon+\beta^+$
α
β^-n
etc.
0 to ~6 datasets

Reactions
(HI,xnγ)
(p,p' γ)
(n, γ)
Coul. Exc.
(α,α')
(d,p)
etc.
0 to ~40 datasets

Access to ENSDF data

90	NDS 82 379 (1997)	1-May-1997
91	NDS 86 1 (1999)	15-Dec-1998
^{91}Kr	ENSDF	29-Dec-2000
^{91}Sr	ENSDF	29-Dec-2000
^{91}Zr	ENSDF	29-Dec-2000
92	NDS 91 423 (2000)	7-Nov-2000
^{92}Kr	ENSDF	21-Jan-2004
^{92}Sr	ENSDF	2-Aug-2003
93	NDS 80 1 (1997)	1-Nov-1996
^{93}Br	ENSDF	26-Feb-2001
^{93}Kr	ENSDF	26-Feb-2001
^{93}Rb	ENSDF	27-Feb-2001
94	NDS 66 1 (1992)	1-Feb-1992
^{94}Pd	ENSDF	5-Sep-2002
^{94}Ag	ENSDF	5-Sep-2002
95	NDS 68 635 (1993)	10-Oct-1995
96	NDS 68 165 (1993)	1-Oct-1992
^{96}Zr	NDS 82 547 (1997)	1-Oct-1997
97	NDS 70 85 (1993)	1-Jul-1993

Segment of Index to ENSDF; choose A or nuclide of interest

Index to ENSDF for ^{92}Kr

- In ENSDF.
- Evaluator(s): CORAL M. BAGLIN
- Cutoff: 21-Jan-2004; Get NSR Entries added since this date.

Back to index.

Choose Dataset(s), Output option

Matching datasets in ENSDF:

	^{92}Kr	COMMENTS	References
☐		ADOPTED LEVELS, GAMMAS	References
☐		92BR B- DECAY	References
☐		93BR B-N DECAY	References
☐		248CM SF DECAY	References
☐		235U(N,FG) E=THERMAL	References

Get selected ENSDF datasets: HTML Download View ENSDF

Get all ENSDF datasets : HTML Download View ENSDF

Reset

HTML output for 184Bi "Adopted"

^{184}Bi **Adopted Levels** 200402

Published: 2004 ENSDF.

S_p=-1.33×10^3 *13* Q_α=8025 *50* 2003Au03

Q_α:The value recommended in 2003Au03 assumes that the highest-energy α emitted by ^{184}Bi is within 50 keV of the g.s. to g.s. α transition energy.

History

Type	Author	Citation	Cutoff Date
Full evaluation	Coral M. Baglin	ENSDF	21-Jan-2004

Production: ^{93}Nb(^{94}Mo,3n), E(^{94}Mo)=444 MeV; pulsed beam; evaporation residues separated by velocity filter SHIP and implanted in position sensitive Si detector; coaxial HPGe detector; measured excit (434-461 MeV), Eα, Eγ, αγ(t), recoil-α-γ, recoil-α-α (2003An27,2003AnZZ).

^{184}Bi levels

E_{level}	$T_{1/2}$ [a]	Comments
0.0+x	13 ms *2*	%α≈100 **%α:** α decay was observed, proton decay was not (2003An27). Based on gross β-decay calculations (1973Ta30), the partial β halflife is ≈1 s implying %ε+%β$^+$≈1.3%. **J$^\pi$:** the strongest α's associated with ^{184}Bi decay appear to be unhindered (2003An27) and have Eα consistent with extrapolated Eα values from 10- and 3+ isomers known in heavier even-A Bi isotopes. This favors Jπ=10- and 3+ for the observed ^{184}Bi isomers. **$T_{1/2}$:** from complex structure containing contributions from many α groups with Eα=7120-7350 (2003An27). Other $T_{1/2}$: 14 ms +6-4 from 7194α(t) (2003An27).

XUNDL Database

Purpose: To provide rapid access to formatted (manipulable) data from the latest papers - in response to request from high-spin physics researchers.

Contents: Compiled (**un**evaluated) data from recent publications, primarily in high-spin physics. Currently contains material for:

- 916 nuclides (A=13-288; N - element 115)
- 1326 papers

Coordination: B. Singh (McMaster).

Updates: as datasets arrive at NNDC (D. Winchell - BNL)

Manpower: primarily, carefully trained and closely supervised undergraduate students.

Data Input: often, data input can be done directly from publication using FINEREADER commercial software.

122

Major products for which ENSDF is primary source

NuDat: recommended level and gamma properties (ENSDF Adopted Levels, Gammas)

WWW Table of Nuclear Structure: website providing alternative interface to ENSDF Adopted Levels, Gammas

MIRD: Medical internal radiation dose from radionuclides

Wallet Cards: ground and isomeric state properties

RADWARE Hi-Spin Database: database providing ENSDF and XUNDL datasets for in-beam gamma-ray studies in RADWARE file format

NuDat Database

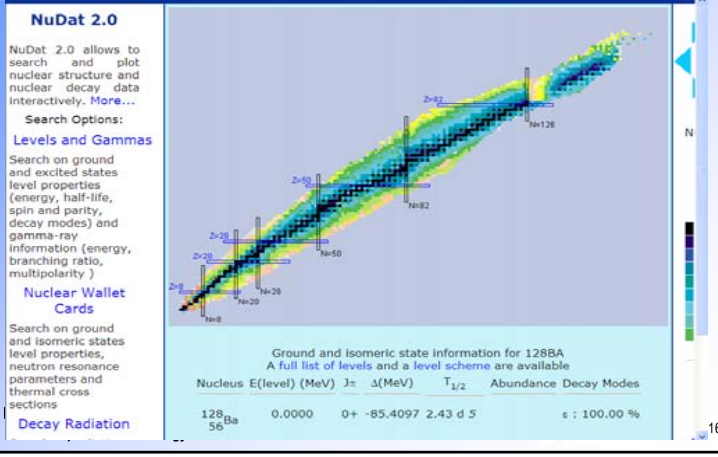

Nuclear Wallet Cards

NNDC

To NNDC

Nuclear Wallet Cards present properties for ground and isomeric states of all known nuclides. Properties given are:

- Spin and parity assignments
- Nuclear mass excesses
- Half-life, isotopic abundances
- Decay modes

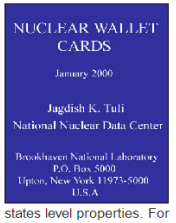

Appendices contain properties of elements, fundamental constants and other userful information. Nuclear Wallet Cards booklet is published by the National Nuclear Data Center and its electronic (current) version is periodically updated by Dr. Jagdish K. Tuli. Nuclear Wallet Cards are distributed as a booklet as well as in PDA-adaptable Palm Pilot format. A web-based version of Nuclear Wallet Cards provides **search** capabilities on ground and isomeric states level properties. For additional nuclear properties see **NuDat 2.0**.

General Information | Current Version | Radioactive Nuclides (Homeland Security) | Nuclear Materials Management & Safeguards | Palm Pilot | Sixth Edition 2000

Last updated by Boris Pritychenko on April 21, 2004.

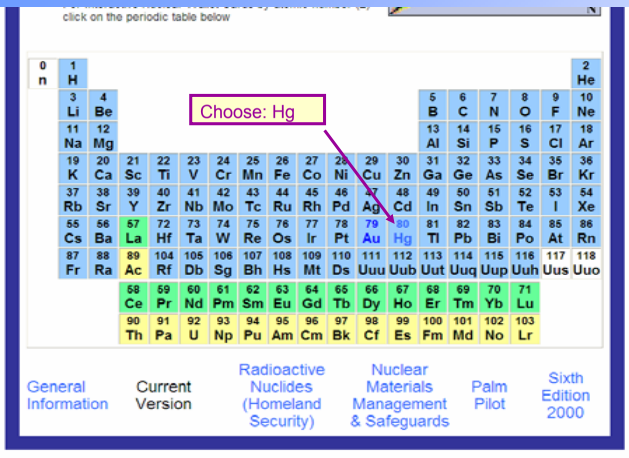

Last updated by Boris Pritychenko on April 21, 2004.

123

Results for Z=80

Nucleus	E(level) (MeV)	Jπ	Δ(MeV)	$T_{1/2}$	Abundance	Decay Modes
$^{171}_{80}$Hg	0.0000			60 μs +40-15		α ≈ 100.00 %
$^{172}_{80}$Hg		0+		0.25 ms +35-9		α
$^{173}_{80}$Hg	0.0000			0.9 ms +6-3		α ≈ 100.00 %
$^{174}_{80}$Hg	0.0000	0+		2.1 ms +18-7		α : 99.60 %
$^{175}_{80}$Hg	0.0000		-8.0000 Syst	8 ms 8		α : 100.00 %
$^{176}_{80}$Hg	0.0000	0+	-11.7245	34 ms +18-9		α ≈ 100.00 %
$^{177}_{80}$Hg	0.0000	(13/2+)	-12.7271	127.3 ms 18		α : 85.00 % ε : 15.00 %
$^{178}_{80}$Hg	0.0000	0+	-16.3232	0.287 s 23		α ≈ 70.00 % ε ≈ 30.00 %
$^{179}_{80}$Hg	0.0000		-16.9690 Syst	0.93 s 11		α ≈ 53.00 % ε ≈ 47.00 % εp ≈ 0.15 %
$^{180}_{80}$Hg	0.0000	0+	-20.2447	2.58 s 1		ε : 52.00 % α : 48.00 %
$^{181}_{80}$Hg	0.0000	1/2(-)	-20.6740 Syst	3.6 s 1		ε : 69.00 % α : 31.00 %

Nuclear Structure Data

- Bibliographic data
- Evaluated data
- Journal preparation

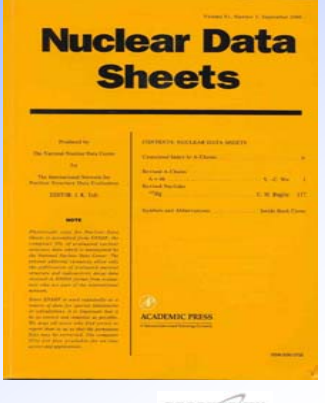

Electronic Access to Nuclear Data

- Electronic access to nuclear physics data bases, computer codes and documents available since 1986.

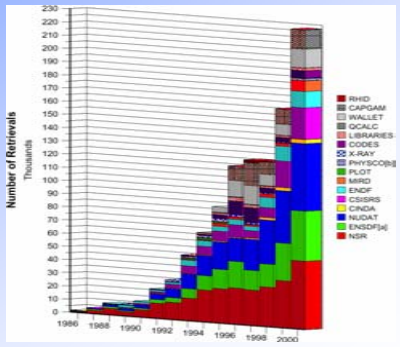

2004 Web Statistics

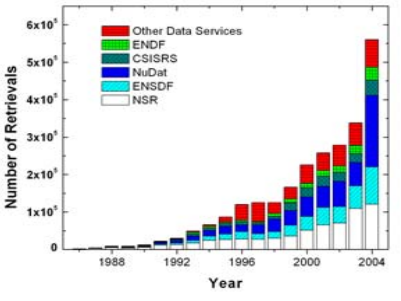

Portal was launched on April 19, 2004

- Number of retrievals went from 338K in 2003 to 560K in 2004, 66% calendar year increase
- Number of database retrievals increased two-folds with a new portal
- Migration + User Interface improvements produce results

Overview of US Nuclear Data Program's nuclear structure and decay data activities

Summary:

- How do our evaluation and dissemination activities fit into the global picture?
- Who is involved?
- What are the major products?
- How can our products be accessed?
- Other activities

IONIZATION CHAMBERS

IONIZATION CHAMBER MEASUREMENT TECHNIQUE AND NUCLEAR DATA

Presented by

M.N. AMIOT
LNHB

IONIZATION CHAMBER INSTRUMENT

Secondary instrument :

- Activity measurements (SIR)
- Memory of standards

Standard Solution

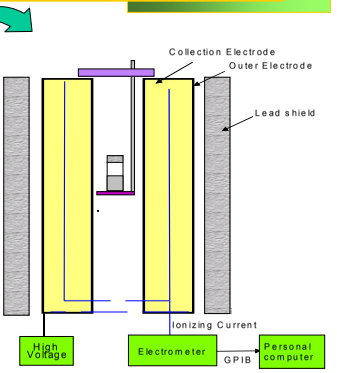

Calibration coefficient

IONIZATION CHAMBERS RESPONSES

- I.C. responses are used for impurity corrections.
- Emission intensities are needed to build I.C. response to photons.
- I.C. response shape depends mainly on the filling gas.

$$C_{Exp} = \frac{I}{A} \quad (pA/MBq)$$

I : ionisation current
A : activity
C_{Exp} : calibration coefficient

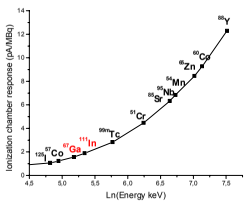

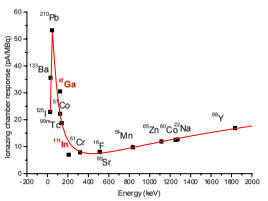

I. C. ACTIVITY MEASUREMENTS

Activity measurements : nuclear data needed

1) Radioactive solution without impurities :

- Half life

2) Radioactive solution with impurities (Simulation) :

- Half life (RN and impurities)
- Emission intensities (X and gamma rays) and uncertainties
- Energies (X and gamma rays) and uncertainties

I. C. ACTIVITY MEASUREMENTS

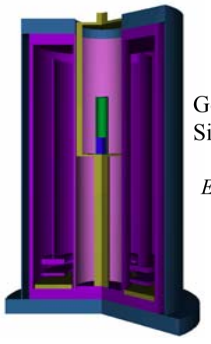

IC MONTE CARLO SIMULATION

Mean energy deposited in the ionised gas per decay for a given RN. E_d (eV)

Geometry and materials modelization
Simulation parameters determination (Cut off E)

$$E_d = \sum_{k=1}^{n} E_k I_k$$

E_k : deposited energy by k^{th} γ-ray
I_k : emission probability per decay for the k^{th} γ-ray

$$C_{Theo} = \frac{E_d}{W} \cdot e$$

e : electron charge
W : mean energy absorbed in gas per ion pair formed

I. C. ACTIVITY MEASUREMENTS

Ionization chamber simulation results

$$C_{Exp} = \frac{I}{A}\ (pA/MBq) \Rightarrow \frac{C_{Theo}}{C_{Exp}}$$

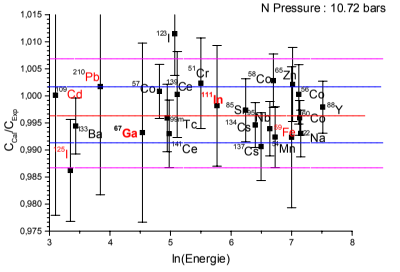

There is a need for more precise X and γ emission intensities for :

^{67}Ga, ^{111}In, ^{59}Fe, ^{210}Pb, ^{125}I, ^{109}Cd.

I. C. ACTIVITY MEASUREMENTS

IC simulation for pure beta emitters

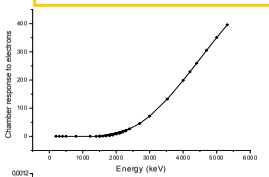

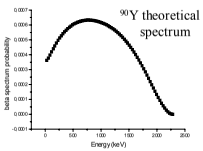

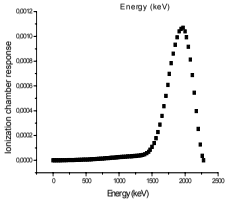

- IC response to monoenergy electrons using MC simulation
- ^{90}Y theoretical beta spectrum
- IC energy distribution response for ^{90}Y

Calibration coefficient for ^{90}Y is the integrale of this IC energy distribution response.

I. C. ACTIVITY MEASUREMENTS

IC simulation for pure beta emitters

Example **^{90}Y**

Beta spectrum : first forbidden unique transition.

The form of the **^{90}Y** beta spectrum is important for the IC simulation study specially for high electron energies which are well detected by the IC.

Problems encountered :

- Many different experimental coefficients in correction Factor C(W),
- Many programs of beta spectra calculation leading to significant deviation of IC response.

We need shapes of beta spectra as precise as possible.

I. C. HALF LIFE MEASUREMENTS

I.C. can provide experimental nuclear data : RN Half life

Half life measurements examples :

0.1% uncertainty on T½ (^{207}Bi) : 30 y measurement time : 20 y
0.03% uncertainty on T½ (^{155}Eu) : 4.7 y measurement time : 10 y
0.04% uncertainty on T½ (^{65}Zn) : 244 d measurement time : 2 y
0.05% uncertainty on T½ (^{88}Y) : 106.7 d measurement time : 1 y
0.02% uncertainty on T½ (^{18}F) : 1.8 h measurement time : 1 d

Stability checking sealed source of ^{226}Ra in equilibrium

I. C. HALF LIFE MEASUREMENTS

Half life determination

- Current measurement,
- Background subtraction,
- Stability checking,
- Impurity checking (γ spectrometry) correction on current knowing impurity half live,
- Non linear least-squares fit to the experimental data.

No nuclear data are needed for half life determination (except when impurities are found).

I. C. HALF LIFE MEASUREMENTS

Typical uncertainties budget

- Current measurement including linearity (0.07 %),
- Background contribution (0.06 %)
- Stability checking (0.03 %)
- Positionning variability (0.065 %)

All these uncertainties are taken into account for the Half life determination.

Uncertainty obtained for ^{88}Y half life measurement 0.05 % : 106.63 (5) d

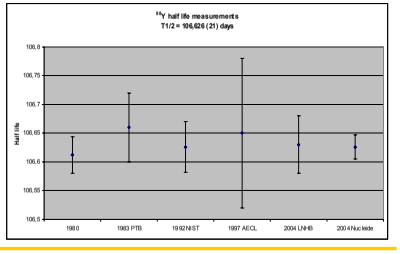

IONIZATION CHAMBER

CONCLUSION

1) Ionization chamber measurement technique can provide :

- Activity measurements
- Half life experimental values

2) Ionization chamber measurement technique needs :

- More precise X and gamma emission intensities (^{67}Ga, ^{111}In, ^{59}Fe, ^{123}I, ^{109}Cd, ^{125}I, ^{210}Pb, ^{51}Cr, ^{200}Tl, ^{202}Tl, …),
- Confident beta spectra (^{90}Y, ^{89}Sr, ^{85}Kr, ^{204}Tl…).

DDEP Training Session

X-ray and Auger electron emissions

Saclay, March 08, 2006

Marie-Martine Bé
LNE – CEA / Laboratoire National Henri Becquerel
91191 Gif-sur-Yvette Cedex
France
mmbe@cea.fr

Processes creating vacancies

The creation of vacancies in the electron cloud leads to a rearrangement of the electronic sub-shells, associated with the emission either of X-rays or of Auger electrons.

1) Gamma transitions with internal conversion process
Internal conversion coefficients for the sub-shells
$\alpha_K, \alpha_{L1}, \alpha_{L2}, \alpha_{L3}, \alpha_{M1}$, etc.

2) Electron capture process

Electron capture transition

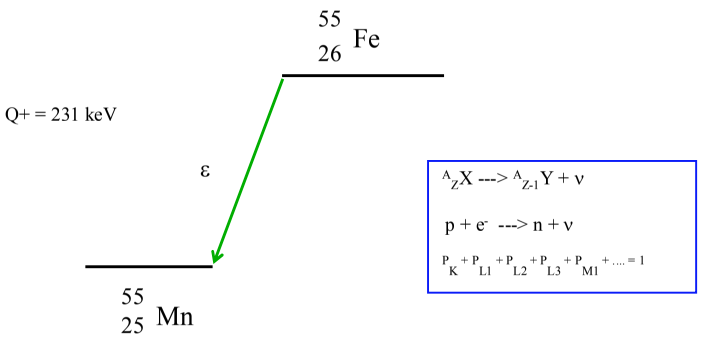

$^{A}_{Z}X \rightarrow {}^{A}_{Z-1}Y + \nu$

$p + e^- \rightarrow n + \nu$

$P_K + P_{L1} + P_{L2} + P_{L3} + P_{M1} + \ldots = 1$

Electron capture transition

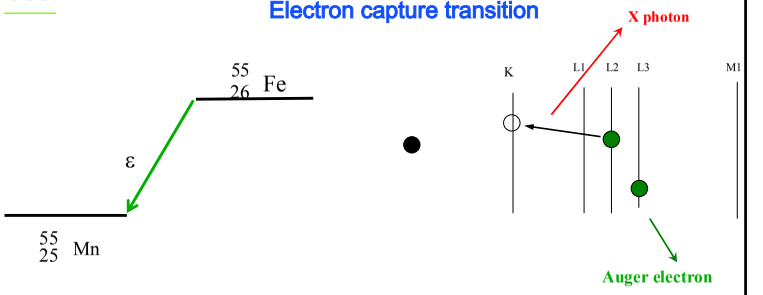

Emissions :
- Manganese K X- Rays
ray : 5,9 keV
- Manganese Auger electrons

K Shell

- For a given radionuclide, the total number of vacancies created in the K shell is :

$$n_K = \Sigma P_e P_K + \Sigma P_g \frac{\alpha_K}{1+\alpha_t}$$

Where P_e is the probability of the electron capture, P_K the probability of the capture in the K shell, Pg the probability of the gamma transition and α the ICCs.

- The K-shell fluorescence yield ω_K is the probability that the filling of a K vacancy is followed by a XK radiation

$$\omega_K = \frac{I_{X_K}}{n_K}$$ where I_{XK} is the intensity of the XK photons

- The K-Auger yield is derived : $a_K = 1 - \omega_K$

- Then the total intensity of XK rays and K Auger electrons are :
  $I_{XK} = \omega_K n_K$ and $I_{AK} = a_K n_K$

K X-rays

- The K X-ray energy for a K – X transition (X = L, M, N, …) is :
  $E_{XK} = E_K - E_X$
  Where E_K and E_X are the binding energies of the electrons in the K and X shells
  They are classified by series :

$K\alpha$ $\begin{cases} K\alpha_2 & KL_3 \\ K\alpha_1 & KL_2 \end{cases}$

$K'\beta_1$ $\begin{cases} K\beta_3 & KM_2 \\ K\beta_1 & KM_3 \\ K\beta_5'' & KM_4 \\ K\beta_5' & KM_5 \end{cases}$

$K'\beta_2$ $\begin{cases} K\beta_2 \begin{cases} K\beta_2^* & KN_2 \\ K\beta_2' & KN_3 \end{cases} \\ K\beta_4 \begin{cases} K\beta_4^* & KN_4 \\ K\beta_4' & KN_5 \end{cases} \end{cases}$

K X-rays

- The emission intensity for the various K X-ray lines can be calculated from the total K X-ray intensity and the relative probability ratios : P(Kβ)/P(Kα) ; $P(K\alpha_1)/P(K\alpha_2)$, etc.
  These ratios being measured or obtained from theoretical calculations.

$$I_{X_{K\alpha}} = I_{XK}\left[1 + \frac{P_{X_{K\beta}}}{P_{X_{K\alpha}}}\right]^{-1} \qquad I_{X_{K\alpha 1}} = I_{X_{K\alpha}}\left[1 + \frac{P_{X_{K\alpha 2}}}{P_{X_{K\alpha 1}}}\right]^{-1}$$

K-Auger electrons

- A vacancy in the K shell is filled by an electron coming from a less bound shell. The available energy is transferred to an electron of another shell, which is also less bound. The latter electron is then ejected (Auger electron) with energy :
  $E_{AK} = E_K - E_X - E_Y - \Delta E$
  Where E_K , E_X and E_Y are the binding energies of the electrons in the K shell and in the two less bound shells (or sub shells). ΔE is a corrective term due to the fact that the binding energy of the excited atom is greater than that of the atom in its ground state.

Three groups of K-Auger electrons are distinguished :

- KLL Auger electrons (X = L, Y = L) with six components : ($KL_1 L_1$, $KL_1 L_2$, $KL_1 L_3$, $KL_2 L_2$, $KL_2 L_3$, $KL_3 L_3$),
- KLX Auger electrons (X = M, N, ...) : $KL_1 M_1$, $KL_1 M_2$, $KL_1 M_3$, $KL_1 M_{4,5}$, $KL_2 M_1$, $KL_2 M_{2,3}$, $KL_2 M_{4,5}$, $KL_3 M_1$, $KL_3 M_{4,5}$, $KL_1 N$, $KL_2 N$, $KL_3 N$,
- KXY Auger electrons (X = M, N, ..., Y = M, N, ...)

K-Auger electrons

- As for the X ray intensities, the detailed K-Auger electron intensities are calculated from the total intensity ($I_{AK} = (1 - \omega_K)\, n_K$) and the relative probability ratios :

with $P_{AKLX}/P_{AKLL} = KLX/KLL$

$$I_{AK} = KLL\left(1 + \frac{KLX}{KLL} + \frac{KXY}{KLL}\right)$$

L Shell

- For a given radionuclide, the total number of vacancies created in the L shell is :

$$n_L = \Sigma P_\varepsilon P_L + \Sigma P_g \frac{\alpha_L}{1+\alpha_t} + n_K\, n_{KL}$$

Where Pε is the probability of the electron capture, P_L the probability of the capture in the L shell, Pg the probability of the gamma transition and α the ICCs, n_K the number of vacancies created in the K shell and n_{KL} the number of L vacancies created by transfer of vacancy from K to L.

$$n_{KL} = \omega_K \frac{K\alpha}{K\alpha + K\beta} + (1-\omega_K)\frac{2KLL + KLX}{KLL + KLX + KXY}$$

$$n_{KL} = \omega_K \frac{1}{1+\frac{K\beta}{K\alpha}} + (1-\omega_K)\frac{2+\frac{KLX}{KLL}}{1+\frac{KLX}{KLL}+\frac{KLY}{KLL}}$$

L Shell

- The L shell is divided in three sub shells L_1, L_2, L_3. This leads to the definition of three L-fluorescence yields :

$$\omega_i = \frac{I_{XLi}}{n_{L_i}} \qquad i = (1,2,3)$$

The L_i- sub shell fluorescence yield ω_i is the probability that the filling of a L_i vacancy is followed by a XL_i radiation with intensity I_{XLi}.

n_{Li} is the number of vacancies created in the L_i sub shell.

(n_{Li} depends on P_{Li} and α_{Li} and n_{KLi})

L X-rays

The L X-ray energy for a L – X transition (X = M, N, …) is :

$E_{XL} = E_L - E_X$

Where E_L and E_X are the binding energies of the electrons in the L and X shells (or sub shells)

They are classified by series :

$L\ell$ L_3M_1

$L\alpha$ α_2 L_3M_4; α_1 L_3M_5

$L\eta$ L_2M_1

$L\beta$ β_4 L_1M_2; β_3 L_1M_3; β_{10} L_1M_4; β_9 L_1M_5; β_1 L_2M_4; β_2 L_3N_5; β_7 L_3O_1; β_5 $L_3O_{4,5}$

$L\gamma$ γ_2 L_1N_2; γ_3 L_1N_3; γ_4 $L_1O_{2,3}$; γ_5 L_2N_1; γ_1 L_2N_4; γ_6 L_2O_4

L-Auger electrons

- A vacancy in the L shell is filled by an electron coming from a less bound shell (M, N, …). The available energy is transferred to an electron of another less bound shell (M, N, …). The latter electron is then ejected (L-Auger electron).

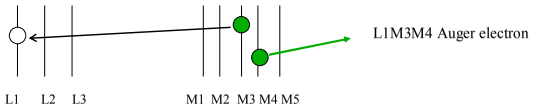

L-Auger electrons

Coster-Kronig :
A Coster-Kronig transition is a special type of Auger effect, it occurs when an Li vacancy (i= 1, 2) moves from a sub shell towards another less bound sub shells, L1 →L2, L1 →L3, L2 →L3.
The ratio of the number of vacancies filled by Coster-Kronig transitions to the total number of initial vacancies; f_{12}, f_{13}, f_{23} are called Coster-Kronig yields.

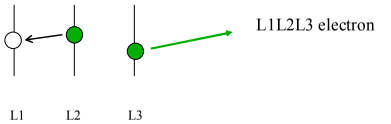

L Shell

- Total number of vacancies :

$$V_{L_1} = N_{L_1}$$
$$V_{L_2} = N_{L_2} + f_{12} N_{L_1}$$
$$V_{L_3} = N_{L_3} + f_{13} N_{L_1} + f_{23}\left(N_{L_2} + f_{12} N_{L_1}\right)$$

Where N_{Li} is the primary number of vacancies

- Mean L-fluorescence yield

$$\overline{\omega}_L = V_{L_1}\omega_1 + V_{L_2}\omega_2 + V_{L_3}\omega_3$$
$$\overline{\omega}_L = N_{L_1}\left[\omega_1 + f_{12}\omega_2 + \left(f_{13} + f_{12}.f_{23}\right)\omega_3\right] + N_{L_2}\left(\omega_2 + f_{23}\omega_3\right) + N_{L_3}\omega_3$$

- Emission intensities

$$X_{L_1} = \omega_1 N_{L_1}$$
$$X_{L_2} = \omega_2 \left(N_{L_2} + f_{12} N_{L_1}\right)$$
$$P_{AL_3} = (1 - \omega_3)\left[N_{L_3} + f_{13} N_{L_1} + f_{23}\left(N_{L_2} + f_{12} N_{L_1}\right)\right]$$

etc….

References

- **Energies**
  - Bearden J.A., X-ray Wavelengths, *Rev. Mod. Physics* 39, 1 (1967) 78
  - Deslattes R.D. *et al.*, X-ray transition energies, *Rev. Mod. Physics* 75 (2003) 35
  - Larkins, F.P., (1977). Semi empirical Auger-electron energies for elements $10 \leq Z \leq 100$. *At. Data and Nuclear Data Tables* 20-4, 313.

- **Relative Intensities**
  - Scofield, J.H., (1974). Exchange corrections of K X-ray emission rates. *Phys. Rev.* A9, 1041.
  - Puri, S., *et al.* (1993). Production of Li subshell and M shell vacancies following inner-shell vacancy production. *Nucl. Instrum. Meth. Phys. Res. B* 83, 21-30.
  - Campbell, J. L. and Wang, J.-X., (1989). Interpolated Dirac-Fock values of L-subshell x-ray emission rates including overlap and exchange effects. *Atomic Data and Nuclear Data Tables* 43, 281-298.
  - Chen, M.H., *et al.*, (1979). Relativistic radiationless transition probabilities for atomic K- and L-shells. *At. Data and Nuclear Data Tables* 24-1, 13.

References

- **Fluorescence yields**

  - Bambynek, W., (1984). X-ray and Inner shell processes in atoms, molecules and solids (X-84), Leipzig, August 20-24, paper P1.

  - Puri, S., *et al.*, (1993). L shell fluorescence yields and Coster-Kronig transition probabilities for the elements with $25 \leq Z \leq 96$. *X-Ray Spectrometry* 22, 358-361.

- **General works**

  - Schönfeld, E., Janssen, H., (1995). Untersuchungen zur Verknüpfung von Konstanten der Atomhülle. *Report PTB-Ra-37*, ISBN 3-89429-624-0.

  - Schönfeld, E., Janssen, H., (2000). Calculation of emission probabilities of x-rays and Auger electrons emitted in radioactive disintegration processes. *Appl. Rad. Isotopes* 52, 595.

  - Bé M.-M., *et al.*, Detailed calculation of K- and L- Auger electron emission intensities following radioactive disintegration. To be published in *Appl. Rad. Isotopes* (2006)

Emission program

- To calculate X ray and Auger electrons energies and intensities following radioactive disintegration
- This program needs to know :
  - All the atomic data (Emission.101 file)
  - All the nuclear data of a particular disintegration (entry file)
- Results are given in an output file

Emission.101

```
; OmegaK ........................... PTB-Ra-37, table 1
; OmegaL ........................... PTB-Ra-37, table 7
; nKL .............................. PTB-Ra-37, table 6
; x = p(KBeta)/p(KAlpha) ........... PTB-Ra-37, table 2
; y = p(KAlpha2)/p(KAlpha1) ........ PTB-Ra-37, table 4
; r = p(KBeta2')/p(KBeta1') ........ Scofield, 1974
; u = p(KLX)/p(KLL) ................ PTB-Ra-37, table 5
; v = p(KXY)/p(KLL) ................ PTB-Ra-37, table 5
; Z   OmegaK      OmegaL       nKL       x          y          r          u          v          Z
;-------------------------------------------------------------------------------------------------
 10  0,0152(8)   0,0001(1)    1,985(6)  0,0(0)     0,5028(25) 0,0(0)     0,0(0)     0,0(0)     10
 11  0,0213(9)   0,00022(11)  1,962(6)  0,0084(25) 0,5029(25) 0,0(0)     0,017(6)   0,00007(4) 11
 12  0,0291(9)   0,00030(12)  1,938(6)  0,017(4)   0,5031(25) 0,0(0)     0,034(8)   0,00029(12) 12
 13  0,0387(12)  0,00042(13)  1,921(6)  0,021(3)   0,5033(25) 0,0(0)     0,042(6)   0,00044(12) 13
 14  0,0504(13)  0,00055(12)  1,895(7)  0,029(3)   0,5037(25) 0,0(0)     0,058(6)   0,00084(17) 14
 15  0,0642(16)  0,00072(15)  1,856(7)  0,043(4)   0,5048(25) 0,0(0)     0,086(8)   0,0018(3)  15
 16  0,0804(19)  0,00093(18)  1,807(7)  0,062(4)   0,5053(25) 0,0(0)     0,124(8)   0,0038(5)  16
 17  0,0989(24)  0,00118(24)  1,751(6)  0,086(4)   0,5056(25) 0,0(0)     0,172(8)   0,0074(6)  17
 18  0,1199(28)  0,00147(30)  1,697(6)  0,1079(30) 0,5049(25) 0,0(0)     0,216(5)   0,0116(6)  18
 19  0,143(4)    0,00181(36)  1,654(6)  0,1225(24) 0,5055(25) 0,0(0)     0,245(5)   0,0150(6)  19
 20  0,169(4)    0,00221(44)  1,621(6)  0,1296(23) 0,5061(25) 0,0(0)     0,259(5)   0,0168(6)  20
 21  0,196(5)    0,00268(54)  1,594(5)  0,1319(21) 0,5069(25) 0,0(0)     0,264(4)   0,0174(6)  21
 22  0,226(5)    0,00321(64)  1,566(5)  0,1325(18) 0,5076(25) 0,0(0)     0,265(4)   0,0176(5)  22
 23  0,256(5)    0,00381(75)  1,539(5)  0,1334(16) 0,5083(25) 0,0(0)     0,267(3)   0,0178(4)  23
 24  0,289(5)    0,00450(90)  1,508(5)  0,1346(14) 0,5091(25) 0,0(0)     0,269(3)   0,0181(4)  24
```


Emission entry file

```
; I125.102
; EMISSION.EXE
; Radionuclide  -- I-125 ---> Te-125
  I-125
  52
  END
; Electron Capture Transitions
; pEC    pK      pL1      pL2      pL3
; Pec(u)     Pk(u)          PL1(u)          PL2(u)      PL3(u)
   100     0,8007(17)     0,1520(15)     0,0041(1)     0(0)
  END
; Gamma Transitions
; E    pGamma     AlphaK    AlphaL1    AlphaL2    AlphaL3
;Energie     Pg           Ak           al1           al2           al3
35,4919     6,67(17)     11,9(2)     1,442(44)     0,1289(40)     0,0443(16)
  END
```

Emission output file

```
EMISSION, V3.10, 28-Jan-2003
============================
Date of calculation ..................: 21.02.2006 10:45
Atomic shell data from file ..........: EMISSION.101
Radionuclide data from file ..........: D:\codes\emi-X\I125.102
Nuclide ..............................: I-125
Z(Daughter) ..........................: 52
Radionuclide data:
------------------
pEC, pK, pL1, pL2, pL3 ..............:
    100,000000(0)       0,8007(17)      0,1520(15)      0,00410(10)     0(0)
E, pGamma, Alpha(K, L1, L2, L3) .....:
    35,491900(0)        6,67(17)        11,90(20)       1,44(5) 0,129(4)        0,0443(16)
Atomic shell data:
------------------
OmegaK ...............................: 0,875(4)
x=p(KBeta)/p(KAlpha) .................: 0,2266(23)
y=p(KAlpha2)/p(KAlpha1) ..............: 0,5370(25)
r=p(K'Beta2)/p(K'Beta1) ..............: 0,217(5)
u=p(KLX)/p(KLL) ......................: 0,453(5)
v=p(KXY)/p(KLL) ......................: 0,0513(10)
<OmegaL> .............................: 0,086(4)
nKL ..................................: 0,917(4)
nKL1 .................................: 0,0540(20)
nKL2 .................................: 0,308(4)
nKL3 .................................: 0,555(6)
Omega1 ...............................: 0,0410(10)
Omega2 ...............................: 0,0780(20)
```


Emission output file

```
Results:
--------
N(K) .................................: 159,4(25)
p(eaK) ...............................: 19,9(7)
p(KLL) ...............................: 13,2(5)
p(KLX) ...............................: 6,00(23)
p(KXY) ...............................: 0,680(28)
p(XK) ................................: 139,5(23)
p(KAlpha2) ...........................: 39,7(7)
p(KAlpha1) ...........................: 74,0(12)
p(KAlpha) ............................: 113,7(19)
p(K'Beta1) ...........................: 21,2(5)
p(K'Beta2) ...........................: 4,60(14)
p(KBeta) .............................: 25,8(5)
……..
p(eaL) ...............................: 157,9(10)
p(eaL)=N(L)*(1-<OmegaL>) .............: 157,7(20)
……
p(XL)=p(XL1)+p(XL2)+p(XL3) ...........: 14,67(30)
p(XL)=N(L)*<OmegaL> ..................: 14,9(7)
  ..... p(XLAlpha) ...........: 7,43(21)
..... p(XLBeta) ............: 6,01(14)
..... p(XLGamma) ...........: 0,844(20)
..... p(XLEta) .............: 0,108(4)
..... p(XL1) ...............: 0,280(9)
p(L1-M2) ..... p(XLBeta4) ............: 0,426(14)
p(L1-M3) ..... p(XLBeta3) ............: 0,685(23)
p(L1-N2) .....p(XLGamma2) ............: 0,0907(30)
p(L1-N3) ..... p(XLGamma3) ...........: 0,150(5)
p(L1-O2,3) .... p(XLGamma4',4) .......: 0,0189(9)
```

Example of Evaluation: Decay of ^{177}Lu (6.647 d)

Filip G. Kondev

kondev@anl.gov

Nuclear Engineering Division

Argonne National Laboratory

A U.S. Department of Energy
Office of Science Laboratory
Operated by The University of Chicago

135

Outline

- Introduction
  - ✓ nuclear structure properties of ^{177}Lu
  - ✓ the relevance to applications
- Nuclear Data Properties
  - ✓ lifetime
  - ✓ beta and gamma emission probabilities
- Atomic Data
- Recipe for Evaluators

Nuclear Structure Properties of ^{177}Lu

✓ deformed rare-earth nucleus with 71 protons and 106 neutrons

Q(7/2+) = 3.39(2) eb
μ(7/2+) = 2.239(11) μ_N

$$Q = \frac{3K^2 - I(I+1)}{(I+1)(2I+3)} Q_0$$

$$\beta_2 \approx 0.271$$

$$\mu = g_R I + (g_K - g_R)\frac{K^2}{I+1}$$

$$g_K \approx 0.68; g_K(7/2[404]) \approx 0.65$$

Q(23/2-) = 5.2(5) eb
μ(23/2-) =2 .337(13) μ_N

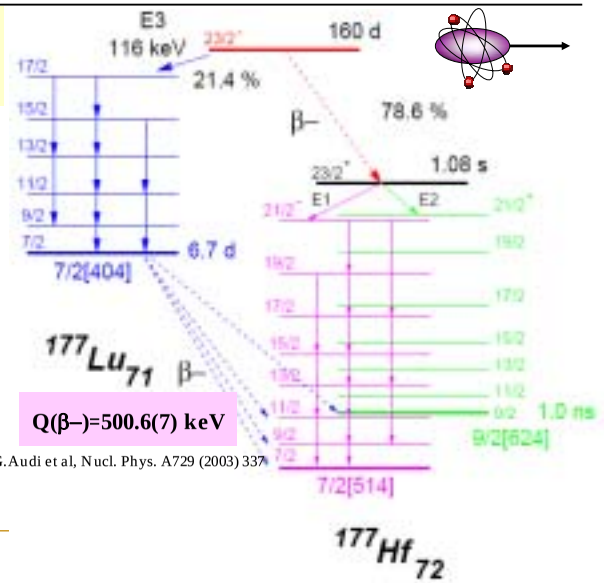

G.Audi et al, Nucl. Phys. A729 (2003) 337

Why of interest to applications

- ^{177}Lu (6.647 d) is a therapeutic radionuclide
  - ✓ used to cure the so-called "metastatic bone disease" – when breast or prostate cancer spreads from their primary sites to the bone – the cure is to use high-energy β– particles to the bone

- ^{177m}Lu (160.44 d) can be used as γ–ray energy & efficiency standards (high multiplicity) & has a potential for energy related applications (e.g. energy storage device)
  - ✓ especially for gamma-ray tracking, where the efficiency depends sensitively on the multiplicity

Nuclear Data

- **Q(β–)**
  - ✓ G. Audi et al, Nucl. Phys. A729 (2003) 337
  - ✓ http://www.nndc.bnl.gov/qcalc/
- **Lifetime**
  - ✓ need to be evaluated
- **Emission energies & probabilities (β– and γ)**
  - ✓ need to know the decay scheme - adopted Ex, J^{π}, mult (ENSDF)
  - ✓ α_T – calc. from Rossel (in the past), but BRICC (in the future)
  - ✓ evaluate E_γ, P_γ, δ, $P_{\beta-}$
  - ✓ calculate $E_{\beta-,\,max}$, log *ft*

Production of ^{177}Lu

$\sigma(n,\gamma) \approx 3.02(5)$ b

- ✓ no contaminants
- ✓ small production CS

$\sigma(n,\gamma) \approx 2090(70)$ b

- ✓ large production CS
- ✓ but be aware of potential complications

Lifetime measurements

$$A(t) = dN(t)/dt = \lambda N(t) = A_0 e^{-\ln(2)t/T_{1/2}}$$

Tag on specific signature radiations (α, β, ce or γ) in a "singles" mode

- usually follow several $T_{1/2}$
- statistical uncertainties are usually small
- systematic uncertainties (dead time, geometry, etc.) dominate, but often these are not reported

Half-life of ^{177}Lu

✓ not a trivial task – depends on the main production mode – all measurements used ^{176}Lu(n,γ)^{177}Lu production

$T_{1/2}$, d	Reference	Comments
6.75 (5) #	1958Be41	
6.74 (4) #	1960Sc19	
6.71 (1) #	1972Em01	
6.7479 (7) #	1990Ab02	
6.645 (30)	1982La25	$T_{1/2}(^{177m}Lu)$=159.5 d (7) was used in the fitting procedure
6.65 (1)	2001Zi01	Corrections for $T_{1/2}(^{177m}Lu)$ have been applied, but the value has not been reported
6.646 (5)	2001Sc23	$T_{1/2}(^{177m}Lu)$=160.4 d was used in the fitting procedure
6.647 (4)	Adopted	

Half-life of ^{177}Lu - cont

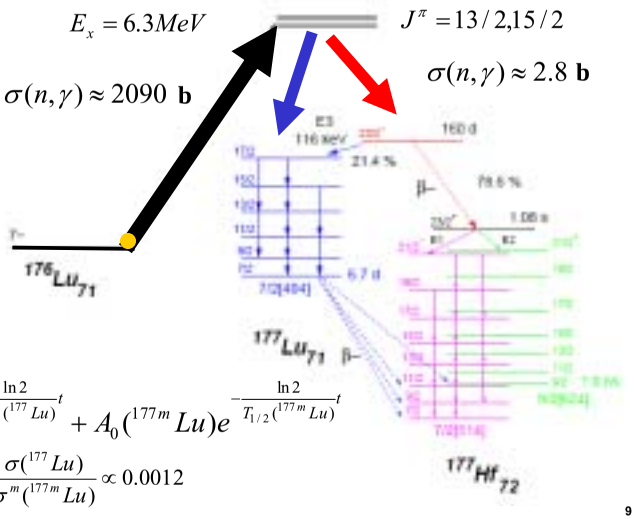

$$A(t) = A_0(^{177}Lu)e^{-\frac{\ln 2}{T_{1/2}(^{177}Lu)}t} + A_0(^{177m}Lu)e^{-\frac{\ln 2}{T_{1/2}(^{177m}Lu)}t}$$

$$\frac{A_0(^{177}Lu)}{A_0(^{177m}Lu)} \propto \frac{\sigma(^{177}Lu)}{\sigma^m(^{177m}Lu)} \propto 0.0012$$

J.RADIOANAL.NUCL.CHEM.,LETTERS 144 /5/ 359-365 /1990/
1990 Ab02

PRECISION MEASUREMENTS OF THE HALF-LIVES OF ^{60m}Co, ^{79m}Se, ^{104m}Rh, ^{149}Nd, ^{176m}Lu, ^{177}Lu AND ^{198}Au

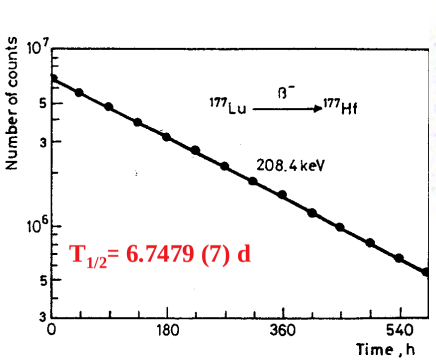

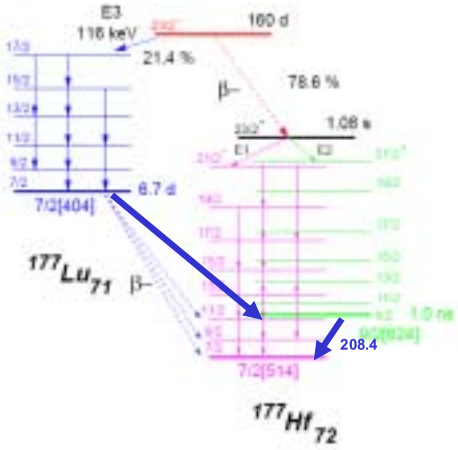

137

$$A(t) = A_{01}e^{-t/\tau_1} + A_{02}e^{-t/\tau_2}$$

ROOT
An Object-Oriented Data Analysis Framework

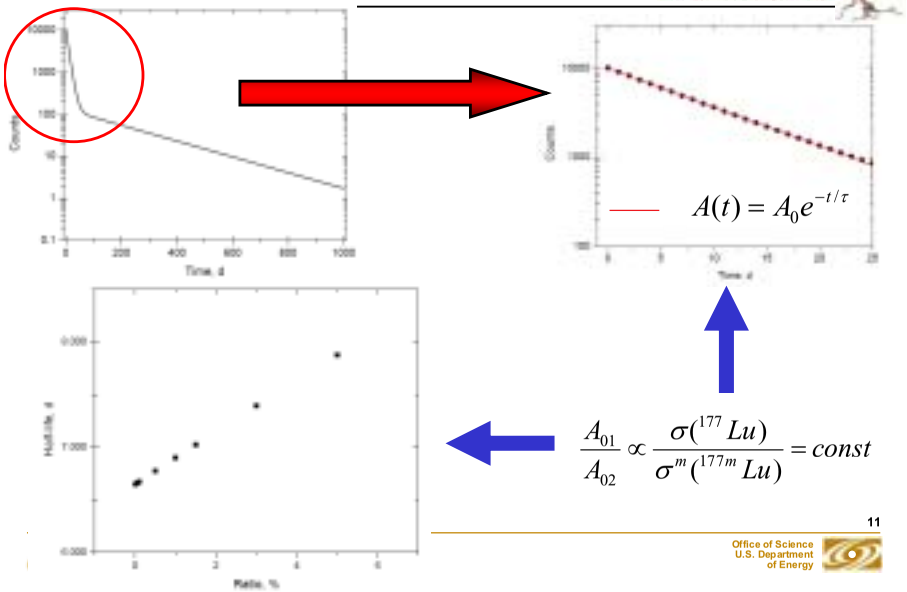

Half-life of ^{177}Lu

$T_{1/2}$, d	Reference	Comments
6.75 (5) #	1958Be41	
6.74 (4) #	1960Sc19	
6.71 (1) #	1972Em01	
6.7479 (7) #	1990Ab02	
6.645 (30)	1982La25	$T_{1/2}(^{177m}Lu)$=159.5 d (7) was used in the fitting procedure
6.65 (1)	2001Zi01	Corrections for $T_{1/2}(^{177m}Lu)$ have been applied, but the value has not been reported
6.646 (5)	2001Sc23	$T_{1/2}(^{177m}Lu)$=160.4 d was used in the fitting procedure
6.647 (4)	Adopted	

- What we want to know accurately:
  - ✓$T_{1/2}$, E_γ, I_γ, mult – δ & α_T

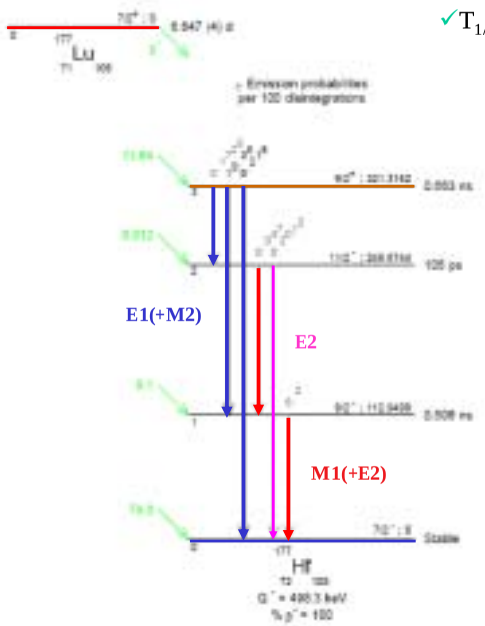

- E_γ – determines Ex and E_β
- I_γ, mult., δ & α_T – determine $P_{\beta(\gamma)}$

$$P_{\beta_i} = \eta[I^{tot}(out) - I^{tot}(in)]$$

$$I^{tot}(out/in) = \sum_i I_{\gamma_i}(1+\alpha_{T\,i})$$

$$\alpha_T(M1+E2) = \frac{\alpha_T(M1)+\delta^2\alpha_T(E2)}{1+\delta^2}$$

Gamma-ray energies – an example

Reference	$\gamma_{1,0}$
1989Ma56	112.9498 (4)
1981Hn03	112.95 (2)
1967Ha09	112.95 (2)
1965Ma18	112.952 (2)
1964Al04	112.97 (2)
1961We11	112.97 (2)
1955Ma12	112.965 (20)
Adopted	**112.9498 (4)**

Lweight

```
INP. VALUE  INP. UNC.     R. WGHT  chi**2/N-1 REFERENCE
.112950E+03 .400E-03 MIN *.960E+00* .101E-01 1989Ma56
.112950E+03 .200E-01       .389E-03  .431E-05 1981Hn03
.112950E+03 .200E-01       .389E-03  .431E-05 1967Ha09
.112952E+03 .200E-02       .389E-01  .104E+00 1965Ma18
.112970E+03 .200E-01       .389E-03  .160E+00 1964Al04
.112950E+03 .200E-01       .389E-03  .431E-05 1961We11
.112965E+03 .200E-01       .389E-03  .990E-01 1955Ma12

No. of Input Values N= 7   CHI**2/N-1=  0.46   CHI**2/N-1(critical)=  2.80

UWM   :.112955E+03  .322039E-02
WM    :.112950E+03  .391056E-03(INT.)  .265051E-03(EXT.)

********** S U M M A R Y **********

      Eg,1 Lu177 GS

CHI**2/N-1 .4575E+00
UWM-|.1130E+03 .32E-02|
WM- |.1129E+03 .39E-03|
LWM-|.1129E+03 .39E-03|
**********
```


Gamma-ray intensities – an example

Reference	$\gamma_{1,0}$
2001Sc23	59.6 (6)
1987Me17	59.6 (11)
1974Ag01	60 (5)
1964Al04	58 (4)
1961We11	62 (2)
1955Ma12	45.5 #
Adopted	**59.7 (5)**

Lweight

```
INP. VALUE  INP. UNC.     R. WGHT  chi**2/N-1 REFERENCE
.596000E+02 .600E+00 MIN *.700E+00* .118E-01 2001Sc23
.596000E+02 .110E+01       .209E+00  .951E-02 1987Me17
.600000E+02 .500E+01       .101E-01  .727E-03 1974Ag01
.580000E+02 .400E+01       .156E-01  .466E-01 1964Al04
.620000E+02 .200E+01       .632E-01  .322E+00 1961We11

No. of Input Values N= 5  CHI**2/N-1=  0.38  CHI**2/N-1(critical)=  3.3

UWM   :.595480E+02  .640000E+00
WM    :.597304E+02  .502727E+00(INT.)  .311843E+00(EXT.)

********** S U M M A R Y **********

      Eg,1 Lu177 GS

CHI**2/N-1 .3868E+00
UWM-|.5904E+02 .64E+00|
WM- |.5973E+02 .50E+00|
LWM-|.5973E+02 .50E+00|
**********
```


Gamma-ray mixing ratios – an example

Reference	$\delta(\gamma_{1,0})$
1974Kr12	-4.7 (2)
1974Ag01	-3.99 (25)
1970Hr01	-3.7 (3)
1961We11	-4.0 (2)
1972Ho54	-4.75 (7)
1972Ho39	-4.5 (3)
1977Ke12	-4.8 (2)
1992De53	-4.85 (5)
Adopted	**-4.4(4)**

```
INP. VALUE  INP. UNC.     R. WGHT  chi**2/N-1 REFERENCE
.400000E+01 .200E+00       .394E-01  .190E+01 1961We11
.370000E+01 .300E+00       .175E-01  .168E+01 1970Hr01
.475000E+01 .700E-01       .922E+00  .134E-01 1972Ho54
.450000E+01 .300E+00       .176E-01  .829E-01 1972Ho39
.399000E+01 .250E+00       .252E-01  .125E+01 1974Ag01
.470000E+01 .200E+00       .394E-01  .291E-02 1974Kr12
.400000E+01 .200E+00       .394E-01  .182E-01 1977Me12
.485000E+01 .561E-01     *.930E+00* .669E+00 1992De53
* Input uncertainty increased .112E+01 times *

No. of Input Values N= 8  CHI**2/N-1=  5.61  CHI**2/N-1(critical)=  2.60

UWM   :.441125E+01  .158232E+00
WM    :.472853E+01  .396960E-01(INT.)  .940027E-01(EXT.)
LWM   :.441125E+01  .436750E+00   Min. Inp. Unc.=.500000E-01
LWM has used unweighted average and expanded the uncertainty so range
includes the most precise value of .485000E+01

********** S U M M A R Y **********

      dg,1 Lu177 GS

CHI**2/N-1 .5605E+01
UWM-|.4411E+01 .16E+00|
WM- |.4729E+01 .40E-01|
LWM-|.4411E+01 .44E+00|
**********
```

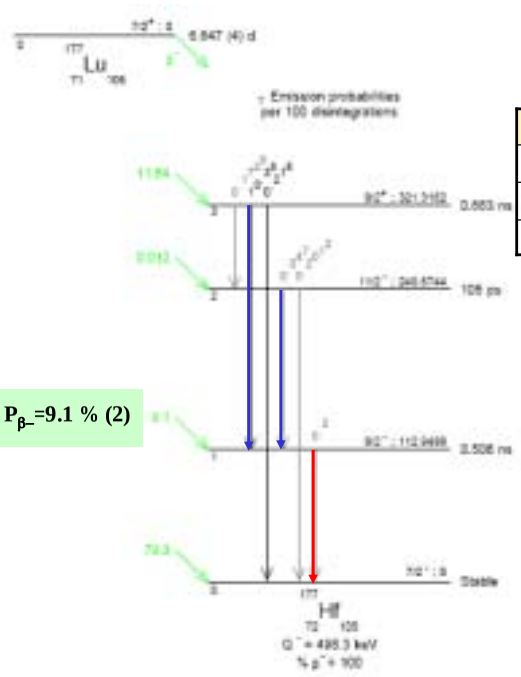

E_γ	Mult	I_γ	δ	α_T
113	M1+E2	6.20 (7)	-4.4 (4)	2.272
137	M1+E2	0.0470 (7)	-3.0 (7)	1.158
208	E1+M2	10.38 (7)	0.074 (13)	0.068

$$\alpha_T(M1+E2)=\frac{\alpha_T(M1)+\delta^2\alpha_T(E2)}{1+\delta^2}$$

$P_{\beta-}$=9.1 % (2)

$I^{tot}(137)+I^{tot}(208)=11.19\ (7)$

$I^{tot}(113)=20.29\ (7)$

$$I_{\gamma i}^{tot}=I_{\gamma_i}(1+\alpha_{T_i})$$

log *ft* values

- ENSDF analysis program LOGFT – both Windows & Linux distribution
  http://www.nndc.bnl.gov/nndcscr/ensdf_pgm/analysis/logft/
- LOGFT Web interface at NNDC http://www.nndc.bnl.gov/logft/

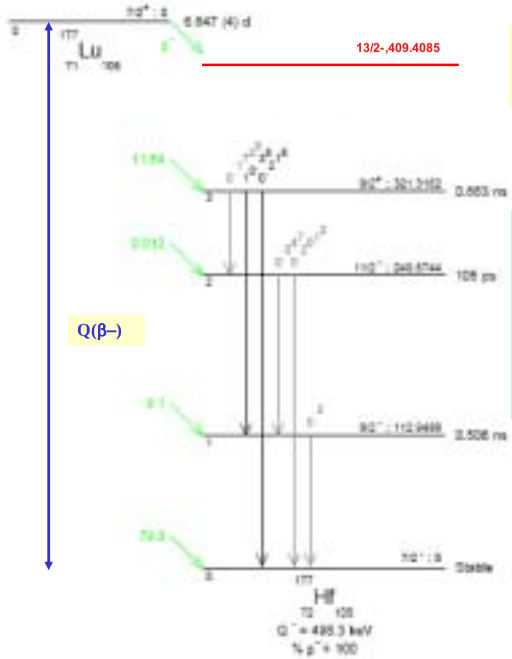

13/2-,409.4085

7/2+→13/2-; ΔI=3; $\pi_i\pi_f$=-1

3rd forbidden

$$\log f+\log T_{1/2}^{\exp}-a=\log P_{\beta_i}$$

$a=\log ft\approx 19$ **from systematics**

$\log f\approx -1.5$ **from LOGFT**

$\log T_{1/2}^{\exp}\approx 5.8$ **from expt.**

Q(β–)

$$P_{\beta_i}(13/2-)\approx 10^{-15}$$

$$Q^{eff}=\sum_{i=1}^{allBR}Q_iBR_i;Q^{calc}=\sum_{j=1}^{all\gamma}E_{\gamma j}P_{\gamma j}+\sum_{k=1}^{all\beta}E_{\beta k}P_{\beta k}+\sum_{l=1}^{all\alpha}E_{\alpha l}P_{\alpha l}+etc.$$

$$Consistency=\left[\frac{Q^{eff}-Q^{calc}}{Q^{eff}}\right]\times 100\%$$

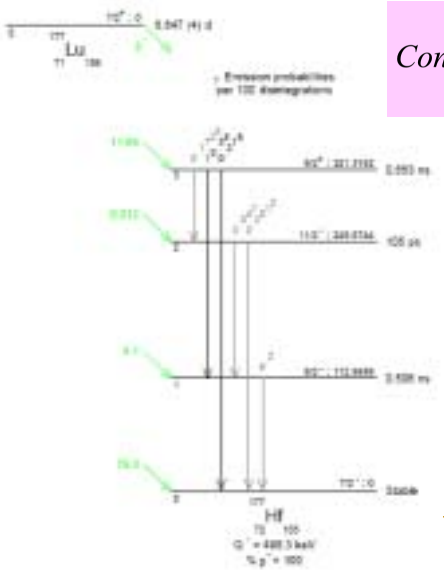

Using RADLST

Decay Mode	Q_i, keV
β– + ν	450.8 (20)
CE + Auger	13.2 (3)
γ	33.41 (18)
Q^{calc}	497.4 (25)
Q^{eff}	498.3 (8)

***Consistency* = 0.18 %**

Atomic Data

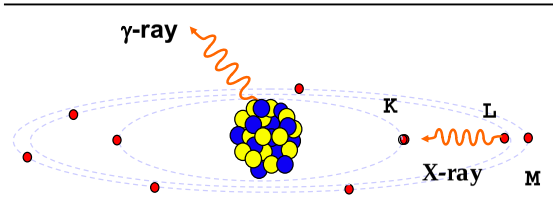

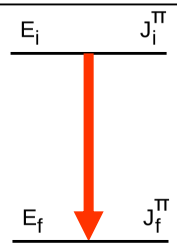

Energetics of CE-decay (i=K, L, M,….)

$$E_i = E_f + E_{ce,i} + E_{BE,i} + T_r$$

- **emission of X-rays**
- **emission of Auger electrons**

Where Data Come From?

- **The X-ray energies:** J.A. Bearden, *Rev. Mod. Phys. 39 (1967) 78* (also TOI)
- **Fluorescence yields:**
  - ✓ ω_K: 1% (Z>35) to 10% (Z=5) -W. Bambynek et al. *Rev. Mod. Phys. 44 (1972) 716*
  - ✓ ω_L: < 4% (Z>29) - E. Schonfeld and H. Janssen, *PTB-Report RA-37 (1995)*
  - ✓ ω_M – J.H. Hubbell et al., *J. Phys. Chem. Ref. Data 23 (1994) 339* (fit to expt. data)
- **Relative K_β/K_α and $K_{\alpha1}/K_{\alpha2}$ emission rates (<1% assumed):**
  - ✓ from E. Schonfeld and H. Janssen, *PTB-Report RA-37 (1995)* and J.H. Scofield, *Phys. Rev. A9 (1974) 1041*, respectively
- **The K- and L-Shell Auger electron energies:**
  - ✓ F.P. Larkins, *ADNDT 20 (1977) 313*
- **Emission probabilities of K-shell Auger electrons:**
  - ✓ deduced from X-ray ratios- E. Schonfeld and H. Janssen, *PTB-Report RA-37 (1995)*

EMISSION

```
;172Hf.102
; V1.01, 25-May-1999
; Input file for program EMISSION.EXE
; 172HF

; The input file contains three blocks of data.
; The first block describes the radionuclide under study.
; The second block contains the primary decay parameters pEC, pK, pL1, pL2, pL3.
; The third block contains photon emission probabilities and conversion
; coefficients.
; Each block is terminated by an END statement.
; The input file may contain comments. Comments are introduced by a semicolon (;).
; The decimal point is either a komma or a dot on the line.

; Radionuclide
  Hf-177        ; Name of radionuclide
  72            ; Atomic number Z of daughter nuclide
  END

; Electron Capture Transitions
; pEC           pK          pL1         pL2         pL3
; One extra line for each additional electron capture transition.
  END

; Gamma Transitions
; In the following table, the photon energies are supplied to guide the user.
; They are not used in the calculations. However, the energies have to be
; in the table, because they are read by the program EMISSION.

; Energy       pGamma          AlphaK          AlphaL1         AlphaL2      AlphaL3
  321.3159     0,216(8)        0,06(5)         0,010(8)        0,0012(11)   0.0007(5)
  249.6742     0,2012(21)      0,091(0)        0,0107(0)       0,00167(0)   0.00109(0)
  208.3662     10,38(7)        0,055(4)        0,0072(8)       0,00115(10)  0.00110(8)
  136.7245     0,0470(7)       0,559(21)       0,068(5)        0,215(7)     0.177(6)
  112.9495     6,20(7)         0,817(12)       0,0879(11)      0,540(4)     0.477(3)
   71.6418     0,1726(23)      0,715(14)       0,078(4)        0,0269(4)    0.0385(11)

; One extra line for each additional gamma transition.
  END
```

```
EMISSION, V3.01, 03-Nov-1999
============================

Date of calculation ..................: 07.09.2000 16:19
Atomic shell data from file ..........: EMISSION.101
Radionuclide data from file ..........: hf177.102

Nuclide ..............................: Hf-177
Z(Daughter) ..........................: 72

Radionuclide data:
------------------
pEC, pK, pL1, pL2, pL3 ...............:

E, pGamma, Alpha(K, L1, L2, L3) .....:
      321,315900(0)      0,216(8)     0,06(5)      0,010(8)     0,0012(11)   0,0007(5)
      249,674200(0)      0,2012(21)   0,091000(0)  0,010750(0)  0,001670(0)  0,001090(0)
      208,366200(0)      10,38(7)     0,055(4)     0,0072(8)    0,00115(10)  0,00110(8)
      136,724500(0)      0,0470(7)    0,559(21)    0,063(5)     0,215(7)     0,177(6)
      112,949500(0)      6,20(7)      0,817(12)    0,0879(11)   0,540(4)     0,477(3)
       71,641800(0)      0,1726(23)   0,715(14)    0,078(4)     0,0269(4)    0,0385(11)

Atomic shell data:
------------------
OmegaK ...............................: 0,951(4)
x=p(KBeta)/p(KAlpha) .................: 0,266(4)
y=p(KAlpha2)/p(KAlpha1) ..............: 0,5714(2
r=p(K'Beta2)/p(K'Beta1) ..............: 0,267(5)
u=p(KLX)/p(KLL) ......................: 0,532(8)
v=p(KXY)/p(KLL) ......................: 0,0708(1

<OmegaL> .............................: 0,260(10)
nKL ..................................: 0,829(4)
nKL1 .................................: 0,9370(20)
nKL2 .................................: 0,299(3)
nKL3 .................................: 0,503(6)
Omega1 ...............................: 0,125(3)
Omega2 ...............................: 0,268(6)
Omega3 ...............................: 0,241(5)
f12 ..................................: 0,186(5)
f13 ..................................: 0,382(8)
f23 ..................................: 0,141(3)
```

```
<OmegaL> ..............................: 0,260(10)
nKL ...................................: 0,829(4)
nKL1 ..................................: 0,0270(20)
nKL2 ..................................: 0,299(3)
nKL3 ..................................: 0,503(6)
Omega1 ................................: 0,125(3)
Omega2 ................................: 0,268(6)
Omega3 ................................: 0,241(5)
f12 ...................................: 0.186(5)
f13 ...................................: 0,392(8)
f23 ...................................: 0,141(3)

p(L1-M2)/p(L1-total) ..................: 0,336(4)
p(L1-M3)/p(L1-total) ..................: 0,436(5)
p(L1-N2)/p(L1-total) ..................: 0,0838(10)
p(L1-N3)/p(L1-total) ..................: 0,1151(10)
p(L1-O2,3)/p(L1-total) ................: 0,0288(5)
p(L1-P2,3)/p(L1-total) ................: 0(0)
```

… similarly p(L2-Mx)/p(L2-total) and p(L3-Mx)/p(L3-total)…


```
N(K) ..................................: 5,82(11)
p(eaK) ................................: 0,285(24)
p(KLL) ................................: 0,178(15)
p(KLX) ................................: 0,095(8)
p(KXY) ................................: 0,0126(11)

N(L) ..................................: 11,82(10)
N(L1) .................................: 0,798(18)
N(L2) .................................: 5,11(6)
N(L3) .................................: 5,91(5)
p(eaL) ................................: 0,93(9)
p(eaL)=N(L)*(1-<OmegaL>) ..............: 8,75(14)
p(eaL1) ...............................: 0,498(16)
p(eaL2) ...............................: 3,74(6)
p(eaL3) ...............................: 4,49(7)

p(XL)=p(XL1)+p(XL2)+p(XL3) ............: 3,18(6)
p(XL)=N(L)*<OmegaL> ...................: 3,07(12)
p(XL1) ................................: 0,100(4)
p(XL2) ................................: 1,41(4)
p(XL3) ................................: 1,67(4)

p(XK) .................................: 5,53(10)
p(KAlpha2) ............................: 1,59(3)
p(KAlpha1) ............................: 2,78(6)
p(KAlpha) .............................: 4,37(8)
p(K'Beta1) ............................: 0,917(23)
p(K'Beta2) ............................: 0,245(8)
p(KBeta) ..............................: 1,162(28)
```


Comparison with experimental data

	Energy KeV		2001Sc23		1987Me17	RADLST	EMISSION
XLα2 (Hf)	7.844	}		}			0.137 (4)
XLα1 (Hf)	7.899	}	1.51 (3)	}	1.59 (6)		1.21 (3)
XLη (Hf)	8.139	}		}			0.0313 (9)
XLβ4 (Hf)	8.905	}		}			0.0335 (12)
XLβ1 (Hf)	9.023	}	1.34 (3)	}			1.15 (4)
XLβ6 (Hf)	9.023	}		}	1.76 (7)		0.0147 (4)
XLβ3 (Hf)	9.163	}		}			0.0435 (15)
XLβ2,15 (Hf)	9.342		0.274 (7)	}			0.248 (7)
XLγ1 (Hf)	10.516	}	0.231 (6)	}			0.222 (6)
XLγ2 (Hf)	10.834	}	0.0223 (14)	}			0.00835 (19)
XLγ3 (Hf)	10.890	}		}			0.0115 (4)
XKα2 (Hf)	54.6120 (7)		1.55 (3)		1.65 (3)	1.59 (5)	1.59 (3)
XKα1 (Hf)	55.7909 (8)		2.73 (6)		2.84 (5)	2.78 (9)	2.78 (6)
XK'β1 (Hf)	62.985-63.662		0.885 (15)		0.919 (16)		0.917 (23)
XK'β2 (Hf)	64.942-65.316		0.238 (5)		0.252 (5)		0.245 (8)
XKβ (Hf)						1.16 (4)	1.16 (3)

CE energies and emission probabilities

	Energy keV	Electrons per 100 disintegrations
$ec_{3,2\,L}$ (Hf)	60.3711 (8)	0.0238 (13)
$ec_{3,2\,M}$ (Hf)	69.0409 (8)	0.0055 (3)
$ec_{2,1\,K}$ (Hf)	71.3737 (8)	0.0263 (14)
$ec_{1,0\,L}$ (Hf)	101.6791 (6)	6.84 (23)
$ec_{1,0\,M}$ (Hf)	110.3489 (6)	1.71 (6)
$ec_{2,1\,L}$ (Hf)	125.4538 (7)	0.0214 (8)
$ec_{2,1\,M}$ (Hf)	134.1236 (7)	0.005306
$ec_{3,1\,K}$ (Hf)	143.0154 (8)	0.57 (5)
$ec_{2,0\,K}$ (Hf)	184.3234 (9)	0.018 (5)
$ec_{3,1\,L}$ (Hf)	197.0955 (6)	0.098 (11)
$ec_{3,1\,M}$ (Hf)	205.7653 (6)	0.022 (3)
$ec_{2,0\,L}$ (Hf)	238.4035 (8)	0.008 (5)
$ec_{2,0\,M}$ (Hf)	247.0733 (8)	0.002 (5)
$ec_{3,0\,K}$ (Hf)	255.9651 (9)	0.013 (11)
$ec_{3,0\,L}$ (Hf)	310.0453 (8)	0.0026 (22)

$E_{CE}=E_x - E_{BEi}$, i=K,L,M,N, …

$P_{CE,\,i}=\alpha_i \times P_\gamma$, i=K,L,M,N, …

β– max. and avg. energies

	Energy keV	Electrons per 100 disintegrations
$\beta^-_{0,3}$		
max:	177.0 (8)	11.64 (10)
avg:	47.66 (23)	
$\beta^-_{0,2}$		
max:	248.6 (8)	0.012 (8)
avg:	78.6 (3)	
$\beta^-_{0,1}$		
max:	385.4 (8)	9.1 (5)
avg:	111.7 (3)	
$\beta^-_{0,0}$		
max:	498.3 (8)	79.3 (5)
avg:	149.4 (3)	

$$E_{\beta\max} = Q_{\beta-} - E_x$$

Recipe for evaluators

- Start with the examination of the known decay scheme
  - ✓ use ENSDF for J^π, mult., etc. as a first approximation – but check for latest references using the NSR database and be aware of potential differences – create your own ENSDF file – you can use some useful ENSDF programs (ALPHAD, BRICC, GABS, GTOL, LOGFT, & RADLST)
- Use Q values from G. Audi et al. mass evaluation (2003Au03)
- Evaluate $T_{1/2}$, I_γ, mult., α_T & δ following DDEP rules
  - ✓ use LWEIGHT for statistical analysis of data
- Deduce level energies using evaluated transition energies, e.g. E_γ +/- ΔE_γ, etc. (using GTOL for example)
- Do the intensity balances of the decay scheme and deduce P_β, P_α, P_γ, etc. for each level (transitions)

Recipe for evaluators-cont.

- Calculated log *ft* and/or HF_α values (using LOGFT and ALPHAD)
- Estimate possible week branches (or missing ones) using systematics of log *ft* and/or HF_α values – get P_β and/or P_α
- Check the decay scheme for consistency (using RADLST)

$$Qeff = \sum_{i=1}^{allBF} Q_i BF_i; Qcalc = \sum_{j=1}^{all\gamma} E_{\gamma j} P_{\gamma j} + \sum_{k=1}^{all\beta} E_{\beta k} P_{\beta k} + \sum_{l=1}^{all\alpha} E_{\alpha l} P_{\alpha l} + etc. \quad Consistency = \left[\frac{Qeff - Qcalc}{Qeff}\right] \times 100\%$$

- Get the atomic data using the EMISSION program
  - ✓ need to provide E_γ+/-ΔE_γ, P_γ+/-ΔP_γ and α_K, α_L, α_M, α_N etc (and their uncertainties)
  - ✓ compare with experimental data, if any, for consistency
- Get $E_{\beta max}$ and $E_{\beta\ av.}$ using LOGFT program

Some personal notes …

- Be critical to the experimental data you are dealing with!
  - ✓ as all nuclei are different, so are the experiments
- A good evaluation is not just simply averaging numbers!
  - ✓ sometime the most accurate value quoted in the literature is not the best one!
- Enjoy what you have been doing!

Evaluation of ^{56}Co Decay Data

Desmond MacMahon

Coral Baglin

DDEP Workshop, Saclay, March 2006

^{56}Co Decay Data

- ^{56}Co decays by positron emission (19.58%) and by electron capture (80.42%) to excited states of ^{56}Fe.
- 46 gamma rays with energies up to 3.6 MeV de-exciting 15 excited states in ^{56}Fe have been reported.
- This energy range makes ^{56}Co useful as a calibration source in gamma ray spectrometry.

^{56}Co Decay Data

- The Q value for the decay is given by Audi *et al*. as **4566 (20) keV.**
- The half-life of ^{56}Co has been evaluated by Woods *et al.* as **77.236 (26) days.**
- The main gamma ray energies are taken from the Helmer & van der Leun evaluation (2000).

^{56}Co Gamma Ray Emission Probabilities

- Relative gamma ray emission probabilities for the 46 gamma rays reported by 31 authors between 1965 and 2002 were tabulated.
- A problem arose when considering the high energy data.
- In many cases detector efficiency curves used measured data up to about 2.5 MeV and were then extrapolated to 3.6 MeV.

^{56}Co Gamma Ray Emission Probabilities

- It was clear from experimentally determined efficiency curves above 3 MeV that the extrapolated curves introduced errors of up to 6%.
- Therefore, of the 31 papers cited, only 8 which had used experimentally determined efficiency curves up to 3.6 MeV were included in the evaluation of data above 3 MeV.

^{56}Co Gamma Ray Emission Probabilities

- The following graph shows the data for the 1140.5 keV gamma ray, for which the reduced chi-squared is 5.2.
- The discrepancies are clear from the graph.

^{56}Co Gamma Ray Emission Probabilities

- The second problem was the significant number of discrepant data.
- Of the 46 gamma rays considered, 18 had data sets with a reduced chi-squared ranging from 2.0 to 7.8, indicating significant discrepancies.

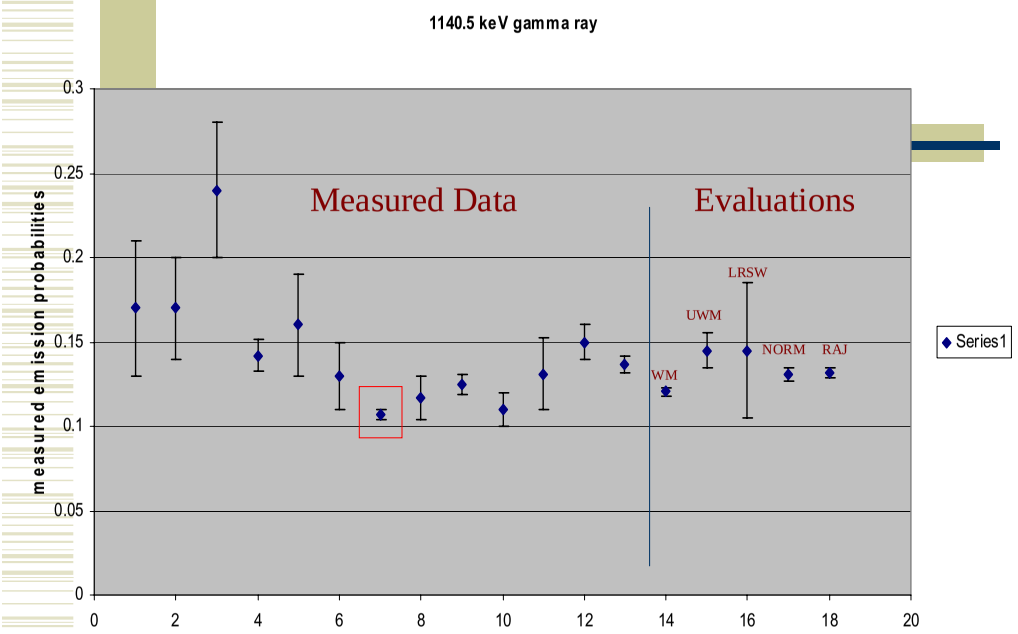

^{56}Co Gamma Ray Emission Probabilities

- On the previous graph points 1 to 13 are the experimental data.
- Point 14 is the weighted mean 0.1204(21)
- Point 15 is the unweighted mean 0.145(10)
- Point 16 is the LRSW 0.145 (38)
- Point 17 is the norm. resid. 0.131(4)
- Point 18 is the Rajeval value

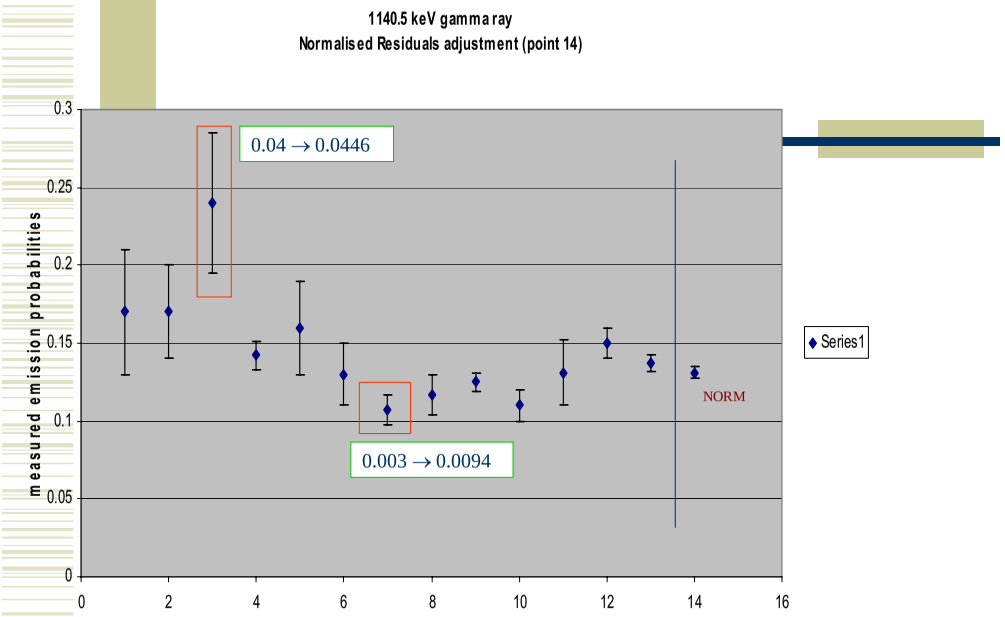

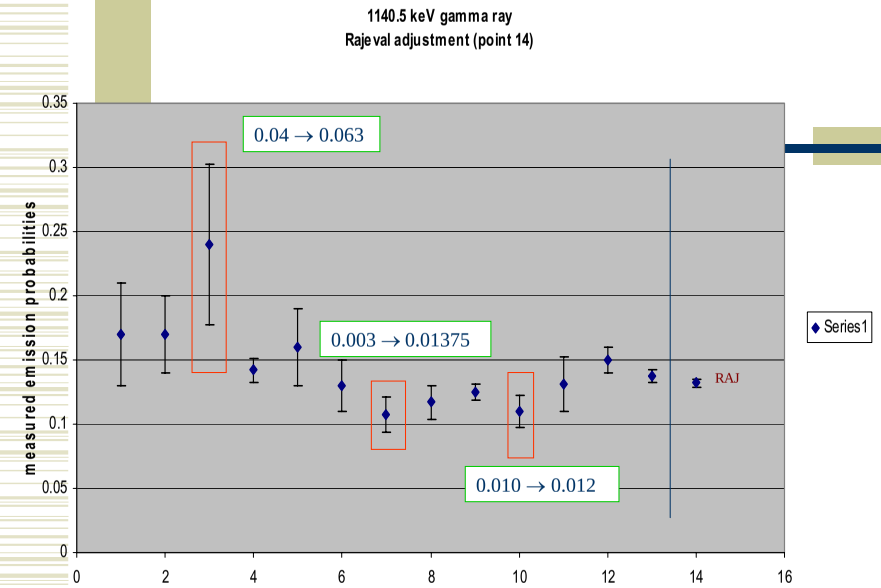

Normalisation

- Evaluated intensities are relative to the strongest 847 keV transition to the ground state.
- Normalisation is accomplished by requiring that all transitions to the ground state add up to 100.

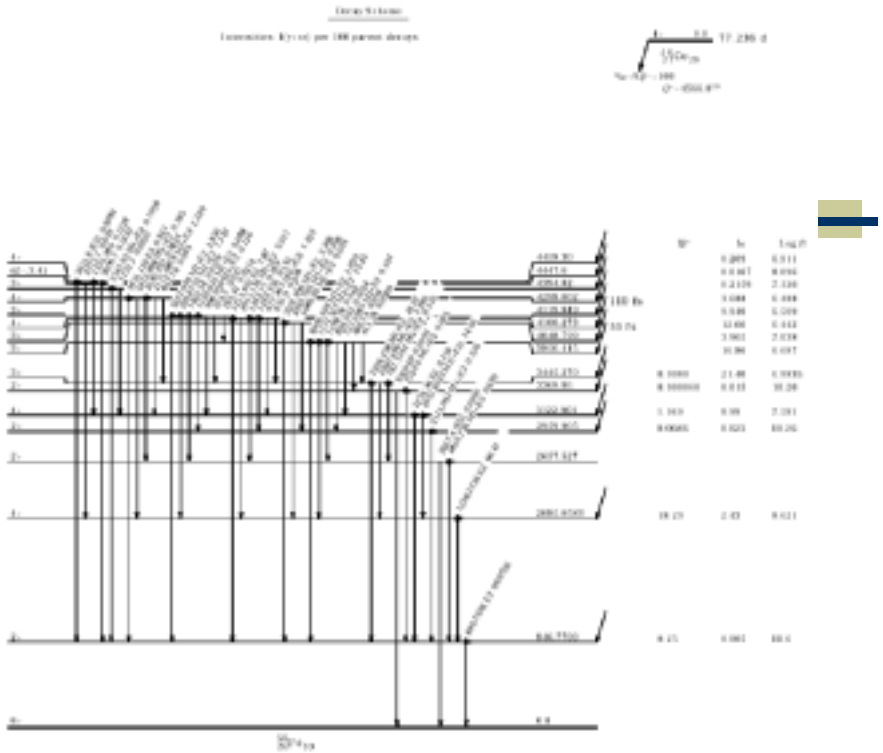

Normalisation

- Assuming zero electron capture/positron feeding from the 4+ ^{56}Co parent to the 0+ ^{56}Fe ground state:

$$\Sigma\left(I\left(\gamma+ce\right)\textit{to the ground state}\right) = 100$$

Normalisation

$$N = \frac{100}{\left[I\left(847\gamma\right)\left(1+\alpha\left(847\gamma\right)\right)+I\left(2657\gamma\right)+I\left(3370\gamma\right)\right]}$$

$$= \frac{100}{100.0303(9)+0.0195(20)+0.0103(8)}$$

$$= 0.999399(23)$$

Evaluated Data

Gamma Energy keV	Relative Iγ	Absolute Pγ
846.772	100	0.999399(23)
1037.840	14.04(5)	0.1403(5)
1238.282	66.45(16)	0.6641(16)
1360.215	4.283(13)	0.04280(13)
1771.351	15.46(4)	0.1545(4)
2034.755	7.746(13)	0.07741(13)
2598.458	16.97(4)	0.1696(4)
3201.962	3.205(13)	0.03203(13)
3253.416	7.87(3)	0.0787(3)

Positron Emission Probabilities

	Energy (keV)	**Probability × 100**	**Nature**	**log *ft***
$\beta^+_{0,7}$	98.7 (20)	0.0080 (7)	allowed	6.984
$\beta^+_{0,6}$	174.3 (20)	6.0 E-5 (20)	2nd forbidden	10.20
$\beta^+_{0,5}$	421.1 (20)	1.040 (20)	allowed	7.581
$\beta^+_{0,4}$	584.1 (20)	0.0086 (22)	2nd forbidden	10.26
$\beta^+_{0,2}$	1458.9 (20)	18.29 (16)	allowed	8.621
$\beta^+_{0,1}$	2697.2 (20)	0.25 (17)	2nd forbidden	11.6

Electron Capture Probabilities

	Energy (keV)	Probability × 100	Nature	log *ft*
$\varepsilon_{0,15}$	107.7(20)	0.209(7)	allowed	6.911(23)
$\varepsilon_{0,14}$	118.4(20)	0.0167(5)	unknown	8.096(21)
$\varepsilon_{0,13}$	171.2(20)	0.2159(18)	allowed	7.320(12)
$\varepsilon_{0,12}$	268.0(20)	3.688(13)	allowed	6.489(7)
$\varepsilon_{0,11}$	446.1(20)	9.940(18)	allowed	6.509(4)
$\varepsilon_{0,10}$	465.7(20)	12.66(4)	allowed	6.442(4)
$\varepsilon_{0,9}$	517.2(20)	3.965(15)	allowed	7.038(4)

Electron Capture Probabilities

	Energy (keV)	Probability × 100	Nature	log *ft*
$\varepsilon_{0,8}$	709.5(20)	16.86(5)	allowed	6.687(3)
$\varepsilon_{0,7}$	1120.7(20)	21.40(5)	allowed	6.984(2)
$\varepsilon_{0,6}$	1195.9(20)	0.015(5)	2nd forbidden	10.20(15)
$\varepsilon_{0,5}$	1443.1(20)	8.99(6)	allowed	7.581(4)
$\varepsilon_{0,4}$	1606.1(20)	0.023(6)	2nd forbidden	10.26(11)
$\varepsilon_{0,2}$	2480.9(20)	2.43(3)	allowed	8.621(5)
$\varepsilon_{0,1}$	3719.2(20)	0.005(3)	2nd forbidden	11.6(3)

X Ray Emissions

	Energy (keV)	Photons per 100 disintegrations
XL	0.615-0.792	0.581 (17)
$XK\alpha_2$	6.39091(5)	7.53 (10)
$XK\alpha_1$	6.40391(3)	14.75 (17)
$XK\beta_3$	} 7.05804(7)	} 3.05 (5)
$XK\beta_1$	}	}
$XK\beta"_5$	7.1083(4)	

Auger Electron Emissions

	Energy (keV)	Electrons per 100 disintegrations
e_{AL}	0.510 – 0.594	111.8 (8)
e_{AK}		46.04 (30)
KLL	5.370-5.645	35.61 (25)
KLX	6.158-6.400	9.76 (13)
KXY	6.926-7.105	0.666 (15)

KRISS Effort on Data Evaluation (Ni-63 & Au-195)

KRISS 한국표준과학연구원

Environment Metrology Group

K.B. Lee

lee@kriss.re.kr

Activity group in KRISS

KRISS is the NMI of Korea.

Our group is mainly responsible for the radionuclide standardization.

- Primary standards
  - 4πβ(PPC)-γ(NaI &HPGe) coincidence system
  - 4πβ(LS)-γ coincidence system
  - TDCR system
  - PPC for radon standard
  - γ-γ coincidence system
  - 2π α proportional counter
  - DCC system
- Secondary standards
  - Two LSC systems
  - Three ion chambers for Metrology
  - One ion chamber for nuclear medicine
  - A number of HPGe systems
  - A number of radionuclide calibrators
  - MWPC
- Standard propagation
  - Calibration services
  - CRMs
    - Standard solutions
    - Mixed gammas in various geometries
  - Radon chamber

Ni-63 evaluation

Decay scheme : 100 % β^- decay to Cu-63 ground state.

Search the bibliography DBs for the reference data on Ni-63 decay properties

Half-life

Reference	Values (years)	Comments
Brosi (1951Br)	85 (20)	Omitted from analysis
Wilson (1950Wi)	61	Omitted from analysis
McMullen (1956Mc)	125 (6)	Omitted from analysis
Horrocks (1962Ho)	93.9 (20)	Revised by Colle (1996Co25)
Barnes (1971Ba89)	101.21 (20)	Revised by Colle (1996Co25)
Colle (1996Co25)	101.06 (197)	

The Horrocks (1962Ho) and Barnes (1971Ba89) values were revised by Colle (1996Co25) using more accurate nuclear data and thereby more rigorously calculated liquid scintillator detection efficiencies.

Using Lweight V3 program,

$\chi^2/\nu = 4.38$

$a_w = 98.7(11)$ internal

(24) external

Program recommended value:98.7 (11) years. But the external uncertainty is adopted as suggested by Eddie.

Ni-63 evaluation (...contd.)

Decay Q value

Reference	Values (keV)	comments
Preiss (1957Pr)	67.0 (5)	Omitted
Hsue (1966Hs01)	65.87 (15)	Omitted
Hetherington (1987He14)	66.946 (20)	Omitted
Kawakami (1992Ka29)	66.9451 (39)	Omitted
Ohshima (1993Oh2)	66.9459 (54)	Omitted
~~Ohshima (1993Oh2)~~	~~66.9433 (126)~~	~~Omitted~~
Holzschuh (1999Ho09)	66.980 (15)	Adopted value

- Holzschuh et al. (1990Ho09) pointed out in the paper that the excitation of atomic electrons (85 eV) was not taken into account in the previous measurements.
- The atomic mass table of Audi et al. (2003Au03) : 66.975(15) keV

- *log ft* and mean energy of beta particles from the LOGFT program.
- The evaluation was reviewed through and the DDEP reviewing process
- TheNi-63 evaluation is on nuclide server.

Au-195 evaluation

KRISS

Still under evaluation…….

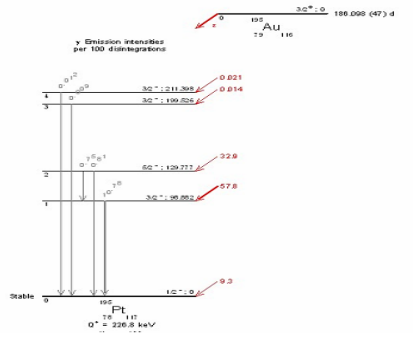

Au-195 evaluation (...contd.)

KRISS

Decay Q value

Reference	Values (keV)	Comments
1959BIXX	234 (2)	
1964Go19	226 (2)	KX+γ coincidence
1964Go19	229 (1)	LX+γ coincidence
1965De20	227 (2)	
1965Ha13	225 (5)	
1968Ja11	224 (2)	
1969Fi08	225 (5)	
1973Go05	230 (1)	Exchange and overlap correction = 1
1980Sa11	227.3 (10)	

$\chi^2/\nu = 1.63$

$a_w = 228.1(5)$ internal

(7) external

the atomic mass table of Audi et al. (2003Au03) :

226.8(10) keV

Half-life

Reference	Values (days)	Comments
????WiXX	185 (3)	
1948StXX	180 (15)	
1958CrXX	90 (1)	
1960BrXX	199 (3)	
1962Bo12	185 (1)	
1963Ha17	182.9 (5)	
2002Un02	186.098 (47)	Recommended

150

Au-195 evaluation (...contd.)

KRISS

EC transition probabilities per 100 disintegrations

Reference	$P(\varepsilon_{0,0})$ (%)	$P(\varepsilon_{0,1})$ (%)	$P(\varepsilon_{0,2})$ (%)	$P(\varepsilon_{0,3})$ (%)	$P(\varepsilon_{0,4})$ (%)	P_{ec} [13] (%)	Comments
1952DeXX		65	35			10	
1959BiXX		57	43				
1964Go19	0 (6)	59 (4)	41 (4)		0.05	4.9 (15)	
1965Ha13	13 (15)	47 (10)	40 (6)			5.2 (10)	
1968Ja11		63	37			6.8	
1967Sc18	0 (3)	70 (5)	30 (3)	0.019	0.025	7.9 (5)	
1969Fi08	12 (4)	50 (12)	38 (6)			6.0 (8)	
1970To19		68 (3)	32 (1)		0.035 (10)	5.5	
1970Ah05	10 (13)	58 (8)	32 (5)	0.019	0.025	7.4	
1973Go05	9.5 (4)	62.1 (27)	28.4 (16)	0.025 (1)	0.032 (1)	11.1 (2)	Used for normalization

- The Goverse values (1973Go73) are much more precise.
- 4π geometry detection technique.
- The values were obtained directly from the experiment without using old unevaluated nuclear data such as the internal conversion coefficients.

Au-195 evaluation (...contd.)

KRISS

Relative sub-shell probabilities for EC : calculated using the table of Schonfeld (1998Sc28).

Experimental values for comparison

- $PK(\varepsilon_{0,1}) = 0.438 \pm 0.011$ (1973Go05)
- $PK(\varepsilon_{0,2}) = 0.196 \pm 0.005$ (1965De20)
- $PK(\varepsilon_{0,2}) = 0.160 \pm 0.017$ (1973Go05)

The gamma-ray energies calculated from the structural details of the decay scheme and the nuclear level energies of 1999Zh11.

Experimental values for comparison

Reference	$\gamma_{2,1}$ (30.9 keV)	$\gamma_{1,0}$ (98.9 keV)	$\gamma_{2,0}$ (129.8 keV)	$\gamma_{3,0}$ (199.5 keV)	$\gamma_{4,0}$ (211.4)
1970Ah05	30.94 (5)	98.84 (5)	129.78 (3)		
1970To19	30.80 (6)	98.84 (20)	129.83 (26)		
1973Ja10		98.90 (5)	129.74 (5)	199.46 (10)	211.32 (10)

Multipolarities and mixing ratios are taken from the 1999Zh11.

Au-195 evaluation (...contd.)

KRISS

Gamma-ray emission probabilities

- Expressed relative to the 129.8 keV gamma.
- The uncertainty of 5 % is arbitrarily assigned.

Reference	$P(\gamma_{2,1})$	$P(\gamma_{1,0})$	$P(\gamma_{2,0})$	$P(\gamma_{3,0})$	$P(\gamma_{4,0})$
1964Go19	9.31*	100 (5)	8.38*		0.24*
1965Ha13		100 (5)	7.7 (8)		
1967Sc18		100 (5)	7.2 (7)		0.12 (1)
1970Ah05	6.8 (4)	100 (5)	7.4 (4)		
1972Ha21	7.1 (4)	100 (5)	7.6 (4)		
1972HSZX		100 (5)	7.3 (4)	0.080 (8)	0.10 (1)
1974HEYW		100 (5)	8.0 (5)	0.078 (8)	0.102 (1)
$\chi 2/v$	0.28		0.32	0.03	1.21
Evaluated	6.95 (28)	100 (5)	7.52 (19)	0.079 (57)	0.1073 (64)

Au-195 evaluation (...contd.)

KRISS

Internal conversion coefficients

- Interpolated from the theoretical values of Rosel et al. (1978Ro21) using ICCV99
- The uncertainty of 3 % is assigned.

Experimental values for comparison

Reference	$\alpha(\gamma_{2,1})$	$\alpha(\gamma_{1,0})$	$\alpha(\gamma_{2,0})$
1964Go19		α_T : 9.9 (10) α_K : 6.01 (15) α_L : 9.9 (10)	
1969Fi08	α_T : 38.9 (50) α_L : 30.2 (39) α_M : 6.9 (9)	α_T : 6.9 (5) α_K : 5.8 (5) α_L : 0.82 (7) α_M : 0.186 (15)	α_T : 1.76 (19) α_K : 0.35 (12) α_L : 1.06 (10)
1970Ah06	α_L : 26 (3)	α_K : 5.6 (7) α_L : 1.0 (1)	α_K : 0.46 (3)
1970To19			
1980Sa11		α_T : 7.24 (31) α_K : 5.98 (13)	

Au-195 evaluation (...contd.)

KRISS

Once I_γ and ICC have been evaluated, we can obtain the normalization factor using the decay scheme balance with the measured EC transition probabilities.

$P(\varepsilon_{0,2}) = N\{I(\gamma_{2,0})(1+\alpha_T(\gamma_{2,0})) + I(\gamma_{2,1})(1+\alpha_T(\gamma_{2,1}))$ — 0.1049 ± 0.062

$P(\varepsilon_{0,1}) = N\{I(\gamma_{1,0})(1+\alpha_T(\gamma_{1,0})) - I(\gamma_{2,1})(1+\alpha_T(\gamma_{2,1}))$ — 0.1180 ± 0.088

$100 - P(\varepsilon_{0,0}) = N\{I(\gamma_{1,0})(1+\alpha_T(\gamma_{1,0})) + I(\gamma_{2,0})(1+\alpha_T(\gamma_{2,0})) + I(\gamma_{3,0})(1+\alpha_T(\gamma_{3,0})) + I(\gamma_{4,0})(1+\alpha_T(\gamma_{4,0}))\}$ — 0.1078 ± 0.043

- In an agreement with each other.
- On the basis of the more accurate determination.

Gamma-ray absolute emission probabilities and gamma transition probabilities

$$\%I(\gamma) = N \cdot I(\gamma) \qquad P_{\gamma+ce} = N \cdot I(\gamma) \cdot \{1 + \alpha_T(\gamma)\}$$

Au-195 evaluation (...contd.)

KRISS

EC transition probabilities

- From the balance of gamma-ray transition probabilities

- Atomic data
  - Fluorescence yields from 1996 Sc06
  - X radiations
    - Energy : 1967Be65
    - Relative emission probabilities : 1996Sc06
  - Auger electrons
    - Energy : 1977La19
    - Relative emission probabilities : 1996Sc06
  - Electron emissions
    - Calculated from Saisnuc program
  - Photon emission
    - Calculated from Saisnuc program

Decay Data Evaluation Project

^{106}Ru/^{106}Rh

- ^{106}Ru: pure beta emitter
- ^{106}Rh: 30 betas and 88 gammas!

1

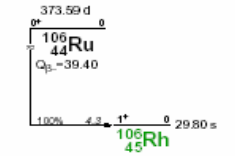

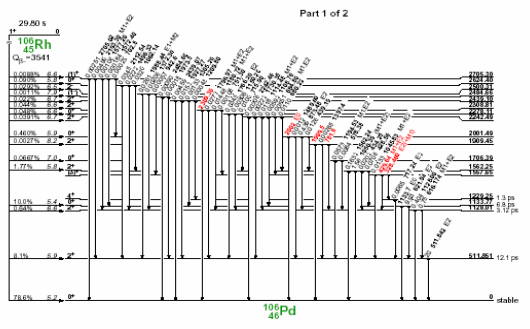

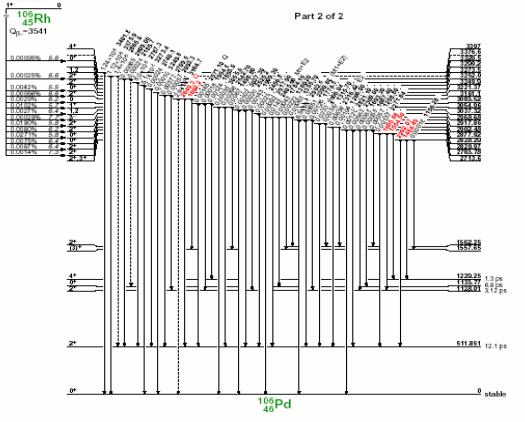

Recently published data

- Half-life data evaluated by M. J. Woods, S.M. Collins, S.A. Woods (NPL, UK), January 2004

^{106}Rh Half-life (d)	Reference
0.0003449 (9)	Kobayashi [H6]
0.0003514 (17)	Middelboe [H7]
0.000348 (4)	

5

^{106}Ru Half-life (d)	Reference
370.5 (6)	Schrader [H1]
373.59 (15)	Houtermans *et al* [H2]
368.0 (18)	Flynn *et al* [H3]
371 (1)	Wyatt *et al* [H4]
365.8 (17)	Easterday and Smith [H5]
371.8 (18)	

6

Half-life references

[H1] H. Schrader, Appl. Radiat. Isot. **60** (2004) 317.
[H2] H. Houtermans, O. Milosevic, F. Reichel, Int. J. Appl. Radiat. Isot. **31** (1980) 153.
[H3] K. F. Flynn, L. E. Glendenin, E. P. Steinberg, Nucl. Sci. Eng. **22** (1965) 416.
[H4] E. I. Wyatt, S. A. Reynolds, T. H. Handley, W. S. Lyons, H. A. Parker, Nucl. Sci. Eng. **11** (1961) 74.
[H5] H. T. Easterday, R. L. Smith, Nucl. Phys. **20** (1960) 155.
[H6] Y. Kobayashi, JAERI-1178 (1969) 21.
[H7] V. Middelboe, Nature **211** (1966) 283.

7

Main gamma-ray emission probabilities evaluated by T.D. MacMahon (NPL, UK), February 2005

E_γ (keV)	P_γ per decay
511.8534 (23)[a]	0.2050 (21)
616.22 (9)[b]	0.00724 (13)
621.93 (6)[b]	0.0986 (11)
873.49 (5)[b]	0.00435 (8)
1050.41 (6)[b]	0.01488 (22)
1128.07 (5)[b]	0.00399 (6)

[a] from Ref. [1].
[b] from Ref. [2].

8

References - radiations

1] R.G. Helmer, C. van der Leun, Nucl. Instrum. Meth. Phys. Res. **A450** (2000) 35.

2] R. Kaur, A.K. Sharma, S.S. Sooch, N. Singh, P.N. Trehan, J. Phys. Soc. Japan **51** (1982) 23.

3] R.L. Robinson, F.K. McGowan, W.G. Smith, Phys. Rev. **119** (1960) 1692.

4] P.V. Rao, R.W. Fink, Nucl. Phys. **A103** (1967) 385.

5] J. Vrzal, E.P. Grigoriev, A.L. Zolotavin, J. Liptak, V.O. Sergeev, J. Urbanets, Bull. Acad. Sci. USSR Phys. Ser. **31** (1968) 692.

6] H. Forest, M. Huguet, C. Ythier, C.R. Acad. Sci., Paris, Series B **264** (1967) 1614.

7] V.V. Ovechkin, T.K. Ragimov, D.F. Rau, Sov. J. Nucl. Phys. **4** (1967) 484.

8] J. Hattula, E. Liukkonen, Ann. Acad. Sci. Fennicae, Series A VI **274** (1968) 3.

9] P. Odru, Radiochim. Acta **12** (1969) 64.

10] Kl.-D. Strutz, H.-J. Strutz, A Flammersfeld, Z. Phys. **221** (1969) 231.

11] E.P. Grigoriev, A.V. Zolotavin, V.O. Sergeev, Sov. J. Nucl. Phys. **17** (1973) 583.

12] C. Marsol, G. Ardisson, Rev. Roum. Phys. **18** (1973) 1101.

13] K. Debertin, U. Schötzig, K.F. Walz, H.M. Weiss, Ann. Nucl. Energy **2** (1975) 37.

14] A.M. Geidelman, V.V. Ovechkin, D.F. Rau, P.I. Fedotov, Yu. V. Kholnov, Bull. Acad. Sci. USSR, Phys. Ser. **39** (1975) 76.

15] S.T. Hsue, H.H. Hsu, F.K. Wohn, W.R. Western, S.A. Williams, Phys. Rev. **C12** (1975) 582.

Papers on $^{106}Ru/^{106}Rh$

- So far, 35 relevant papers have been collected…
- Most recent paper is from 1993 and the oldest from 1960
- Fair amount of papers on E0 transition

Beta branching ratio for ^{106}Ru

	Greenwood et Al 1992	Okano et Al 1977	Hsue et Al 1975
Ru-106 ground state	79.1 (16)	78.72 (70)	80.5 (14)
511.85 keV		8.40 (59)	6.5 (11)
1133.69 keV		9.70 (58)	9.6 (10)
1562.23 keV		1.71 (11)	1.77 (17)

Eventual problems?

- Data available not very recent
- Balancing the decay scheme
- E0 transition
- Any advice?

Welcome to the BUREAU INTERNATIONAL DES POIDS ET MESURES

1. **The BIPM, its role and its activities Short presentation of the Bureau (about 30 minutes)**
2. **The SIR and its efficiency curves (about 30 minutes)**

Metre Convention and BIPM

- 20 May 1875 : Signature of the *Metre Convention* (Convention du Mètre). This diplomatic treaty, signed to date by 51 Member States among the most developed countries, established the Bureau International des Poids et Mesures (BIPM).
- in September 1889 at the first Conférence Générale des Poids et Mesures (CGPM) the international prototypes of platinum-iridium of the metre and of the definitions of the units of length and mass

Prototypes of the kilogram and of the metre

- The BIPM is an inter-governmental organisation, the seat of which is established at the Pavillon de Breteuil on grounds graciously placed at the disposal of the Comité International des Poids et Mesures by the French Government in the Park of Saint-Cloud.

Metre Convention and BIPM

- The BIPM is placed under the authority of a diplomatic conference, the General Conference on Weights and Measures (CGPM), which meets every 4 years and of a committee of scientific experts, the International Committee for Weights and Measures (CIPM).

Prototypes of the kilogram and of the metre

- The annual budget of the BIPM, supported at the common expenses of the signatory countries, is in 2006 higher than 10 Million Euros.
- About 75 people from 16 different countries are working at the BIPM.

The role of the BIPM

The goal of the BIPM is worldwide uniformity of measurement. It achieves this goal by providing the necessary scientific and technical basis for such uniformity and by collaborating with other institutions and organizations that have related missions.

Its principal tasks are:

The International System of Units (SI)

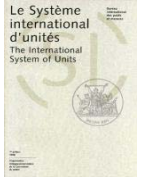

- to keep up-to-date and disseminate the text of the International System of Units known as the SI Brochure;

The role of the BIPM

Basic scientific and technical tasks

- to conserve and disseminate the primary standard of mass, the International Prototype of the kilogram;
- to establish and disseminate the International Atomic Time (TAI) and, in collaboration with the International Earth Rotation Service, the Coordinated Universal Time (UTC);
- to make its own realizations of other base and derived units of the SI and, if necessary, other units that are not yet possible to link to the SI;

The role of the BIPM

- to participate in the development of primary methods of measurement and procedures in chemical analysis and bio-analysis and where necessary to maintain its own standards in this field;
- to undertake research focused on the development of present and future measurement units and standards, including appropriate fundamental research, studies of the conceptual basis of primary standards and units and determination of physical constants, and to publish the results of the research.

The role of the BIPM

Specific technical services in support of NMIs

- to carry out certain international comparisons of practical realizations of certain base and derived units of the SI, as may be necessary to meet the needs of the ensemble of the National Metrology Institutes (NMI);
- to provide a specialized calibration service for NMIs for selected national measurement standards whenever this is desirable and feasible;

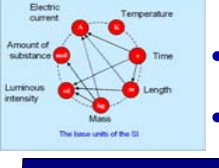

- to provide opportunities for technology transfer during calibrations and comparisons organized by the BIPM;
- to provide facilities for the exchange of scientific staff between the BIPM and NMIs;
- to provide certain consultancy services to NMIs related to peer review of their activities.

The role of the BIPM

Global coordination of metrology

- to provide support as necessary in the operation of the CIPM Mutual Recognition Arrangement (MRA) of national measurement standards and of calibration and measurement certificates issued by NMIs through the operation of the BIPM key comparison database, the management of the Joint Committee of the Regional Metrology Organizations and the BIPM (JCRB) and through participation in meetings of Consultative Committees and appropriate meetings of the RMOs and through the publication of the results of key and supplementary comparisons;

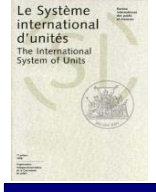

- to provide the scientific and administrative Secretariat for the General Conference on Weights and Measures, the CIPM and its Consultative Committees as well as the secretariat for meetings of directors of NMIs and the various Joint Committees and to publish reports of their deliberations.

The role of the BIPM

Relations with other organizations

- to enter into agreements with intergovernmental and international organizations where such agreements would help in the coordination of the work of these organizations with that of the BIPM or the CIPM and where it may stimulate corresponding coordination at the national or regional level;
- to collaborate, and where appropriate enter into agreements to establish Joint Committees with intergovernmental and international bodies having related missions;
- to act on behalf of the NMIs of Member States of the Metre Convention in representing their common interest as the occasion arises.

The role of the BIPM

Information and publicity

To promote as widely as possible using all appropriate methods, the activities carried out under the Metre Convention, in particular:

- to provide through the BIPM website, a centre for information on matters related to the Metre Convention, the CIPM, its Consultative Committees, Joint Committees, the CIPM MRA, including the BIPM key comparison database, and matters related to international metrology;

- to edit and arrange for the publication of *Metrologia*, the international scientific journal of metrology;

The role of the BIPM

- to ensure, with other appropriate organizations, that basic documents needed for uniformity of measurements, such as those on the vocabulary in metrology (VIM) and on the expression of uncertainty in measurement (GUM), are kept up-to-date and widely disseminated;
- to organize workshops and summer schools for the benefit of staff from the NMIs.

Main activities in the Ionizing Radiation section of the BIPM Dosimetry

- Maintenance of standard chambers for measurements in x-ray beams and γ beams (^{60}Co and ^{137}Cs) as international reference standards for most national comparisons in dosimetry (Mesurement in water, air and graphite);
- Link of the comparisons run by the WHO/IAEA for the Secondary Standards Dosimetry Laboratories (SSDL) to those carried out for the primary laboratories through the BIPM standards;
- Development of a calorimeter for the determination of the absorbed dose in water;
- Setup of reference radiation qualities used in mammography.

Example of a BIPM key comparison du BIPM in dosimetry: measurement of absorbed dose in water

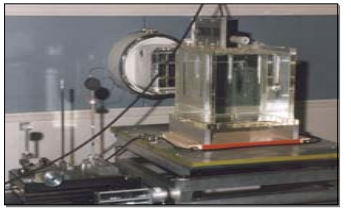

Water phantom used for the determination of absorbed dose in water

Example of a BIPM key comparison in dosimetry: measurement of absorbed dose in water

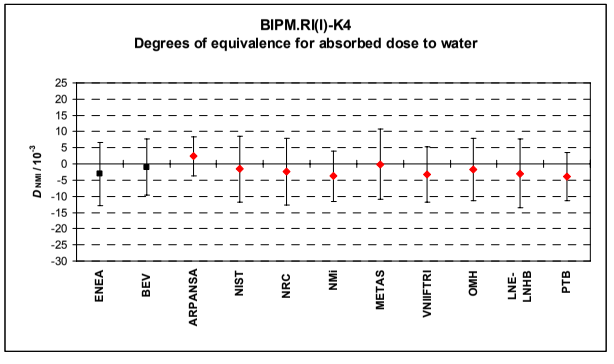

Main activities in the Ionizing Radiation section of the BIPM Radioactivity Measurements

- International reference System for activity measurements of gamma-ray emitting nuclides (SIR);
- Development of a NaI(Tl) travelling detector for extending the SIR to the measurement of short-lived nuclides;
- Development of the TDCR method as an absolute method for measuring β emitters and in view of a possible extension of the SIR to the measurements of β emitters;
- Calibration of a HPGe spectrometer for determination of impurities.

View of the experimental setup of the Système International de Référence (SIR)

The SIR in figures:

Since 1976

- **891 ampoules received**
- **651 independent results**
- **63 radionuclides measured**
- **59 without the pure β emitters**

Example of a BIPM key comparison in radioactivity: measurement of the equivalent activity of ^{18}F

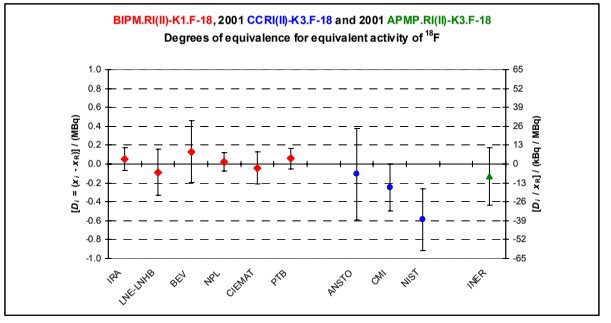

Example of a BIPM key comparison in radioactivity: measurement of the equivalent activity of ^{131}I

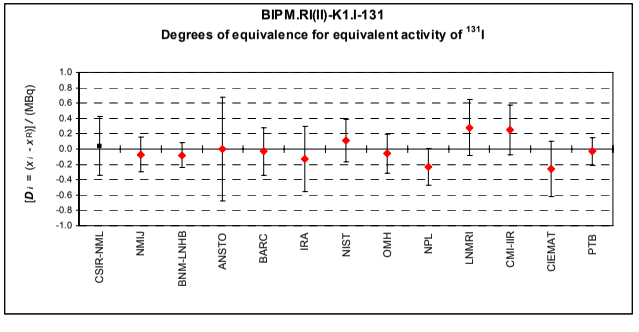

Example of a BIPM key comparison in radioactivity: measurement of the equivalent activity of ^{99}Tc^{m}

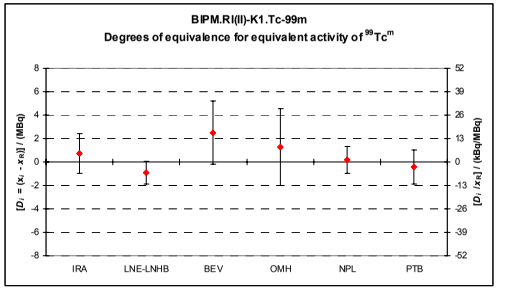

Conclusion

- The task of the BIPM is to ensure world-wide uniformity of measurements and their traceability to the International System of Units (SI).
- It does this with the authority of the Convention of the Metre, a diplomatic treaty between fifty-one nations, and it operates through a series of Consultative Committees, whose members are the national metrology laboratories of the Member States of the Convention, and through its own laboratory work.
- The BIPM carries out measurement-related research. It takes part in, and organizes, international comparisons of national measurement standards, and it carries out calibrations for Member States.

Aerial view of the BIPM site

Ionizing Radiation building

The SIR and its photon and beta efficiency curves

C. Michotte

SIR = International Reference System for activity measurements of γ-emitting nuclides

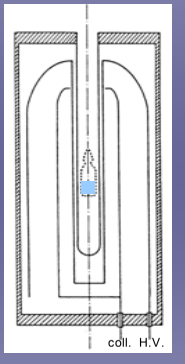

ionization chamber (IC) filled with N_2 (2 MPa)

At any time, NMIs send their own standardized radioactive solutions to the BIPM where they are measured in the SIR IC

$$\frac{(I-I_{\mathrm{bg}})_{i,l}}{(I_{\mathrm{Ra},n}-I_{\mathrm{bg}})_{i,l}} = \varepsilon_{i,l}\, A_{\mathrm{NMI}}\, \frac{e^{-\lambda_i (t_{\mathrm{m}}-t_{\mathrm{r}})}}{e^{-\lambda_{\mathrm{Ra}} (t_{\mathrm{m}}-t_0)}}\, F_n C_{i,l}$$

Correction for impurities

$\varepsilon_{i,l}$ = IC detection efficiency for radionuclide i, measured with solution of NMI l
$u(I/I_{\mathrm{Ra}}) << u(A_{\mathrm{NMI}})$

Definition: $(A_e)_{i,l} = 1/\varepsilon_{i,l}$ "equivalent activity / Bq"

Comparison result

163

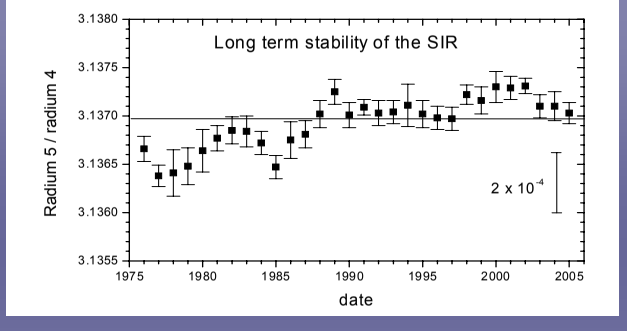

Statistics since 1976:
- 891 ampoules measured
- 650 independent SIR comparison results
- 25 participating countries + IRMM + IAEA
- 63 different radionuclides
- 57 key comparisons in the MRA

Degrees of equivalence for ^{60}Co

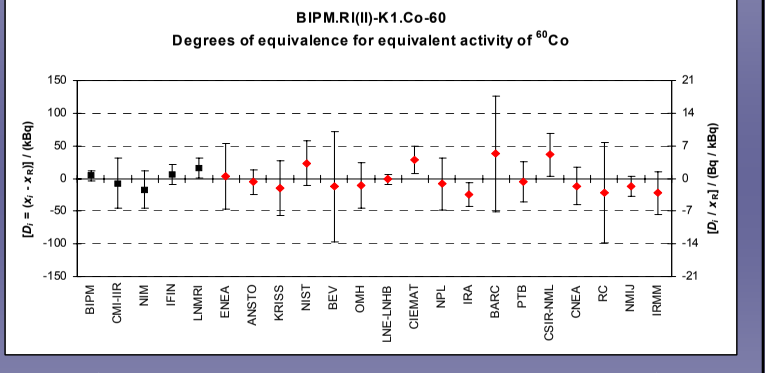

30 years

Influence of impurities on the SIR result

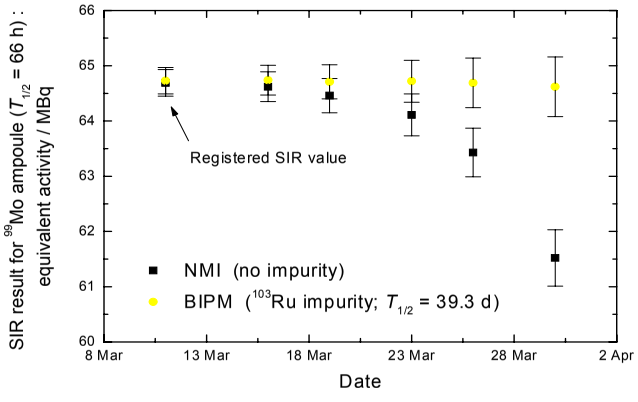

Need for IC efficiency curves

SIR correction for impurities

$$C_{i,l} = 1 + \sum_k R_{i,l,k} H_{i,l,k} (A_e)_i \,/\, (A_e)_k$$

$R_{i,l,k}$ activity ratio for impurity k (γ-spectrometry at NMI and/or BIPM)
$H_{i,l,k}$ decay correction

but for some impurities, $(A_e)_k$ is not known experimentally
=> need to calculate the equivalent activity

SIRIC

BIPM

NPL National Physical Laboratory

Andy Pearce and Maurice Cox
DTI

SIRIC: complete SIR measurement model

$$\frac{1}{(A_e)_i^{\text{model}}(\boldsymbol{B})} = \sum_j P_{i,j} F(\boldsymbol{B}^{(1)}, E_{i,j}) + \sum_{j'} \beta P_{i,j'} \int_0^{W_{i,j'}} S_{i,j'}(W) G(\boldsymbol{B}^{(2)}, W) dW$$

β spectrum shape

Efficiency curves

$$F(\boldsymbol{B}^{(1)}, E_{i,j}) = E_{i,j} \exp\left(\sum_h B_h^{(1)} \phi_h(\ln E_{i,j}) \right)$$

$$G(\boldsymbol{B}^{(2)}, W) = W \exp\left(\sum_h B_h^{(2)} \phi_h(W) \right)$$

F/*E* versus ln*E* : asymmetric bell shape, always positive

ϕ_h : Chebyshev polyn.

$$(A_e)_{i,l}^{\text{meas}} = A_{i,l}\, M_{i,l}^{-1}\, C_{i,l}(R, H, (A_e)^{\text{KCRV}}, N, \boldsymbol{B})$$

279 equations

$$C_{i,l} = 1 + \sum_k R_{i,l,k} H_{i,l,k} (A_e)_i \,/\, (A_e)_k$$

$M_{i,l}$ SIR current measurements and decay corrections
N nuclear data (thousands of values)

Non-linear least squares (LS) problem

Fortran 95, NAG libraries

$$\min_{\boldsymbol{B}} \sum_i \sum_l \left(A_{i,l} M_{i,l}^{-1} - \frac{(A_e)_i^{\text{model}}(\boldsymbol{B}, N)}{C_{i,l}(\boldsymbol{B}, N, R, H, A_e^{\text{KCRV}})} \right)^2 \Big/ u(A_{i,l} M_{i,l}^{-1})^2$$

+ propagation of uncertainties after minimization to take account of $u(R)$, $u(H)$, $u(A_e^{\text{KCRV}})$ and $u(N)$

- $A_{i,l}$ and $M_{i,l}$ are considered as independent, as well as $R_{i,l,k}$ and $H_{i,l,k}$
- The possible correlation between photon emission intensities due to a normalization factor is taken into account

INPUTS: SIR results
nuclear data
DDEP Sept. 2004
ENSDF Dec. 2004
initial values

OUTPUTS: efficiency curves (photon and β)
A_e^{model} values
with uncertainty budget and covariance matrix
impurity corrections
outliers

SIRIC : Consistency check

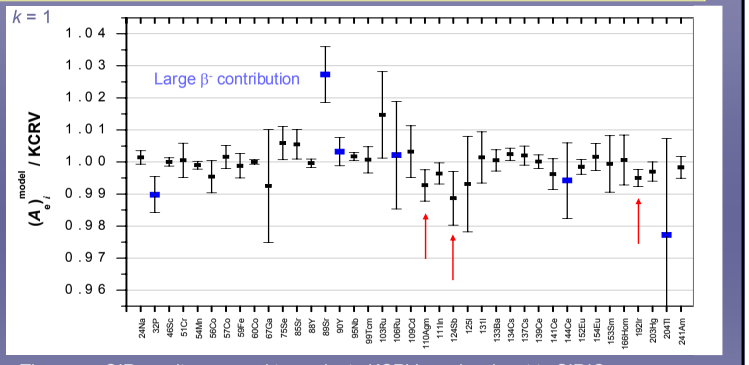

- The same SIR results are used to evaluate KCRVs and as input to SIRIC
  Recall : A_e^{model} can come from a combination of dozens of photons of very different energies
- Discrepancies may come from SIR data, nuclear data, SIRIC efficiency curves

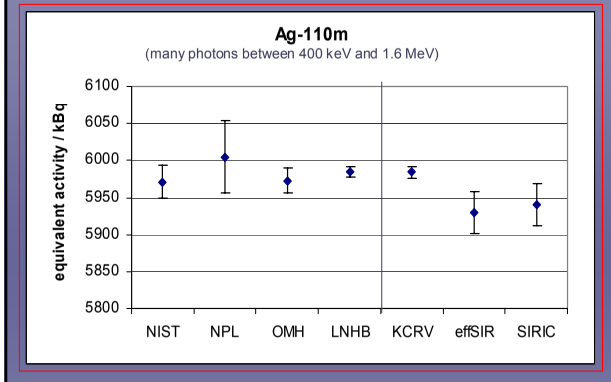

Problem in the decay scheme ?

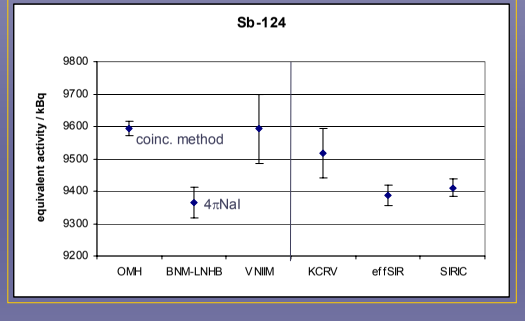

Problem in the primary standardizations ?

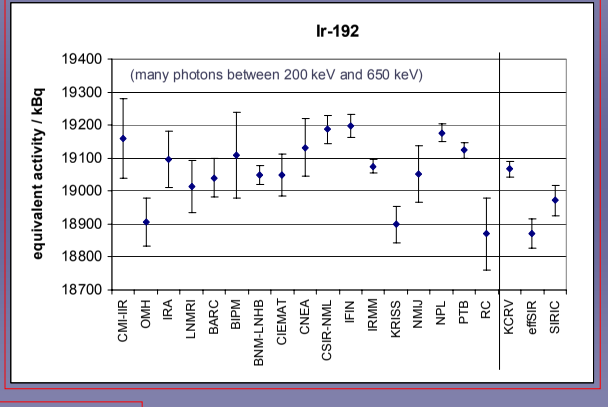

Problem in the decay scheme ?

The case of ^{65}Zn

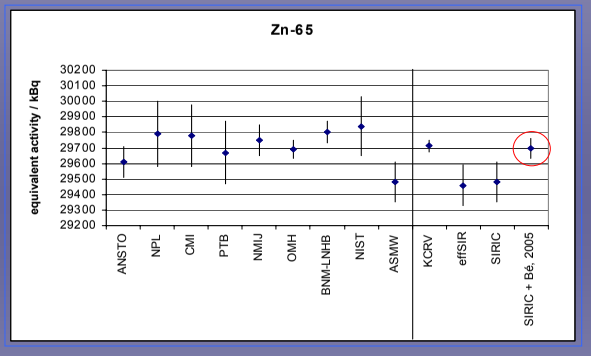

Very good agreement when 2005 DDEP emission intensities are used

Note : ^{65}Zn not used in SIRIC to obtain the efficiency curves

Conclusions and perspectives

- The SIR is a very efficient comparison tool since 1976 and the basis for key comparisons of the MRA for 57 radionuclides.
- SIRIC software is being finalized at NPL and will be used for the calculation of impurities in the SIR. SIRIC will be made available for all NMIs.
- $^{110}Ag^{m}$, ^{153}Gd, ^{192}Ir, ^{201}Tl, ^{207}Bi, ^{243}Am:

  the observed discrepancies between the SIR results and the efficiency curves motivate new research on measurement methods and/or decay scheme parameters for these nuclides.

Liquid Scintillation Counting and Atomic & Nuclear Data

Philippe Cassette, Laboratoire National Henri Becquerel, France

DDEP workshop, Saclay, March 2006

A short history of LSC

Date of birth: 1950, by 2 independent teams:

•H. Kallmann, Scintillation counting with solutions, *Phys. Rev*., 1950
•G.T. Reynolds, F.B. Harrison, G. Salvine, Liquid scintillation counters, *Phys. Rev*., 1950

First detector: 1954, Packard instruments

First LSC conference: August 1957, Chicago USA
Last conference: October 2005, Katowice, Poland

Development of primary methods: premises in the 70's, development in the 80's, still going on…

LSC in short

- Mix the radioactive solution with a LS cocktail
- place in ad-hoc vial
- count the number of light flashes per unit of time
- calculate detection efficiency
- activity = count rate / detection efficiency

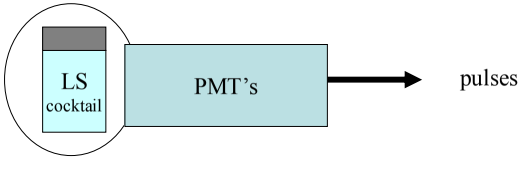

LSC

Advantages:

- 4π detection
- no physical barrier between the radionuclide and the detector
- easy-to-prepare sources
- high detection efficiency for most radionuclides

Drawbacks:

- low intrinsic light yield
- disastrous spectroscopic resolution
- source stability problems

Energy transfer in a LS cocktail

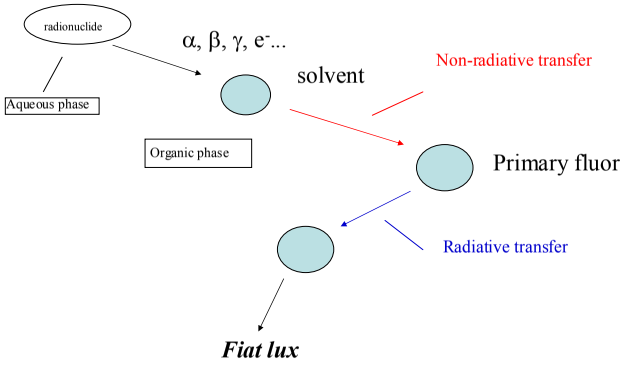

5

Example of energy transfer in a toluene-PPO cocktail

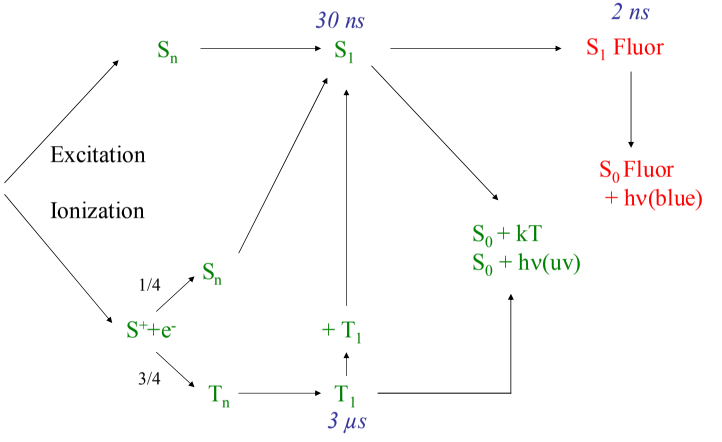

6

168

Some numbers:

- The energy of a 5 keV electron, if totally converted into light (425 nm) would produce — 1700 quanta
- About 99% of the energy is lost — 17 quanta
- The quantum efficiency of a PMT is ~25 %, so at the first dynode we expect — 4.3 electrons
- But, considering the ionization quenching (influence of stopping power) we get — 2.6 electrons

Low number of quanta -> big fluctuations (Poisson) -> bad energy resolution

7

The LS counter

The scintillation counter is a converter of:

- **electron energy into light**
- **light into photoelectrons at the photocathode of the PMT**
- **Photoelectron into charge pulse at the anode of the PMT**
- **Charge pulse into logic signal at the discriminator**

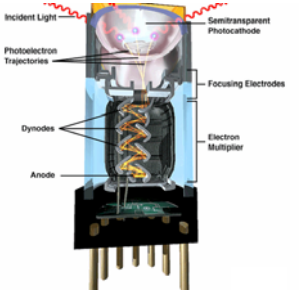

8

Coincidence circuit

- **Coincidence counting is needed to reduce the PMT noise.**
- **Coincidence resolving time: few 10 ns**
- **A larger coincidence resolving time imposes accidental coincidence correction (including coincidences due to after-pulses)**
- **Dead-time must be added to eliminate the effect of after-pulses (A few 10 μs are adequate)**

9

LSC Triple Counter

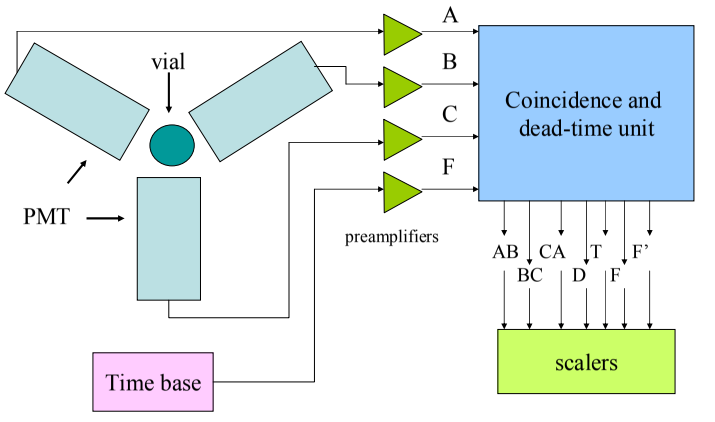

10

The Triple to Double Coincidence Ratio (TDCR) method

LS counter with 3 PMT 's : A, B, C
Coincidence counting:

- 3 double coincidences: AB, BC,CA
- Logical sum of double coincidences: D
- Triple coincidences: T
- Live-time clock (clock pulses sampled by the dead-time signal)

11

Statistical distribution of the number of photons emitted after the absorption by the LS-cocktail of a monoeneregetic electron E

(for example a Poisson law)

$$P(x/m) = \frac{m^x e^{-m}}{x!}$$

Probability of emission of x photons for an average value $m(E)$

12

Statistics of photoelectrons distribution for a weak light source

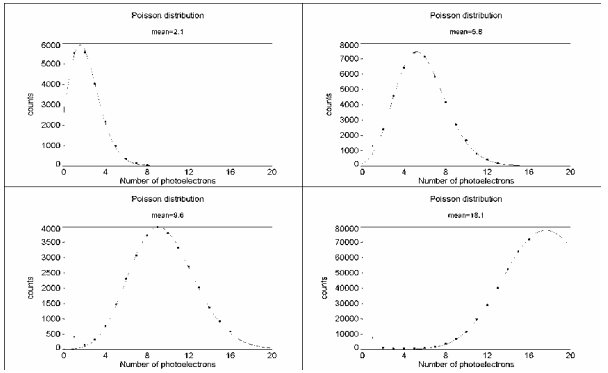

If the detection probability of 1 photon is not 0

Detection probability = 1- non-detection probability

For 1 PMT:

$$R = 1 - P(0/m) = 1 - \frac{m^0 e^{-m}}{0!} = 1 - e^{-m}$$

But PMT are affected by thermal noise, so this equation is useless …

In a symmetrical LS-counter (3 PMT 's 120° apart) assuming that the quantum efficiency of each PMT is the same ν, we get:

- Detection efficiency for 1 PMT: $R_1 = 1 - e^{-\frac{\nu m}{3}}$
- Detection efficiency for 2 PMT's in coincidence: $R_2 = (1 - e^{-\frac{\nu m}{3}})^2$
- Detection efficiency for 3 PMT's in coincidence: $R_T = (1 - e^{-\frac{\nu m}{3}})^3$
- Detection efficiency for the logical sum of the double coincidences:

$$R_D = 3(1 - e^{-\frac{\nu m}{3}})^2 - 2(1 - e^{-\frac{\nu m}{3}})^3$$

Experimental evidence:

The number of photons emitted **is not** proportional to the energy released in the LS cocktail

For a given energy, the number of photons emitted by alpha particles is lower than the one emitted by electrons

The light emission is an inverse function of the stopping power of the incident particle

Relative scintillation yield

Type of particle	Fraction of particle energy converted to photons compared to electrons
Electrons (>80 keV)	**1.00**
Protons (1-10 MeV)	**0.20 - 0.50**
Alpha (4-6 MeV)	**0.08 - 0.12**
Fission (180 MeV)	**0.013**

Scintillator non linearity :

mean number of photons emitted non-proportional to the energy released in the scintillator

Birks formula (integral form) :

$$m(E) = \int_0^E \frac{AdE}{1 + kB\frac{dE}{dx}}$$

m(E) : mean number of photons emitted after absorption of *E*

If the absorbed energy is not monoenergetic, but with a normalized spectrum density *S(E)*

- Detection efficiency for 2 PMT's in coincidence: $R_2 = \int_0^{E_{max}} S(E)(1-e^{-\frac{\nu\eta}{3}})^2 dE$
- Detection efficiency for 3 PMT's in coincidence: $R_T = \int_0^{E_{max}} S(E)(1-e^{-\frac{\nu\eta}{3}})^3 dE$
- Detection efficiency for the logical sum of double coincidences:

$$R_D = \int_0^{E_{max}} S(E)3(1-e^{-\frac{\nu\eta}{3}})^2 \text{-}2\,(1-e^{-\frac{\nu\eta}{3}})^3 dE$$

with $$\eta = \frac{\nu}{3}\int_0^E \frac{AdE}{1 + kB\frac{dE}{dx}}$$

The TDCR value is:

$$\frac{R_T}{R_D} = \frac{\int_{spectre} S(E)(1-e^{-\eta})^3 dE}{\int_{spectre} S(E)((3(1-e^{-\eta})^2 - 2(1-e^{-\eta})^3))dE}$$

with $$\eta = \frac{\nu}{3}\int_0^E \frac{AdE}{1 + kB\frac{dE}{dx}}$$

For a large number of events the ratio of frequencies equals the ratio of probabilities:

$$\frac{R_T}{R_D} = \frac{T}{D} = RCTD$$

Resolution method:

Find a value of the free parameter (νA) giving:

R_T/R_D calculated = T/D experimental

How many solutions ?

Pure-beta radionuclides: 1 solution

Beta-gamma, electron capture: up to 3 solutions...

21

Example of usual detection efficiencies

^{3}H: 60 %
^{55}Fe: 60 %
^{63}Ni: 80 %
^{241}Pu: 50 %
^{14}C: 95 %
^{32}P, ^{90}Y > 99 %
^{241}Am: ≈ 100 %
^{222}Rn$_{eq}$: ≈ 495 %

Average light yield ≈ 5 photons/keV
Or ≈ 1 photoelectron/keV

22

172

CALCULATION OF BETA SPECTRA
Fermi theory

Number of electrons with energy W emitted per unit of time in the $[W, W+dW]$ interval :

$$N(W)dW = \alpha p W (W_0 - W)^2 F(\pm Z, W) C(W) dW$$

With :

electron energy (m_0c^2 units) :

$$W = \frac{E}{m_0 c^2} + 1$$

Electron momentum (m_0c^2 units) :

$$p = \sqrt{W^2 - 1}$$

Beta max energy : W_0

Atomic number : Z

Fermi function : $F(\pm Z, W)$

Shape factor : $C(W)$

Neutrino momentum : $q = W_0 - W$

23

β transitions selection rules

$L=J_i-J_f$	$\pi_i\pi_f$	transition
0,1	+1	allowed
0,1	-1	1st forbidden non-unique
>1	$(-1)^L$	Lth forbidden non-unique
>1	$(-1)^{L-1}$	Lth forbidden unique

$J_i J_f$ $\pi_i\pi_f$ spin and parity of initial and final nuclear states

24

Shape factors

H. Behrens and L. Szybisz, (Shapes of beta spectra, Physics Data, ZAED 6-1, 1976)

- allowed : $C(W)=1$ or $C(W)=1+aW+b/W+cW^2$ with (a,b,c) smalls
- 1st forbidden non-unique : $C(W)=1+aW+b/W+cW^2+d(q^2+\lambda_2 p^2)$
- 1st forbidden unique : $C(W)= q^2+\lambda_2 p^2$ or $C(W)=1+aW$
- 2nd forbidden non unique : $C(W)= q^2+B_0\lambda_2 p^2$
- 2nd forbidden unique : $C(W)=q^4+\lambda_2 p^2 q^2 10/3+\lambda_3 p^4$
- 3rd forbidden non unique : $C(W)= q^4+A\lambda_2 p^2 q^2+B\lambda_3 p^4$
- 3rd forbidden unique : $C(W)= q^6+7\lambda_2 p^2 q^4+7\lambda_3 p^4 q^2+\lambda_4 p^6$

Beta spectra

- Uncertainty of shape factor and $E_{\beta max}$ is considered in the evaluation of detection efficiency uncertainties, especially for forbidden non unique transitions
- but … we need data and models for spectra shape factors
- Rule: the lower the detection efficiency, the higher the required accuracy of the calculated spectrum
  -> for high $E_{\beta max}$ the shape factor is not so important
- Example of critical nuclides : Rb-87, Cl-36, Tc-99, I-129, Cs-137, Pu-241…

Electron capture (example of ^{55}Fe)

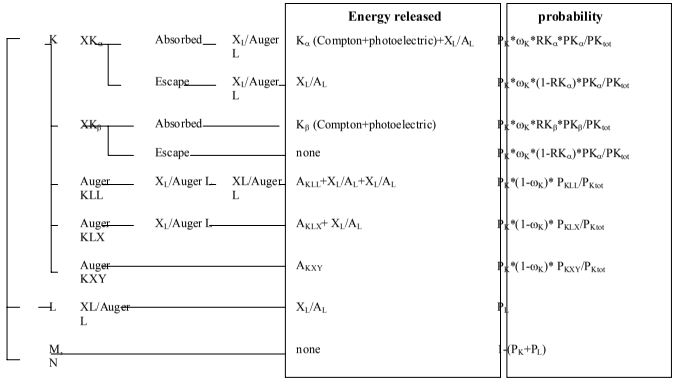

So, we need

- P_K, P_L, P_M,…
- ω_K, ϖ_L,…
- Detailed energies and intensities of X rays (KLL,KLX, L)
- Detailed energies and intensities of Auger electrons (KLL, KLX, KXY, L, M,…)

- Very important data: P_K (this governs the energy emission)
- Important data: P_{KLL}/P_{KLX} (scintillator non-linearity)
- Not so important data: ω_K (similar energy of X_K and $Auger_K$)
- Not important data: ω_L (low value, low energy of L events)

More complex decay-scheme: e.g. β or e.c. followed by γ transition

β followed by γ:

- Absorbed
  - Compton
  - Photoelectric
- Not absorbed
- Conversion electron

Idem for electron capture…

With even simple decay schemes, the number of decay paths can be very important…

-> The method is generally restricted to simple decay scheme radionuclides

29

Calculation of the energy absorbed by the LS-cocktail

Possible assumptions:

- Auger and conversion electrons totally absorbed
- X_L totally absorbed
- γ and X_K energy transfer calculated using a Monte Carlo model

Dominant decay data parameters:

- E_γ, E_{XK}, etc. (energy available)
- P_K, P_L, $P_{M,N}$ (energy available after e.c.)
- ω_K, etc. (radiation yield)
- α_K, α_L, $\alpha_{M,N}$ (conversion probability)

30

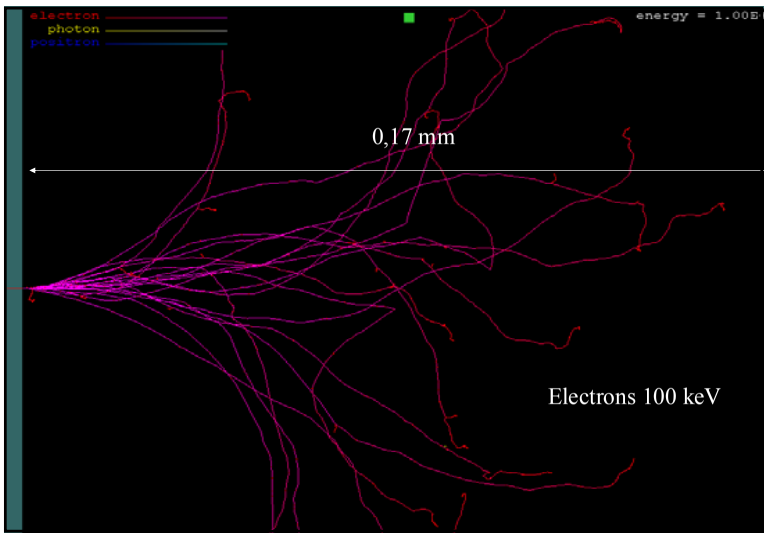

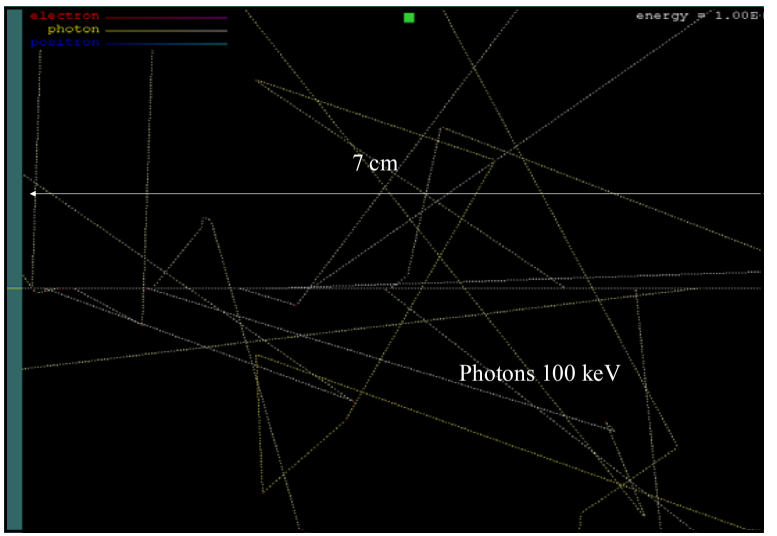

Uncertainty evaluation

Uncertainty : parameter, associated with the result of a measurement that characterizes the dispersion of the values that could reasonably (sic) be attributed to the measurand

Uncertainty of measurement means “doubt about the validity of the result of a measurement”

Uncertainty evaluation method (GUM)

1. Model the measurement
   (get the transfer function between input quantities and measurement result)
2. Evaluate standard uncertainties of input quantities (experimental data, parameters, *etc.*) and covariances between input quantities
3. Combine the standard uncertainties and covariances
4. Expand uncertainty (if you really need it…)

Uncertainty evaluation method

Model the measurement transfer function :

$$y = f(x_1, x_2, \ldots x_n)$$

y is the result and x_i are all the parameters used in the measurement : experimental, theoretical, etc.

The combined standard uncertainty u_c is calculated using :

$$u_c^2(y) = \sum_{i=1}^{n} \left[\frac{\partial f}{\partial x_i}\right]^2 \cdot u^2(x_i) \quad +2\sum_{i=1}^{n-1}\sum_{j=i+1}^{n} \frac{\partial f}{\partial x_i} \cdot \frac{\partial f}{\partial x_j} \cdot u(x_i, x_j)$$

Standard uncertainties on TDCR input parameters

Experimental:

- Double coincidences: D
- Triple coincidences: T
- TDCR: T/D

$$s_D^2 = \frac{1}{n-1}\sum_{i=1}^{n}(D_i - \overline{D})^2$$

$$s_T^2 = \frac{1}{n-1}\sum_{i=1}^{n}(T_i - \overline{T})^2$$

$$s_{DT} = \frac{1}{n-1}\sum_{i=1}^{n}(D_i - \overline{D})(T_i - \overline{T})$$

$$s_{TDCR} = TDCR\sqrt{\frac{s_T^2}{T^2} + \frac{s_D^2}{D^2} - \frac{2s_{DT}}{DT}}$$

Data:

Standard deviation of: $E_{\beta max}$, shape factor, P_K, P_L, P_M, X-ray energies and probabilities, Auger electrons energies and probabilities, ω_K, ϖ_L,.. α_K, α_L, α_M…

And covariance of correlated data!

Covariance matrix example measurement input data set (example of electron capture to excited level)

	D	TDCR	PK	PL	PM	wK	wL	AKLL/AK	AKLX/AK	AKXY/AK	Ka/K	PecK	PecL	PecM
D	exp	exp	0	0	0	0	0	0	0	0	0	0	0	0
RCTD		exp	0	0	0	0	0	0	0	0	0	0	0	0
PK			2,0E-06	-6,0E-07	-6,0E-07	0	0	0	0	0	0	0	0	0
PL				1,2E-06	-6,0E-07	0	0	0	0	0	0	0	0	0
PM					3,00E-07	0	0	0	0	0	0	0	0	0
wK						1,6E-05	0	0	0	0	0	0	0	0
wL							1,4E-06	0	0	0	0	0	0	0
AKLL/AK								5,3E-04	1,0E-04	1,0E-04	0	0	0	0
AKLX/AK									7,0E-05	1,0E-04	0	0	0	0
AKXY/AK										8,0E-06	0	0	0	0
Ka/K											3,0E-05	0	0	0
PecK												2,8E-03	5,0E-03	5,0E-03
PecL													2,2E-02	5,0E-03
PecM														5,2E-03

Combination of variances

- TDCR efficiency is calculated using numerical algorithms

  No analytical calculation of partial derivatives

  - Option 1: Numerical evaluation of the partial derivatives
  - Option 2: Monte Carlo method

Option 1: numerical calculation of derivatives

$$\frac{\partial F(x_1, x_2, .., x_n)}{\partial x_i} = \frac{F(x_1, ..., x_i + h, ..x_n) - F(x_1, ..., x_i - h, ..., x_n)}{2h}$$

- If ε_F : relative error on the evaluation of F around x_i
- If the choice of h is optimum
  - Then : the relative error on the derivative is about $(\varepsilon_F)^{2/3}$

The number of evaluations of F for each derivative calculation is 6 to 12 with the algorithm used (Numerical recipes, Press et *al.*)

Option 2: Monte Carlo method

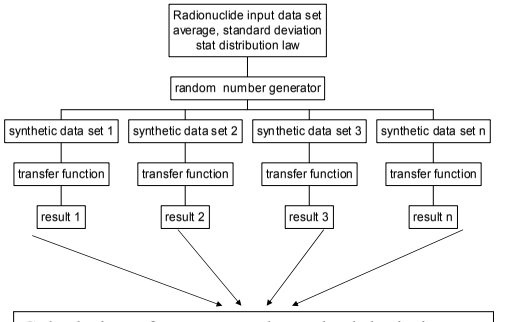

Application: measurement of the half-life of ^{79}Se

a cooperation between

COGEMA (La Hague),

CEA-LNHB (Saclay),

CEA-LARC (Cadarache)

41

^{79}Se

Long half-life fission product

	Concentration in REP fuel	Activity in FP solutions (after 10 years)
^{79}Se	7,7 mg/kg	$1,5\ 10^5$ Bq/l
Total FP	34 g/kg	10^{12} Bq/l

Major concern for waste management…

42

^{79}Se – decay scheme

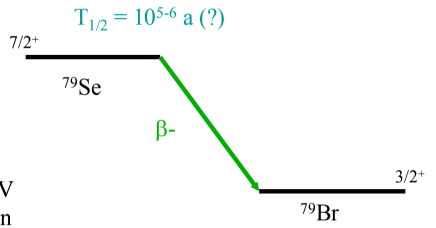

Q = 151 keV
1st forbidden
unique

43

^{79}Se – half-life

I- Historical values

1949, Parker *et al.*	**≤ 6,5 × 10^4 a**
1951, Glendenin	**7 × 10^6 a**

II – Historical values revisited

1993, in NDS	**6,5 × 10^5 a**

II- Recent measurements

1995, Yu Runlan	**4,8 (4) × 10^5 a**
1997, Jiang Songsheng	**1,1 (2) × 10^6 a**
2000, same authors	**1,24 (19) × 10^5 a**
2002, same authors	**2,95 (38) × 10^5 a**

44

Why so few ^{79}Se half-life measurements ?

- Pure ^{79}Se is a very rare product
- ^{79}Se is a pure beta emitter, difficult to measure in a mixture of radionuclides
- The mass of ^{79}Se is difficult to measure by ICP-MS (interference with argon compounds)

45

This measurement

COGEMA : initial solution and first separation
LARC : purification and mass spectrometry
LNHB : activity measurement

Activity and mass ⟶ half-life

46

1 Sample preparation

Initial juice : **1,4 10^{11} Bq/l β, ec** and **5 10^{9} Bq/l α !**

Se initial separation using ion-exchange resins in hot cells (La Hague reprocessing plant)

Se purification (Cadarache)

Some impurities still present: Sb, Ru,…

-> 2 samples about 2,5 g of ^{79}Se solution in 7,2 M HNO_3 (^{79}Se activity of « a few Bq/g »)

47

Impurity determination

Liquid sample

GeHP detector with anti-cosmic guard in underground laboratory:

standardization with point-source at 10 cm

Efficiency transfer calculation: ETNA software

48

Measurement

Measurement time 604 800 s

- For each peak:

$$A(Bq) = \frac{N(E)}{I_\gamma(E) \cdot [R(E) \cdot C^R(E)] \cdot t} \cdot C^T \cdot C^{coinc}$$

- N(E) : surface
- $I\gamma(E)$ = gamma emission intensity (Nucléide)
- R(E) : detector efficiency for point source
- t = measurement duration (s)

- C^T : decay correction
- $C^R(E)$: efficiency correction (ETNA)
- C^{coinc} (E) : coincidence correction (about 2 %, ETNA)

49

Spectrum

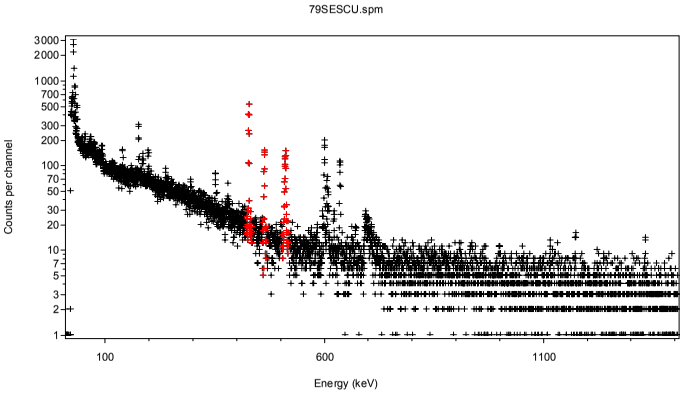

50

Impurities

- Uncertainties :
  - Counting statistics (2-5 % for ^{125}Sb, 25% for ^{137}Cs, 10% for ^{106}Ru)
  - Efficiency (0,4 %)
  - Geometry transfer (2 %)
  - Gamma emission intensities (1 %)
  - Coincidence corrections (0,1 %)

  - Activity of the sample
- ^{125}Sb : 1,6 Bq ± 4 %
- ^{137}Cs : 0,06 Bq ± 25 %
- ^{106}Ru : 0,3 Bq ± 11 %

51

LSC

• Test of 3 cocktails: Ultima Gold AB, Hionic Fluor (Perkin Elmer) and Ready Safe (Beckman Coulter)

• Test source using ^{36}Cl and various volume ratio:

• Criteria: stability and ^{36}Cl detection efficiency)

52

Measurement method: ^{3}H efficiency tracing (CIEMAT/NIST method)

Same principle than TDCR method but free parameter deduced from the measurement of a tritium standard source in the same chemical condition than the ^{79}Se source

$$R_D = \int_{spectrum} S(E)(1-e^{-\eta})^2\, dE \qquad \eta = \frac{\nu}{2}\int_0^E \frac{AdE}{1+kB\frac{dE}{dx}}$$

νA is calculated using a ^{3}H standard
R_D is calculated for any radionuclide using νA

Measurement system

Low activity LS counter Quantulus (Perkin Elmer)
low-activity lead
anticoincidence guard (LS)

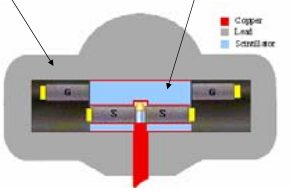

Measurement time: 5 x 1500 minutes
Blank measurement time: 5 x 5000 minutes

Experimental spectrum

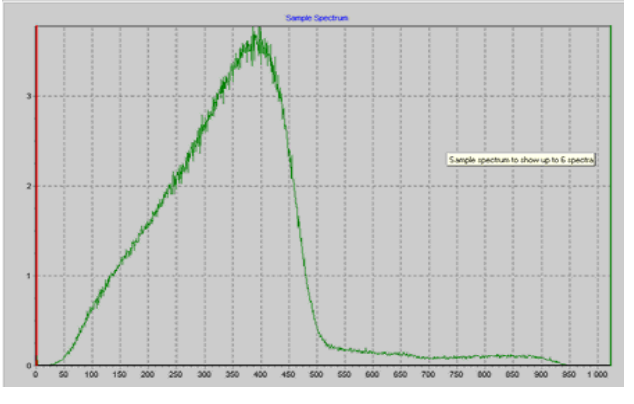

Activity calculation

$$N_{\exp} = A_{Se}\varepsilon_{Se} + A_{Sb}\varepsilon_{Sb} + A_{Ru}\varepsilon_{Ru} + A_{Rh}\varepsilon_{Rh}$$

N_{exp} : count rate of the sample
A_X : activity of radionuclide X
ε_X : detection efficiency of radionuclide X

Known: N_{exp}, A_{Sb}, A_{Ru} and A_{Rh} (SL and γ–spectrometry)

ε_{Sb}, ε_{Se}, ε_{Ru} and ε_{Rh} can be calculated

$\rightarrow \quad A_{Se}$

Scintillator intrinsic light yield

$\varepsilon_{H\text{-}3} = 0{,}00142\ SQPE - 0{,}82262$

In the measurement conditions:

$n = 0{,}4734 \pm 0{,}0054$ photoelectron per keV

Spectra calculation

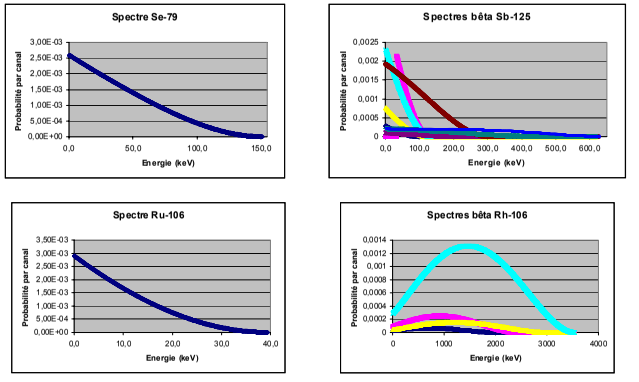

Detection efficiencies

Radionuclide	$E_{\beta max}$ (keV)	ε	s_ε
^{79}Se	151,1	0,8916	0,0018
^{125}Sb	95,4	0,8956	0,0027
	95,4+ec	0,9606	0,0029
	124,7	0,9157	0,0018
	130,8	0,9271	0,0019
	241,6	0,9638	0,0008
	303,4	0,9720	0,0007
	445,7	0,9879	0,0004
	662,0	0,9885	0,0002
^{125}Sb	total	0,9613	0,0020
^{106}Rh		1	0
^{106}Ru	39,4	0,7233	0,0043

Final result:
^{79}Se activity per unit of mass of the sample

$13{,}35 \pm 0{,}06$ Bq/g
$(4{,}5\ 10^{-3})$

Pure beta impurity ?

• Bad resolution of LSC spectroscopy but it is possible to compare the experimental spectrum and the theoretical expected spectrum

61

Experimental spectrum

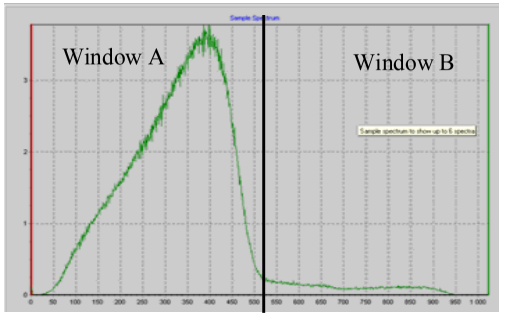

Channel 525 is about 150 keV (^{79}Se $E_{\beta max}$)
The count ratio is A/B = 0,053

62

Theoretical spectrum (log)

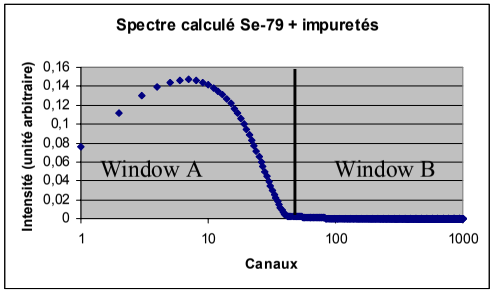

The ratio A/B = 0,051

→ No evidence of pure-beta impurity

63

3. Mass measurement of ^{79}Se

ICP-MS measurement using isotopic ratio of Se isotopes ^{79}Se, ^{77}Se and ^{82}Se

$$[^{79}Se]_f = (^{79}Se/^{82}Se)_i \cdot [^{82}Se]_f$$

[79Se]f = 29,2 ± 1,6 ng/g

64

4. Half-life calculation

$$T_{1/2} = \frac{Ln2}{A} N_0 \frac{m}{M} \frac{1}{s}$$

$T_{1/2}$: half-life (a)
A : ^{79}Se activity (Bq)
N_0 : Avogadro number (6,022 1415 (10) 10^{23} mol^{-1})
m : mass of ^{79}Se (g)
M : molecular mass of ^{79}Se (78,9184991 (18) g/mol)
s : number of s in a year (365,242 x 86400 s/a)

65

Uncertainty of the half-life

$$s_{T_{1/2}} = \sqrt{\left(\frac{s_A}{A}\right)^2 + \left(\frac{s_m}{m}\right)^2}$$

s_A : standard uncertainty of ^{79}Se activity
s_m : standard uncertainty of ^{79}Se mass

Other uncertainties are negligible
No *a priori* covariance between A and m

66

^{79}Se half-life

$T_{1/2} = (3,67 \pm 0,20)\ 10^5$ a

67

Nuclear Instruments and Methods in Physics Research A265 (1988) 541–547
North-Holland, Amsterdam

UNCERTAINTIES OF PARTICLE EMISSION PROBABILITIES

Directly measured particle emission probabilities

$$p_1(\%) = \frac{100 I_1}{I_1 + I_2} \quad \text{and} \quad p_2(\%) = \frac{100 I_2}{I_1 + I_2},$$

The emission probability of the ith particle group is given by

$$p_i(\%) = \frac{B I_i}{\sum_k I_k}, \tag{1}$$

where I_i is the relative spectral intensity of the ith particle group (with statistical uncertainty $\mathrm{d}I_i$), B is the percentage particle branching (with statistical uncertainty $\mathrm{d}B$), and the summation is over all particle groups k.

The fractional uncertainty of $p_i(\%)$, calculated in first order approximation in a Taylor series expansion, as in ref. [1], is

$$\frac{\mathrm{d}p_i(\%)}{p_i(\%)} = \left(\left(\frac{\mathrm{d}I_i}{I_i} \right)^2 \left(1 - \frac{2I_i}{\sum_k I_k} \right) + \frac{\sum_k \mathrm{d}I_k^2}{\left(\sum_k I_k \right)^2} + \left(\frac{\mathrm{d}B}{B} \right)^2 \right)^{1/2}. \tag{2}$$

The first term in the second member of this equation gives the contribution from the uncertainty of the relative spectral intensity of the ith particle group, and the second term, that of the normalizing factor $(100/\Sigma_k I_k)$. For an isotope emitting two particle groups, eq. (2) shows that the uncertainties of both emission probabilities are equal, irrespective of the statistical uncertainties of the relative spectral intensities of the two peaks, i.e.,

$$\mathrm{d}p_1(\%) = \mathrm{d}p_2(\%) = \frac{100}{(I_1 + I_2)^2} \left(I_1^2\, \mathrm{d}I_2^2 + I_2^2\, \mathrm{d}I_1^2 \right)^{1/2}$$

Additionally, if the particle groups have equal relative spectral intensities ($I_1 = I_2$) and uncertainties ($\mathrm{d}I_1 = \mathrm{d}I_2$), then

$$\frac{\mathrm{d}p_1(\%)}{p_1(\%)} = \frac{\mathrm{d}p_2(\%)}{p_2(\%)} = \frac{\sqrt{2}}{2} \frac{\mathrm{d}I}{I}. \tag{3}$$

From eq. (3), one can see that the fractional uncertainties of the emission probabilities are smaller than those of the corresponding relative spectral intensities.

4. Typical examples

4.1. Uncertainties of directly measured particle emission probabilities: ^{240}Pu alpha decay

The alpha-decay data of ^{240}Pu from ref. [2] are listed in table 1, along with the emission probabilities calculated in the present work.

Using eq. (2) and assuming that the uncertainties given in the second column of table 1 are for the relative spectral intensities, the calculated uncertainties of the emission probabilities (given in the third column) become

$$\mathrm{d}p_1(\%) = \left(\left(\frac{0.36}{73.51}\right)^2\left(1 - \frac{2\times 73.51}{99.9}\right) + 1.737\times 10^{-5}\right)^{1/2} \times 73.51 = 0.18,$$

$$\mathrm{d}p_2(\%) = \left(\left(\frac{0.21}{26.39}\right)^2\left(1 - \frac{2\times 26.39}{99.9}\right) + 1.737\times 10^{-5}\right)^{1/2} \times 26.39 = 0.18,$$

and

$$\mathrm{d}p_3(\%) = \left(\left(\frac{0.001}{0.071}\right)^2\left(1 - \frac{2\times 0.071}{99.9}\right) + 1.737\times 10^{-5}\right)^{1/2} \times 0.071 = 0.001.$$

Note that the emission probabilities of the two most intense alpha groups have the same uncertainty (= 0.18). This is because collectively they represent 99.9% of the total alpha-decay intensity. Additionally, this uncertainty is 50% smaller than that of the relative spectral intensity of the 5168-keV alpha group.

Table 1
^{240}Pu alpha decay

Alpha energy [keV]	Intensity (relative)	Emission probability [a] [%]
5168.17 ± 0.15	73.51 ± 0.36	73.51 ± 0.18
5123.62 ± 0.25	26.39 ± 0.21	26.39 ± 0.18
5021.5 ± 0.5	0.071 ± 0.001	0.071 ± 0.001

[a] Present work.

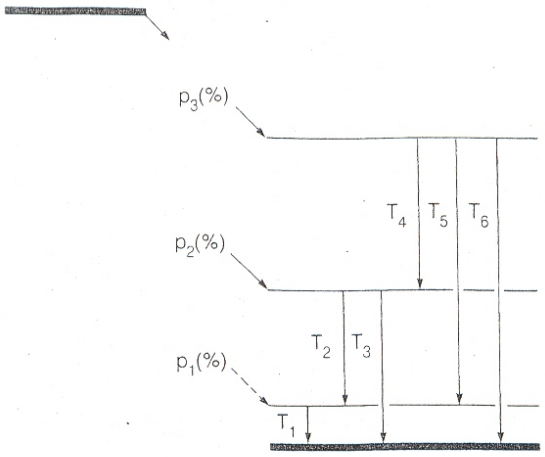

Fig. 1. Simple decay scheme.

3. Particle emission probabilities derived from decay schemes

Let us consider a hypothetical radioactive nucleus with the simple decay scheme shown in fig. 1. Three particle branches (p) and six γ-ray transitions (T) are involved.

Since there is no particle branching to the ground state, the three respective particle emission probabilities may be derived from the γ-ray transition intensities (photons plus conversion electrons):

$$p_1(\%) = \frac{T_1 - T_2 - T_5}{T_1 + T_3 + T_6} \times 100, \quad p_2(\%) = \frac{T_2 + T_3 - T_4}{T_1 + T_3 + T_6} \times 100, \quad p_3(\%) = \frac{T_4 + T_5 + T_6}{T_1 + T_3 + T_6} \times 100.$$

Notice that $p_1(\%)$, $p_2(\%)$, and $p_3(\%)$ are functions of the γ-ray transition intensity imbalances $(T_1 - T_2 - T_5)$, $(T_2 + T_3 - T_4)$, and $(T_4 + T_5 + T_6)$, respectively, as well as of the normalizing factor $100/(T_1 + T_3 + T_6)$. These are dependent quantities, and their corresponding uncertainties are affected by cancellation effects. Using

$$\mathrm{d}p_i^2(\%) = \sum_{k=1}^{6} \left(\frac{\partial p_i}{\partial T_k} \mathrm{d}T_k \right)^2, \tag{4}$$

the uncertainties become

$$\begin{aligned}
\mathrm{d}p_1(\%) &= \frac{100}{(T_1 + T_3 + T_6)^2} \big(\mathrm{d}T_1^2 (T_2 + T_3 + T_5 + T_6)^2 \\
&\quad + (\mathrm{d}T_2^2 + \mathrm{d}T_5^2)(T_1 + T_3 + T_6)^2 + (\mathrm{d}T_3^2 + \mathrm{d}T_6^2)(T_1 - T_2 - T_5)^2 \big)^{1/2}, \\
\mathrm{d}p_2(\%) &= \frac{100}{(T_1 + T_3 + T_6)^2} \big(\mathrm{d}T_3^2 (T_1 - T_2 + T_4 + T_6)^2 \\
&\quad + (\mathrm{d}T_2^2 + \mathrm{d}T_4^2)(T_1 + T_3 + T_6)^2 + (\mathrm{d}T_1^2 + \mathrm{d}T_6^2)(T_2 + T_3 - T_4)^2 \big)^{1/2},
\end{aligned} \tag{5}$$

and

$$\begin{aligned}
\mathrm{d}p_3(\%) &= \frac{100}{(T_1 + T_3 + T_6)^2} \big(\mathrm{d}T_6^2 (T_1 + T_3 - T_4 - T_5)^2 \\
&\quad + (\mathrm{d}T_4^2 + \mathrm{d}T_5^2)(T_1 + T_3 + T_6)^2 + (\mathrm{d}T_1^2 + \mathrm{d}T_3^2)(T_4 + T_5 + T_6)^2 \big)^{1/2}.
\end{aligned}$$

Further, for example, if it is reasonable to assume that there is no particle population to the first excited state, i.e., $p_1(\%) = 0$, the γ-ray intensity balance gives

$$T_1 = T_2 + T_5.$$

The particle emission probabilities then become

$$p_2(\%) = \frac{T_2 + T_3 - T_4}{T_2 + T_3 + T_5 + T_6} \times 100 \quad \text{and} \quad p_3(\%) = \frac{T_4 + T_5 + T_6}{T_2 + T_3 + T_5 + T_6} \times 100,$$

and their corresponding uncertainties become equal, i.e.,

$$\begin{aligned}
\mathrm{d}p_2(\%) = \mathrm{d}p_3(\%) &= \frac{100}{(T_2 + T_3 + T_5 + T_6)^2} \big(\mathrm{d}T_4^2 (T_2 + T_3 + T_5 + T_6)^2 \\
&\quad + (\mathrm{d}T_2^2 + \mathrm{d}T_3^2)(T_4 + T_5 + T_6)^2 + (\mathrm{d}T_5^2 + \mathrm{d}T_6^2)(T_2 + T_3 - T_4)^2 \big)^{1/2}.
\end{aligned} \tag{6}$$

These equal uncertainties are consistent with the conservation of the total probability $p_2(\%) + p_3(\%)$ $(= 100)$. Note that if the assumption $p_1(\%) = 0$ is not used, the uncertainties $\mathrm{d}p_2(\%)$ and $\mathrm{d}p_3(\%)$ given in eq. (5) are consistent with a possible particle branch to the first excited state, and, consequently, they are not necessarily equal.

Nuclear Instruments and Methods in Physics Research A249 (1986) 461–467
North-Holland, Amsterdam

CALCULATED UNCERTAINTIES OF ABSOLUTE γ-RAY INTENSITIES AND DECAY BRANCHING RATIOS DERIVED FROM DECAY SCHEMES

2. Description of the framework

2.1. Absolute γ-ray intensities

Let us consider first a hypothetical β^- emitter which populates the first excited state in the daughter nucleus, as shown in fig. 1. The absolute intensity ($\gamma(\%)$) for the subsequent γ-ray is

$$\gamma(\%) = \frac{100}{1+\alpha}, \tag{1}$$

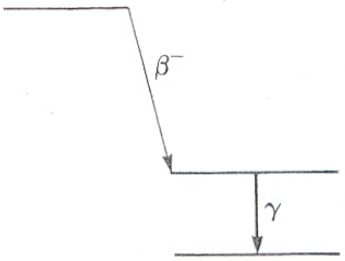

Fig. 1. Simple single-mode decay scheme

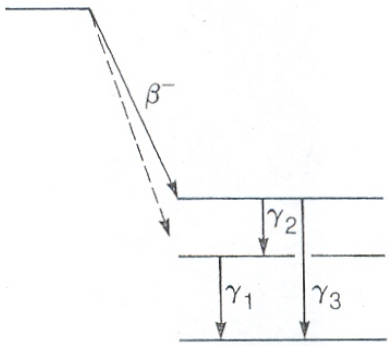

Fig. 2. Simple single-mode decay scheme.

where α is the total γ-ray conversion coefficient, i.e., the ratio of the total number of conversion electrons to the number of photons. Notice that the accuracy of this absolute intensity is independent of the photon intensity measurement, and depends only on the accuracy of α. Let us consider now the decay scheme shown in fig. 2. A normalizing factor N_1 between the relative and absolute intensity scales is

$$N_1 = \frac{100}{I_{\gamma 1}(1+\alpha_1) + I_{\gamma 3}(1+\alpha_3)}, \tag{2}$$

where $I_{\gamma 1}$, $I_{\gamma 3}$, α_1 and α_3 are the relative γ-ray intensities and their corresponding total conversion coefficients. Notice that an alternative normalizing factor is

$$N_2 = \frac{100}{I_{\gamma 2}(1+\alpha_2) + I_{\gamma 3}(1+\alpha_3)}. \tag{3}$$

This latter factor assumes no direct β^- population of either the ground state or first excited state, where N_1 assumes only no direct β^- population of the ground state. The accuracy of N_1 depends on the values of the relative γ-ray intensities, on their corresponding total conversion coefficients, and on the one decay-scheme assumption.

Choosing N_1, the absolute intensity of γ_1 is given by

$$\gamma_1(\%) = N_1 I_{\gamma 1} = \frac{100 I_{\gamma 1}}{I_{\gamma 1}(1+\alpha_1) + I_{\gamma 3}(1+\alpha_3)}. \tag{4}$$

The uncertainty of the normalizing factor similarly affects the absolute intensities of all of the γ-rays. Its numerical value, however, may not be the same for each γ-ray, because the normalizing factor and the relative γ-ray intensities are not always independent quantities. The maximum contribution to the uncertainty of the absolute intensity applies to those γ-rays which have not been included in the calculation of the normalizing factor, i.e., γ_2. Other γ-rays have lower uncertainties because of a cancellation effect, e.g., γ_1 (see eq. (4))

3. General formulation

3.1. Uncertainties of absolute γ-ray intensities

Let us consider the case of an isotope which decays through several decay modes (t), where only a fraction G_t of each mode does not populate the corresponding ground state in the daughter nucleus (i.e., $1 - G_t$ is the fraction for that decay mode which directly populates the ground state). The absolute intensity of the lth γ-ray associated with the ith decay mode is

$$\gamma_{li}(\%) = \frac{100 I_{li}}{\sum_{j,t} \frac{1}{G_t} T_{jt}}, \tag{6}$$

where $T_{jt} (= I_{jt}(1 + \alpha_{jt}))$ is the total transition intensity, α_{jt} is the total conversion coefficient of the jth γ-ray, and the summation is over all γ-rays (j) from the various decay modes (t) used in the normalizing procedure. Notice that for each decay mode there may be several γ-rays.

The relative uncertainty of $\gamma_{li}(\%)$ may be derived by first defining the variable

$$Y_{li} = \frac{100}{\gamma_{li}(\%)} = \left(\frac{\sum_{jt} \frac{1}{G_t} T_{jt}(1 - \delta_{jl})}{I_{li}} + \sum_{jt} \frac{1}{G_t}(1 + \alpha_{jt}) \delta_{jl} \delta_{ti} \right), \tag{7}$$

where δ is the Kronecker delta function, and then by calculating $\mathrm{d}Y_{li}/Y_{li}$ $(= \mathrm{d}\gamma_{lt}(\%)/\gamma_{li}(\%))$ in first order approximation in a Taylor series expansion.

Using

$$\frac{\mathrm{d}Y_{li}}{Y_{li}} = \frac{1}{Y_{li}} \left(\sum_{j,t} \left(\frac{\partial Y_{li}}{\partial T_{jt}} \mathrm{d}T_{jt} \right)^2 + \sum_{t} \left(\frac{\partial Y_{li}}{\partial G_t} \mathrm{d}G_t \right)^2 \right)^{1/2}, \tag{8}$$

the relative uncertainty of $\gamma_{li}(\%)$ becomes

$$\frac{\mathrm{d}\gamma_{li}(\%)}{\gamma_{li}(\%)} = \frac{\mathrm{d}Y_{li}}{Y_{li}} = \left[D_l^2 + C_l^2 \left(\frac{\mathrm{d}I_{li}}{I_{li}} \right)^2 + \left(\frac{\sum_{j} \frac{1}{G_i} \mathrm{d}\alpha_{jt} \delta_{jl}}{\sum_{j,t} \frac{1}{G_t} T_{jt}} I_{li} \right)^2 + \frac{\left(\sum_{j,t} T_{jt} \right)^2 \sum_{t} \frac{1}{G_t^2} \left(\frac{\mathrm{d}G_t}{G_t} \right)^2}{\left(\sum_{j,t} \frac{1}{G_t} T_{jt} \right)^2} \right]^{1/2}, \tag{9}$$

where

$$D_l^2 = \frac{\sum_{j,t} \frac{1}{G_t^2} \mathrm{d}T_{jt}^2 (1 - \delta_{jl})}{\left(\sum_{j,t} \frac{1}{G_t} T_{jt} \right)^2} \quad \text{and} \quad C_l^2 = \frac{\left(\sum_{j,t} \frac{1}{G_t} T_{jt}(1 - \delta_{jl}) \right)^2}{\left(\sum_{j,t} \frac{1}{G_t} T_{jt} \right)^2}.$$

For one decay mode, $t = 1$ and eq. (9) becomes

$$\frac{\mathrm{d}\gamma_l(\%)}{\gamma_l(\%)} = \left[D_l^2 + C_l^2 \left(\frac{\mathrm{d}I_l}{I_l} \right)^2 + \left(\frac{\sum_{j} \mathrm{d}\alpha_j \delta_{jl}}{\sum_{j} T_j} I_l \right)^2 + \left(\frac{dG}{G} \right)^2 \right]^{1/2} \tag{10}$$

where

$$D_l^2 = \frac{\sum_{j} \mathrm{d}T_j^2 (1 - \delta_{jl})}{\left(\sum_{j} T_j \right)^2} \quad \text{and} \quad C_l^2 = \frac{\left(\sum_{j} T_j (1 - \delta_{jl}) \right)^2}{\left(\sum_{j} T_j \right)^2}.$$

Eq. (10) is equivalent to one given by Browne and Firestone [1]. Notice that for γ-rays which have not been included in the calculation of the normalizing factor (i.e., for γ-rays with $l \neq j$), $C_l^2 = 1$ and the third term vanishes in eqs. (9) and (10). Eq. (10) then becomes

$$\frac{\mathrm{d}\gamma_l(\%)}{\gamma_l(\%)} = \left(D_l^2 + \left(\frac{\mathrm{d}I_l}{I_l} \right)^2 + \left(\frac{\mathrm{d}G}{G} \right)^2 \right)^{1/2}, \tag{11}$$

where the first and third terms in the second member of the equation represent the contribution from the uncertainty of the normalizing factor, and the second term, that from the relative photon intensity. These contributions are independent quantities.

2.2. Decay branching ratios

Decay branching ratios may be calculated from relative γ-ray intensities and decay-scheme considerations. Let us consider the hypothetical decay scheme shown in fig. 3.

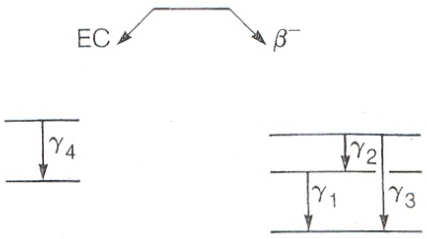

Fig. 3. Simple double-mode decay scheme.

If we assume no direct population to the ground states of the respective daughter nuclei, the β^- branching ratio ($B_{\beta-}$) is given by

$$B_{\beta-} = \frac{I_{\gamma1}(1+\alpha_1) + I_{\gamma3}(1+\alpha_3)}{I_{\gamma1}(1+\alpha_1) + I_{\gamma3}(1+\alpha_3) + I_{\gamma4}(1+\alpha_4)}. \tag{5}$$

As with N_1 above, the accuracy of $B_{\beta-}$ is affected by cancellation effects, i.e., the numerator and the denominator in eq. (5) are not independent quantities.

3.2. Uncertainties of decay branching ratios

The following expression gives the branching ratio (B_i) for the ith decay mode of an isotope which decays through several decay modes (t):

$$B_i = \frac{\frac{1}{G_i}\sum_j T_{ji}}{\sum_{j,t}\frac{1}{G_t}T_{jt}}. \tag{12}$$

Here the summation in the numerator is over all γ-rays (j) which carry the total decay intensity through the ith decay mode, and the summation in the denominator includes all γ-rays which carry the full disintegration intensity through all decay modes (t). Since once again the numerator and the denominator in the equation are not independent quantities, the relative uncertainty of B_i may be derived by first defining the variable

$$Z_i = \frac{1}{B_i} = 1 + \frac{\sum_{jt} R_{ti}T_{jt}(1-\delta_{ti})}{\sum_j T_{ji}}, \tag{13}$$

where $R_{ti} = G_i/G_t$, and then by calculating $\mathrm{d}Z_i/Z_i\ (= \mathrm{d}B_i/B_i)$ in a manner analogous to that in sect. 3.1.

The relative uncertainty of B_i becomes

$$\frac{\mathrm{d}B_i}{B_i} = \frac{1}{\sum_{j,t} R_{ti}T_{jt}}\left[\left(\frac{\sum_{jt} R_{ti}T_{jt}(1-\delta_{ti})}{\sum_j T_{ji}}\right)^2 \sum_j \mathrm{d}T_{ji}^2 + \sum_{jt} R_{ti}^2\,\mathrm{d}T_{jt}^2(1-\delta_{ti}) + \left(\sum_{jt} T_{jt}(1-\delta_{ti})\right)^2 \sum_t \mathrm{d}R_{ti}^2\right]^{1/2}, \tag{14}$$

where

$$\mathrm{d}R_{ti}^2 = R_{ti}^2\left[\left(\frac{\mathrm{d}G_i}{G_i}\right)^2 + \left(\frac{\mathrm{d}G_t}{G_t}\right)^2\right].$$

If the γ-rays used in the calculation carry the full intensity for each decay mode, i.e., if there is no direct ground-state population of the daughter nuclei, $G_t = 1$, $R_{ti} = 1$, and $\mathrm{d}R_{ti} = 0$ for all values of t and i. Eq. (14) is then

$$\frac{\mathrm{d}B_i}{B_i} = \frac{1}{\sum_{j,t} T_{jt}}\left[\left(\frac{\sum_{j,t} T_{jt}(1-\delta_{ti})}{\sum_j T_{ji}}\right)^2 \sum_j \mathrm{d}T_{ji}^2 + \sum_{j,t} \mathrm{d}T_{jt}^2(1-\delta_{ti})\right]^{1/2}, \tag{15}$$

4. Application to the decay of ^{192}Ir

As shown in the partial decay scheme in fig. 4, ^{192}Ir decays to ^{192}Pt by β^-, and to ^{192}Os by electron capture, with no direct ground-state population of the respective daughter nuclei. Data given in table 1, along with the decay scheme and eqs. (10) and (15), can be used to calculate the decay branching ratios and the absolute γ-ray intensities, and their corresponding uncertainties [2–4].

4.1. Decay branching ratios

The β^- percentage branching is given by

$$B_{\beta-}(\%) = 100\,\frac{T(316.5\gamma) + T(612.5\gamma) + T(1378.5\gamma)}{T(316.5\gamma) + T(612.5\gamma) + T(1378.5\gamma) + T(205.8\gamma) + T(489.1\gamma)} = 95.2,$$

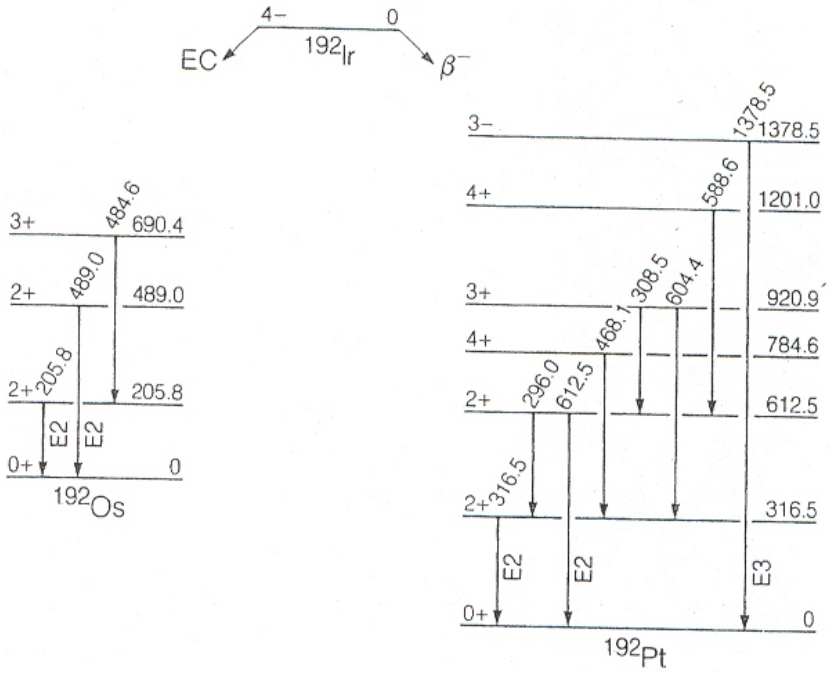

Fig. 4. ^{192}Ir partial decay scheme.

Table 1
^{192}Ir γ-rays populating the ground states of ^{192}Pt and ^{192}Os [a]

Energy (E_γ) [keV]	Relative intensity (I_γ) [rel]	Multipolarity and conversion coefficient (α)	Transition intensity (T) $T = I_\gamma(1+\alpha)$
205.8	4.01 ±0.06	E2, 0.305	5.233 ±0.145
316.5	100.0 ±0.5	E2, 0.085	108.5 ±1.0
489.1	0.527 ±0.009	E2, 0.0242	0.540 ±0.009
612.5	6.365 ±0.025	E2, 0.0155	6.464 ±0.027
1378.5	0.0016 ±0.0005	E3, 0.0035 ±0.0009 [b]	0.0016 ±0.0005

[a] γ-ray energies and intensities are from ref. [3]. Conversion coefficients are theoretical values from ref. [3], with 10% assumed uncertainty, except as otherwise indicated.
[b] Experimental value from ref. [4].

and the corresponding relative uncertainty by

$$\frac{\mathrm{d}B_{\beta-}}{B_{\beta-}} = \frac{1}{120.74}\left(\left(\frac{5.773}{114.96}\right)^2 1.0 + 0.021\right)^{1/2} = 0.00127.$$

Therefore B_{β}-(%) = 95.2 ± 0.1, and B_{EC}(%) = 4.8 ± 0.1.

4.2. Absolute γ-ray intensities

The normalizing factor for the absolute intensities is

$$N = \frac{100}{120.74} = 0.8282.$$

The relative uncertainty of the intensity for the 316.5-keV γ-ray (which has been used for calculating the normalizing factor N) is

$$\frac{\mathrm{d}\gamma(\%)}{\gamma(\%)} = \left[D_I^2 + C_I^2\left(\frac{0.5}{100}\right)^2 + \left(\frac{0.0085}{120.74}100\right)^2\right]^{1/2},$$

where

$$D_I^2 = \frac{0.145^2 + 0.009^2 + 0.027^2 + 0.0005^2}{120.74^2} = 1.50 \times 10^{-6}$$

and

$$C_I^2 = \left[\frac{5.233 + 0.540 + 6.464 + 0.0016}{120.74}\right]^2 = 1.02 \times 10^{-2}.$$

$\mathrm{d}\gamma(\%)/\gamma(\%)$ then becomes 0.00716 and the absolute intensity,

$$\gamma(\%) = 82.8 \pm 0.6.$$

For the 468-keV γ-ray (which has not been used for calculating the normalizing factor N),

$$\frac{\mathrm{d}\gamma(\%)}{\gamma(\%)} = \left[D_I^2 + C_I^2\left(\frac{0.23}{57.76}\right)^2\right]^{1/2},$$

in which

$$D_I^2 = \frac{0.145^2 + 0.009^2 + 1.0^2 + 0.027^2 + 0.0005^2}{120.74^2} = 7.0 \times 10^{-5} \quad \text{and} \quad C_I^2 = 1.0.$$

Table 2
Absolute intensities of the strongest γ-rays from ^{192}Ir decay

Energy (E_γ) [a] [keV]	Relative intensity (I_γ) [a] [rel]	Absolute intensity (γ(%))[%]	
		Ref. [2]	Present work
205.8	4.01 ±0.06	3.32 ±0.5	3.32 ±0.06
296.0	34.69 ±0.17	28.73 ±0.28	28.73 ±0.28
308.5	35.87 ±0.19	29.7 ±0.3	29.7 ±0.3
316.5	100.0 ±0.5	82.8 ±0.6	82.8 ±0.6
468.1	57.76 ±0.23	47.8 ±0.5	47.80 ±0.44
484.6	3.828 ±0.018	3.17 ±0.03	3.17 ±0.03
588.6	5.423 ±0.021	4.49 ±0.04	4.49 ±0.04
604.4	9.79 ±0.04	8.11 ±0.08	8.11 ±0.08
612.5	6.365 ±0.025	5.27 ±0.05	5.27 ±0.05

[a] From ref. [2].

$d\gamma(\%)/\gamma(\%)$ then becomes 0.00927 and the absolute intensity,

$$\gamma(\%) = 47.80 \pm 0.44.$$

Table 2 shows the absolute γ-ray intensities and their corresponding uncertainties for the strongest γ-rays from the decay of ^{192}Ir. The uncertainties calculated in the present work agree well with those of Iwata et al. [2], as seen in the third column.

^{134}Cs *Evaluation*

Ruy M. Castro — IEAv-CTA, UNITAU

Paulo R. Pascholati — IF/USP
Vito R. Vanin — IF/USP
Edgardo Browne — LBNL

CRP

^{134}Cs *Evaluation*

- References
- Half life
- Energy
- Intensity
- Other evaluations

^{134}Cs *Evaluation*

Decay Scheme

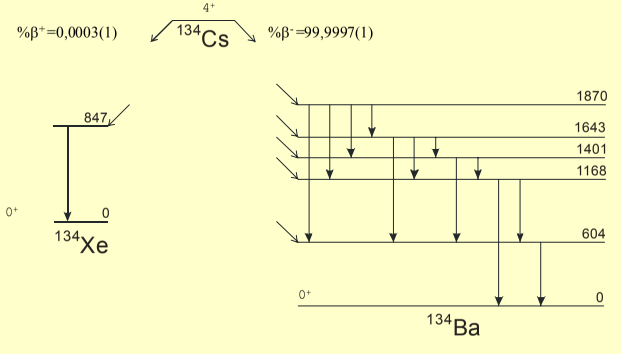

^{134}Cs *Evaluation*

References

~ 380 in NSR

~ 1/4 with information about: $T_{1/2}$, E_γ , I_γ , etc.

Compilations: TECDOC (1991), NDS (2004) and CRP

Since CRP

~ 25 in NSR,

4 with information about: $T_{1/2}$ and $I\gamma$

^{134}Cs *Evaluation* Half life

Ref.	Woods 2004Ni03	Paulo P.	TECDOC	$T_{1/2}$ (d)	Used	Comments
1972LA14	X	X	X	751,7(15)	X	Uncertainty in the work for 99,7% confidence level.
1973DI01	X		X	753,1(6)	X	Uncertainty in the work for 99,7% confidence level and uses $T_{1/2}$ of ^{137}Cs
1978BU		X	X	745(11)		Outlier - Uses $T_{1/2}$ of ^{137}Cs and the uncertainty is not reliable
1980RUZY		X	X	753,78(3)	X	The same Lab of 1997Ma75, but it is a different measurement (?)
1980HO17	X	X	X	754,50(7)	X	
1982HOZJ		X	X			Superseded by 2002Un02
1992UN01	X					Superseded by 2002Un02
1997MA75	X	X		754,52(18)	X	The same Lab of 1980RuZY, but it is a different measurement (?)
2002Un02				753,88 (15)	X	

^{134}Cs *Evaluation* Half life

```
HALF-LIFE         ....

INP. VALUE  INP. UNC.      R. WGHT  chi**2/N-1 REFERENCE
.751700E+03 .150E+01       .248E-02  .590E+00 1972LA14                OUTL(CHAUV)
.753100E+03 .600E+00       .155E-01  .769E+00 1973DI01
.753780E+03 .300E+00       .620E-01  .548E+00 1980RUZY
.754500E+03 .106E+00     *.500E+00* .896E+00 1980HO17
* Input uncertainty increased .151E+01 times *
.754520E+03 .180E+00       .172E+00  .366E+00 1997MA75
.753880E+03 .150E+00       .248E+00  .140E+01 2002UN02

No. of Input Values N= 6  CHI**2/N-1=  4.57  CHI**2/N-1(critical)=  3.00

Data rejection parameters for deviation from weighted average.
OUTL(CHAUV)...Chauvenet's PS*SIG=.181E+01

UWM   :.753580E+03  .433005E+00
WM    :.754276E+03  .746843E-01(INT.)  .159584E+00(EXT.)
LWM   :.753580E+03  .920000E+00   Min. Inp. Unc.=.700000E-01
LWM has used unweighted average and expanded the uncertainty so range
includes the most precise value of .754500E+03

****************************** S U M M A R Y ******************************
     HALF-LIFE
CHI**2/N-1 .4566E+01
UWM-|.7536E+03 .43E+00|
WM- |.7543E+03 .75E-01|
LWM-|.7536E+03 .92E+00|
***************************************************************************
```


^{134}Cs *Evaluation* Half life

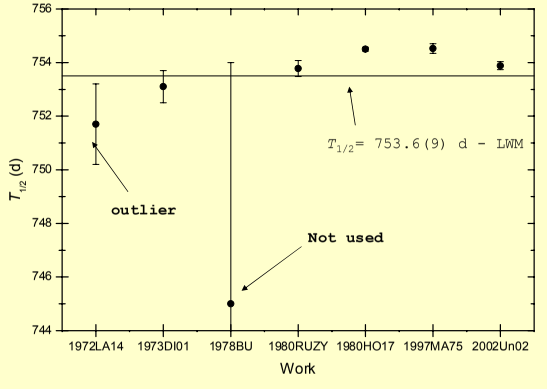

^{134}Cs *Evaluation* Energy

Works	TECDOC	Paulo	NDS	Used	Comments
1965Br02		X		X	
1966Ba57					Many transitions that not "fit" in the decay scheme.
1967Ra10		X	X	X	
1968Ab01		X		X	
1968Na11		X		X	
1975Al21			X	?	I don't have the ref.
1975Va12		?	X	?	Same data of 1990Me15.
1976De??					I don't have the ref.
1976Gr11		X	X	X	
1978MeZZ					I don't have the ref.
1985GoZK			XX		
1987Wa28	X	X	XX	X	
1990ChZB			o		Handbook (?)
1990Me15		?		?	Same data of 1975Va12 (?)
1991BaZS			o		TECDOC

^{134}Cs *Evaluation* Energy

E_γ(keV)	$\sigma_{E\gamma}$(keV)	#	χ^2/(n-1)	χ^2/(n-1) Critical
242,76	0,05	3	4,9	4,6
326,585	0,013	3	1,25	4,6
475,364	0,003	6	0,32	3,0
563,240	0,004	7	1,09	2,8
569,327	0,003	7	0,61	2,8
604,718	0,003	7	1,98	2,8
795,83	0,03	7	2,89	2,8
801,944	0,005	7	2,42	2,8
1038,605	0,007	7	1,35	2,8
1167,966	0,005	7	1,24	2,8
1365,183	0,007	7	0,38	2,8

- No systematic behavior in the data

9

^{134}Cs *Evaluation* Energy

Level Energy - GTOL

```
0   604.722  3    604.720  3
                  604.718  3

0  1167.966  4   1167.961  4   563.243  3
               1167.966  5   563.240  4
             ****1*****
0  1400.584  6   1400.576  6   795.859  6   232.617  5
                              795.83   3

0  1643.331  4   1643.321  4  1038.605  4   475.364  3   242.747  6
                             1038.605  7   475.364  3    242.76  5

0  1969.912 1969.912 5   1969.897  5  1365.183  5   801.943  4   569.327  3   326.581  5
                                     1365.183  7   801.944  5   569.327  3   326.585 13
```

χ^2/(6) = 0.4	χ^2/(6) Critical = 2.8

10

197

^{134}Cs *Evaluation* Iγ

	TECDOC	Paulo	NDS	Use	Comments
1962Ha10		X		X	Only 3 lines
1965Br02	X	X		X	
1966Ba57	X				Presents many transitions
1967Ra10	X	X		X	
1968Ab01	X	X		X	
1968Na11	X	X		X	
1970Ho06	X	X		X	
1973St14	X			X	Data in a decay scheme
1975Va12	X	X	X	X	
1976De??	X		X		I don't have the ref.
1978MeZZ	X				Is it a compilation?
1978Tr04		X			Only for 605 and and 796 keV
1980Yo05	X	X	X	X	
1987Wa28	X	X	X	X	
1988Ch44		X	X	X	
1990Me15					Same data of 1975Va12
2002Mi06			X	X	

11

^{134}Cs *Evaluation* Relative Intensity

E_γ(keV)	Ir_γ	$\sigma_{Ir\gamma}$	#	χ^2/(n-1)	χ^2/(n-1) Critical
242	0,027	0,006	6	3,9	3,0
326	0,0167	0,0010	5	0,6	3,3
475	1,515	0,007	10	0,6	2,4
563	8,545	0,014	12	0,4	2,2
569	15,740	0,017	12	1,7	2,2
604	100,00	0,08	12	0,0	2,2
795	87,54	0,06	10	0,1	2,4
801	8,904	0,015	10	0,7	2,4
1038	1,015	0,003	10	0,5	2,4
1168	1,834	0,005	10	0,8	2,4
1365	3,093	0,007	10	1,5	2,4

12

^{134}Cs *Evaluation* Normalization

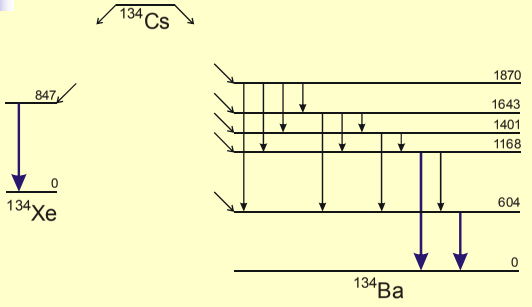

$$NR \cdot \left[Ir_{847}(1+\alpha_{847}) + Ir_{1168}(1+\alpha_{1168}) + Ir_{604}(1+\alpha_{604}) \right] = 100$$

NR = 0,9762(11)

^{134}Cs *Evaluation* Emission Probabilities

E_γ(keV)	Ir_γ	σ_{Ir_γ}	P	σ_P
242	0,027	0,006	0,026	0,006
326	0,0167	0,0010	0,0163	0,0010
475	1,515	0,007	1,477	0,007
563	8,545	0,014	8,342	0,014
569	15,740	0,017	15,366	0,017
604	100,00	0,08	97,623	0,018
795	87,54	0,06	85,46	0,06
801	8,904	0,015	8,692	0,015
1038	1,015	0,003	0,991	0,003
1168	1,834	0,005	1,790	0,005
1365	3,093	0,007	3,019	0,007

per 100 disintegrations

Gabs

^{134}Cs *Evaluation* Normalization

$$NR \cdot \left[Ir_{847}(1+\alpha_{847}) + Ir_{1168}(1+\alpha_{1168}) + Ir_{604}(1+\alpha_{604}) \right] = 100$$

$$NR = \frac{100}{\left[Ir_{847}(1+\alpha_{847}) + Ir_{1168}(1+\alpha_{1168}) + Ir_{604}(1+\alpha_{604}) \right]}$$

$$I_{604} = Ir_{604} \cdot NR = Ir_{604} \cdot \frac{100}{\left[Ir_{847}(1+\alpha_{847}) + Ir_{1168}(1+\alpha_{1168}) + Ir_{604}(1+\alpha_{604}) \right]}$$

$$I_{604} = \frac{100}{\left[\frac{Ir_{847}(1+\alpha_{847}) + Ir_{1168}(1+\alpha_{1168})}{Ir_{604}} + (1+\alpha_{604}) \right]}$$

$$\sigma_{I_{604}} \approx I_{604} \cdot \sigma_{\alpha_{604}} \approx\sim 97,623 \cdot 0,006 \cdot 0,03 \sim 0,018$$

I_{604} = 97,623(18) per 100 disintegrations

^{134}Cs *Evaluation*

Other evaluations

No new experimental information since 2002

Q value → Audi(2003)

Multipolarities → NDS

I_β →

Log*ft* →

Atomic Data →

NPL
National Physical Laboratory

Decay Data of Uranium-232

Andy Pearce, National Physical Laboratory, UK

(work in progress..)

Introduction to Radioactivity at NPL

- Radioactivity at NPL dates back to 1930s (at least) when radioactivity measurement consisted of weighing lumps of radium
- Primary function of the radioactivity group is to support "users" in medical physics and the nuclear industry in making activity measurements
- This support consists of providing calibration standards ("bucket science"), measuring customer samples - and of course providing nuclear data!

NPL

Measurement Techniques

- Gamma spectrometry – suite of high resolution and high efficiency gamma spectrometers - potential for absolute gamma measurements with all standards produced "in house"
- High resolution alpha spectrometry (same equipment as Eduardo Garcia-Torano but without the expertise) for p-alpha measurements
- Ionisation Chambers – previously used for half life determinations on short lived radionuclides
- Liquid scintillation counters, proportional counters, absolute (coincidence) counters – essential but less useful for nuclear data

NPL

Why Uranium-232

- Increased interest in thorium fuel cycles due to non-proliferation considerations (see IAEA TECDOC-1450)
- Uranium-232 is produced as a by-product in thorium-based fuels by neutron activation and the strong gamma emissions of some daughters (^{212}Bi, ^{208}Tl) make the resulting fuel "proliferation resistant"
- Selected as a candidate for evaluation at the CRP meeting in October

NPL

Background information

Uranium-232

Almost exclusively decays by alpha emission to excited states in ^{228}Th

Alpha branch consists of 9 alpha lines and 15 gamma transitions

VERY small fraction of decays are by ^{24}Ne radioactivity: NUBASE gives the branching ratio as $8.9 \pm 0.7 \times 10^{-10}$ per 100 decays

Maybe also some spontaneous fission (2000Bo46 suggests branching ~10^{-12})?

Half life is somewhere in the region of 70 years: NUBASE gives 68.9 ± 0.4 years

NPL

Uranium-232 Alpha Decay

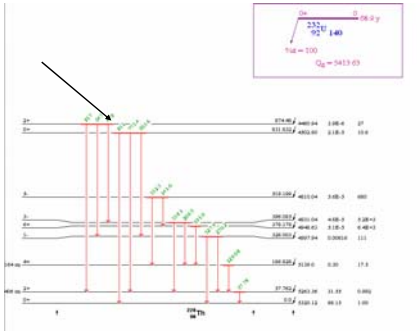

NPL

Work to Date

- Have to apologise I have little to present in terms of results!
- Have performed literature search (using NSR) and turned up around 60 papers which could be potentially relevant
- Haven't yet got papers from Nuclear Physics or looked at references section in ENSDF (I will soon!)
- Have ruled out all but three of those papers held at NPL* as not relevant

*one of those turned out to be the same paper I photocopied twice by mistake

NPL

Gamma Energies

- Paper by Börner (1979) gives curved crystal measurements of energies of Uranium-232
- Plan to use this paper will be used to scale energies in other publications – unless there are other curved crystal measurements (haven't looked in Helmer's paper yet)

Gamma Energy (keV)	Uncertainty (keV)
150.059	0.003
184.101	0.009
387.884	0.004
421.932	0.007
453.655	0.005
472.390	0.006
515.607	0.009
563.197	0.007
581.398	0.008
819.187	0.013
863.892	0.031
866.760	0.019
894.351	0.012
969.315	0.011
1003.280	0.039
1125.480	0.166

NPL

Half Life Measurement

- Only one paper detailing measurement of half life obtained so far (although it does reference four other measurements which I need to look at)
- Methods vary from specific activity (mass spec) to relative activity $^{232}U/^{233}U$ and ingrowth rate from ^{236}Pu

NPL

Potential problems

- Shortage of data in some areas (although I'm not exactly out of ideas about where to look next – just a little disorganised and haven't looked hard enough yet)
- Decay scheme not wildly complicated although I will need to look again braced with new information on what to look for!

NPL

International Atomic Energy Agency

Nd-147 Evaluation

M.A. Kellett
IAEA Nuclear Data Section
A-1400 Vienna, Austria

DDEP Evaluation Workshop,
6-10 March 2006, LNHB/CEA Saclay

Nd-147 – Basic Information

10.98 days half-life

100% beta- decay to Pm-147

Various betas (>7) and gammas (>15)

Nd-147 – Starting point

Nuclear Data Sheets vol.66 (1992)
cut-off date 1 April 1992

ENSDF – same data as NDS-66

6 levels and 7 beta transitions (including to ground)

15 gamma lines given

Nd-147 – Level Scheme - 1992

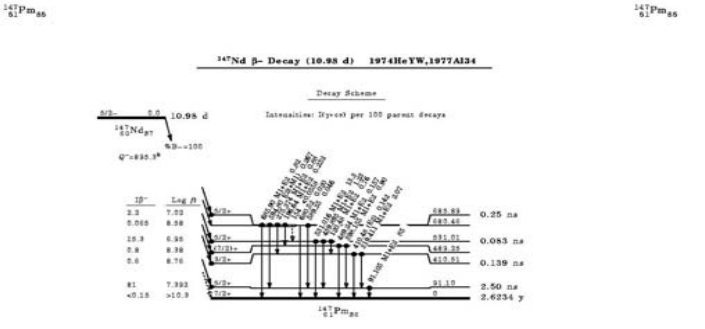

Nd-147 – Current status

Three main papers published since 1992:

1) Phys.Rev. C56, 2468 (1997), M.Sainath, K.Venkataramaniah, P.C.Sood, "*Level Structures in 147Pm from 147Nd Decay*"
2) *Bull.Rus.Acad.Sci.Phys. 67, 752 (2003), V.A.Zheltonozhsky, N.V.Strilchuk, V.P.Khomenkov, "Penetration effects in l-forbidden M1-transition in 147Pm nucleus"*
3) *Bull.Rus.Acad.Sci.Phys. 67, 1667 (2003), I.N.Vishnevsky, V.A.Zheltonozhsky, N.V.Strilchuk, "Simultaneous emission of two K-electrons by 123mTe and 147Pm nuclei"*

Nd-147 – Current status

Phys.Rev. C56, 2468 (1997), M.Sainath, K.Venkataramaniah, P.C.Sood, "*Level Structures in 147Pm from 147Nd Decay*"

Contains new decay scheme with 11 levels and 29 gamma transitions (2 without intensities!?!) and ICCs

Normalised to 531.069 keV line (as in NDS)

Nd-147 – Current status

Bull.Rus.Acad.Sci.Phys. 67, 752 (2003), V.A.Zheltonozhsky, N.V.Strilchuk, V.P.Khomenkov, *"Penetration effects in l-forbidden M1-transition in 147Pm nucleus"*

Bull.Rus.Acad.Sci.Phys. 67, 1667 (2003), I.N.Vishnevsky, V.A.Zheltonozhsky, N.V.Strilchuk, *"Simultaneous emission of two K-electrons by 123mTe and 147Pm nuclei"*

Measured gamma energies and intensities and ICCs

Nd-147 – What to do now?

Evaluate the nuclide using DDEP methodology!!

BUT…

How to evaluate ONE measurement?

How to deal with a previous evaluation?

Special topics

The following two topics were added to the agenda:

1) Nominal gamma-ray with Iγ = 100 and NO uncertainty
2) Rounding off uncertainties

1) How to handle a nominal gamma-ray intensity of 100 with an (or without any) uncertainty given.

The following procedure has been suggested and approved by consensus:

a) If authors clearly describe their uncertainties and explain that the uncertainty in Iγ = 100 has been folded into the uncertainties of the other γ rays, then use Iγ = 100 (with no uncertainty) in the DDEP evaluation.
b) If authors do not describe their uncertainties, then include a reasonable guess for the uncertainty of Iγ = 100 (for example: Iγ = 100 ± 2), and use this value in the DDEP evaluation.

After doing these changes, then normalize gamma-ray intensities to "intensities per 100 decays of the parent nuclide".

2) Rounding off uncertainties

The following two proposals for presenting uncertainties were suggested:

a) Uncertainties where the two most significant digits are between 10 and 25 should be rounded off to those two digits. Uncertainties > 25 should be rounded off to one significant digit.

b) "To produce a central value with a number of figures compatible with its uncertainty in the measurement, this value should be rounded off so its error due to rounding would be less than 1/10 the uncertainty in the measurement".
This rule is commonly expressed as follows: if the most significant figure in the uncertainty is between 5 and 9, then the central value is rounded off to that figure and its uncertainty should have just one digit. If the most significant figure is less than 5, then the central value is rounded off to the next significant figure and its uncertainty should have two digits.

Details are given in the two following appendixes.

Conclusions

The participants concurred that it was a fruitful meeting and made the following remarks :

- Most lectures were very appropriate and helpful;
- It would have been useful to have more time available for practicing with the use of data analysis software tools at this workshop.
- They had difficulties starting their own evaluations before attending this workshop. Also, they anticipated a need for ongoing support from senior evaluators as they proceed with their own evaluations.
- They suggested the creation of a "DDEP WEB FORUM" in the Internet for members of the collaboration to discuss various topics of data evaluation.
- They suggested another training workshop by the end of 2007 or the beginning of 2008.

The participants received each a CD-ROM that contained both all the DDEP software tools and the slides from these workshop presentations.

(Note: the DDEP web forum is now available at: http://laraweb.free.fr/DDEP_forum)

APPENDIX 1

Proposed guidelines for rounding of uncertainties (Draft 2)

Desmond MacMahon

1. The UKAS document M3003, The Expression of Uncertainty and Confidence in Measurement states:

   Para 8.6
   "The number of figures in a reported uncertainty should always reflect practical measurement capability. In view of the process for estimating uncertainties it is seldom justified to report more than two significant figures. Uncertainties should normally be rounded up to the appropriate number of figures but may be rounded down when this does not significantly reduce confidence in a measurement result."

   Para 8.7
   "The numerical value of the measurement result should normally be rounded to the least significant figure in the value of the expanded uncertainty quoted unless there are justifiable reasons for quoting more figures. The normal rules of rounding apply, however, if the rounding decreases the value of the uncertainty by more than 5%, the rounded-up value should be used. Rounding of results and uncertainties should be carried out only at the final stages of the calculation in order to prevent cumulative rounding errors having a significant effect."

2. It is not usually justified to quote a final uncertainty to more than two significant figures and, in many cases one digit is sufficient, as indicated below.

3. In the calculation of final uncertainties up to 3 digits should be retained during the calculations.

4. The effect of the 5% rule would be: -

uncertainties of greater than	945	and less than	1050	become	10
"	840	and up to	945	become	9
"	735	"	840	become	8
"	630	"	735	become	7
"	525	"	630	become	6
"	420	"	525	become	5
"	315	"	420	become	4
" greater than, or equal to	255	"	315	become	3

   uncertainties, where the two most significant digits are from 10 to 25, are rounded in the normal manner to two significant digits.

5. The number of significant digits quoted in the parameter value is then adjusted to match those quoted in the final (k=1) uncertainty. If the uncertainty has been expressed as a percentage, this is not straightforward. It is necessary to express the uncertainty in absolute terms, i.e. in the same units as the parameter value, to determine the number of significant figures in that parameter value.

6. Where uncertainties are quoted with the coverage factor k=2, rounding should take place for the k=1 uncertainty and the result doubled to obtain the k=2 uncertainty.

Desmond MacMahon
20th February 2004

BNM BUREAU NATIONAL DE MÉTROLOGIE

COMMISSARIAT À L'ÉNERGIE ATOMIQUE

LABORATOIRE NATIONAL
HENRI BECQUEREL

Note technique LNHB/04-13

Rounding of measurement results

Number of significant figures

M.M. Bé, P. Blanchis, C. Dulieu

28 avril 2004

I- Introduction

This document states the manner of presenting results in scientific and technical reports with special reference to the number of significant figures of the values of quantities and the associated uncertainty.

How many significant figures should be given for uncertainty of measurement? It is to be noted that, whatever the case, if absolute uncertainty is indicated, the number of figures must be consistent with that of the quantity.
Example: A = (123.45 ± 0.08) Bq and not A = (123.45 ± 0.081) Bq.

The following rule is justified below:

If the first significant figure of the uncertainty is between 5 and 9, the result is rounded off to that decimal (uncertainty then has been given to one significant figure); if the first significant figure is less than 5, the result is rounded off to the next decimal (2 significant figures for uncertainty).

Application functions are given in the appendix.

II- Notation

The notation used is in accordance with the recommendation in the "Guide to the expression of uncertainty in measurement", i.e. preferably:
"A = 123.456 (11) Bq where the number between brackets is the numerical value of the combined standard uncertainty relating to the last two figures corresponding to the result given". The third component of the result is the unit in which the numerical value is expressed.

Examples:
A = 123.0 (1) Bq means A = (123.0 ± 0.1) Bq
A = 123 (1) Bq means A = (123 ± 1) Bq
A = 123.0 (11) Bq means A = (123.0 ± 1.1) Bq

III- Rounding of results

"Scientific common sense" (?) would suggest that a number with a string of decimals is not significant and that it "needs" to be rounded off.
By convention, the following empirical rule is applied "if the number that follows the decimal at the point where it is to be rounded off is 5 or greater, the figure is rounded off to the higher figure and otherwise the lower figure".

Example:

Gross figure	5.6789123	5.432167
Rounded off to	0.001	0.001
Number rounded off to 3 decimal places	5.679	5.432
Rounding error	+ 0.0000877	- 0.000167
Rounding off to 5 decimal places	5.67891	5.43217

But rounding off the gross figure introduces error into its value. This error is less than 5/9 of the decimal it is rounded off to.

IV- Determination of the number of significant figures

However, all the readings given in a technical memorandum need to have three components:
- the value of the quantity;
- the associated uncertainty;
- the unit.

Knowledge of the uncertainty imposes the number of significant figures of the quantity.

The following rules determine the number of decimal places it is rounded off to:
- truncation of the number must not result in loss of decimals that contain meaningful information (i.e. significant decimals);
- meaningless decimals must not be left (i.e. non-significant figures).

The number of significant figures of a result depends on the value of its uncertainty. Before any calculations are made, the following considerations need to be reviewed.

Taking the above example:

m	gross number	5.6789123	5.6789123
u	uncertainty	0.006243	0.002341
x	rounding factor	5	5
u/x		0.0012486	0.0004682
s	decimal rounded off to	0.001	0.0001
m_r	number rounded off to *s* decimals	5.679	5.6789
	final number	5.679 (6)	5.6789 (23)
r	rounding error	+ 0.0000877	- 0.0000123

A number *x* is sought such that the rounding of a number *m* does not result in an error in its value greater that *u/x*, where *u* is the uncertainty of measurement and *x* a factor to be determined (set at 5 in the above example).

It will be noted that:

- The straightforward rounding off a number is consistent with *r £ s/2*, which always remains true.

- The number of decimal places to be rounded off to is determined by the uncertainty, i.e. finding a number of *x*, such that $s \leq u/x$, where *u* is the uncertainty associated with the result. However, to avoid leaving non-significant decimal, a relationship of the $u/10x < s$ type must be complied with.

This results in a rounded-off value such that: *r £ u/2x*.

• If $x < 1$ then: $u/x > u$; therefore in certain cases it could be possible for: $r > u/2$ and the result of the rounding being outside the interval $m \pm u$. Which implies that $x > 1$.

• If $x > 5$, then $r \leq u/10$ and the number of significant figures of the uncertainty can, in certain cases, be greater than 2. Which is unthinkable.

=> **The number *x* to be adopted must therefore be between 1 and 5**.

Notes concerning values of *x* :

1) Number $x = 5$ corresponds to the recommendations of former French Standard AFNOR NF X 06-044 which are: "To obtain a final result containing a number of figures compatible with the uncertainty of measurement, the result is to be rounded off in such a manner that the error due to rounding is less than 1/10 of the uncertainty of measurement".

This rule is also commonly expressed as follows: if the first significant figure of the uncertainty is between 5 and 9, the result is rounded off to that decimal (uncertainty then has been given to one significant figure); if the first significant figure is less than 5, the result is rounded off to the next decimal (2 significant figures for uncertainty).

Taking the proceeding example:

m	gross figure	5.6789123	5.6789123
u	uncertainty	0.006243	0.002341
x	rounding factor	5	5
	results	5.679 (6)	5.6789 (23)

2) Our colleagues at PTB use $x = 3$, with the result that the rounding error remains less than 1/6.

V- Value of rounding error

What value should be adopted for *x*? Can this value be more precisely estimated in view of the measurements commonly made in the laboratory? What rounding error can reasonably be accepted?

For a series of *n* measurements {*Xi* }, the average value of the results { *Xi* } is given by:

$$m = \frac{1}{n}\sum_i Xi$$

and the experimental variance of the average of the *n* measurements { *Xi* }as follows:

$$s_m^2 = \frac{1}{n(n-1)}\sum_i (Xi - m)^2$$

If quantity s_m is determined on the basis of experimental data, what is its uncertainty?

If the quantity *X* is distributed *in accordance with a normal law*, the variance of s_m^2 is:

$$D\left(s_m^2\right)=\overline{\left(s_m^2-\overline{s_m^2}\right)^2}$$

The relative uncertainty concerning the value of the experimental value is:

$$d\left(s_m^2\right)=\frac{\sqrt{D\left(s_m^2\right)}}{\overline{s_m^2}}=\sqrt{\frac{2}{n-1}}$$

The uncertainty U_X associated with the experimental value *m* is proportional of the square root of s_m^2 and its relative uncertainty is:

$$d\left(U_X\right)=\frac{U\left(U_X\right)}{U_X}=\frac{1}{2}d\left(s_m^2\right)\approx\sqrt{\frac{1}{2\left(n-1\right)}}$$

It is thus necessary to make some fifty measurements to obtain a relative uncertainty of the experimental standard deviation of 10 %.

a) How many measurements are commonly made to determine the radioactivity of a sample for instance? In the case of international comparison ? Of a standardization ?

Most specific radioactivity measurements are made with a maximum of 10 sources, and in an experimental standard deviation uncertainty of 24%. With 5 sources, the uncertainty amounts to 36%. And this is based on the assumption that the distribution is Gaussian, which is hard to prove.
Furthermore, in view of the inevitable approximations and interpretations made during determination of the uncertainties by type B methods (the distribution law is generally unknown except in certain specific cases, Poisson's law for instance) the combined uncertainty of the result is rarely known within more than 50 %.

b) And what of rounding after "evaluation"of data?

A data set for a given quantity rarely exceeds around ten items.
In a certain number of cases, the final uncertainty adopted is the external uncertainty, with the result that the relative uncertainty of this uncertainty is necessarily greater than 1/10.
In other cases, the final uncertainty is the standard uncertainty obtained from the experimental standard uncertainties given by the researchers. Here, the calculation of the variance is correct, i.e. the relative uncertainty concerning the evaluated standard uncertainty is as reliable as the relative uncertainties relating to the experimental standard uncertainties.
This begs the question as to what is the relative uncertainty for the experimental standard uncertainty?

Conclusions :

1) The 1/10 rule: “To obtain a final result containing a number of figures compatible with the uncertainty of measurement, the result is to be rounded off in such a manner that the error due to rounding is less than 1/10 of the uncertainty of measurement” appears to be optimistic.

2) But this rule is applicable in a few cases.

3) Besides, the results of measurements obtained are frequently subsequently used in calculation programs where new sources of error are present. In particular, the following rule should be born in mind: “complete the calculations before rounding”. It is accordingly preferable to retain the 1/10 rule: if the first significant figure of the uncertainty is between 5 and 9, the result is rounded off to that decimal (uncertainty then has been given to one significant figure); if the first significant figure is less than 5, the result is rounded off to the next decimal (2 significant figures for uncertainty).

4) Examples:

value	uncertainty	Result
123.567 8912	0.000 512 3	123.567 9 (5)
123.567 891 2	0.000 492 3	123.567 89 (49)
987.21	10.567	987 (11)
987.21	1.056 7	987.2 (11)
98 765.432 1	56.123	98 770 (60)
98 765.432 1	5.612 3	98 765 (6)
98 765.432 1	0.561 23	98 765.4 (6)

The appendix contains the functions for rounding off a number and its uncertainty.

Appendix

Excel functions:

```
'
'Returns the rounded value of a result (or its uncertainty) as a function of its uncertainty
' for x = 5

    Function ResRond(Result, Uncertainty)
      With Application
        ResRond = .Round(Result, -1 - Int(.Log(Uncertainty/ 50)))
      End With
    End Function

'
'Returns the value of a result (or its uncertainty) as a function of its uncertainty
' for x = 3

    Function ResRond(Result,Uncertainty)
      With Application
        ResRond = .Round(Result, -1 - Int(.Log(Uncertainty / 30)))
      End With
    End Function

'
'Returns in TEXT FORMAT the rounded value of a result and of its uncertainty (e.g. 12.345(26) )
' for x = 5
'
    Function ResRondTxt(Result, Uncertainty)
      With Application
        nb_chif = -1 - Int(.Log(Uncertainty / 50))
        ResRondTxt = .Fixed(ResRond(Result, Uncertainty), nb_chif) + _
                "(" + .Fixed(ResRond(Uncertainty, Uncertainty) * 10 ^ nb_chif, 0) + ")"
      End With
    End Function
```